



DEPARTMENT OF ENERGY
Environmental Management Los Alamos Field Office (EM-LA)
Los Alamos, New Mexico 87544

Mr. John E. Kieling
Bureau Chief
Hazardous Waste Bureau
New Mexico Environment Department
2905 Rodeo Park Drive East, Building 1
Santa Fe, NM 87505-6303



AUG 29 2019

Dear Mr. Kieling:

Subject: Submittal of the Investigation Report for Royal Demolition Explosive in Deep Groundwater

Enclosed please find two hard copies with electronic files of the "Investigation Report for Royal Demolition Explosive in Deep Groundwater." The report summarizes information on the occurrence and concentration of Royal Demolition Explosive (RDX) in deep groundwater. The report satisfies Milestone 15 of the fiscal year 2019 version of Appendix B, Milestones and Targets, of the 2016 Compliance Order on Consent (Consent Order).

Pursuant to Section XXIII.C of the Consent Order, pre-submission review meetings were held with the U.S. Department of Energy Environmental Management Los Alamos Field Office (EM-LA); Newport News Nuclear BWXT-Los Alamos, LLC (N3B); and the New Mexico Environment Department (NMED) on February 5, March 28, and May 16, 2019, to discuss project status and elements of this report. NMED acknowledged its support for the report's contents in an email on July 17, 2019.

If you have any questions, please contact Pat McGuire at (505) 709-7918 (patrick.mcguire@em-la.doe.gov) or Cheryl Rodriguez at (505) 665-5330 (cheryl.rodriguez@em.doe.gov).

Sincerely,

Arturo Q. Duran
Compliance and Permitting Manager
Environmental Management
Los Alamos Field Office

Enclosures:

1. Two hard copies with electronic files – Investigation Report for Royal Demolition Explosive in Deep Groundwater (EM2019-0235)

cc (letter with hard-copy enclosure[s]):

C. Rodriguez, EM-LA

cc (letter with CD enclosure[s]):

L. King, EPA Region 6, Dallas, TX

R. Martinez, San Ildefonso Pueblo, NM

D. Chavarria, Santa Clara Pueblo, NM

S. Yanicak, NMED

P. McGuire, N3B

emla.docs@em.doe.gov

N3B Records

Public Reading Room (EPRR)

PRS Website

cc (letter emailed without enclosure[s]):

W. Alexander, N3B

E. Day, N3B

M. Erwin, N3B

E. Evered, N3B

M. Everett, N3B

D. Holgerson, N3B

J. Hyatt, N3B

D. Katzman, N3B

K. Lebak, N3B

J. Legare, N3B

F. Lockhart, N3B

E. Lowes, N3B

P. Maestas, N3B

J. Moore, N3B

G. Morgan, N3B

L. Patten, N3B

G. Pool, N3B

B. Robinson, N3B

T. Vigil, N3B

S. White, N3B

J. Yarbrough, N3B

A. Duran, EM-LA

T. McCrory, EM-LA

D. Nickless, EM-LA

EM-LA-40AD-00484

August 2019
EM2019-0235

Investigation Report for Royal Demolition Explosive in Deep Groundwater




Newport News Nuclear BWXT-Los Alamos, LLC (N3B), under the U.S. Department of Energy Office of Environmental Management Contract No. 89303318CEM000007 (the Los Alamos Legacy Cleanup Contract), has prepared this document pursuant to the Compliance Order on Consent, signed June 24, 2016. The Compliance Order on Consent contains requirements for the investigation and cleanup, including corrective action, of contamination at Los Alamos National Laboratory. The U.S. government has rights to use, reproduce, and distribute this document. The public may copy and use this document without charge, provided that this notice and any statement of authorship are reproduced on all copies.

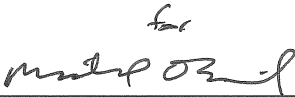
Investigation Report for Royal Demolition Explosive in Deep Groundwater

August 2019


Responsible program director:

Bruce Robinson		Program Director	Water Program	8/22/2019
Printed Name	Signature	Title	Organization	Date

Responsible N3B representative:

Erich Evered		Program Manager	N3B Environmental Remediation Program	8/23/19
Printed Name	Signature	Title	Organization	Date

Responsible DOE EM-LA representative:

Arturo Q. Duran		Compliance and Permitting Manager	Office of Quality and Regulatory Compliance	
Printed Name	Signature	Title	Organization	Date

EXECUTIVE SUMMARY

This deep groundwater investigation report (DGIR) for Royal Demolition Explosive (RDX) at Los Alamos National Laboratory (the Laboratory) fulfills the requirements of the 2016 Compliance Order on Consent (Consent Order), Fiscal Year 2019 Appendix B, Milestones and Targets. Appendix B, Milestone 15, requires a report characterizing the nature and extent of RDX in deep groundwater (i.e., perched-intermediate and regional groundwater).

Fiscal year 2019 Appendix B, Milestone 15, describes the milestone as an “Investigation Report that culminates results of investigation activities associated with deep groundwater and includes a groundwater risk assessment.” This report integrates applicable information from groundwater-related investigations conducted to date at the site and also addresses groundwater risk by incorporation of the following elements:

- Screening of groundwater data against applicable risk- and standards-based criteria
- Characterizing the extent of the RDX above the NMED tap water screening level in deep groundwater
- Evaluating the extent of RDX in deep groundwater and its spatial relationship to the nearest water supply well
- Assessing the land-use restrictions present for the Laboratory property and their function in preventing exposure to the present day location of RDX in deep groundwater

The purpose of this DGIR is to present a comprehensive description of the current conditions of RDX contamination in deep groundwater, for this report defined as the perched-intermediate and regional groundwater zones. The objectives of this DGIR are to summarize information on the occurrence and concentration of RDX in deep groundwater, use this information to define the nature and extent of RDX in deep groundwater, update the conceptual site model (CSM), describe current conditions, and recommend next steps. To meet the objectives, the DGIR summarizes and evaluates deep groundwater analytical results collected since 2000 and presents additional information to address the uncertainties identified by NMED in their review of the 2007 “Corrective Measures Evaluation Report for Intermediate and Regional Groundwater.”

In accordance with the 2005 Consent Order (superseded by the 2016 Consent Order), the U.S. Department of Energy (DOE) submitted the corrective measures evaluation (CME) to the New Mexico Environment Department (NMED) in August 2007. NMED subsequently issued a notice of disapproval (NOD) for the CME in April 2008. In the NOD, NMED required the Laboratory to conduct additional characterization to assess the extent of RDX in the perched-intermediate groundwater and in the regional aquifer and to further evaluate the feasibility of the remedial alternatives proposed in the CME.

In response to NMED’s 2008 NOD, the Laboratory developed the “Supplemental Investigation Work Plan for Intermediate and Regional Groundwater at Consolidated Unit 16-021(c)-99.” In this work plan, the Laboratory proposed additional characterization activities to address uncertainties in the hydrogeologic conceptual model at Technical Area 16 (TA-16).

To address sources of RDX to the deep groundwater, several remedial actions were performed in shallow soils and sediment between 1999 and 2010. These efforts included removal of approximately 1500 yd³ of RDX-contaminated material and in situ stabilization of residual RDX in permeable rock. In September 2017, DOE submitted to NMED the “Remedy Completion Report for Corrective Measures Implementation at Consolidated Unit 16-021(c)-99,” with the purpose of closing out the surface corrective

measures implementation (CMI). On November 27, 2017, NMED approved the surface CMI closure with modification (i.e., long-term monitoring requirement) and concluded that no further action was required to address any remaining surficial RDX concentrations.

Monitoring at TA-16 continues under the interim facility-wide groundwater monitoring plan (IFGMP). In addition to deep groundwater, springs, alluvial wells, and surface waters are sampled as part of the IFGMP. The IFGMP program also monitors RDX concentrations in groundwater in other wells downgradient of TA-16 and upgradient of public water supply wells PM-5, PM-4, and PM-2. These wells include R-60, R-17, R-46, and R-14. These wells could be considered sentinel wells for the public water supply wells, which are also monitored for RDX on a semiannual basis.

This DGIR describes the nature and extent of RDX in deep groundwater by screening analytical data collected from January 2000 to March 2019. This screening process confirms that RDX is the primary chemical of potential concern. The extent of RDX in perched-intermediate groundwater remains stable, and at 6 of the 9 sampling locations where RDX is detected, RDX concentrations are stable or decreasing. In regional groundwater, RDX was detected in 5 of the 10 monitoring wells, with 3 wells showing trends of increasing RDX concentration. The extent of RDX in regional groundwater is limited to an area underlying TA-16 and is approximately 3 mi from the nearest public water supply extraction well.

This report summarizes the main elements of the physical system CSM that describe the fate and transport of RDX in the TA-16 area, with particular emphasis on pathways that affect deep groundwater. The discussion builds on the CSM presented in the “Investigation Report for Water Canyon/Cañon de Valle” that is modified to include new and updated information collected since 2011. The conceptual model includes descriptions of the surface water environment, vadose zone pathways, and deep groundwater.

Conditions at the Laboratory necessitate that institutional controls be put in place to eliminate the possibility of using the water underlying TA-16 for consumption now and in the foreseeable future. There is no imminent threat to the public water supply because the extent of deep groundwater that contains RDX is more than 3 mi from the nearest public water supply well.

The Consent Order provides a course of action to be taken if RDX concentrations were to exceed the New Mexico tap water screening level, which would lead to a risk assessment to determine if there exists an unacceptable risk to human health. This DGIR concludes that RDX concentrations in perched-intermediate and regional groundwater do not pose a current unacceptable risk to human health; however, RDX concentrations in the perched-intermediate groundwater are the source of RDX that has been detected in the underlying regional groundwater. The RDX in the regional aquifer might pose a future unacceptable risk to human health if the RDX were to migrate to the public water supply well in sufficient concentration and quantities. To assess this uncertainty and support the evaluation of potential remedial alternatives in a CME, a fate and transport groundwater model evaluation and further risk characterization should be performed.

CONTENTS

1.0	INTRODUCTION	1
1.1	DGIR Purpose and Objectives	3
1.2	Regulatory Context	3
2.0	BACKGROUND	4
2.1	Site Description	4
2.2	Current and Future Land Use	5
2.3	Regional and Structural Geology	5
2.4	TA-16 Stratigraphy	6
2.5	Site Hydrogeology	9
2.6	Site History	10
2.6.1	TA-16 History	10
2.6.2	260 Outfall Operation	10
2.6.3	TA-16 RDX Source and Release History	11
2.6.4	Other Potential Sources of RDX at TA-08 and TA-09	12
2.7	Early Investigations and Source Removal	13
2.7.1	Phase I RFI	13
2.7.2	Phase II RFI	13
2.7.3	Source Removal Interim Measure	14
2.7.4	Phase III RFI	14
2.7.5	2009–2010 CMI	16
2.8	2006 Intermediate and Regional Groundwater Investigation and the 2007 CME	18
2.9	Post 2007 CME Supplemental Investigations	20
2.9.1	2014 Direct Current Resistivity Survey of Cañon de Valle	20
2.9.2	Post 2007 Monitoring Well Installations	22
2.9.3	2011 Extended Duration Aquifer Tests at Wells CdV-16-4ip and R-25b	27
2.9.4	2014 Extended Duration Aquifer Tests at Well CdV-16-4ip	28
2.9.5	2016 Extended Duration Cross-Hole Aquifer Tests at Wells CdV-9-1(i), CdV-16-4ip, and CdV-16-1(i)p	30
2.10	2018 RDX Compendium Report Investigations	31
2.10.1	Updated RDX Inventory	31
2.10.2	Geologic Investigation	32
2.10.3	Hydrogeochemical Studies	32
2.10.4	RDX Fate and Transport Studies	35
2.10.5	RDX Biostimulation and Microbial Community Profiling	36
2.10.6	Hydrogeology and Model Calibration for Contaminant Fate and Transport at TA-16	38
2.10.7	Tracer Study	38
3.0	CONCEPTUAL SITE MODEL	40
3.1	Nature and Extent	40
3.1.1	Groundwater Chemical Screening Assessment	41
3.1.2	Major-Ion Characteristics of Waters in Different Hydrologic Zones	46

3.2	Updated Conceptual Site Model	48
3.2.1	Surface Water Pathways	48
3.2.2	Vadose Zone Pathways	49
3.2.3	Regional Groundwater	57
4.0	SUMMARY AND CONCLUSIONS	59
5.0	RECOMMENDATIONS	62
6.0	REFERENCES AND MAP DATA SOURCES	64
6.1	References	64
6.2	Map Data Sources	75

Figures

Figure 1.0-1	Location TA-16 within LANL	77
Figure 1.0-2	TA-16 boundary	78
Figure 1.0-3	TA-16 Monitoring Group	79
Figure 2.3-1	Geologic map of TA-16 and surrounding areas	80
Figure 2.4-1	Stratigraphy of the geologic units at TA-16	81
Figure 2.5-1	Map of regional water table at Los Alamos National Laboratory	82
Figure 2.6-1	TA-16 source locations	83
Figure 3.1-1	Time series trend plots for alluvial wells (circle), springs (square), and baseflow (triangle) monitoring locations	84
Figure 3.1-2	Time series trend plots for intermediate (triangle) and regional (square) monitoring wells	85
Figure 3.1-3	Map showing RDX extent and water table contours for the upper perched-intermediate groundwater zone at TA-16	86
Figure 3.1-4	Southwest to northeast cross section of RDX concentrations in the regional aquifer at TA-16	87
Figure 3.1-5	Map view of RDX concentrations in the regional aquifer at TA-16	88
Figure 3.1-6	Trilinear (Piper) plots for springs, surface water, alluvial groundwater, perched-intermediate groundwater, and regional groundwater	89
Figure 3.1-7	Stiff diagrams for surface and near-surface water systems	90
Figure 3.1-8	Stiff diagrams for perched-intermediate groundwater	91
Figure 3.1-9	Stiff diagrams for regional groundwater	92
Figure 3.2-1	Conceptual E-W cross section showing of groundwater in the vicinity of TA-16	93
Figure 3.2-2	Conceptual block diagram showing RDX release sites and monitoring wells in the vicinity of TA-16	94
Figure 3.2-3	Southwest-northeast geologic cross section showing groundwater pathways from the 260 Outfall to well R-18	95
Figure 3.2-4	Structure contour maps for geologic contacts in the TA-16 area	96
Figure 3.2-5	Map showing approximate extent of perched-intermediate groundwater zones at TA-16	97

Figure 3.2-6	North-south geologic cross-section for the lower part of the vadose zone showing geologic contacts and groundwater occurrences in wells CdV-9-1(i), CdV-16-1(i), R 25b, and R-25.....	98
Figure 3.2-7	Northwest-southeast geologic cross-section for the lower part of the vadose zone showing geologic contacts and groundwater occurrences in wells CdV-9-1(i) and CdV-16-4ip	99
Figure 3.2-8	West-northwest to east-southeast geologic cross-section for the lower part of the vadose zone showing contacts and groundwater occurrences in wells CdV-9-1(i), R-63i, R-63, and CdV-16-2(i)r	100
Figure 3.2-9	Geologic media hosting perched-intermediate groundwater at TA-16	101
Figure 3.2-10	Block diagram showing conceptual facies model of Puye Formation proximal alluvial fan deposits at TA-16	102
Figure 3.2-11	Regional water table map for the Pajarito Plateau and geologic units intersected by the water table.....	103
Figure 3.2-12	R-17 screen 1 and screen 2 water levels along with pumping rates at municipal water-supply wells PM-2, PM-4, and PM-5.....	104
Figure 3.2-13	Map showing the location of RDX concentrations >9.66 µg/L in regional groundwater relative to the existing groundwater monitoring wells and downgradient water supply wells	105

Tables

Table 1.0-1	TA-16 Activities Summary.....	107
Table 2.6-1	TA-16 Contaminant Sources and Ranking Based on their Potential to Impact Groundwater	112
Table 3.1-1a	Analytes, Field Preparation, and Analytical Methods Used by Accredited Contract Laboratories for Samples Collected under the IFGMP	113
Table 3.1-1b	Analytical Methods Used by Contract Laboratories for Samples Collected under the IFGMP	114
Table 3.1-2	Sample Location Descriptions for Water Samples Collected in Alluvial Wells, Base Flow, Intermediate Wells, and Regional Wells	121
Table 3.1-3	Frequency of Detections for Inorganic Constituents in Water Samples Collected in Intermediate and Regional Wells	123
Table 3.1-4	Frequency of Detections for Organic Constituents in Water Samples Collected in Intermediate and Regional Wells	125
Table 3.1-5	Mean, Most Recent Values, and Mann-Kendall Trend Analysis of the RDX Concentrations in Water Samples	136
Table 3.1-6	Frequency of Detections for Radionuclide Constituents in Water Samples Collected in Intermediate and Regional Wells	138
Table 3.2-1	Vertical Head Gradients in Multiscreen Wells.....	143

Appendixes

- Appendix A Acronyms and Abbreviations, Metric Conversion Table, and Data Qualifier Definitions
- Appendix B Well Completion Diagrams
- Appendix C Tracer Data (on CD included with this document)
- Appendix D Groundwater Analytical Results from 2000 to 2019 (on CD included with this document)
- Appendix E 2019 Update of RDX Inventory in the Regional Aquifer

1.0 INTRODUCTION

This deep groundwater investigation report (DGIR) for Technical Area 16 (TA-16) at Los Alamos National Laboratory (LANL or the Laboratory) fulfills the requirements of the 2016 Compliance Order on Consent (Consent Order), Fiscal Year 2019 Appendix B, Milestones and Targets. Appendix B, Milestone 15, requires a report characterizing the nature and extent of RDX (Royal Demolition Explosive) in deep groundwater. Deep groundwater in this report refers to the perched-intermediate zone beneath TA-16 and in the regional aquifer.

Fiscal year 2019 Appendix B, Milestone 15, specifies an “Investigation Report that culminates results of investigation activities associated with deep groundwater and includes a groundwater risk assessment.” This report integrates applicable information from groundwater-related investigations conducted to date at the site and addresses groundwater risk by incorporating the following elements:

- Screening of groundwater data against applicable risk- and standards-based criteria
- Characterizing the extent of the RDX above the New Mexico Environment Department (NMED) tap water screening level in deep groundwater
- Evaluating the extent of RDX in deep groundwater and its spatial relationship to the nearest water supply well
- Assessing the land-use restrictions present for Laboratory property and their function in preventing exposure to the present day location of RDX in deep groundwater.

TA-16 was established to develop explosive formulations, cast and machine explosive charges, and assemble and test explosive components for the nuclear weapons program. Work conducted at TA-16 has been in support of developing, testing, and producing explosive charges for atomic weapons. Present-day use of this site is essentially unchanged, although the facilities have been upgraded and expanded as explosives and manufacturing technologies have advanced. The location of TA-16 relative to the Laboratory is shown in Figure 1.0-1. Details of TA-16 are shown in Figure 1.0-2.

The 2005 Consent Order (superseded by the 2016 Consent Order) required that a corrective measures evaluation (CME) be submitted by U.S. Department of Energy (DOE) to NMED in 2007. In August 2007, the DOE submitted to NMED the “Corrective Measures Evaluation Report for Intermediate and Regional Groundwater” (LANL 2007, 098734). The CME recommended a remediation strategy for monitoring natural attenuation in the perched-intermediate and regional groundwater, with including possible pump-and-treat actions to reduce high explosives (HE) concentrations in groundwater.

NMED subsequently issued a notice of disapproval (NOD) for the CME in April 2008 (NMED 2008, 101311). In the NOD, NMED required the Laboratory to conduct additional characterization to assess the extent of contamination in perched-intermediate groundwater and in the regional aquifer, and to further evaluate the feasibility of the remedial alternatives proposed in the CME. NMED’s direction was based on its assessment that insufficient information was available to determine whether the Laboratory’s proposed actions were appropriate and protective.

In response to NMED’s 2008 NOD, the Laboratory developed the “Supplemental Investigation Work Plan for Intermediate and Regional Groundwater at Consolidated Unit 16-021(c)-99” (LANL 2008, 103165). In this work plan, the Laboratory proposed additional characterization activities to address uncertainties in the hydrogeologic conceptual model at TA-16. These activities included installing additional perched-intermediate and regional groundwater monitoring wells, performing additional groundwater monitoring, and conducting single-well aquifer tests to further characterize hydraulics of the perched-intermediate and

the regional aquifers. To address hydrogeologic uncertainties, subsequent work plans were submitted, proposing multi-well aquifer tests and cross-hole tracer tests.

Several additional activities were conducted since the NOD. A geophysical study was performed to better understand underlying geologic structures. Hydrogeochemical studies evaluated different groundwater flow regimes and the potential for groundwater mixing. Fate and transport studies and biological studies assessed how RDX moves or is degraded in deep groundwater.

To address sources of HE to the deep groundwater, several remedial actions were performed in shallow soils and sediment between 1999 and 2010. These actions included an interim action and a corrective measures implementation (CMI). These efforts included removal of approximately 1500 yd³ of RDX-contaminated material and the in situ stabilization of residual RDX in permeable rock (LANL 2010, 108868). In September 2017, DOE submitted to NMED the “Remedy Completion Report for Corrective Measures Implementation at Consolidated Unit 16-021(c)-99” (LANL 2017, 602597) to close out the surface CMI. On November 27, 2017, NMED approved the surface CMI closure with modification (i.e., adding a long-term monitoring requirement) and concluded no further action was required to address surficial RDX contamination; however, monitoring of alluvial groundwater, surface water, and springs continue under the RDX Characterization Campaign’s “Long-Term Monitoring and Maintenance Plan for Corrective Measures Implementation at Consolidated Unit 16-021(c)-99.”

This DGIR focuses on the perched-intermediate and regional groundwaters containing RDX. Monitoring at TA-16 continues under the interim facility-wide groundwater monitoring plan (IFGMP) (N3B 2018, 700000). In addition to deep groundwater, springs, alluvial wells, and surface waters are sampled as part of the IFGMP. The results from sampling spring, alluvial groundwater, and surface water are reported in the annual long-term monitoring and maintenance report for Consolidated Unit 16-021(c)-99. Figure 1.0-3 shows the location of the TA-16 260 monitoring group. Sampling locations, analytical suites, and monitoring frequencies for the TA-16 260 monitoring group are presented in the IFGMP, Table 6.4-1 (N3B 2018, 700000). Monitoring of deep groundwater from the perched-intermediate and regional aquifers represents a long-term data set that indicates what constituents are present and their trends and variability. The sampling frequency for most locations in the TA-16 260 monitoring group is primarily semiannual, although select locations are sampled quarterly.

The IFGMP program also monitors HE concentrations in groundwater in other wells downgradient of TA-16 and upgradient of public water supply wells PM-5, PM-4, and PM-2. These wells include R-60, R-46, R-17, and R-14. R-19 will become part of the IFGMP sampling program after the sampling equipment in the well is reconfigured. These wells could be considered sentinel wells for the public water supply wells, which are also monitored on a semiannual basis for HE.

In this DGIR, groundwater results obtained from January 2000 to March 2019 were screened to verify that RDX is the only chemical of potential concern (COPC) in perched-intermediate and regional groundwaters. The process prescribed in the Consent Order is used to evaluate the risk posed by RDX in perched-intermediate and regional groundwater, to assess if there is an imminent risk to human health, and to aid in determining next steps.

This report summarizes the main elements of the physical system conceptual site model (CSM) that describe the fate and transport of HE in the TA-16 area, with particular emphasis on pathways that affect groundwater. The discussion builds on the CSM presented in the “Investigation Report for Water Canyon/Cañon de Valle” (LANL 2011, 207069) that was modified to include new and updated information collected since 2011. The conceptual model includes descriptions of the surface water environment, vadose zone pathways, and regional groundwater.

There is a long history of investigating and studying soil and groundwater containing HE at the Laboratory. In the 1990s, environmental assessment activities began with a Resource Conservation and Recovery Act (RCRA) Phase I site characterization. Subsequent soil, sediment, surface water, springs, alluvial groundwater, vadose zone groundwater, and regional groundwater investigations, remedial interim actions, and corrective measures have been conducted and continue to be performed (e.g., IFGMP sampling and annual reporting). Table 1.0-1 provides a listing of over 40 activities performed and pertinent correspondence generated since TA-16 was first investigated in 1990. This DGIR is not intended to present all the information gathered since 1990, but instead to summarize information relevant to deep groundwater that may have been impacted by operations conducted at TA-16.

In the remaining parts of section 1, this DGIR presents the purpose and objectives of this report and regulatory background pertinent to the preparation and submission of this document. Section 2 presents a summary of investigations and studies conducted over the past 18 years to understand the sources and extent of contamination and to update the CSM. Section 3 describes the process of screening the analytical data collected since 2000, and it verifies that RDX is the primary COPC. Section 3 also describes the current nature and extent of RDX in deep groundwater and presents the updated CSM. Section 4 provides a summary of the pertinent information included in this DGIR and states conclusions based on current site conditions. Section 5 presents recommendations.

1.1 DGIR Purpose and Objectives

The purpose of this DGIR is to present a comprehensive description of the current conditions of RDX in perched-intermediate and regional groundwater at TA-16. The objectives of this DGIR are to summarize information on deep groundwater containing RDX, use this information to define the nature and extent of RDX in perched-intermediate and regional groundwater, update the CSM, describe current conditions, assess current risk to human health, and recommend next steps. To meet the objectives, the DGIR summarizes and evaluates perched-intermediate and regional groundwater analytical results collected since 2000 and presents additional information to address the uncertainties identified by NMED in their review of the 2007 CME.

1.2 Regulatory Context

NMED issued the Consent Order to DOE pursuant to Section 74-4-10 of the New Mexico Hazardous Waste Act. The Consent Order was also issued under (1) Section 74-9-36(D) of the New Mexico Solid Waste Act (SWA) and (2) 20.9.9.14 New Mexico Administrative Code (NMAC), for the limited purpose of addressing the corrective action activities, including requirements, concerning groundwater contaminants listed at 20.6.2.3103 NMAC, toxic pollutants listed at 20.6.2.7.WW NMAC, and Explosive Compounds as defined herein. Although DOE consents to SWA jurisdiction for enforcement of the corrective action activities, including requirements, of this Consent Order relating to groundwater contaminants listed at 20.6.2.3103 NMAC, toxic pollutants listed at 20.6.2.7.WW NMAC, and Explosive Compounds, DOE otherwise reserves any and all rights, claims, and defenses with respect to the applicability of the requirements of the SWA, including the defenses enumerated in Section 74-9-34.

The Consent Order provides the process by which investigation and remediation of contamination from legacy waste management activities at the Laboratory occurs. The Consent Order both guides and governs the ongoing cleanup of legacy waste at the Laboratory through a campaign-based approach and the annual planning process. The annual planning process allows for revisions to cleanup campaigns based on actual work progress, changed conditions, and funding, with DOE updating the milestones and targets listed in the Consent Order, Appendix B, Milestones and Targets.

DOE proposed to use the annual planning process described in Section VIII.C of the 2016 Consent Order to discuss and establish a new target date for the final CME report based upon data from the new monitoring wells and progress with the studies proposed since NMED issued the CME NOD.

DOE proposed to replace the CME report milestone in Appendix B with a report summarizing additional information obtained since the NOD. The 2016 Consent Order included a milestone date for submission of the revised CME of September 30, 2017. During the 2017 annual planning process, the Appendix B milestone table showed a revised CME being submitted in March 2020 and an investigation report for perched-intermediate and regional groundwater being submitted in March 2019. During the 2018 planning process, the deep groundwater investigation report submission date was set as August 30, 2019.

The Consent Order also establishes a process to assess if contaminant concentrations in groundwater pose an unacceptable risk to human health. Section 4 of this DGIR discusses the comparison of RDX concentrations in perched-intermediate and regional groundwater to the 2019 NMED Risk Assessment Guidance tap water screening level (NMED 2019, 700550) and the potential for unacceptable risk to human health.

2.0 BACKGROUND

2.1 Site Description

TA-16 is located in the southwestern corner of the Laboratory and covers 2410 acres (3.8 mi²). The U.S. Department of the Army acquired the land for the Manhattan Project in 1943. Figure 1.0-2 shows the boundary of TA-16. Bandelier National Monument borders TA-16 along New Mexico State Highway 4 to the south. The Santa Fe National Forest along New Mexico State Highway 501 borders TA-16 to the west. To the north and east, TA-16 is bordered by TA-08, TA-09, TA-11, TA-14, TA-15, TA-37, and TA-49. TA-16 is fenced and posted along New Mexico State Highway 4. Water Canyon, a 200-ft-deep ravine with steep walls, separates New Mexico State Highway 4 from active sites at TA-16. Cañon de Valle forms the northern border of TA-16.

Building 260, located on the north side of TA-16 (Figure 1.0-2), has been used for processing and machining HE since 1951. Water is used to machine HE, which is slightly water-soluble. Effluent from machining operations contains dissolved HE and may contain entrained HE cuttings. At building 260, effluent treatment consists of routing the water to 13 settling sumps to recover any entrained HE cuttings. From 1951 to 1996, the water from these sumps was discharged to the 260 Outfall that drained into Cañon de Valle. In 1994, outfall discharge volumes were measured at several million gallons per year. The discharge volumes were probably higher during the 1950s when HE production output from building 260 was substantially greater than it was in the 1990s (LANL 1994, 076858). In the past, barium was a constituent of certain HE formulations and inert components and was present in the outfall effluent from building 260.

The HE machining building (16-260) and associated sumps, drain lines, and troughs discharged effluent into the 260 Outfall drainage channel. The 260 Outfall drainage channel consisted of a settling pond and an upper and lower drainage channel that extends from the 260 Outfall downgradient to the confluence of the drainage and Cañon de Valle. The former approximately 50 ft-long x 20-ft wide settling pond was located within the upper drainage channel, approximately 45 ft below the 260 Outfall. The drainage channel runs approximately 600 ft northeast from the 260 Outfall to the bottom of Cañon de Valle. Historically, HE-containing water from the outfall entered the former settling pond and drained into the 260 Outfall drainage channel.

2.2 Current and Future Land Use

Current and future land use at TA-16, according to the Laboratory's 25-year site plan for 2013 to 2037 (LANL 2012, 601095), is designated as HE research, development, testing, assembly, and production, in addition to weapons engineering tritium research. Most areas within TA-16 are active sites for the Weapons Engineering Technology Division of the Laboratory. As described in the site plan, construction of new facilities is planned during this 25-year period. As shown in Figure 1.0-2, numerous roads and utilities are present at the site.

In addition, on Laboratory property there are inherent restrictions that regulate land use at TA-16. For example, institutional control requirements for security and land transfer. Security controls prevent unknowing entry and minimize the possibility for unauthorized entry of persons or livestock onto TA-16, thus ensuring no wrongful, clandestine land use.

Land transfer controls govern any transfer of property from DOE to another entity. These land transfer controls require a notice to NMED when DOE transfers property. DOE will include in the deed a restriction that limits future use of the property to the particular use scenario.

These institutional controls together establish safeguards that prevent access to LANL property by people and restrict the installation of an unapproved, clandestine water supply well now and in the foreseeable future. Additionally, if in the future the property is transferred to another entity, deed restrictions can be put in place to control and constrain the use of deep groundwater underlying LANL property.

2.3 Regional and Structural Geology

TA-16 is located in the western part of the Española basin near the active rift basin margin defined by the Pajarito fault system. The Española basin of the Rio Grande rift is a west-tilted, half graben (Kelley 1978, 011659) filled with Miocene and Pliocene sedimentary deposits derived from highlands located to the west, north, and east (Griggs and Hem 1964, 092516; Galusha and Blick 1971, 021526; Cavazza 1989, 021501; Turbeville et al. 1989, 021587). These deposits thicken westward across the basin and may be as much as 9000 ft thick near the Pajarito fault system (Kelley 1978, 011659). Ferguson et al. (1995, 056018) identified a northeast-trending intrabasin graben beneath the western Pajarito Plateau based on gravity data; this structure represents the deepest part of the Española basin. Figure 2.3-1 is a geologic map of TA-16 and surrounding areas.

During early stages of volcanism in the Jemez Mountains volcanic field, the western structural margin of the Española basin coincided with a broad zone of north-trending faults that traversed the central part of the volcanic field (Gardner and Goff 1984, 044021). These early rift-margin faults became inactive about 6 million years ago (Ma), and the active rift margin migrated eastwards to the Pajarito fault system. The Pajarito fault system has been active since at least the mid-Miocene (Golombek 1983, 601748; WoldeGabriel et al. 2013, 601750). The Pajarito fault system is a narrow band of north- and northeast-trending normal faults with displacement dominantly down to the east (Griggs and Hem 1964, 092516; Smith et al. 1970, 009752; Gardner and Goff 1984, 044021). West of NM 501, the fault forms a 400-ft-high escarpment that has the surface expression of a large, north-trending, faulted monocline (Gardner et al. 1999, 063492; Gardner et al. 2001, 070106). Along strike, the fault varies from a simple normal fault to broad zones of small faults and faulted and unfaulted monoclines. These varied styles of deformation are all expressions of deep-seated normal faulting (Gardner et al. 1999, 063492). West of TA-16, the fault zone is segmented into two major splays that form stepped, east-facing escarpments.

Stratigraphic separation on the Tshirege Member of the Bandelier Tuff (1.22 Ma) ranges between 260 and 400 ft along the fault west of the Laboratory (Gardner et al., 2001, 070106). Episodic faulting is

indicated by progressively larger offsets in older rock units (Griggs and Hem 1964, 092516), though fault displacement for older rock units is poorly known because thick deposits of Bandelier Tuff cover critical relations. Continuing displacement along this fault system is reflected by Holocene movements and historic seismicity (Gardner and House 1987, 006682; Gardner et al. 1990, 048813).

The Pajarito fault system exerts a major influence on the thickness and juxtaposition of geologic units at the mountain block/basin interface. It is the principal structural feature in the area and probably plays a significant, but poorly understood, role in the movement of groundwater across the mountain block/basin interface. Because of intense fracturing, the fault zone probably is also an important infiltration zone for mountain-front recharge.

High-precision bedrock mapping of a 2.9 mi² area, including most of the RDX study area, found that a broad zone of deformation extends eastwards from the Pajarito fault system to the 260 Outfall area (Gardner et al. 2001, 070106; Lewis et al. 2002, 073785) (Figure 2.3-1). The mapping conducted by the Laboratory's Seismic Hazards program identified the following structural elements in this zone of deformation: (1) a north-south graben, referred to as the TA-09 graben that lies between building 16-260 and Material Disposal Area P (MDA P); (2) north-northwest-striking fractures and rare faults that bound the zone of deformation and may be the surface expression of deeper faulting; (3) northeast trending open or rubble-filled fissures within the Tshirege Member, some of which are very large; and (4) rare small east-west-trending faults (Gardner et al. 2001, 070106; Lewis et al. 2002, 073785).

The largest structure in the 260 Outfall area is the north-trending TA-09 graben (Figure 2.3-1) (Lewis et al. 2002, 073785). The graben is about 2000 ft wide at its southern end between building TA-16-260 and MDA P, narrowing to about 1000 ft wide at its northern end in Pajarito Canyon. The western bounding fault of the TA-09 graben is a high-angle normal fault with 5 ft of down-to-the-east displacement. The eastern boundary of the graben is defined by three closely spaced high-angle normal faults with a total of 20 ft of down-to-the-west displacement. A shallow north-trending syncline adjacent to the eastern bounding fault accounts for an additional 10 ft of down-to-the-west displacement. The bounding faults of the TA-09 graben offset old mesa top alluvial fan deposits, indicating some displacements post-date the Tshirege Member (Lewis et al. 2002, 073785).

Lewis et al. (2002, 073785) conducted a total station survey of open and filled fractures of large aperture (up to 3.3 ft wide) at MDA P. A total of 454 fractures were measured in the Bandelier Tuff to determine possible tectonic influences on fracturing. The fractures are generally steep and have a statistically significant north-northwest-preferred orientation (mean direction of N14W \pm 16°). Fractures in the densely welded Qbt 3t (Figure 2.3-1) are generally subhorizontal and have a statistically significant east-northeast preferred orientation (mean direction of N69E \pm 32°). Fractures in densely welded Qbt 3 are subhorizontal-to-steep and have north-northwest-preferred orientation (mean direction of N25W \pm 32°). The overall map pattern of high-angle fractures in all units is polygonal, suggesting most are cooling joints (Lewis et al. 2002, 073785). Subhorizontal fractures within densely welded units Qbt 3t and Qbt 3 appear to be associated with compaction foliation, and some may be partings between flow units. The presence of tectonic fractures is indicated by fracture densities and apertures that are greater on the western side of MDA P near the eastern border faults of the TA-09 graben. The association of elevated fracture density and fractures of large aperture with the TA-09 graben appears to mark a north-northwest-trending zone of diffuse deformation that extends 2 km east of the Pajarito fault system (Lewis et al. 2002, 073785).

2.4 TA-16 Stratigraphy

The character of volcanic and sedimentary rocks at TA-16 reflects their deposition in the western Española basin near the tectonically active Pajarito fault system during periods of active volcanism in the

Jemez Mountains volcanic field. Rock units include thick Quaternary ash-flow tuff sheets erupted from calderas located in the central part of the volcanic field and Pliocene alluvial fan deposits shed from the mountain block west of the Pajarito fault system. The stratigraphy in the vicinity of TA-16 includes surficial deposits, ash-flow tuffs of Quaternary Bandelier Tuff (including interbedded sedimentary deposits of the Cerro Toledo Formation), alluvial fan deposits of the Pliocene Puye Formation, and Pliocene dacite lavas of the Tschicoma Formation (Figure 2.4-1).

There is a large variety of surficial deposits at TA-16, including canyon-bottom alluvium and colluvium, mesa-top soils, and older alluvial fans on mesa tops. In Cañon de Valle near the 260 Outfall and MDA P, the thickness of alluvium ranges between 5.0 ft in well CdV-16-02657 and 9.0 ft in well CdV-16-1(i) (LANL 1998, 059891; Kleinfelder 2004, 087844). Alluvium in Cañon de Valle includes medium-to fine-grained sands derived from the Tshirege Member and dacitic cobbles, gravels, and sands derived from the Tschicoma Formation. These deposits host persistent alluvial groundwater in the vicinity of the 260 Outfall and MDA P; the saturated thickness of this alluvial groundwater ranges from 3.3 to 6.6 ft (LANL 2011, 207069). Mesa tops at TA-16 include widespread remnants of dacite-rich gravels deposited by early Pleistocene streams draining the Sierra de los Valles that pre-dated incision of the canyons (Reneau and McDonald 1996, 055538; Reneau et al. 1996, 055539). Because of their thickness and high porosity, mesa top alluvial fans may play a role storing water from storm runoff and snowmelt.

The Jemez volcanic field began to develop approximately 13 to 10 Ma with the eruption of predominantly basaltic and rhyolitic rocks of the Keres Group (Gardner et al. 1986, 059104). Activity in the volcanic field reached a climax with eruption of the Bandelier Tuff (Griggs and Hem 1964, 092516; Smith and Bailey 1966, 021584; Bailey et al. 1969, 021498; Smith et al. 1970, 009752).

The Bandelier Tuff has two members, each consisting of a basal pumice fall overlain by a petrologically related succession of ash-flow tuffs (Bailey et al. 1969, 021498). Eruption of the two members was accompanied in each case by caldera collapse. The Otowi Member (1.61 Ma) (Izett and Obradovich 1994, 048817; Spell et al. 1996, 055542) was erupted from the earlier of the two calderas. This early caldera was coincident with, and largely destroyed by, the younger Valles Caldera that formed during the eruption of the Tshirege Member (1.22 Ma) (Izett and Obradovich 1994, 048817; Spell et al. 1996, 055542). Deposition of widespread ash-flow tuff sheets over the western Española basin, including the TA-16 area, formed the Pajarito Plateau, an east-sloping tableland bounded on the west by the eastern Jemez Mountains (Sierra de los Valles) and on the east by the Rio Grande River.

The Tshirege Member of the Bandelier Tuff is a compound cooling unit that resulted from emplacement of successive rhyolite ash-flow tuffs separated by periods of inactivity that allowed for partial cooling before subsequent flows were deposited (Smith and Bailey 1966, 021584; Broxton and Reneau 1995, 049726). Because of the episodic nature of deposition, physical properties such as density, porosity, degree of welding, fracture density, and mineralogy vary as a function of stratigraphic position. Vertical variations in tuff properties were used to subdivide the Tshirege Member into mappable subunits that reflect localized emplacement temperature, thickness, gas content, and composition of the tuff deposits (Broxton and Reneau 1995, 049726; Lewis et al. 2002, 073785). Subunits of the Tshirege Member are described in Attachment 2 of "Compendium of Technical Reports Related to the Deep Groundwater Investigation for the RDX Project at Los Alamos National Laboratory" (LANL 2018, 602963). The Tshirege Member is 430 ft thick in well CdV-9-1(i). The base of the Tshirege Member is marked by the Tsankawi Pumice Bed, a 2-ft-thick stratified, fines-depleted fall deposit of gravel-sized vitric pumice and quartz and sanidine crystals.

Sedimentary deposits of the Cerro Toledo Formation are a diverse group of rocks that include extrusive volcanic domes, lava flows, tephras, and sedimentary rocks that record landscape evolution in the time interval between the Tshirege and Otowi Members of the Bandelier Tuff (Gardner et al. 2010, 204421).

The Cerro Toledo Formation at TA-16 is a well-stratified alluvial fan sequence deposited on partly eroded Otowi Member ash-flow tuffs on the west alluvial slope of the Española basin. The Cerro Toledo Formation is largely made up of beds of tuffaceous sandstone, siltstone, and ash and pumice falls, and locally includes dacitic gravel- and cobble-rich alluvial deposits eroded from the Tschicoma Formation exposed in the eastern Jemez Mountains. The Cerro Toledo Formation is 102 ft thick in well CdV-9-1(i), but its thickness varies greatly because of the channelized nature of the deposits. The Cerro Toledo Formation is an important component of a perched-intermediate groundwater zone in well R-26, near the Pajarito fault system.

The Otowi Member of the Bandelier Tuff is a thick sequence of nonwelded vitric ash-flow tuffs and thin beds of intercalated ash and pumice falls. The Otowi Member differs from the Tshirege Member notably in its generally lesser degree of welding compaction (Bailey et al. 1969, 021498). The unit is characterized by fully inflated vitric pumices whose supporting tubular structures have not collapsed as a result of welding. The pumices are supported by a matrix of poorly sorted ash, glass shards, broken pumice fragments, phenocrysts (primarily sanidine and quartz), and volcanic lithics. The sequential deposition of flow and fall deposits resulted in stratification of the unit on a regional scale. The Otowi Member is 298 ft thick in well CdV-9-1(i). The Guaje Pumice Bed is the basal fall deposit of the Otowi Member, and it was deposited atop the Puye Formation on the west alluvial slope of the Española basin. The base of the Otowi Member is marked by the Guaje Pumice Bed, a stratified, fines-depleted pumice fall deposit. The Guaje Pumice Bed ranges between 5 and 15 ft thick at TA-16. The Otowi Member is an important component of the perched-intermediate groundwater zones beneath Cañon de Valle in the vicinity of the 260 Outfall. Potential clay-silt soil horizons have been identified at the top of the underlying Puye Formation in wells CdV-16-4ip, R-25, and R-26 and may act as confining beds for perched-intermediate groundwater.

The Pliocene Puye Formation was deposited as broad, coalescing alluvial fans shed eastward from the Jemez Mountains volcanic field into the western Española basin (Griggs and Hem 1964, 092516; Bailey et al. 1969, 021498). The sources for these alluvial-fan deposits were overlapping dacite to low-silica rhyolite dome complexes of the Tschicoma Formation that were active in the eastern Jemez Mountains between about 3 and 5 Ma (Broxton et al. 2007, 106121). The complex lithologic character of the Puye Formation is discussed further in section 3.2. The Puye Formation is more than 1092 ft thick in well R-25, but the base of the unit was not penetrated by wells in the TA-16 area. The Puye Formation is an important component of the perched-intermediate and regional groundwater aquifer beneath Cañon de Valle in the vicinity of the 260 Outfall.

In the southern part of the TA-16 area, a thick lobe of Tschicoma dacite lavas originating in the mountain block to the west flowed eastward into the western part of the Española basin. These lava flows were subsequently down-faulted and buried by younger Puye alluvial fan deposits. These dacite lavas correlate to the dacite of Cerro Grande exposed in the mountain block to the west based on similarities in rock chemistry and petrography (Samuels et al. 2007, 204422).

Dacite lava is not present in areas of perched groundwater beneath Cañon de Valle, but it is a major component of the regional aquifer over a broad area in the southern part of TA-16, TA-11, and probably most, if not all, of TA-37 and TA-28. The dacite of Cerro Grande was partially penetrated in wells CdV-R-37-2, R-48, and R-58. Where penetrated by wells, the Cerro Grande dacite has two main facies, monolithologic flow breccias and massive, dense, flow-banded lavas. The Cerro Grande dacite is more than 400 ft thick in well R-48.

2.5 Site Hydrogeology

The hydrologic system in the watershed includes surface water, springs, alluvial groundwater, shallow bedrock and perched-intermediate groundwater, springs, and regional groundwater. These components of the hydrologic system are briefly described below and in more detail in section 3.2.

Water Canyon and its main tributary Cañon de Valle have their headwaters west of the Laboratory in the Sierra de los Valles within the Santa Fe National Forest. Surface water in Cañon de Valle is predominantly ephemeral and seasonally dependent on snowmelt and storm runoff. Only short reaches with perennial flow occur in Cañon de Valle, and these reaches are dependent on spring discharges. Alluvial groundwater in Cañon de Valle is recharged by stream flow and runoff from local precipitation and snowmelt runoff.

Perched groundwater occurs at both shallow (referred to as shallow-bedrock) and deep (referred to as perched-intermediate) levels of the vadose zone in the TA-16 area. Shallow bedrock groundwater zones occur at depths 200 ft in upper units of the Tshirege Member of the Bandelier Tuff, and they include springs that discharge into canyons and small zones of saturation in tuff that are penetrated by shallow wells. Perched-intermediate groundwater occurs at depths generally 600 ft in the lower part of the vadose zone, primarily in the Cerro Toledo Formation, the Otowi Member of the Bandelier Tuff, and Puye Formation. Groundwater in the two perched-intermediate zones is a mixture of mountain-block recharge (MBR) and mountain-front recharge (MFR). MBR occurs in the highlands west of the Pajarito fault zone and consists of diffuse subsurface infiltration of snow melt and surface water that percolates through the rock and recharges the regional aquifer. MFR consists of mountain overland flow (generally streamflow) that infiltrates at the mountain front and the adjacent basin.

The regional groundwater table beneath Cañon de Valle has an easterly sloping gradient that extends from an elevation of approximately 6600 ft at the Pajarito fault to approximately 5500 ft at the Rio Grande, over a distance of approximately 9.3 mi. Much of the 1100-ft decline in elevation occurs within the 1.3-mi distance between the Pajarito fault zone and well R-63. Recharge of the regional aquifer takes place largely in the Jemez Mountains west of the Pajarito fault zone; however, the presence of HE in some regional aquifer monitoring wells indicates that local infiltration at TA-16 contributes to recharge of the regional aquifer. A regional water table map is presented in Figure 2.5-1.

Los Alamos County maintains three well fields that tap the regional aquifer as part of the public water supply system: the Guaje, Otowi and Pajarito well fields. Within the three well fields there are 12 supply wells: 5 in Guaje (G-1A, G-2A, G-3A, G-4A, G-5A), 2 in Otowi (O-1 and O-4), and 5 in Pajarito (PM-1, PM-2, PM-3, PM-4, PM-5). These wells, with depths up to 3000 ft below ground surface (bgs), all draw water from the regional aquifer. According to the Los Alamos County Water Supply Plan, the regional aquifer is the only aquifer in the area capable of serving as a water supply—the perched-intermediate groundwater has limited beneficial use (Daniel B. Stephens & Associates Inc. 2018, 700540).

The Water Canyon and Cañon de Valle watershed is more than 1.5 mi from the nearest water-supply wells, PM-5, PM-4, and PM-2. (As discussed in section 3.2, the downgradient edge of RDX in regional aquifer is approximately 3 mi upgradient of the public water supply wells.) DOE voluntarily supplements the county's water quality monitoring program, collecting groundwater samples that are analyzed for HE. To date, HE has not been detected above NMED's tap water screening level in the public water supply wells.

2.6 Site History

2.6.1 TA-16 History

Early activities at TA-16 supported the development of the first implosion-type atomic bombs. The high explosives components of the implosion design were developed, manufactured, and tested at TA-16 during World War II. TA-16 was the principal site that manufactured HE castings and lenses to produce a means of detonating an explosive charge (McGehee et al. 2003, 700541).

Building 260, located on the north side of TA-16, has been used for processing and machining HE since 1951. Water is used to machine HE, which is slightly water soluble, and effluent from machining operations contains dissolved and entrained HE cuttings. At building 260, effluent treatment consists of routing the effluent to 13 settling sumps to recover any entrained HE cuttings. From 1951 to 1996, the water from these sumps was discharged to the 260 Outfall that drained into Cañon de Valle.

2.6.2 260 Outfall Operation

The 260 Outfall drainage channel consisted of the outfall, a former settling pond, and the upper and lower portions of the drainage channel leading to Cañon de Valle. From 1951 to 1996, the water from the building 260 sumps was discharged to the 260 Outfall, with millions of gallons discharged per year. Discharges from the 260 Outfall were greatest in the 1950s and then fell significantly, although they were sustained at low levels for more than 30 yr afterward (Gard and Newman 2005, 093651, p.19). There are limited data on the amounts of HE-containing discharge released from the 260 Outfall into Cañon de Valle between 1950 and 1996, when the outfall was decommissioned and remediation programs commenced.

Water containing HE and barium flowed from the sumps into the settling pond to capture entrained HE cuttings in the concrete trough and ultimately to the 260 Outfall, located 200 ft east of building 260. The outfall discharged into Cañon de Valle, providing a pathway for contaminants to enter the alluvial groundwater, vadose zone, and deeper groundwater (LANL 2003, 077965).

During the late 1970s, the 260 Outfall was permitted by the U.S. Environmental Protection Agency (EPA) to operate as EPA Outfall No. 05A056 under the Laboratory's National Pollutant Discharge Elimination System (NPDES) permit (EPA 1990, 012454). The last NPDES-permitting effort for the 260 Outfall occurred in 1994. The NPDES-permitted 260 Outfall was deactivated in November 1996. EPA officially removed it from the Laboratory's NPDES permit in January 1998. This waste stream is currently managed by pumping the sumps and treating the water at the TA-16 HE wastewater treatment plant.

Because of the historic discharge, soil in the 260 Outfall drainage channel was contaminated, primarily with HE and barium. The sumps and drain lines of this facility are designated as Solid Waste Management Unit (SWMU) 16-003(k), and the 260 Outfall and drainage are designated as SWMU 16-021(c), as defined in the Consent Order Appendix A. Because of the Laboratory's consolidation of SWMUs, these two SWMUs were collectively referred to as Consolidated Unit 16-021(c)-99.

The HE compounds RDX and HMX (octahydro-1,3,5,7-tetranitro-1,3,5,7-tetrazocine) and barium, associated with the 260 Outfall discharges have been detected in alluvial groundwater and springs (N3B 2018, 700089) RDX and HMX have also been detected in perched-intermediate groundwater (LANL 2003, 077965) and in the regional aquifer (LANL 2016, 601779), but elevated barium concentrations have not been detected in deeper groundwater.

Other contaminants associated with the 260 Outfall include TNT (2,4,6-trinitrotoluene), which is more sorptive (and therefore less mobile) than RDX and HMX (Her Majesty's Explosive), but TNT has not been detected in groundwater in recent years. A wide range of other contaminants, including low levels of volatile organic compounds (VOCs), metals, and HE byproducts and degradation products are also associated with 260 Outfall discharges.

The 260 Outfall is the primary source of HE that impacted groundwater at TA-16 (LANL 2011, 203711). The 260 Outfall released large quantities of contaminants, particularly RDX, at high concentrations and large volumes of water that provided a significant hydrologic driving force for infiltration of contaminants (LANL 2011, 203711; LANL 2012, 213573).

2.6.3 TA-16 RDX Source and Release History

Effluent from the machining of HE charges was produced at TA-16 over several decades, much of which was discharged at the surface through the 260 Outfall. Although other types of HE effluent, including HMX, TNT, and TATB (triaminotrinitrobenzene) were released at the outfall, the principal waste component was RDX.

RDX contaminant sources with the potential to impact groundwater were evaluated by the Laboratory and reported in "Technical Area 16 Well Network Evaluation and Recommendations" (LANL 2012, 213573). These sources include the losing reach of Cañon de Valle downstream from the 260 Outfall, the former retention pond at the 260 Outfall, other HE retention ponds, HE process building outfalls and drainages, contaminated alluvial aquifers, and large surface MDAs. The sources were grouped and ranked by their potential to impact groundwater. A summary of the sources locations and their prioritization are shown on Figure 2.6-1 and summarized in Table 2.6-1. Sources ranked as having high potential for groundwater impact are known to have received large quantities of contaminants, particularly RDX and other HE, and to have received large volumes of water that provide a significant hydrologic driving force for infiltration of contaminants into perched-intermediate zones at TA-16.

Sources with high potential for groundwater impact included the most highly contaminated reach in Cañon de Valle and the 260 Outfall pond and drainage. These were hypothesized to be the principal sources for contamination in the perched-intermediate groundwater located at a depth of >600 ft beneath Cañon de Valle and the northern portion of TA-16 (LANL 2011, 207069).

Sources categorized as having medium potential for groundwater impact have known contaminants in water and received large volumes of water, providing a hydrologic driving force for contaminant infiltration into the vadose zone (LANL 2011, 207069). These sites are not known to have contributed to contamination in the perched-intermediate groundwater at TA-16 but are still of potential concern. Sources with medium potential impact included the 30s Line and 90s Line HE retention ponds (LANL 2010, 108279); the losing reach within Fishladder Canyon (LANL 2009, 105061.17), particularly downgradient of the TA-16 Burning Ground; and the westernmost losing reach within S-Site/Martin Spring Canyon (LANL 2011, 207069).

Sources with low potential for groundwater impact either lack known large contaminant concentrations (particularly RDX) or lack large volumes of water to provide a hydrologic driving force to promote contaminant infiltration. The lower-priority sources included the alluvial aquifer in Water Canyon, the TA-16-430 drainage, the TA-16-460 drainage, the HE retention pond at V-Site, MDA P and the TA-16 Burning Ground, MDA R, K-Site, and the Zia shops drum storage area.

The 260 Outfall channel runs approximately 600 ft from the outfall to the bottom of Cañon de Valle (LANL 2003, 077965). Levels of RDX ranged to >10 wt%, and total HE was highly elevated in the

drainage from the 260 Outfall to Cañon de Valle (LANL 1993, 020946; LANL 1996, 055077; LANL 1998, 059891; LANL 2000, 064355; LANL 2002, 073706). These levels were 1-to-2 orders of magnitude higher than the highest RDX concentrations detected at other SWMUs within the watershed, and the extent of high-level soil contamination of RDX at the 260 Outfall was 1 to 2 orders of magnitude larger than other sites within the watershed.

MDA P is an approximately 9.25-acre site located along the southern slope of Cañon de Valle approximately 1800 ft east of the 260 Outfall area. MDA P contained wastes from the synthesis, processing, and testing of HE; residues from the burning of HE-contaminated equipment; and construction debris. HE waste-disposal activities at this site began in the early 1950s and ceased in 1984. MDA P underwent a clean closure under RCRA in which approximately 55,000 yd³ of soil and debris was removed (LANL 2005, 092251). Closure was approved by NMED and no further actions are needed (NMED 2005, 093247).

MDA R (SWMU 16-019) is an approximately 2.25-acre site located north of the 260 Outfall area along the mesa top and edge and extends onto the southern slope of Cañon de Valle. MDA R was constructed in the mid-1940s and used as a burning ground and disposal area for waste explosives and possibly other debris. Potential contaminants at MDA R include HE, HE byproducts, and metals (particularly barium). Use of this site was discontinued in the early 1950s (LANL 2003, 077965, p. 1-10). Soil removal and site investigations were conducted at MDA R following the Cerro Grande fire (LANL 2001, 069971).

SWMUs at the TA-16 Burning Ground are 16-005(g), 16-006(e), 16-010(a,b,c,d,e,f,g,h,i,j,k,l,m,n), 16-016(c), and 16-028(a). These SWMUs are located on the mesa in the northeast corner of TA-16 within the Fishladder Canyon watershed. The burning ground was constructed in 1951 for HE waste treatment and disposal. Over the years, hundreds of thousands of pounds of HE and HE-containing waste material has been burned at this location. The remaining noncombustible material was subsequently placed either in MDA P, north of the Burning Ground (through 1984), or taken to TA-54 for disposal (1984 to present). A barium nitrate pile was located at the TA-16 Burning Ground for many years. SWMU 16-010(b) underwent RCRA clean closure, and SWMUs 16-006(e), 16-010(a), 16-016(c) underwent a voluntary corrective action (VCA) concurrently with the MDA P clean closure. The closure and VCA were approved by NMED (2005, 093247) and no further actions are needed.

Sites associated with the 30s and 90s Line Ponds are SWMUs 16-007(a), 16-008(a), 16-017(a,b,c,d,e)-99, 16-024(d,e), 16-025(e,f), 16-026(m,n,o,p), and 16-029(k,l,s,u) and Area of Concern (AOC) C-16-007. These sites consist of former HE process and storage buildings and associated sumps, drain lines, outfalls, and settling ponds. Cleanup of the 30s and 90s Line Ponds was completed in 2009 and no further actions are needed (LANL 2010, 108279).

2.6.4 Other Potential Sources of RDX at TA-08 and TA-09

TA-08 (Anchor West) and TA-09 (Anchor East) are located in the western part of the Laboratory within the drainage basins of Pajarito and Twomile Canyons and the south fork of Pajarito Canyon. These TAs contain some of the earliest Manhattan Project sites at the Laboratory and are considered potential sources of HE observed in regional aquifer wells in the RDX investigation area. SWMUs and AOCs located in these TAs include firing sites, outfalls, septic tanks, sumps, storage areas, an incinerator ash pond, and surface and subsurface disposal areas.

At TA-09, effluent release volumes at TA-09 outfalls totaled about 4.7 million gal./yr, which was a greater volume than the 2.5 million gal./yr released from TA-16 260 outfall (DOE 1995, 700539); however, the TA-09 site was primarily a research laboratory site that produced small amounts of RDX compared to the production facility at building 260. Also, environmental media in the vicinity of TA-09, including springs,

alluvial wells, and sediments, show relatively low concentrations of HE compounds, suggesting TA-09 was a secondary source of HE compared to TA-16. Consequently, TA-09 is unlikely to be an important source of RDX observed in regional aquifer.

Monitoring of RDX concentrations in groundwater, spring, and surface water at TA-08 and TA-09 are prescribed in the Consolidated Unit 16-021(c)-99 long-term monitoring and maintenance program and the IFGMP. Spring samples from Bulldog Spring show RDX concentrations ranging from 1.8 to 7.7 µg/L. Base-flow samples collected in Pajarito Canyon below the confluences of South and North Anchor East Basin contain concentrations of RDX ranging from 0.09 to 4.6 µg/L. RDX is detected in base-flow samples at concentrations ranging from 0.17 to 0.20 µg/L collected above the confluence with Twomile Canyon. In groundwater HE compounds have not been consistently detected at wells PCO-1, PCO-2, PCO-3, 18-BG-1, 18-MW-8, 18-MW-9, 18-MW-11, and 18-MW-18; they have not been detected in the newly installed alluvial wells PCAO-5, PCAO-6, PCAO-7a, PCAO-7b2, PCAO-7c, PCAO-8, and PCAO-9.

2.7 Early Investigations and Source Removal

2.7.1 Phase I RFI

In 1995, the Laboratory performed a Phase I RCRA Facility Investigation (RFI) pursuant to its Hazardous Waste Facility Permit. The RFI Report (LANL 1996, 055077) for TA-16: PRS 16-021(c) and 16-003(k) was submitted to NMED on September 23, 1996, and approved by NMED on January 20, 1998. The Phase I RFI site characterization concentrated on the drainage channel and its intersection with Cañon de Valle, including alluvial sediment, surface water, and groundwater. The Phase I data showed widespread HE contamination at SWMU 16-021(c)-99, extending from the 260 Outfall discharge point down to the sediment and waters of Cañon de Valle. NMED approved the Phase I RFI Report in March 1998 (NMED 1998, 093664).

2.7.2 Phase II RFI

A Phase II RFI was performed in 1996 and 1997 to further characterize the site and determine extent of contamination. The Phase II RFI report (LANL 1998, 059891) further delineated contamination in tuff surge beds beneath the drainage channel and in Cañon de Valle sediment and waters. The goal of a Phase II RFI was the collection of sufficient data to characterize the site and to quantify the extent of contamination for three purposes: (1) developing a physical site conceptual model, (2) performing a site-specific risk assessment, and (3) initiating a corrective measures study (CMS) process.

The Phase II RFI included the sampling of surface and near-surface material within the drainage channel and the sampling of 13 boreholes drilled to depths between 17 and 115 ft in and near the drainage. The Phase II RFI also included extensive field screening for RDX and TNT using immunoassay methods, as well as sampling for other chemicals. A risk characterization was also performed. NMED approved the report in September 1999 (NMED 1999, 093666).

Results of the outfall and drainage area investigation indicated high levels of HE and barium within the outfall and drainage, from the surface to the soil-tuff interface. Phase II surface sampling confirmed previous results by demonstrating that surface contamination did not extend laterally beyond the reasonably well-defined drainage. Downgradient within the drainage, concentrations of contaminants (barium, HMX, RDX, and TNT) decreased rapidly. Subsurface sampling in the outfall and drainage indicated that concentrations also decrease rapidly below the soil/tuff interface; however, there was subsurface contamination—up to 1000 mg/kg of HE in tuff—within the uppermost tuff unit beneath the upper part of the drainage, including the former pond. Higher levels, a total of almost 1 wt% HE, were

reported in a sample of saturated material from a surge bed that was encountered at a depth of about 16 ft beneath the source area. Below the level of this surge bed, HE is observed only sporadically and at much lower concentrations (typically <5 mg/kg). While HE and barium were the principal contaminants at the TA-16-260 outfall, several other metals—including cadmium, chromium, copper, lead, nickel, vanadium, and zinc—were consistently observed above background levels in the drainage.

Organic compounds, particularly anthracene and phthalates, were also detected in several samples. Surface water and sediment samples were collected in Cañon de Valle. There were elevated concentrations of barium, HMX, and RDX in the canyon sediments and waters.

The proposed recommendations from the Phase II report were

- perform a source removal IM to remove high levels of contamination in the outfall and drainage;
- collect additional data to improve the hydrogeologic conceptual model, perform a site-specific risk assessment, and make conclusions as to the impact on deeper groundwater; and
- continue with the CMS process to evaluate the appropriate alternatives for water/sediment remediation and continued monitoring of the watershed system.

These conclusions led the Laboratory to conduct an IM to address shallow soils and sediment, prepare a Phase III RFI, and submit a CMS, with NMED selecting a final remedy for shallow soils and shallow bedrock groundwater.

2.7.3 Source Removal Interim Measure

During 2000–2001 IM activities, RDX concentrations in soil exceeding 100 mg/kg were targeted for removal from the settling pond area. More than 1300 yd³ of contaminated soil was removed (LANL 2003, 077965), some of the material with HE concentrations of 2 wt% (20,000 mg/kg) or more. In the IM report (LANL 2002, 073706), the HE compounds removed were estimated at 18,740 lb, or 90% of the total. The remaining part was estimated at 1435 lb based on post-removal analytical data, high-performance liquid chromatography screening data, and estimates of volume and bulk density.

Additionally, the 1435 lb estimate included HE present in a surge bed located below the settling pond area and the upper and lower sections of the drainage channel (LANL 2002, 073706). As described below, the source of HE contained in the surge bed was stabilized during the 2009-2010 corrective measures.

2.7.4 Phase III RFI

The Phase III RFI site characterization and Phase III RFI report (LANL 2003, 077965) included further analysis of shallow water and sediment data collected since the Phase II RFI, a study of spring dynamics, a geomorphic alluvial sediment study, geophysical studies, and baseline risk assessments for the outfall source area and for selected reaches of Cañon de Valle and Martin Spring Canyon. In addition, a baseline ecological risk assessment was performed for Cañon de Valle. NMED approved the Phase III RFI report in June 2004 (NMED 2004, 093248).

The Phase III RFI was conducted from 1999 to 2002 and was part of the CMS. The CMS plan divided the evaluation of transport pathways and the selection of remedial alternatives into an alluvial groundwater CMS and a regional groundwater CMS. The alluvial groundwater CMS focused on the Cañon de Valle source area, alluvial groundwater system, and the subsurface tuff and saturated system, including canyon springs. The regional groundwater CMS for SWMU 16-021(c)-99 was a separate investigation into the

extent of contamination in the perched-intermediate zone and the regional aquifer. One important goal of the Phase III RFI was to investigate, and incorporate into the conceptual model, the hydrogeologic and contaminant transport dynamics of the Cañon de Valle and Martin Springs alluvial and subsurface groundwater systems.

The conclusions from the RFI Phase III report were as follows:

- Although the volume of the residual soil within the former outfall source area is $<100 \text{ yd}^3$ (based on field observations), the soil contains elevated concentrations of HE and barium that could be mobilized by stormwater runoff.
- The potential risk for residual contamination in the former outfall source area soil is marginally above NMED's target risk levels for reasonable maximum exposure (RME) for the environmental worker (cancer risk) and the construction worker (noncancer hazard) and may be within EPA's target risk range; potential risks for central tendency exposures and other RMEs for the receptors were below these NMED target levels.
- Sediments in Cañon de Valle and Martin Spring Canyon represent a widely dispersed secondary source for HE and barium that is potentially mobilized by surface water and alluvial groundwater. Moreover, the perennial reach of Cañon de Valle alluvial groundwater provides a high potential for subsequent infiltration of mobilized contaminants.
- The drought has influenced the hydrogeology of the area by reducing mesa vadose zone groundwater recharge, reducing canyon alluvium saturated thickness, and causing Sanitation Wastewater Systems Consolidation (SWSC) Spring and Martin Spring to dry up.
- Contaminant transport in the mesa vadose zone is dominated by a fracture or surge bed flow regime, of which contaminated springs are a known manifestation. With the IM source removal, a substantial source for this contamination is gone, though reductions in spring contaminant concentrations are not yet evident. More wells were planned in both the mesa vadose zone groundwater and the regional aquifer to further assess the importance of these pathways.
- Cañon de Valle and Martin Spring Canyon surface water, groundwater, springs, and sediment do not pose a potential unacceptable human health risk to the trail user (i.e., potential risks and hazards are below 10^{-5} and hazard index of 1.0 for all exposures).
- The ecological risk assessment conducted in Cañon de Valle found that COPCs have no adverse effects on terrestrial receptors and have negligible adverse effects on aquatic receptors.

In November 2003, the Laboratory issued a CMS report for the SWMU 16-021(c)-99 alluvial system. The report was a companion document to the Phase III RFI report and relied heavily on the understanding of site hydrogeology and contaminant behavior outlined in the Phase III RFI report. This CMS report proposed corrective measures and associated monitoring programs for remediating SWMU 16-021 (c)-99 surface and shallow subsurface soils within the outfall source area, as well as alluvial sediments, surface water, alluvial groundwater, and springs located within Cañon de Valle and Martin Spring Canyon. Regional groundwater and perched-intermediate groundwater were not addressed in this report but they were addressed by a second CMS focusing on these areas.

The remediation systems were detailed in the CMS report (LANL 2003, 085531) and approved by NMED in 2006 (NMED 2006, 095631). The remediation activities consisted of

- installing a pilot permeable reactive barrier (PRB) for treatment of HE and barium;

- removing residual soil exceeding risk-based media cleanup standards (MCSs) in the 260 Outfall drainage channel and removing the concrete outfall trough;
- maintaining an existing low-permeability cap on the former settling pond within the 260 Outfall drainage channel;
- grouting a contaminated surge bed within tuff beneath a former settling pond along the drainage channel;
- installing a carbon filter for the treatment of spring water at Burning Ground Spring in Cañon de Valle and modifying the existing carbon filter at Martin Spring in Martin Spring Canyon; and
- sampling soil for silver in the SWSC cut of Cañon de Valle. Installing a carbon filter at SWSC Spring was proposed as part of the CMS, but this spring has been dry since 2001.

2.7.5 2009–2010 CMI

The objective of the 2009–2010 CMI was to remediate HE and other contaminants (i.e., RDX; TNT; and barium) detected at the 260 Outfall, including a concrete trough, former settling pond, and outfall drainage channel, and in the alluvial systems of Cañon de Valle and Martin Spring Canyon as described in the 2007 CMI plan for Consolidated Unit 16-021(c)-99 (LANL 2007, 098192). The CMI was conducted in accordance with the approved CMI plan (LANL 2007, 098192; NMED 2007, 098449).

The 2009–2010 CMI remediation activities included

- removing the concrete trough outfall adjacent to building 16-260 at the 260 Outfall channel,
- removing approximately 40 yd³ of soil and sediment within the former settling pond within the 260 Outfall drainage channel,
- replacing a low-permeability cap on the former settling pond,
- removing soil and tuff from the 260 Outfall drainage channel,
- sampling soil in the SWSC Cut of Cañon de Valle,
- installing surge bed injection grouting within the former settling pond at the 260 Outfall channel,
- installing carbon filter treatment systems of spring waters at SWSC and Burning Ground Springs in Cañon de Valle and modifying the existing carbon filter at Martin Spring in Martin Spring Canyon, and
- installing a pilot PRB for treatment of HE and barium in Cañon de Valle.

In March 2010, the Laboratory submitted to NMED the “Summary Report for the Corrective Measures Implementation at Consolidated Unit 16-021(c)-99” (LANL 2010, 108868) and the “Addendum to the Summary Report for the Corrective Measures Implementation at Consolidated Unit 16-021(c)-99” (LANL 2010, 108868) describing the corrective action performed pursuant to the 2007 CMI Plan.

Between June 26 and August 3, 2011, the Las Conchas fire consumed more than 156,000 acres across the Santa Fe National Forest in Sandoval, Los Alamos, and Rio Arriba counties. Located in these counties and impacted by the fire were Santa Clara Pueblo, Jemez Pueblo, Cochiti Pueblo, Santo Domingo Pueblo, Bandelier National Monument, Valles Caldera National Preserve, and state and private land holdings (LANL 2011, 206408). The Cañon de Valle watershed and large areas upgradient of the PRB and 260 Outfall sustained moderate to severe fire damage. While Laboratory property, the PRB, and

the 260 Outfall were not directly burned in the Las Conchas fire, the subsequent burn scar left the watershed vulnerable to flash flooding.

Between July 28 and August 21, 2011, a series of storms produced damaging floods in Cañon de Valle watershed, resulting in flooding in Cañon de Valle that significantly damaged many parts of the PRB, rendering the treatment unit inoperable. Floodwater, sediment, and ash infiltrated the PRB vessel chambers, significant head cutting occurred in the Cañon de Valle channel immediately east (downgradient) of the PRB cutoff wall, and piping and sampling components of the PRB sustained considerable damage. Additionally, the severe flooding in Cañon de Valle destroyed a number of alluvial wells in Cañon de Valle and caused considerable additional damage to 8 of the 20 PRB monitoring wells and piezometers (LANL 2011, 206408).

In response to the damage, NMED directed the Laboratory to prepare a report evaluating issues relevant to the CMI and proposed an approach to resolving these issues. The “Evaluation Report for Surface Corrective Measures Implementation Closure, Consolidated Unit 16-021(c)-99” was submitted to NMED on September 29, 2016 (LANL 2016, 601837).

The CMI evaluation report included

- recommendations for removal of the damaged PRB and associated debris in Cañon de Valle;
- plans to plug and abandon damaged PRB wells or wells not being used;
- evaluation of the alluvial groundwater monitoring network in Cañon de Valle alluvium to be used for long-term monitoring, including the addition of the PRB alluvial seep and a replacement alluvial monitoring well (CdV-16-02657r); and
- in-depth review of RDX trends in Cañon de Valle and Martin Spring Canyon springs and alluvium and recommendations for removing the treatment units and restoring the sites because of declining trends in RDX concentrations in alluvial wells.

NMED approved the CMI evaluation report on October 21, 2016 (NMED 2016, 601914), and the Laboratory implemented the recommendations from the report during the period from November 2016 to June 2017. The damaged PRB and debris were removed; the PRB monitoring wells were plugged and abandoned; the carbon-filtration units at SWSC, Burning Ground, and Martin Springs were removed and the springs restored; and replacement alluvial monitoring well CdV-16-02657r was installed.

In September 2017, the Laboratory submitted the “Remedy Completion Report for Corrective Measures Implementation at Consolidated Unit 16-021(c)-99” (LANL 2017, 098192). NMED approved the report on November 27, 2017 (NMED 2017, 602758). This report summarized the activities conducted to close out the CMI. In addition, the report provided an overview of the CMI activities conducted in 2009–2010 at Consolidated Unit 16-021(c)-99, in addition to a conceptual model of the fate and transport of RDX and barium, the primary contaminants in shallow groundwater in Cañon de Valle. Furthermore, this report summarized the performance of the pilot PRB during its brief operational period from 2010 to 2011 and evaluated whether additional PRBs were necessary to remove residual RDX and barium from shallow groundwater in Cañon de Valle and Martin Spring Canyons. The report concluded that given RDX concentrations in alluvial groundwater are at or near the groundwater screening levels. Given that the elevated barium concentrations do not threaten deeper groundwater because of barium’s sorptive geochemical characteristics, additional PRBs are not needed in either.

Completion of these activities fulfilled the requirements of the CMI work plan for Consolidated Unit 16-021(c)-99 (LANL 2007, 098192) and the evaluation report for the surface CMI closure (LANL 2016, 601837). Because the Laboratory considered the CMI remedy completed; it recommended

that monitoring related to Consolidated Unit 16-021(c)-99 including monitoring of alluvial groundwater, base flow, and springs, transition to long-term monitoring. The results from the long-term monitoring and cap inspection is reported annually to NMED in the "Long-Term Monitoring and Maintenance Plan for the Corrective Measures Implementation at Consolidated Unit 16-021(c)-99."

2.8 2006 Intermediate and Regional Groundwater Investigation and the 2007 CME

The completion of the CMI for shallow soil, sediment, and groundwater allowed activities to focus on RDX in perched-intermediate and regional groundwater. Per the 2005 Consent Order, the Laboratory was required to submit to NMED an investigation report for perched-intermediate and regional groundwater and upon approval prepare a CMS report.

The principal goal of the investigation was to determine the extent of RDX in perched-intermediate and regional groundwater resulting from operation of the former 260 Outfall. The secondary goals of the investigation were (1) to determine the rate at which RDX is moving downgradient toward the Pajarito well field or other potential exposure points, (2) to investigate the directions of groundwater flow and the hydrologic gradients within the intermediate and regional zones at TA-16, and (3) to identify COPCs for the TA-16 regional groundwater CME.

An investigation of intermediate and regional groundwater was conducted (LANL 2006, 093798). In addition, the Laboratory conducted an evaluation of area-monitoring well screens to assess the validity of intermediate and regional groundwater analytical data (LANL 2007, 095787). These reports reached the following conclusions.

- The analytical results for perched-intermediate groundwater samples showed concentrations (<80 $\mu\text{g/L}$) of HE within the area defined by wells R-25, CdV-16-1(i), and CdV-16-2(i)r. In CdV-16-1(i) and R-25, RDX exceeded the EPA Region 6 tap water screening limit of 0.61 $\mu\text{g/L}$ (EPA 2003, 093662). (Note: In 2006, RDX concentrations were screened against EPA's tap water screening level using a 10^{-6} target risk. Currently, NMED uses a target risk of 10^{-5} , resulting in a tap water screening level of 9.66 $\mu\text{g/L}$). For regional groundwater samples, analytical results from R-25 showed RDX and TNT concentrations exceeding the EPA Region 6 tap water screening limits (EPA 2003, 093662). The results from other wells located to the east of (downgradient of) R-25 showed that RDX was detected once in R-19 during 2000 but at a concentration less than the tap water screening limit. RDX was detected in well R-18 at very low levels (1 $\mu\text{g/L}$).
- The wells evaluated in these reports include downgradient regional groundwater wells CdV-R-15-3, CdV-R-37-2, R-17, R-18, R-19, R-25, and R-27; downgradient intermediate wells/BHs CdV-16-1(i), CdV-16-2(i)r, CdV-16-3(i); and upgradient well R-26. At least 18 of 26 well screens provided reliable and representative data for RDX, which does not degrade easily in the environment.
- Hydrologic evaluations of wells in the monitoring network were also completed as part of the well screen evaluation (LANL 2007, 095787). The majority of the well screens provides reliable head (pressure) data.
- Based on a compilation of existing well data, it was determined that the average permeability of the intermediate and regional aquifers at TA-16 is approximately 3.2×10^{-9} cm^2 . Extreme local variability in permeability, however, is present, as demonstrated by collocated monitoring wells CdV-16-2(i) and CdV-16-2(i)r, the former of which was dry and was replaced by CdV-16-2(i)r.
- Perched-intermediate groundwater is likely a groundwater mound recharge feature associated with Cañon de Valle, with hydraulic heads in existing wells [CdV-16-1(i), R-25 Screen 2, and

CdV-16-2(i)r], indicating local groundwater-flow components both laterally (to the south) and to the east. Presumably, local lateral flow occurs to the north also; however, no monitoring wells are located in sufficient proximity in that direction.

- The presence of productive fractures in both intermediate-zone well screens installed [CdV-16-1(i) and R-25 Screen 2] within the Bandelier Tuff of intermediate groundwater suggests a significant fracture density within this horizon. If this is the case, vertical groundwater and contaminant travel times through this zone may be relatively rapid.

The 2006 Investigation Report compared investigation results to standards and screening levels and identified COPCs for the regional groundwater. As a first step, these COPCs were identified by screening groundwater analytical data against New Mexico Water Quality Control Commission (NMWQCC) standards (20 NMAC 6.2.3103 Parts A and B) and EPA MCLs (EPA 2003, 093662). If neither of these standards existed for a chemical, the EPA Region 6 tap water screening limit (EPA 2005, 091002) was used. If that was not available, the EPA Region 9 tap water screening limit was used (EPA 2004, 093663). After screening the analytical results, the list of chemicals was evaluated with respect to (1) prevalence of detection, (2) which ones were detected in an upgradient well (R-26), and (3) which ones were part of the alluvial system. Using this process, it was concluded that RDX and TNT were identified as COPCs for intermediate and regional groundwater (LANL 2006, 093798).

Upon completion of the 2006 investigation and in accordance with the 2005 Consent Order, the Laboratory prepared a CME. The CME proposed MCSs for groundwater, presented monitoring points, evaluated remediation technologies, provided corrective measure alternatives, and recommended preferred alternatives. The CME was based on a previous investigation of perched-intermediate and regional groundwater, which identified the COPCs as RDX and TNT. The investigation concluded that groundwater contamination does not pose an imminent threat to public water supply wells located approximately 3 mi to the east.

NMED subsequently issued a NOD for the CME in April 2008 (NMED 2008, 101311). In the NOD, NMED required the Laboratory to conduct additional characterization to assess the extent of contamination in perched-intermediate groundwater and in the regional aquifer, and to further evaluate the feasibility of the remedial alternatives proposed in the CME based on their assessment that insufficient information was available to determine whether the Laboratory's proposed actions were appropriate and protective.

Specifically, NMED requested in the NOD that the Laboratory develop a supplemental investigation work plan to

- characterize the extent of the contaminant plume in the perched-intermediate zone;
- characterize the extent of contaminant plume in the regional aquifer;
- characterize the hydrogeologic properties in the regional aquifer;
- characterize the hydrogeologic and hydrogeochemical properties in the perched-intermediate zone;
- determine HE degradation rates;
- provide recommendations for additional monitoring wells;
- provide recommendations for the replacement of monitoring wells unsuitable for the well network;
- collect site-specific data for use in evaluating the feasibility of remedy implementation for remedial alternatives; and

- propose actions to reduce uncertainties associated with the conceptual model, including uncertainties related to infiltration rates, groundwater travel times, and the contaminant source.

2.9 Post 2007 CME Supplemental Investigations

In response to NMED's 2008 NOD, the Laboratory developed the "Supplemental Investigation Work Plan for Intermediate and Regional Groundwater at Consolidated Unit 16-021(c)-99" (LANL 2008, 103165). In this document, the Laboratory proposed additional characterization activities to address uncertainties in the hydrogeologic conceptual model at TA-16. These activities included installing additional perched-intermediate and regional groundwater monitoring wells, performing additional groundwater monitoring, and conducting single-well aquifer tests to further characterize hydraulics of the perched-intermediate and the regional aquifer. To address hydrogeologic uncertainties, subsequent work plans were submitted, proposing multiwell aquifer tests and cross-hole tracer tests (LANL 2012, 210352; LANL 2015, 600535; LANL 2015, 600686).

Activities subsequently completed include

- conducting an electrical resistivity geophysical survey to map the electrical structure of the vadose zone in the vicinity of Cañon de Valle (LANL 2014, 259157);
- installation and monitoring of perched-intermediate monitoring wells R-25b, R-25c (dry), R-47i, R-63i, CdV-9-1(i), and CdV-16-4ip;
- installation and monitoring of regional monitoring wells R-48, R-58, R-68, and R-69;
- reconfiguration of wells CdV-R-37-2 and CdV-R-15-3 from Westbay sampling systems to single-screened wells with purgeable sampling systems;
- conducting short-duration aquifer tests in new monitoring wells;
- conducting extended duration aquifer tests at CdV-16-4ip in 2011 and 2014;
- deploying groundwater tracers in perched-intermediate well CdV-9-1(i) with two piezometers (PZs), and in monitoring wells R-25b and CdV-16-1(i), and performing subsequent sampling for tracers in monitoring wells near tracer-injection points; and
- conducting extended-duration (3-d) cross-hole aquifer tests using CdV-9-1(i), CdV-16-4ip, and CdV-16-1(i) as pumping locations and monitoring the effects in surrounding wells.

In 2012, the Laboratory conducted an evaluation of the TA-16 well network to (1) evaluate its adequacy to support the selection of corrective action alternatives for a future CME, (2) support ongoing investigations in the area, and (3) detect potential contaminants upgradient of water supply wells (LANL 2012, 213573). The network evaluation resulted in recommendations to (1) convert several multiscreen wells to single-screen wells to improve their reliability, (2) install a monitoring well in the perched-intermediate zone north of Cañon de Valle, and (3) install two additional monitoring wells in the regional aquifer to characterize contaminant flow paths and to monitor for contaminants. NMED approved the TA-16 well network evaluation with modifications in June 2012 (NMED 2012, 520747).

2.9.1 2014 Direct Current Resistivity Survey of Cañon de Valle

A direct-current (DC) electrical resistivity geophysical survey collected six lines of electrical resistivity within and next to Cañon de Valle in 2014 (LANL 2014, 600004). The work was performed according to the "Work Plan for Direct Current Resistivity Profiling in Cañon de Valle" (LANL 2012, 215111). Three electrical lines were run parallel to the canyon, and three lines were run perpendicular to the canyon to

help tie resistivity features together. A total of 27,848 ft of electrical resistivity data points were collected in the survey. The investigation included acquiring, modeling (in both two- and three-dimensions), and interpreting six lines of electrical resistivity within and next to Cañon de Valle. Three of the resistivity lines (Lines 3, 4, and 5) also acquired induced-polarization (IP) measurements to test chargeability effects of the different lithological units. The IP was not part of the original scope but was added during the investigation to enhance understanding of the subsurface. HydroGeophysics, Inc. (HGI) conducted this survey in May and June 2014.

The main objective of the direct-current (DC) resistivity survey was to map the electrical structure of the vadose zone in the vicinity of Cañon de Valle (LANL 2012, 215111). Of particular interest was the identification of low resistivity regions indicative of increased moisture content, clay-rich zones associated with groundwater pathways, changes in geologic lithologies, or perched water. The primary goals included the following:

- Assess the relative importance of surface water infiltration below mesa tops versus canyon floors.
- Evaluate Cañon de Valle as an important infiltration pathway and determine the eastern extent of infiltration.
- Determine if perched-intermediate groundwater is likely to be found north of Cañon de Valle based on the deep electrical structure of the vadose zone.
- Identify other low resistivity features that may indicate groundwater pathways (e.g., vertical infiltration zones and faults) or perching horizons (e.g., bedding.)
- Evaluate the location of a new perched-intermediate groundwater zone monitoring well CdV-9-1(i) proposed north of Cañon de Valle.

Results of the DC resistivity survey include the following:

- The vadose zone exhibits a layered electrical structure. Mesa-top alluvium and weathered Qbt 4 of the Tshirege Member form a low resistivity surface layer that is relatively thin and has a horizontal structure. The remaining subunits of the Tshirege Member are highly resistive. The Otowi Member and Puye Formation are characterized by low resistivity, and the Puye Formation is less resistive than the units above it.
- The electrical line collected along the axis of Cañon de Valle showed that the tuffs beneath the canyon floor, including normally resistive Tshirege tuffs, have low resistivity west of MDA P. Similar results were obtained in a smaller scale resistivity survey conducted in Cañon de Valle by HGI in 2001. The similar results increase the confidence in the data acquired in both surveys.
- Vertical low resistivity features are associated with several of the mapped faults in the area.
- Vertical low resistivity features are associated with a few small mesa-top drainages and may indicate the presence of local infiltration pathways.
- The attempt to determine whether perched-intermediate groundwater is likely to be found north of Cañon de Valle was inconclusive based on the DC resistivity survey.
- The spatial resolution of the resistivity survey decreases with increasing depth and it was not possible to resolve lower vadose zone features of hydrogeological interest such as perched-intermediate groundwater zones or potential perching horizons.
- Infrastructure affected the resistivity data where cables traversed or passed near buried pipelines, overhead power lines, and wells. Steps were taken to eliminate the infrastructure's influence, specifically by removing data from electrodes near it. These steps had limited success.

2.9.2 Post 2007 Monitoring Well Installations

The Laboratory developed the “Supplemental Investigation Work Plan for Intermediate and Regional Groundwater at Consolidated Unit 16-021(c)-99” (LANL 2008, 103165) in response to NMED’s 2008 NOD. In this work plan, the Laboratory proposed additional characterization activities to address uncertainties in the hydrogeologic conceptual model at TA-16. These activities included installing additional perched-intermediate and regional groundwater monitoring wells. The wells installed after the 2008 NOD included perched-intermediate wells R-25b, R-25c, R 47i, R 63i, CdV-9-1(i), and CdV-16-4ip and regional wells R-48, R-58, R-68, and R-69. The work plan also proposed reconfiguration of wells CdV-R-37-2 and CdV-R-15-3 from Westbay sampling systems to single-screened wells with purgeable sampling systems. Each well’s attributes are summarized below, with well completion diagrams provided in Appendix B. Water quality data collected from each well is discussed in section 3.

Well R-25b

Well R-25b is a single-screen perched-intermediate monitoring well installed in October 2008 at TA-16 on the south rim of Cañon de Valle (Figure 1.0-3) (LANL 2017, 602539). Well installation was performed in accordance with the “Drilling Work Plan for Intermediate Aquifer Well R-25b” (LANL 2007, 098121) that was approved by NMED (NMED 2007, 098996). Details are presented on the drilling, installation and testing of R-25b in “Completion Report for Well R-25b, Revision 1” (LANL 2008, 105018). The well screen was designed to monitor the upper part of perched-intermediate groundwater downgradient of HE release sites at TA-16. Well R-25b replaces well R-25 screen 1 that was impacted by repair activities to R-25 screen 3 (Broxton et al. 2002, 072640).

The well borehole was drilled to a total depth of 786 ft bgs. A monitoring well was installed with the well screen placed between 750 to 770.8 ft bgs within the Otowi Member of the Bandelier Tuff. The depth to perched water in the completed well was 759.1 ft bgs.

Well R-25c

Well R-25c is a single-screen perched-intermediate monitoring well installed in September 2008 at TA-16 on the south rim of Cañon de Valle as described in the “Completion Report for Well R-25c” (LANL 2008, 103408). Well installation was performed in accordance with the “Drilling Work Plan for Intermediate Aquifer Well R-25c” (LANL 2008, 100696) that was approved by NMED (NMED 2008, 100575). The well screen was designed to monitor the perched-intermediate groundwater downgradient of HE release sites at TA-16. Well R-25c was intended to replace well R-25 screen 3 that was damaged during construction of well R-25 (Broxton et al. 2002, 072640).

The presence of perched-intermediate groundwater was detected at approximately 848 ft bgs near the Guaje Pumice Bed-Puye Formation contact. A water level of 787 ft bgs was measured in the borehole when the drilling was halted at 850 ft bgs.

The well borehole was drilled to a total depth of 1140 ft bgs. A monitoring well was installed with the well screen placed between 1039.6 to 1060 ft bgs within the Puye Formation. Although the borehole contained water during drilling, the well was dry at completion and did not retain water during attempted slug testing (LANL 2008, 103408). It was concluded that the well screen was installed in unsaturated rocks and that groundwater observed during drilling was produced by perched groundwater in overlying strata. A seismometer was installed at the bottom of the well in September 2010 as part of the Laboratory’s Seismic Hazards Program.

Well R-47i

Well R-47i is a single-screen perched-intermediate monitoring well installed in November 2009 at TA-14 on the north rim of Cañon de Valle (Figure 1.0-3). Details on the drilling, installation, and testing are discussed in the "Completion Report for Intermediate Aquifer Well R-47i" (LANL 2010, 109188). Well installation was performed in accordance with the "Work Plan for Redrilling Well R-47" (LANL 2009, 107505). The original plan for this location was to drill and install a regional well to be called R-47 that would augment the TA-16 monitoring well network by providing a regional monitoring well northeast of the 260 Outfall. However, due to problems encountered during well construction, the regional well was abandoned, and a perched-intermediate zone well named R-47i was installed instead. Well R-47i provides hydrologic and groundwater quality data for perched-intermediate groundwater downgradient of TA-16.

Perched-intermediate groundwater was first recognized in the Puye Formation during video logging. Increased moisture was first noted on the borehole wall at approximately 834 to 835 ft bgs. Strong flow of water on the borehole wall was observed at 842 ft. By 857 ft, the flow was continuous around the full diameter of the borehole. These observations were made when the borehole was 1034 ft deep.

The borehole was drilled to a total depth of 1350.5 ft bgs and regional groundwater was encountered at 1245.3 ft bgs. Initially, the regional aquifer well casing and screen were installed during well construction; however, bentonite associated with the annular seals intruded into the well screen, and the Laboratory, NMED, and DOE decided to abandon the lower portion of the borehole and complete the well in the intermediate zone as well R-47i. The regional aquifer well casing and screen were removed, the borehole was backfilled, and a new well was installed with a 20-ft screen placed between 840.0 and 860.6 ft bgs. The depth to water after well installation was 832.2 ft bgs (LANL 2010, 109188).

Well R-63i

Well R-63i is a single-screen perched-intermediate monitoring well installed in November 2014 at TA-16 on the mesa top south of Cañon de Valle (Figure 1.0-3). Details on the drilling, installation, and testing of R-63i is presented in the "Completion Report for Intermediate Aquifer Well R-63i" (LANL 2015, 600934). Well R-63i was installed to satisfy a requirement made in the "Approval with Modifications, Technical Area 16 Well Network Evaluation and Recommendations" by NMED (NMED 2012, 520747). This letter required the installation of a perched-intermediate groundwater monitoring well east of MDA P. The well was sited next to existing regional aquifer well R-63. Well installation was performed in accordance with the "Drilling Work Plan for Well R-63i" (LANL 2013, 235924) that was approved by NMED (NMED 2013, 522166). Well R-63i was installed to monitor contaminant releases from the 260 Outfall and MDA P as well as recharge from Cañon de Valle. Secondary objectives were to establish water levels in the perched-intermediate groundwater and to identify potential perched groundwater.

A possible upper perched-intermediate groundwater zone was encountered in the lower Otowi Member and top of the Puye Formation with a depth to water of about 750 ft bgs. This upper-perched groundwater was sealed out of the borehole by landing 18-in. drill casing in bentonite at 852 ft bgs. Based on borehole video logs, flow of groundwater from a perched-intermediate zone occurred on borehole walls at 1190 ft bgs at R-63i and 1178 ft bgs at R-63.

The well borehole was drilled to a total depth of 1245 ft bgs. A monitoring well was installed with the well screen placed between 1122.5 and 1189 ft bgs within the Puye Formation. A 66.5-ft-long screen was installed because there were large uncertainties about the depths where stringers of groundwater were entering the borehole. The depth to perched water in the completed well was 1175.9 ft bgs.

Well CdV-9-1(i)

Well CdV-9-1(i) is a two-screen perched-intermediate monitoring well installed in January 2015 at TA-09 on the north rim of Cañon de Valle (Figure 1.0-3). Details on the drilling, installation, and testing of CdV-9-1(i) are discussed in the “Completion Report for Intermediate Aquifer Well CdV-9-1(i)” (LANL 2015, 600503). Well installation was performed in accordance with the “Drilling Work Plan for Well CdV-9-1(i)” (LANL 2013, 239226) that was approved by NMED (NMED 2013, 522693). The objective of well CdV-9-1(i) was to characterize the northern extent of HE in perched-intermediate groundwater associated with the 260 Outfall. The drilling work plan called for completion of a monitoring well tentatively designed with a single well screen to be placed near the depth of CdV-16-4ip screen 2 in the Puye Formation. Secondary objectives were to identify and establish water levels in perched-intermediate aquifers.

No perched groundwater was recognized as the 16-in. drill casing was advanced to 924 ft bgs; however, when the drill casing was retracted to 624 ft bgs, water levels were observed to rise from 791 to 661 ft bgs. A video log documented groundwater flow into the borehole starting at 650 ft bgs. The formation appeared to be relatively dry from 1000 ft bgs to 1020 ft bgs, suggesting a potential perching zone.

The well borehole was drilled to a total depth of 1220 ft bgs. A two-screen monitoring well was installed with screened intervals between 937.4 and 992.4 ft bgs and from 1023.7 to 1045.0 ft bgs within the Puye Formation. The lower well screen was abandoned after a single-set inflatable packer was emplaced but could not be retrieved after preliminary development of the upper well screen. The depth to water of 892.8 ft bgs was recorded after well installation and preliminary development of the upper well screen.

Two PZs were installed outside the well casing with screened intervals set between 662.9 to 672.4 ft bgs in the Otowi Member of the Bandelier Tuff and between 852.9 to 862.4 ft bgs in the Puye Formation. The two piezometers are designed to measure pressure responses to pumping in nearby perched-intermediate wells. The depth to water in PZ-1 and PZ-2 after installation was 604.3 ft bgs and 685.1 ft bgs, respectively.

Well CdV-16-4ip

Well CdV-16-4ip is a two-screen perched-intermediate monitoring well installed in August 2010 at TA-16 on the south rim of Cañon de Valle (Figure 1.0-3). Information on the drilling, construction, and testing of Well CdV-16-4ip is discussed in the “Completion Report for Intermediate Well CdV-16-4ip” (LANL 2011, 111608). Well installation was performed in accordance with the “Drilling Work Plan for Perched-Intermediate Pumping Well CdV-16-4ip” (LANL 2010, 109268). CdV-16-4ip was drilled at the direction of NMED as a pumping well to be used for pumping tests in the perched-intermediate groundwater beneath Consolidated Unit 16 021(c) 99. The pumping tests, coupled with an analysis of the response in nearby wells, were designed to assess the potential to pump and treat RDX-containing perched-intermediate groundwater. The hydrologic testing program is presented in the “Hydrologic Testing Work Plan for Consolidated Unit 16-021(c)-99” (LANL 2010, 108534). Results of pump tests at well CdV-16-4ip are summarized in sections 2.9.3 and 2.9.4 of this report.

The well borehole was drilled to a total depth of 1153.7 ft bgs. Perched-intermediate groundwater was encountered in the Puye Formation, and video logs showed strong water flow entering the borehole below 811 ft bgs before well construction. A two-screen monitoring well was installed with a screen interval between 815.6 to 879.2 ft bgs within the upper perched-intermediate zone and from 1110 to 1141.1 ft bgs within the lower perched-intermediate zone. The lower screen targets the same depth as screen 4 at well R-25. The depth to water in the upper screen was 808.2 ft bgs after well completion and was 1058 ft bgs in the lower screen after well development.

In 2012, the Laboratory proposed to reconfigure CdV-16-4ip to a single-screen well to prevent cross-flow from screen 1 to 2 due to large hydraulic head differences between the screens. The Laboratory submitted the “Work Plan to Reconfigure Well CdV-16-4ip” in November 2012 (LANL 2012, 232222), and NMED approved this work plan with modifications in December 2012 (NMED 2012, 521747). In its approval with modifications, NMED requested the Laboratory develop a work plan to conduct interim measures to hydraulically contain dissolved HE (e.g., RDX) and VOCs [e.g., tetrachloroethylene] in the vicinity of CdV-16-4ip screen 1. In June and July 2013, the Laboratory reconfigured CdV-16-4ip to a single-screen monitoring well (LANL 2013, 249519). During the reconfiguration, the lower screen was plugged and the sampling system installed in the upper screen.

Well R-48

Well R-48 is a single-screen regional aquifer well installed in September 2009 approximately 1800 ft southeast of well R-25 in TA-16 (Figure 1.0-3). Details on the drilling, installation, and testing of R-48 are discussed in the “Completion Report for Regional Aquifer Well R-48” (LANL 2010, 108778). A borehole originally designated CdV-16-3(i) was drilled in 2004 to a total depth of 1405 ft bgs. Drilling was performed in accordance with the “Drilling Work Plan for Well CdV-16-3(i)” (LANL 2008, 101875.11) that was approved by NMED (NMED 2008, 101114). The borehole was believed to have entered the regional aquifer around 1350 ft bgs in massive Tschicoma dacitic lavas. Due to the poor water production experienced in the lavas, it was determined that the borehole would be advanced further in an attempt to encounter more permeable strata, and the designation was changed to R-48. The purpose of well R-48 was to enhance the TA 16 monitoring well network by providing a regional aquifer well to the southeast of the 260 Outfall and northeast of S-Site Canyon.

The R-48 borehole was successfully advanced to a total depth of 1705 ft bgs using open-hole drilling methods. The entire interval, from 1405 to 1705 ft bgs, was drilled in dacite lava flows of the Tschicoma Formation. The well was completed with a single-screened interval from 1500 to 1520.6 ft bgs. The screen interval was selected to optimize the goals of sampling water as close to the water table as feasible while ensuring adequate groundwater flow to the screen. The depth to water after well installation and well development was 1352.5 ft bgs.

Well R-58

Well R-58 is a single-screen regional aquifer well installed in November 2015 approximately 1850 ft south of Cañon de Valle and 3640 ft southeast of well R-48, in TA-16 (Figure 1.0-3). The “Completion Report for Regional Aquifer Well R-58” (LANL 2016, 601364) describes the drilling, installation, and testing activities conducted at R-58. Drilling was performed in accordance with the “Drilling Work Plan for Regional Aquifer Well R-58” (LANL 2012, 212117) that was approved by NMED (NMED 2012, 521741). Regional aquifer well R-58 was installed to satisfy a recommendation made in the “Technical Area 16 Well Network Evaluation and Recommendations” (LANL 2012, 213573) and approved with modifications by NMED (NMED 2012, 520747). This assessment recommended installing one new regional groundwater monitoring well downgradient of S-Site Canyon and Fishladder Canyon. The primary purpose of R-58 was to increase the overall detection efficiency of the TA-16 monitoring network for the high- and medium- priority sources at TA-16. Water-level data from this location was also intended to constrain the shape of the regional water table and groundwater flow directions at TA-16.

The R-58 borehole was drilled to a total depth of 1378.4 ft bgs. A monitoring well was installed with a screened interval between 1257 and 1277.3 ft bgs within dacite breccia of the Tschicoma Formation. The depth to regional groundwater water after well installation was 1238.3 ft bgs.

Well R-68

Well R-68 is a single screen regional aquifer well installed in February 2017 at TA-09 on the mesa north of Cañon de Valle (Figure 1.0-3). Details on the drilling, installation, and testing of R-68 are discussed in the “Completion Report for Regional Aquifer Well R-68” (LANL 2017, 602539). This work was performed in accordance with the “Groundwater Investigation Work Plan for Consolidated Unit 16-021(c)-99, Including Drilling Work Plans for Wells R-68 and R-69” (LANL 2016, 601779). The well was installed to address uncertainties about potential flow paths related to increasing concentrations of RDX observed in monitoring well R-18. Groundwater data from the completed well and from screening samples collected from perched water collected during drilling help to constrain the nature and extent of perched-intermediate groundwater and RDX concentrations in the regional aquifer. Water-level data from the well provide information for the elevation of the regional water table and groundwater flow direction north of Cañon de Valle.

Perched-intermediate groundwater was noted in the R-68 borehole by drillers in the lower part of the Otowi Member of the Bandelier Tuff at a depth of 770 ft bgs. The 17-in. open borehole was advanced to the Guaje Pumice Bed/ Puye Formation contact at a depth 810 ft, and the water level was measured at 683 ft bgs. Following collection of natural gamma ray, induction, and video logs, 16-in. drill casing was tripped into the open borehole to 810 ft bgs. The cased borehole was advanced to 912 ft bgs, and the water level was measured at 804 ft bgs.

The well borehole was drilled to a total depth of 1422.8 ft bgs. A monitoring well was installed with a screened interval between 1340 and 1360.4 ft bgs within the Puye Formation. The water level was 1325.7 ft bgs after well installation (LANL 2017, 602539).

Well R-69

Well R-69 is a two-screen regional aquifer well installed in October 2018 at TA-14 on the mesa approximately 1100 ft north of Cañon de Valle (Figure 1.0-3) (N3B 2019, 700346). This work was performed in accordance with the “Groundwater Investigation Work Plan for Consolidated Unit 16-021(c)-99, Including Drilling Work Plans for Wells R-68 and R-69” (LANL 2016, 601779). The need to install well R-69 was contingent on findings at well R-68, where screening-level data collected during drilling showed that RDX-containing perched groundwater occurs northeast of well CdV-9-1(i), and the regional aquifer contains RDX at higher concentrations than any of the regional wells installed up to that point in time. Well R-69 was installed to determine the northeast extent of perched-intermediate groundwater containing RDX and to assess potential hydraulic connections between the perched zone and the regional aquifer. Well R-69 is located between wells R-18 and R-68, and its location was selected to provide a better understanding of the increasing concentrations of RDX observed in R-18. The two well screens in R-69 provide the ability to monitor water quality in the regional aquifer at two discrete depth intervals. Water-level data from the well provide information for the elevation of the regional water table, groundwater flow direction north of Cañon de Valle, and vertical hydraulic gradients.

The well borehole was drilled to a total depth of 1443.4 ft bgs. A monitoring well was installed with well screens placed at 1310 to 1330.2 ft bgs and 1375.5 to 1395.8 ft bgs within the Puye Formation. A Baski sampling system was installed to isolate and sample the two well screens. No perched-intermediate groundwater was identified during drilling of the R-69 borehole. Depth to the regional aquifer was 1292.5 ft bgs (composite head from both screens) after well installation (N3B 2019, 700346).

2.9.3 2011 Extended Duration Aquifer Tests at Wells CdV-16-4ip and R-25b

Aquifer testing was conducted in 2011 at wells CdV-16-4ip and R-25b to collect data on aquifer properties of perched-intermediate groundwater below Consolidated Unit 16-021(c)-99. The results are described in “Hydrologic Testing Report for Consolidated Unit 16-021(c)-99” (LANL 2011, 203711). This work was developed to meet the requirements of NMED’s “Approval with Modifications: Supplemental Investigation Work Plan for Intermediate and Regional Groundwater at Consolidated Unit 16-021(c)-99” (NMED 2009, 104973). A description of the test plan is provided in the “Hydrologic Testing Work Plan for Consolidated Unit 16-021(c)-99” (LANL 2010, 108534). The tests were conducted to better understand the hydrogeological settings of the area, to quantify the aquifer properties, and ultimately to assess the potential for pumping and treatment of RDX-containing perched groundwater beneath the northern portion of TA-16.

Well CdV-16-4ip Aquifer Test

Well CdV-16-4ip was completed with two screens, with screen 1 located in the upper perched-intermediate zone and screen 2 located in the lower perched-intermediate zone. Screen 1 is 63.6 ft long and extends from 815.6 to 879.2 ft bgs, whereas screen 2 is 31.1 ft long and extends from 1110.0 ft to 1141.1 ft bgs. Both well screens are located in the Puye Formation. The static water level at the upper screen is around 809 ft bgs (i.e., about 7 ft above the top of upper screen). The static water elevation at screen 2 is around 1098 ft bgs, 12 ft above the top of screen.

Pump tests were performed on both of the screens of CdV-16-4ip. Testing of each zone included a brief step-drawdown test followed by a 10-day pump test. Each step-drawdown test was followed by recovery data collection overnight. Each 10-day test was started the morning after the step-drawdown test and was followed by a minimum of 12 days of monitored recovery. During the pumping tests at CdV-16-4ip, water levels were recorded in several nearby wells. The wells and screen zones included in the monitoring effort, along with their horizontal distances from CdV-16-4ip, were R-25 screens 1, 2, 4, 5, 6, 7, and 8 (430.4 ft); R-25b (477.1 ft); CdV-16-1(i) (554.2 ft); CdV-16-2(i)r (1086.4 ft); and R-63 (1064.3 ft). During the pumping events at screen 1, water-level responses were observed only at the monitoring location R-25 (screen 2). Pumping at screen 2 of CdV-16-4ip resulted in no water-level responses at any of the nearby monitoring locations.

Test data showed that CdV-16-4ip screen 1 is located in a laterally limited pocket or channel of highly transmissive sediments, surround by material with lower transmissivity. The data indicate screen 1 is completed in a zone with an estimated lower-bound transmissivity of 4000 to 7000 gal. per day (gpd)/ft, corresponding to a lower-bound hydraulic conductivity on the order of 13 ft/day). Large initial pumping rates quickly dewatered those sediments, reflecting a much lower effective transmissivity (about 130 gpd/ft) for the broader perched zone, suggesting limited water production potential. The perched zone appeared to recharge at a rate of about 4.8 gallons per minute (gpm) from laterally adjacent sediments during the 10-day pumping period and during the recovery period. The only monitored location that showed a response to pumping CdV-16-4ip screen 1 was R-25 screen 2, located 430.4 ft away. The drawdown response was muted, suggesting an indirect hydraulic connection between these zones. The pumping test data collected at CdV-16-4ip screen 2 in the lower perched zone indicated this zone is spatially extensive and has a transmissivity of approximately 660 gpd/ft, with an average hydraulic conductivity of 2.0 ft/day. Late-time pumping test data suggest the perched zone might be recharged from the vadose zone above (delayed yield under phreatic conditions). Late-time pumping test behavior might also result from lateral or vertical heterogeneities (vertical stratification or lateral facies boundaries with different transmissivity). The 10-day pumping test of screen 2 showed no measurable drawdown at any of the nearby monitoring locations.

The static water level observed in screen 1 of CdV-16-4ip was substantially higher (281 ft) than that in screen 2, showing a strong downward hydraulic gradient and highly resistive sediments separating the two screened zones, and little hydraulic connection between the screens. The aquifer testing confirmed this finding, showing no drawdown in either zone as a result of pumping the other zone. Based on the pumping test data, the two perched-intermediate zones above the regional aquifer in the vadose zone beneath the northern portion of TA-16 do not appear to be hydraulically connected. There is also no apparent indication the lower perched-intermediate zone is hydraulically connected with the regional aquifer.

Well 25b Aquifer Test

Well R-25b was completed with one screen within the Otowi Member of the Bandelier Tuff. The well screen is 20.8 ft long, extending from 750.0 to 770.8 ft bgs. Several wells and screen intervals were monitored during the R-25b pumping test; however, only R-25 screens 1 and 2 showed a response to pumping R-25b. Well R-25 is 55 ft from R-25b. R-25 screen 1 is 20.8 ft long and is located within the Otowi Member of the Bandelier Tuff. R-25 screen 2 is 10.8 ft long and lies within the Puye Formation.

Because of the drawdown response observed in R-25 screens 1 and 2 during the R-25b pumping test, it was assumed that the three screened intervals were within the same hydrologic unit. The zone of saturation was considered to extend from the R-25 screen 1 static water level (6779.3 ft above mean sea level [amsl]) to the base of R-25 screen 2 (6622.7 ft amsl), a span of 156.6 ft. R-25b was tested by operating a dedicated Bennett pump for 24 hr at a constant discharge rate averaged 0.60 gpm. Following shutdown of the pump test, recovery data were recorded for a little more than 2 days.

Water levels in R-25b and R-25 screens 1 and 2 showed steep downward gradients suggesting significant vertical anisotropy. The anisotropy was judged to be more severe in the upper portion of the perched-intermediate groundwater zone where heads between R-25b and R-25 screen 1 were substantially different although the elevation intervals spanned by the two screens overlap slightly. Storage effects and discharge rate variations precluded analysis of the pumping portion of the test. The late (post-storage) recovery data yielded an estimated hydraulic conductivity of 0.29 ft/d. Analysis of the drawdown data from R-25 screen 2 produced hydraulic conductivity values averaging slightly more than 0.3 ft/day.

2.9.4 2014 Extended Duration Aquifer Tests at Well CdV-16-4ip

Source-removal pump tests were conducted at CDV-16-4ip screen 1 in 2014, and the results are presented in "Interim Measures Report for Source-Removal Testing at Well CdV-16-4ip" (LANL 2014, 600004). The investigation was originally requested by NMED in its "Approval with Modification Work Plan to Reconfigure Well CdV-16-4ip" (NMED 2012, 521747). In response to this request, the Laboratory prepared the "Interim Measures Work Plan for Source Removal Testing at Well CdV-16-4ip" (LANL 2013, 239235). NMED approved this work plan and provided additional requirements for the testing in its "Approval with Modifications: Interim Measures Work Plan for Source Removal Testing at Well CdV-16-4ip" (NMED 2009, 104973). The primary objectives of the work were to determine whether source removal from this zone could be conducted to limit potential migration of RDX and other constituents to the underlying regional aquifer and to determine if long-term pumping in the perched-intermediate zone is a viable source removal option. Secondary objectives included refinement of the conceptual model regarding the spatial extent and hydraulic characteristics of perched-intermediate groundwater.

Source-removal testing consisted of active pumping at CdV-16-4ip screen 1 for 57 days, followed by recovery monitoring and sampling. Testing consisted of an initial 29-day pumping period at 6.8 gpm to

6.1 gpm, followed by a 3-day hiatus in pumping to collect data on the recovery responses in the pumping well. Pumping was then resumed at 5 gpm for a final 28 days of pumping before recovery monitoring and rebound sampling for 3 weeks. Collectively, the pumping removed 472,684 gallons of groundwater from the perched-intermediate zone at CdV-16-4ip screen 1. Water levels were monitored in perched-intermediate well screens R-25 screen 1, R-25 screen 2, R-25 screen 4, R-25b, CdV-16-1(i), and CdV-16-2(i)r. Water levels were also monitored in regional well screens R-25 screen 5, R-25 screen 6, R-25 screen 7, R-25 screen 8, and R-63.

CdV-16-4ip pumping generated more than 40 ft of drawdown at the pumping well. During aquifer testing, pumping drawdown was clearly detected at R-25 screen 2 (>3 inches). Wells CdV-16-1(i), CdV-16-2(i)r, R-25b, and R-47i also potentially responded to the pumping, but the estimated drawdowns were much smaller (on the order of an inch). Water-level transients observed at the pumping well were heavily influenced by localized boundary effects; however, the boundary effects were not detected at the observation wells (for example, at R-25 screen 2), indicating the boundary effects are localized near the pumping well only. Based on water-level data from R-63, no drawdown response was observed in the regional aquifer. This is expected, considering the vertical hydraulic separation and variable saturation in the vadose zone between pumping and observation screens.

The water-level drawdown curve observed during the pumping test demonstrates the high degree of hydrogeologic heterogeneity of the pumped zone of saturation. The water-level transients are characterized by a series of inflection points at which the shape of water-level curve changes abruptly. The slope of water-level decline and recovery between the inflection points is almost linear. The elevations of the inflections in the water-level curve may reflect the elevations of the hydrostratigraphic contacts. The more permeable hydrostratigraphic zones are believed to be located between elevations of 6603 to 6620 ft. The pumped screen is also recharged by strata at an elevation higher than 6635 ft. The hydrostratigraphic units with elevation between 6635 and 6620 ft and below 6603 ft seem to have very low permeability and may not contribute to the groundwater flow pumped at CdV-16-4ip.

The pump test indicates the large-scale effective transmissivity of the saturated zone between R-25 screen 2 and CdV-16-4ip screen 2 is on the order of 485 ft²/day to 968 ft²/day, with a hydraulic conductivity on the order of 7.4 ft/day. The estimated storativity of the upper perched-intermediate zone is 0.2, a reasonable value for an unconfined perched zone.

Daily groundwater samples were collected for onsite analysis of RDX at the Laboratory's Geochemistry and Geomaterials Research Laboratory (GGRL). Weekly groundwater samples were collected for onsite analysis of metals, anions, and alkalinity and pH at GGRL. Weekly groundwater samples were also collected for offsite analyses of HE and VOCs at General Engineering Laboratory. RDX concentrations in groundwater averaged 161 µg/L. During the initial 30 days when pumping rates gradually diminished from 6.8 to 6.1 gpm, RDX concentrations slowly trended up from approximately 143 µg/L to approximately 155 µg/L (with a maximum of around 159 µg/L). Following a 3-day hiatus when pumping was temporarily stopped, RDX concentrations continued to increase slowly, ending at approximately 170 µg/L. RDX concentrations in groundwater remained fairly constant thereafter and throughout the remainder of the pumping test and throughout the recovery period. Recovery data showed RDX ending at 166.1 µg/L.

Activated charcoal treatment was used successfully during the pumping test to treat groundwater pumped from the well. During the pumping tests, the RDX concentrations in groundwater averaged 161 µg/L, and the treatment effluent was always below 3.8 µg/L for a minimum removal efficiency of about 98%. At an average flow rate of 5.75 gpm, approximately 0.63 lb of RDX was removed during the pump test.

2.9.5 2016 Extended Duration Cross-Hole Aquifer Tests at Wells CdV-9-1(i), CdV-16-4ip, and CdV-16-1(i)p

Cross-well pumping tests were conducted at monitoring wells CdV-9-1(i), CdV-16-1(i), and CdV-16-4ip, completed in the upper perched-intermediate groundwater zone as described in “Summary Report for Intermediate Groundwater System Characterization Activities at Consolidated Unit 16-02I(c)-99” (LANL 2017, 602288). This work was performed in accordance with the “Work Plan for Intermediate Groundwater System Characterization” (LANL 2015, 600535). Objectives of the pumping-test activities were to evaluate the degree of hydraulic connection horizontally and vertically in the perched groundwater zones beneath Cañon de Valle near the 260 Outfall to assess transport pathways for RDX and other contaminants. The pumping test was also used to evaluate the hydraulic connection between perched groundwater in the Puye Formation and in the Otowi Member of the Bandelier Tuff. An additional objective was to evaluate contaminant characteristics in the perched zone and contaminant transport properties by monitoring temporal variations in RDX during the extended pumping.

During the pumping tests, water levels were monitored at the following monitoring well locations: CdV-9-1(i) screen 1; CdV-9-1(i) PZ-1; CdV-9-1(i) PZ-2; CdV-16-1(i); CdV-16-2(i)r; CdV-16-4ip screen 1; R-25 screen 1, screen 2, and screen 4; R-25b; R-47i; R 63; and R-63i.

As described in Section 2.9.2, Well CdV-9-1(i) was completed as a dual-screen perched-intermediate monitoring well with screened intervals set between 937.4 and 992.4 ft bgs and between 1023.7 and 1045.0 ft bgs in Puye Formation. Two PZs (PZ-1 and PZ-2) were installed outside the well casing with screened intervals set between 662.9 and 672.4 ft bgs in the Otowi Member of the Bandelier Tuff and between 852.9 and 862.4 ft bgs in the Puye Formation. The lower well screen was abandoned after a single-set inflatable packer was emplaced but could not be retrieved after preliminary development of the upper well screen. Well CdV-16-1(i) was completed as a single-screen perched-intermediate monitoring well with screened interval of 624.0 to 634.0 ft bgs in the Otowi Member of the Bandelier Tuff. Well CdV-16-4ip was constructed as a two-screen perched-intermediate groundwater well with screen intervals at 815.6 to 879.2 ft bgs and 1110.0 to 1141.1 ft bgs.

The primary pumping test at CdV-9-1(i) was followed by recovery monitoring and rebound. One month before the pumping test, a significant recharge event occurred, manifested in water levels increasing by approximately 12 ft in CdV-9-1(i) screen 1. Water levels were also observed to increase in CdV-9-1(i) PZ-2 but at a small magnitude. The pumping test activities at CdV-9-1(i) were initiated 9 days after the peak was observed, even while water levels were still declining from the recharge event. The potentiometric responses during the pumping test were significantly greater than the declines from the recharge event, allowing pumping test activities to continue; however, the large-scale recharge event added additional complexity to the analysis of the data.

Each of the three pumping wells were pumped for approximately 30 days. Pumping rates at CdV-9-1(i) screen 1 varied between 2.1 gpm and 1.6 gpm. Well CdV-16-1(i) was pumped at variable pumping rates ranging from 0.38 to 0.60 gpm, averaging 0.43 gpm. Pumping rates at CdV-16-4ip screen 1 ranged from 3.9 to 7.8 gpm.

Key findings of the cross-well pump tests include the following:

- Lateral hydraulic communication was observed between some of the screens relatively proximal to each other and completed in the upper Puye Formation. Pumping responses demonstrated that lateral hydraulic pathways occur over an area at least as large as the triangle formed by CdV-9-1(i), CdV-16-4ip, and R-25 screen 2. The preferential communication across the upper Puye Formation is likely driven by stratification (i.e., high anisotropy) in the Puye strata.

- In 30 days of pumping of CdV-9-1(i) screen 1, no water-level response was generated in CdV-9-1(i) PZ-2 even though both screens are completed in the Puye Formation, demonstrating the upper perched-intermediate zone is highly anisotropic. Pumping from any of wells within the upper Puye Formation caused little or no response in monitored screens within the lower perched-intermediate zone of the Puye Formation and the portion of the upper perched-intermediate zone located in the Otowi Member, including monitoring points that are very close to the pumping locations. In one case, limited hydraulic communication may have been observed across the Otowi/Puye boundary, based on an apparent water-level responses in CdV-9-1(i) PZ-2 as a result of pumping at CdV-16-1(i). These observations suggest a high lateral-to-vertical anisotropy ratio is an important characteristic of the upper perched-intermediate zone, and that the Otowi/Puye contact is a potentially important hydrostratigraphic boundary.
- The apparent boundary effect observed during pumping at CdV-16-4ip in 2014 (LANL 2014, 600004) is believed to reflect contrasts in aquifer properties rather than a spatially limited perched body based on the good hydraulic responses in nearby upper Puye wells during the pumping tests.
- RDX concentrations showed some correlation with water levels at CdV-9-1(i) and CdV-16-1(i) but not at CdV-16-4ip. RDX concentrations in wells CdV-9-1(i) and CdV-16-1(i) declined during pumping as water levels dropped and then appeared to increase during recovery.
- Because of the relatively low sustainable pumping rates at CdV-16-1(i), CdV-9-1(i), and CdV-16-4ip, the total mass of RDX removed during 90 days of pumping was an estimated 0.17 kg, representing approximately 0.02% to 0.08% of the estimated RDX inventory believed to be present in perched-intermediate groundwater beneath the TA-16 area.

2.10 2018 RDX Compendium Report Investigations

The characterization activities discussed above in Section 2.9 were directed by the 2008 NOD (NMED 2008, 101311). These investigations have associated work plans, completion reports, and various technical reports documenting these activities and their data. This section summarizes additional studies that were conducted to address questions initially posed in the 2008 NOD (NMED 2008, 101311) regarding the nature and extent of contamination and data collection to be used to evaluate potential corrective actions for high explosives in the vadose zone and groundwater. Some of these additional studies and their results had not been provided to NMED, so the “Compendium of Technical Reports Related to the Deep Groundwater Investigation for the RDX Project at Los Alamos National Laboratory” (hereafter referred to as the Compendium) (LANL 2018, 602963) was developed as a vehicle to complete the administrative record. In addition to nature and extent of contamination, the Compendium reports provide information used to update the CSM and support RDX fate and transport assessments. Each compendium study is summarized below and where appropriate updated information is included.

2.10.1 Updated RDX Inventory

Attachment 1 of the Compendium presents an updated estimate of the mass of RDX in the subsurface environment in the vicinity and downgradient of the 260 Outfall in Cañon de Valle. This estimate was developed based on the latest characterization results from installed monitoring wells and boreholes in TA-16 and TA-9. Although a similar analysis was conducted in 2005, the 2017 update uses recent data from a substantially larger set of monitoring wells and boreholes and addresses the reduction of the near-surface contamination at the 260 Outfall as a result of the 2009–2010 “Summary Report for the Corrective Measures Implementation at Consolidated Unit 16-021(c)-99” (LANL 2010, 108868). The mass of RDX was estimated for (1) the near-surface soils and sediments around the 260 Outfall and in Cañon de Valle,

(2) the underlying vadose zone beneath the outfall and Cañon de Valle, (3) the vadose zone beneath the mesa discharge to SWSC and Burning Ground Springs, and (4) the perched-intermediate groundwater and the regional aquifer.

Overall, the 2017 inventory estimates that between 1533 and 3608 kg of RDX is distributed among all components of the hydrologic system at TA-16. The regional groundwater zone contains between 35 and 415 kg of RDX. The intermediate groundwater zone is estimated to contain between 263 and 1478 kg. The saturated zones feeding SWSC and Burning Ground Springs are estimated to contain between 33 and 56 kg. The vadose zone directly beneath the TA-16 area, including the former pond, outfall area, drainage channel, and surge bed below the pond, is estimated to contain between 545 and 940 kg RDX. Based on a geomorphology study of alluvial sediments (LANL 2011, 207069), it is estimated that between 5 and 10 kg RDX is stored in Cañon de Valle sediments. The vadose zone beneath Cañon de Valle contains is estimated to contain between 8 and 64 kg RDX, but the lack of concentration data in the vadose zone make these estimates highly uncertain.

2.10.2 Geologic Investigation

Attachment 2 of the Compendium summarizes geologic investigations that were undertaken to identify hydrogeologic features that control the occurrence and distribution of RDX-containing groundwater in the vicinity of TA-16. The geological investigations focused on three tasks to improve the geologic model that underpins the site conceptual model for contaminant transport. The three tasks consisted of (1) updating the stratigraphic contacts within the Bandelier Tuff and the Cerro Toledo Formation, (2) using the contacts to define internal bedding surfaces and orientations within the major units, and (3) updating the geological and structural features at TA-16 and adjacent areas.

Stratigraphic contacts were examined and updated using multiple lines of evidence, including drill hole cuttings, geophysical logs, and geochemical analyses. Updated contacts were used to make cross-well correlations, generate structure contour maps showing the bedding orientations and dips of units, and locate and measure displacements of faults. The data was used to update the site-wide geologic model that provides the framework for groundwater flow and transport models for the RDX deep groundwater investigation.

The report also highlights the role of faults and fractures as potential moisture pathways in the upper vadose zone. The eastern margin of the TA-09 graben and its associated structures crosses Cañon de Valle downstream of the 260 Outfall where quantities of HE at high concentrations were released in large volumes of water that provided a significant hydrologic driving force for infiltration of contaminants. The faults and fractures may be important infiltration pathways through the strongly welded tuffs that underlie the canyon floor.

2.10.3 Hydrogeochemical Studies

Six different studies using isotope data, geochemistry, and field measurements were conducted to update the hydrogeochemical conceptual model for the RDX study area that is presented in Attachment 3 of the Compendium. The studies included

- a factorial analysis of the geochemical signatures of waters from different hydrostratigraphic units used to evaluate recharge and flow pathways,
- a review of concentration-discharge relationships used to evaluate contaminant residence times in the near-surface environment,

- a study of infiltration along Cañon de Valle to assess deep MBR,
- a review of stable isotope and temperature data to evaluate recharge sources,
- a study of post-fire water chemistry data to determine if fire-induced changes can be used as a tracer, and
- the analysis of mountain block and local recharge using a simple mixing-model approach and geochemical modeling. This work focused on the main saturated zones at TA-16, including the regional aquifer, perched-intermediate groundwater zones, springs, alluvial groundwater zone, and Cañon de Valle stream flow.

The investigation included a comprehensive evaluation of all TA-16 geochemistry samples and employed a statistical approach to characterize water sources and flow paths as well as highlight important geochemical differences between groundwater zones. Factor analysis was performed to understand the global TA-16 geochemistry data set collected over several years and identify possible relations among analytes. Using the factor analysis results, specific analytes were used to test for statistically significant differences between groundwater zones. The results of this evaluation are described below:

- Comparison tests show that the perched-intermediate zone and regional aquifer are geochemically distinct; however, this is likely because of the difference in lithology of flow paths rather than recharge sources.
- Both groundwater zones contain high lithium and low chloride, suggesting recharge via long, deep flow paths consistent with a mountain block recharge (MBR).
- Stable isotope data indicate that alluvial groundwater is primarily recharged by spring water and that perched-intermediate groundwater and the regional aquifer likely share similar recharge sources.
- Surface, spring, and alluvial zone waters are highly variable compared to perched-intermediate and regional waters, indicating increased mixing and homogenization deeper in the hydrologic system.
- Groundwater samples with young, contaminated signatures are concentrated in close proximity to the perennial reach of Cañon de Valle and in the top approximately 100 ft where they occur in the regional aquifer.

These observations indicate that the perched-intermediate zone and regional aquifer are impacted by localized contaminated recharge associated with the perennial reach of Cañon de Valle.

A simple binary (two source) mixing model was used in conjunction with the conservative tracer chloride to determine the relative proportions of mountain block vs. local recharge. The simple mixing model approach was compared to a second approach that used the geochemical code PHREEQC to examine mountain block vs. local TA-16 recharge. The PHREEQC analysis is based on the background chemistry of TA-16 wells and potential source waters (e.g. MBR), and the potentially relevant water/rock interactions such as mineral dissolution, precipitation, and ion exchange. The simple mixing models and the PHREEQC analysis produced broadly similar results and resulted in the conclusions below:

- Regional aquifer recharge is nearly all from mountain block sources (>90% MBR).
- The perched-intermediate zone has a much larger component of local TA-16 recharge (typically 10%–40%).

- There are RDX hotspots in the regional aquifer that seem to be related to localized higher infiltration areas in and around Cañon de Valle.

The proportion of MBR to deep groundwater via upper Cañon de Valle and the Pajarito fault zone was also estimated using water balance data. Cañon de Valle discharge upstream of the fault zone was measured by portable flume gauging under different conditions between March 2016 and May 2017. Historical measurements were also used to provide additional reference points for upper canyon springs and channel discharge. Conclusions reached from this evaluation are shown below:

- In the upper canyon above the Pajarito fault zone, discharge data demonstrate distinct gaining and losing reaches.
- Springs emerging from Tschicoma Formation bedrock supply the bulk of base flow, which is lost to the subsurface in various places depending on season and flow volume.
- The overall impact is that all upper Cañon de Valle flow is lost at or above the Pajarito fault zone. Flow across the fault, which was occasionally seen in older data, no longer occurs. This shift occurred as a result of scouring and heavy silting of the stream channel during flood events that followed the Cerro Grande fire. The fault appears to accept virtually all upper canyon surface water, and losses along the fault zone were certainly substantial before the fire.
- The highest estimated mountain block loss to deeper zones was found to occur during spring (up to 98% of upper Cañon de Valle streamflow), when snowmelt runoff dominates.
- The lowest values occurred during June through July and December through January (<10%).
- Based on these observations, the majority of net recharge to deep groundwater is sourced from above the Pajarito fault zone during the snowmelt period.
- Spring discharge into lower Cañon de Valle comes mainly from Burning Ground Spring. SWSC Spring is a secondary and intermittent source.
- Comparison of average monthly total spring flows (Burning Ground and SWSC) with average E256 gage flows downstream of the flows indicate that for much of the year, water from these two springs supplies a substantial fraction of the channel flow. Small differences between the total lower canyon spring flow and the E256 gauge is probably attributable to local TA-16 overland flow or interflow contributions to the lower canyon.
- Peak surface water flows in the upper canyon and the lower canyon (at E256) are both in April, while the peak flow in the springs is in June. The lag in peak flow in the springs is consistent with subsurface flow contributions from the mountain block. The timing of peak flow at E256 is best explained by direct snowmelt runoff at TA-16 to the lower canyon.

Water chemistry data collected after the May 2000 Cerro Grande and June 2011 Las Conchas fires from springs and alluvial, intermediate, and regional groundwater wells were evaluated to determine if fire-induced changes to water chemistry can be used as a natural tracer of flood waters. Concentration and water level data for this study were obtained from the Intellus New Mexico public database (<http://intellusnm.com/>). Conclusions drawn from this assessment include the following:

- Overall, fire-induced changes to water chemistry were difficult to trace through the groundwater systems.
- Large spikes in calcium concentration occurred in surface water following both fires at Water Canyon above State Route 501 (gauge E252), but responses were only observed at a small number of the groundwater wells.

- R-25 screen 4 showed the clearest indication of a fire-induced flood water response. Following a flood event in May 2005, calcium concentrations in R-25 screen 4 increased by a factor of four; however, it did not respond to the large floods following the Las Conchas fire.

Recharge events have caused water level responses in some perched-intermediate zone wells in the vicinity of the 260 Outfall. Canyon-bottom well CdV-16-1(i) showed a strong snowmelt signal after the Cerro Grande and Las Conchas fires. Alkalinity and water level both increased during the snowmelt period, although this response was only evident during years with relatively high snowfall.

2.10.4 RDX Fate and Transport Studies

Attachment 4 of the Compendium describes an investigation of the physicochemical interactions of RDX with the minerals of the different geologic formations that make up the perched-intermediate zone and regional aquifer beneath TA-16 and their effect on RDX transport and potential degradation. Volcanic and sedimentary rocks used in the investigation included three cores collected at TA-16 and adjacent areas. One core was a sample of the Otowi Member of the Bandelier Tuff obtained from core hole SHB-3 and represents the geology of the perched- intermediate groundwater zone within the Bandelier Tuff. The second core was a sample of the Puye Formation from core hole SHB-3 and represents the portion of the intermediate perched zone that occurs within the Puye Formation. The third core was a sample of the Puye Formation from well R-25 and represents the geology of the regional aquifer.

The investigation used batch experiments to characterize the partitioning of RDX onto both bulk rocks and mineral separates obtained from the three core samples. The transport of both RDX and its degradation products were also characterized using columns packed using the same crushed cores. Geochemical conditions that are representative of the subsurface conditions at TA-16 were used in all experiments, and biotic interactions of the indigenous microbes present in the groundwater were limited by using sterile water and autoclaved samples. The potential for the abiotic degradation of RDX in contact with minerals was also examined. Transport of the degradation products was only examined for the column containing SHB-3 Otowi bulk tuff.

The findings of the investigation are listed below:

- There was little to no sorption of RDX to the sediments used to pack the columns.
- The partitioning coefficients obtained in batch experiments are zero for the bulk Otowi core from SHB-3 and bulk Puye core from R-25. There was some adsorption observed in batch experiments using their mineral separates, which could have been caused by an increased availability of clay surfaces or increased surface area.
- The strongest retardation measured in column experiments occurred in the sample of Puye Formation collected from directly beneath the Bandelier Tuff in core hole SHB-3 ($K_d = 0.18 \text{ L/kg}$). In batch experiments, the largest partitioning coefficient measured was in the finest fraction of this sample (0.70 L/kg), which was dominated by clays
- The K_d calibrated using the RDX column experiment for the SHB-3 Puye sample agrees with results from both the mineral separates and bulk samples of the same materials studied in the batch experiments.

The results from this study suggest that RDX will migrate conservatively through aquifer materials dominated by the Bandelier Tuff. Some retardation might occur in the perched-intermediate groundwater zone and the regional aquifer in beds of the Puye Formation that contain higher clay contents. The results of the column experiment containing SHB-3 Otowi bulk tuff indicates that transport of MNX

(hexahydro-1-nitroso-3,5-dinitro-1,3,5-triazine), DNX (hexahydro-1,3-dinitro-5-nitro-1,3,5-triazine), and TNX (2,4,6-trinitroxylylene) is similar to RDX. It is likely that these degradation products will also transport conservatively throughout the majority of the rocks making up the perched- intermediate groundwater zone and the regional aquifer, although some additional retardation will occur in areas of the Puye Formation with higher clay content.

2.10.5 RDX Biostimulation and Microbial Community Profiling

Attachments 5, 6, and 7 of the Compendium summarize the study of the microbiome in the perched- intermediate groundwater and the regional aquifer and the response of the microbial population to biostimulation under varying geochemical conditions. The investigation characterized the microbial profile of RDX-containing groundwater to determine if microorganisms are playing any active role in RDX degradation. It also examined the potential existence of RDX biodegradation signatures and evaluated the response of endogenous microbes to biostimulation. Additionally, a microcosm experiment was performed to examine how environmental factors such as the availability of oxygen, sediments, and alternate sources of carbon affected RDX degradation. The microbial profile of the microcosms with the most RDX-degrading activity was also determined.

Water samples collected from well CdV-16-4ip in the Puye Formation within perched-intermediate groundwater zone were used for the study. The groundwater is well oxygenated, with oxygen concentrations varying from 7.5 to 8.0 mg/L. The concentration of RDX was about 160 µg/L and the concentrations of the degradation products TNX, MNX, and DNX were typically <1 µg/L. Culturable cell counts as enumerated using Luria-Bertani agar medium were about 3.6×10^2 CFU (colony-forming units)/ml. In contrast, total bacteria counted using hemocytometer was 8.7×10^4 cells/ml.

A total of 98,405 bacterial 16S ribosomal ribonucleic acid (rRNA) gene sequences were recovered for the CdV-16-4ip sample and used for community analyses by Quantitative Insights Into Microbial Ecology (QIIME) software package v1.9.1 (Caporaso et al. 2012, 700548). Operational taxonomic units (OTUs) were assigned by clustering sequences with over 96% sequence identity. The study results were as followed:

- 1605 OTUs distributed in 15 phyla were identified, indicating high microbial diversity in the sample, including genera known to degrade RDX. The groundwater microbiome was dominated by Actinobacteria and Proteobacteria.
- In the 1605 OTUs, 96 bacterial genera were identified. *Rhodococcus* was the most abundant genus (30.6%). A total of 46 OTUs were annotated as *rhodococcus*.
- One OTU comprising 25.2% of total sequences was closely related to a RDX-degrading strain R. erythropolis HS4. A less abundant OTU from the *Pseudomonas* family, closely related to RDX-degrading strain P. putida II-B, was also present.

Biostimulation studies were conducted using acetate and safflower oil amendments. RDX degradation was examined under variable geochemical conditions to determine which factors are most relevant to RDX degradation. The study results were as follows:

- Biostimulation significantly enriched proteobacteria but decreased/eliminated the population of actinobacteria.
- Consistent with RDX degradation, the OTU closely related to the RDX-degrading P. putida strain II-B was specifically enriched in the RDX-degrading samples.

- Acetate amendment stimulated microbial growth, with a stronger effect under microoxic conditions; however, RDX concentrations were not significantly reduced in these samples over 5 weeks.
- A similar effect was observed for safflower oil under microoxic conditions. Even though the microbes grew to densities of 7.9×10^9 cells/ml, no significant RDX degradation was observed.
- Safflower oil enhanced bacterial growth to the same level and promoted RDX degradation under more strict anaerobic conditions.
- Analysis of the accumulation of RDX-degradation products revealed that during active RDX degradation, there was a transient increase in the concentration of the degradation products MNX, DNX, and TNX and 4-nitro-2,4-diazabutanal. The accumulation of these degradation products suggests that RDX is degraded via sequential reduction of the nitro functional biodegradation groups followed by abiotic ring-cleavage.

The results suggest that strict anaerobic conditions are needed to stimulate RDX degradation. Groundwater at TA-16 is characterized by nonreducing conditions, abundant HCO_3^- , and low concentrations of soluble carbon nutrients. These conditions are not optimal for vigorous microbial activity that would lead to RDX degradation by anaerobic respiration or utilization of RDX as a nitrogen source.

Exploratory experiments designed to assess the rate of degradation of RDX contamination in sediments treated by chemical and biostimulant amendments under simulated TA-16 site-specific conditions were performed. Batch and column experiments were used to examine RDX degradation by sediments treated chemically using sodium dithionite, potassium permanganate, and sodium bicarbonate. RDX degradation was also examined in columns packed with sediments and biostimulated by the addition of molasses and safflower oil. The experiments were conducted using representative sediments from the Puye Formation. Groundwater from well CdV-16-4ip was used as the source water for the experiments. The following results were reported:

- RDX degraded within a few hours in all sediment samples treated chemically in batch testing.
- Under continuous flow conditions in columns pretreated with the same chemicals, the sediments treated with sodium dithionite were the only sediments that had a complete RDX degradation.
- All chemical treatments resulted in a transient pulse of elevated dissolved metals and anions, which was attributed to either partial dissolution of the mineral species in the sediments or desorption of adsorbed metals caused by the excessive concentrations of sodium and potassium present in the pretreatment solutions.
- No known degradation products could be identified in the column effluents.
- RDX attenuation capacity in the biostimulated columns was not very high. RDX reached the injection concentration after 6 pore volumes in the molasses column. The column biostimulated by safflower oil clogged after 4 pore volumes.
- Degradation products (MNX and DNX), and TNX were measured in the biostimulated column effluents.
- Low attenuation capacity in the biostimulated columns is attributed to the rapid oxygenation of the columns' sediments in the absence of a carbon substrate.
- Frequent additions of amendments are required to sustain strict anaerobic conditions required for RDX degradation under TA-16 site conditions.

2.10.6 Hydrogeology and Model Calibration for Contaminant Fate and Transport at TA-16

Attachment 8 of the Compendium describes the development of a three-dimensional (3-D) flow and transport model of the vadose zone and upper saturated zone in the vicinity of the Cañon de Valle to serve as a platform for (1) the integration of TA-16 site information and models developed over the past several years and (2) quantitative predictions for the fate and transport of RDX at TA-16. Results are also presented from a blind source separation (BSS) statistical method and an analytical screening-level model.

Preliminary observations from the modeling effort included the following:

- Based on the BSS analysis, four mixed groundwater source types represent the aqueous geochemistries of all the monitoring wells investigated within the RDX site. Further work is needed to refine these conclusions; however, the MBR source and the local TA-16 recharge source represent the two primary “uncontaminated” end-member components.
- The overall mixing ratio between deep MBR infiltration and local TA-16 infiltration is approximately 4:1 for the perched-intermediate end-member, consistent with site geochemical constraints.
- There are no indications that additional groundwater source types are required to explain R-18 concentration measurements, suggesting that a separate TA-9 source (groundwater type) is not necessary to explain the data. Results from the analytical screening tool (the pipes-and-disks model) also suggest that a single source can be used to explain R-18 and R-68 data assuming groundwater velocities are small in the area.
- R-68 and R-18 have different mixing signatures and contaminant concentrations; however, these wells are probably located along the same regional aquifer groundwater flow pathway. The higher RDX concentrations in well R-68 are occur because of higher local recharge/MBR mixing ratios. Differences in the mixing ratios between the two wells will result in either greater RDX contamination in R-68 from local recharge sources and/or contaminant dilution in R-18 because of MBR.

The preliminary calibrated 3-D vadose zone/source zone model depicts the emerging arrival of a relatively small portion of the total RDX mass to the regional aquifer, with the majority of the contaminant mass predicted to still be in the vadose zone where it has the potential to remain a source to the regional aquifer for decades.

2.10.7 Tracer Study

Attachment 9 of the Compendium describes tracer tests that were conducted to test connectivity of various parts of the TA-16 hydrological system and how that might affect HE transport. Large-scale tracer deployments were made in November 2015 in wells R-25b, CdV-9-1(i) (screen 1, piezometer 1, and piezometer 2), and CdV-16-1(i). Tracers were monitored on a quarterly basis through December 2017 in these wells and in perched-intermediate wells CdV-16-2(i)r, CdV-16-4ip, and R-47i, as well as in regional aquifer wells R-18, R-25, R-47, R-48, R-58, and R-63. This investigation also includes results from higher frequency sampling during pump tests and high-water level periods in some wells. (Noted that monitoring for the tracer chemicals breakthrough continues and the results reported in the “Annual Progress Report for the Corrective Measures Evaluation for the Deep Groundwater Investigation for Consolidated Unit 16-021(c)-99” (N3B 2018, 700127).

Tracers were introduced into the injection wells, and periodic sampling measured their dilution trends under ambient flow conditions. A group of naphthalene sulfonates was determined as most suitable for the tests. The tracers 1,5-disulfonate (NDS) and 1,6-NDS were injected into CdV-16-1(i) and R-25b, respectively. Four tracers were deployed in well CdV-9-1(i): 1,3,6-trisulfonate (NTS) in PZ-1; 1,3,5-NTS in PZ-2; and 2,6-NDS and bromide in screen 1. Because of the small-diameter configuration, the two piezometers could not be sampled after tracer deployment, and only screen 1 was monitored.

The large-scale tracer tests showed the following results:

- There were clear dilution effects in all three deployment wells.
- Implied rates based on concentration differences suggest the groundwater flow velocity at R-25b is much lower than the flow velocity at CdV-16-1(i).
- Flow velocity in CdV-9-1(i) is greater than the flow velocity at CdV-16-1(i).
- Pump tests in CdV-9-1(i) and CdV-16-1(i) affected the deployed tracers in these wells, removing some of the mass from the groundwater in the vicinity of these wells. The effects in CdV-9-1(i) were minor in terms of mass removed and affected only bromide and the tracers introduced into the piezometers.
- The test in CdV-16-1(i) showed a more substantial effect, with removal of an estimated 29% of the original tracer mass during the aquifer test.

The spatially variable flow conditions implied by the large-scale tracer results support the idea of a heterogeneous flow system as described by the TA-16 conceptual model.

Another key result is that tracers from both CdV-9-1(i) PZs have been detected in CdV-9-1(i) screen 1, and that large pulses of PZ tracers arrived in screen 1 in spring 2017. The relatively large concentration increases of the two PZ tracers in spring 2017 are clearly linked to increases in water levels observed in multiple wells in the TA-16 area, including the CdV-9-1(i) PZs. The implication is that snowmelt/springtime recharge to the shallower PZ zones facilitated a downward transport pulse to screen 1. Concentrations of both tracers peaked and declined rather rapidly. Although PZs 1 and 2 are separated by about 200 ft, the two PZ tracers arrive in screen 1 almost simultaneously, and concentrations increase and fall off again at the same time. Arrival of PZ tracers in screen 1 clearly demonstrates vertical flow path connections, although it is unclear whether these detections represent naturally occurring flow conditions or if they are the result of short-circuiting along the well bore or in the adjacent damaged zone (from drilling).

The large-scale tracer tests are still under way, and continued tracer monitoring is being conducted to quantify the complete dispersal behavior of tracers from the wells where they were deployed and to observe any potential transport to downgradient monitoring wells. So far, no credible cross-well detections have been observed. It has taken some time for the tracers to move beyond the vicinity of the deployment screens.

In November 2018, the Laboratory submitted an update on the results from tracer monitoring (N3B 2018, 700127). The update concluded that most of the tracers had not yet fully moved beyond the vicinity of the screens where they were deployed and no cross-well detections have occurred. As of third quarter of FY 2019, there has been no observation of tracers beyond the injection wells. The tracer data are provided in Appendix C.

3.0 CONCEPTUAL SITE MODEL

3.1 Nature and Extent

This section describes the nature and extent of inorganics, organics, and radionuclides in the intermediate and regional wells. The nature and extent of RDX was last assessed in the “Investigation Report for Water Canyon/Cañon de Valle,” with RDX being the primary COPC (LANL 2011, 207069). To verify if this remains the case, data from January 2000 to March 2019 (provided in Appendix D) underwent a screening assessment consistent with the process prescribed in the IFGMP (N3B 2018, 700000). Per the IFGMP process:

Regulatory criteria related to groundwater quality form the basis for the screening values to which groundwater monitoring results are compared in this report. These criteria include the NMWQCC groundwater standards, EPA MCLs, EPA regional screening levels for tap water, and NMED screening levels for tap water. These criteria are used to screen results in accordance with the process specified in Section IX of the 2016 Consent Order

For each individual substance, the lower of the NMWQCC groundwater standard of EPA MCL is used as the screening value.

If the NMWQCC groundwater standard or an MCL has not been established for a specific substance for which toxicological information is published, the NMED screening level for tap water is used as the groundwater screening value. NMED screening levels are established for either a cancer- or noncancer-risk type; for the cancer-risk type, screening levels are based on a 10^{-5} excess cancer risk.

If the NMED screening level for tap water has not been established for a specific substance for which toxicological information is published, the EPA regional screening level for tap water is used as the groundwater screening value. The EPA screening levels are established for either a cancer- or noncancer-risk type. For the cancer-risk type, the Consent Order specifies screening at a 10^{-5} excess cancer risk. The EPA screening levels for tap water are at 10^{-6} excess cancer risk; therefore, 10 times the EPA 10^{-6} screening levels are used in the screening process.

This screening assessment was prepared using the May 2019 EPA regional screening levels for tap water, the NMWQCC groundwater standards published December 21, 2018, and the NMED tap water screening levels specified in the March 2019 Table A-1 of the Risk Assessment Guidance for Site Investigations Remediation.

The NMWQCC groundwater standards apply to the dissolved (filtered) portion of specified contaminants; however, the standards for mercury, organic compounds, and nonaqueous-phase liquids apply to the total unfiltered concentrations of the contaminants. For this report, EPA MCLs are applied to both filtered and unfiltered sample results.

The dataset evaluated to screening values included the following filters: (1) sample purpose-regular (REG); (2) sample type- water (W) and groundwater (WG); (3) best value- yes; and (4) sample usage code- investigation (INV) or blank. No screening values, test data, or field duplicates were included in the dataset.

If an analyte was detected but did not exceed its respective criteria, it was not considered a COPC. If there was no regulatory criteria for a specific substance, then no screening was performed. For each analyte exceeding its respective criteria, further evaluation is done by assessing the frequency of detection for that analyte. If the analyte exceeds its respective criteria but its frequency of detection is <10%, the analyte is not considered a potential COPC. If the analyte is detected above its respective criteria and its frequency of detection is >10%, additional assessment is done to determine if it is a COPC. Each analyte detected above its respective criteria is discussed below.

Water samples collected and analyses performed by the analytical laboratories are presented in Table 3.1-1a and 3.1-1b, the data are provided in Appendix D. Sampling locations are presented in Table 3.1-2 and Figure 1.0-3. The discussions in this report are similar to those presented in earlier investigation reports, particularly the RFI reports for the 260 Outfall (LANL 1998, 059891; LANL 2003, 077965; LANL 2011, 207069), with new data primarily being highlighted when these data modify the existing CSM for contaminant transport.

Section 3.1.1 describes the screening process and presents the results. Section 3.1.2 presents an analysis of the March 2019 groundwater monitoring cation and anion data. Both sections support the CSM, described in Section 3.2.

3.1.1 Groundwater Chemical Screening Assessment

Intermediate and regional groundwater samples were screened, as described above, for all perched-intermediate and regional well locations within and immediately adjacent to the Cañon de Valle/ Water Canyon watershed. Only investigation sample data were used; test, screening, waste, or quality assurance data were not included in the screening dataset. These locations are listed in Table 3.1-2. Inorganic and organic chemicals were first assessed by the frequency of detection and if the concentration exceeded the screening standard. Chemicals that exceeded standards are discussed in detail in the following subsections.

3.1.1.1 Inorganic Constituents

Inorganic constituents detected above standards include beryllium, chromium, cobalt, iron, manganese, nickel, nitrate-nitrite, and thallium (Table 3.1-3). Concentrations of these inorganic constituents tend to be highly variable in any individual location, with few localities showing consistently elevated values (Attachment D-1 to Appendix D). Several (e.g., beryllium, chromium, and nitrate) only exceeded the standard for a single sample. In general, most inorganic concentrations that exceeded standards were associated with reducing conditions at some of the Westbay well screens. Many of these wells are being reconfigured to remove the Westbay systems and replace them with Baski sampling systems.

Beryllium was detected in 3% of the filtered groundwater samples, with only one sample exceeding the screening level of 4 µg/L (Table 3.1-3). The sample was collected from well R-25 screen 4 in 2001 and had a concentration of 10.1 µg/L. No other beryllium results exceeded the standard since this single event. Beryllium is not considered a COPC.

Chromium was detected in 38% of the filtered groundwater samples, with only one sample exceeding the screening level of 50 µg/L (Table 3.1-3). The sample was collected from well R-25 screen 1 in 2016 and had a concentration of 3080 µg/L. No other chromium results exceeded the standard. Chromium is not considered a COPC.

Cobalt was detected in 14% of the filtered groundwater samples, with four samples exceeding the screening level of 50 µg/L (Table 3.1-3). The maximum concentration (95 µg/L) was from a sample

collected at R-26 PZ-2 in 2015. No other samples from R-26 PZ-2 have exceeded the standard. The other three exceedances occurred in well R-25. There were two exceedances in R-25 screen 2, one in 2012 and one in 2016. R-25 screen 1 had one exceedance in 2016. Cobalt is not considered a COPC.

Iron was detected in 28% of the filtered groundwater samples, with 32 samples exceeding the screening level of 1000 µg/L (Table 3.1-3). The maximum concentration (29300 µg/L) was from a sample collected at R-25 screen 1 in 2016. The other locations that exceeded the screening level include R-17, R-25 screen 2, R-25 screen 4, R-25 screen 8, R-19 screen 3, R-19 screen 5, CdV-R-37-2 S2, R-25b, and R-26 PZ-2. R-25, R-19, and CdV-R-37-2 were Westbay wells. CdV-R-37-2 has since been converted to a dual screen well with a Baski sampling system and has not reported elevated iron since the well was converted. The exceedances in R-17, R-25b, and R-26 PZ-2 were all single samples with concentrations above the screening level. Iron is not considered a COPC.

Manganese was detected in 45% of the filtered groundwater samples, with 39 samples exceeding the screening level of 200 µg/L (Table 3.1-3). The maximum concentration (3720 µg/L) was from a sample collected at CdV-R-37-2 screen 2 in 2003. The other locations that exceeded the screening level include R-25 screen 1, R-25 screen 2, R-25 screen 5, R-19 screen 5, R-29, and R-26 PZ-2. R-25, R-19, and CdV-R-37-2 were Westbay wells, and the high manganese and iron concentrations are associated with reducing conditions within the screened interval. The exceedance in R-29 was a single sample above the screening level in 2010, and R-26 PZ-2 reported exceedances in 2015 and 2016. Manganese is not considered a COPC.

Nickel was detected in 67% of the filtered groundwater samples, with 13 samples exceeding the screening level of 200 µg/L (Table 3.1-3). The maximum concentration (7520 µg/L) was from a sample collected at R-25 S1 in 2016. The other location that exceeded the screening level was R-25 screen 2. Both locations are screens in Westbay well R-25. Nickel is not considered a COPC.

Nitrogen as Nitrate-Nitrite was detected in 92% of the filtered groundwater samples, with only one sample exceeding the screening level of 10mg/L (Table 3.1-3). The sample was collected from well R-19 screen 4 in 2010 and the concentration was 793,000 µg/L. No other nitrate results exceeded the standard since this single event. Nitrate is not considered a COPC.

Thallium was detected in 8% of the filtered groundwater samples, with four samples exceeding the screening level of 2 µg/L (Table 3.1-3). The maximum concentration (5.2 µg/L) was from a sample collected at R-25 S4 in 2000. There was one other exceedance in R-25 screen 4 in 2001. R-25 screen 1 had one exceedance in 2001 and R-25 S5 had one exceedance in 2000. Thallium is not considered a COPC.

3.1.1.2 Organic Chemicals

Organic chemicals were historically used as solvents and process components for nuclear weapons research and production at TA-16 and are present in perched-intermediate and regional groundwater.

Because no groundwater background values are available for organic chemicals, all organic chemicals that exceed a criteria are discussed in terms of detection frequency, occurrence, and exceedance of screening values.

Of the 257 organic compounds analyzed in groundwater between 2000 and 2019, 63 compounds were detected. Table 3.1-4 lists the frequency of detection for organic chemicals. Many of the detections of other organic chemicals, solvents in particular, were collocated with detections of RDX, suggesting a broadly similar contaminant CSM for release sites and pathways.

The organic chemicals detected at a frequency >10% include HEs (RDX, HMX, and trinitrobenzene[1,3,5-]), HE breakdown products (amino-2,6-dinitrotoluene[4-], MNX, TNX, DNX, and amino-4,6-dinitrotoluene[2-]), solvents (tetrachloroethene, trichloroethene, and toluene), and methyl tert-butyl ether (MTBE) (Table 3.1-4). Tetrachloroethene, trichloroethene, and toluene are recognized contaminants associated with operations at Consolidated Unit 16-021(c)-99 and the 340 Complex in TA-16 (LANL 2006, 092717). MTBE is a common gasoline additive, and its localized frequent detections in perched-intermediate groundwater may be an indicator of an historical fuel spill.

Of the 63 detected compounds, only 5 exceed screening criteria: bromodichloromethane, nitrosodimethylamine[N-], phenol, RDX, and tetrachloroethene. Only RDX was detected frequently and at multiple locations.

Bromodichloromethane was detected in 1% of the groundwater samples, with only two samples exceeding the screening level of 1.34 µg/L (Table 3.1-4). The maximum concentration was 16.2 µg/L. The sample was collected from well CdV-R-37-2 screen 2 in 2015, and there have not been any detections in subsequent samples collected. The other location was R-25b, with a concentration of 2.18 µg/L in 2016. Bromodichloromethane is not considered a COPC.

Nitrosodimethylamine[N-] was detected, with only one sample exceeding the screening level of 0.00491 µg/L (Table 3.1-4). The sample was collected from well R-47 in 2016 and the concentration was 1.57 µg/L. No other nitrosodimethylamine[N-] results exceeded the standard since this single event. Nitrosodimethylamine[N-] is not considered a COPC.

Phenol was detected, with only one sample exceeding the screening level of 5 µg/L (Table 3.1-4). The sample was collected from well R-17 screen 1 in 2007 and the concentration was 15.8 µg/L. No other phenol results exceeded the standard since this single event. Phenol is not considered a COPC.

Tetrachloroethene was detected in 28% of the groundwater samples, with only one sample exceeding the screening level of 5 µg/L (Table 3.1-4). The sample was collected from well 16-26644 in 2011 and the concentration was 5.03 µg/L. No other tetrachloroethene results exceeded the standard since this single event. Tetrachloroethene is not considered a COPC.

RDX was detected in 49% of the groundwater samples, with 164 samples exceeding the screening level of 9.66 µg/L (Table 3.1-4). RDX is selected as the primary HE COPC for the following reasons:

- RDX is present at greater concentrations than the other HE, so it is detected in more locations than the other HE.
- RDX was discharged in large quantities at virtually all of the major HE-processing facilities at TA-16.
- RDX breaks down relatively slowly in the environment, so it tends to define HE releases more widely than other constituents.
- RDX is a relatively conservative constituent (it does not interact strongly with environmental materials, such as clay minerals), so it is more widely distributed than many other HE that are less conservative.
- RDX is typically collocated with other HE.
- RDX is moderately soluble in water (approximately 40 mg/L at room temperature), so it is mobilized by exposure to water, as is present during HE machining.

- RDX has one of the lowest screening levels (9.66 µg/L in groundwater) for the HE analyte suite because it is classified as a possible human carcinogen.

RDX trends for surface system, intermediate, and regional hydrologic systems

This section details concentrations and trends of RDX in the surface system inclusive of springs, baseflow, and alluvial wells as well as in the intermediate and regional aquifers.

RDX in the Surface System

Figure 3.1-1 shows the RDX time-series trends for springs, baseflow, and alluvial wells, and Table 3.1-5 lists the mean, most recent values, concentration range, and results from the Mann-Kendall trend analysis of the RDX concentrations. RDX concentrations for SWSC Spring (mean RDX 51 µg/L), Burning Ground Spring (mean RDX 20 µg/L), and Martin Spring (mean RDX 98 µg/L) all show decreasing trends per Mann-Kendall trend analysis, but are all above the RDX screening level of 9.66 µg/L (Figure 3.1-1, Table 3.1-5). RDX concentrations in the Cañon de Valle baseflow monitoring point below MDA P shows concentrations generally less than the NMED tap water screening level of 9.66 µg/L except at Cañon de Valle below MDA P (E256), with occasionally higher concentrations associated with wet periods (Figure 3.1-1). There are no trends in RDX concentrations for the baseflow location, based on the Mann-Kendall trend analysis (Table 3.1-5).

The most recent RDX concentrations in alluvial groundwater are less than the NMED screening value of 9.66 µg/L, except at CDV 16-02657r and no alluvial wells show increasing trends based on Mann-Kendall trend analysis (Figure 3.1-1, Table 3.1-5). Occasionally during the past 15 years of monitoring, there have been higher concentrations of RDX (>50 µg/L) observed in alluvial monitoring wells downstream of the 260 Outfall, and these transient values were associated with spring snowmelt wet periods.

RDX in Shallow Bedrock and Perched-Intermediate Groundwater

Perched groundwater zones at TA-16 contain RDX, in most cases at levels above the NMED tap water screening level of 9.66 µg/L. Perched groundwater contaminated with RDX includes shallow bedrock perched groundwater (<200-ft depth) in the upper vadose zone (well 16-26644); and perched-intermediate groundwater (>600-ft depth) in R-25 (screens 1, 2, and 4), CdV-9-1(i) S1, CdV-16-1(i), CdV-16-2(i)r, and CdV-16-4ip 1 screen 1 (Figure 1.0-3).

Figure 3.1-2 shows the RDX time series trends for perched-intermediate zone monitoring wells, and Table 3.1-5 lists the mean, most recent values concentration range, and results from the Mann-Kendall trend analysis of the RDX concentrations. The estimated extent of RDX in perched-intermediate groundwater is shown in Figure 3.1-3. RDX concentrations and temporal trends are variable within this group of perched-intermediate wells. RDX concentrations increase with time in wells R-25 screen 2 (mean RDX 8 µg/L), CdV-16-2(i)r (mean RDX 84 µg/L) and R-25 screen 4 (mean RDX 14 µg/L) (Table 3.1-5 and Figure 3.1-2). RDX concentrations in well CdV-16-1(i) (mean RDX 28.1 µg/L), 16-26644 (mean RDX 11 µg/L), CdV-16-4ip S1 (mean RDX 133 µg/L) show no temporal trend, and wells R-25 screen 1 (mean RDX 42.5 µg/L), CdV-9-1(i) screen 1 (21), and R-25b (mean RDX 3 µg/L) show decreasing trends (Table 3.1-5 and Figure 3.1-2). Well R-25b also shows residual impacts from the 2015 tracer deployment (LANL 2018, 602963). RDX was not detected at wells CdV-37-1(i), R-26 PZ-2, R-26 screen 1, 63i, and R-47i for the period of record. RDX concentrations are significantly greater in the upper perched-intermediate zone (wells CdV-16-4ip screen 1, CdV-16-2(i)r, CdV-16-1(i), and CDV-9-1(i) screen 1) relative to the lower perched zone (wells R-25 screen 4 and CdV-16-4ip screen 2).

RDX concentrations in perched-intermediate groundwater are variable, with the highest RDX values occurring in CdV-16-4ip screen 1 ($>100 \mu\text{g/L}$), which is located in the upper perched-intermediate zone within the Puye Formation. At nearby wells completed in the same formation (CdV-16-1[i]; CdV-16-2[i]; R-25 screen 1, 2; R-25b), RDX concentrations are typically a factor of 2 lower than those in CdV-16-4ip screen 1 (Figure 3.1-2). There are no obvious systematic relations between these concentration variations and screened interval. These observations suggest RDX-bearing groundwater recharges the upper perched zone in the Puye Formation along multiple discontinuous pathways through the vadose zone, such as fracture zones or preferential pathways, rather than by a single RDX recharge pathway.

RDX in Regional Groundwater

RDX is detected in regional groundwater in wells R-18, R-25 (screens 5 and 6), R-63, R-68, and R-69. Figure 3.1-2 shows the RDX time-series trends for the regional zone monitoring wells (except R-69 since there is insufficient data to develop a time-trend analysis), and Table 3.1-5 lists the mean, most recent values, concentration range, and results from the Mann-Kendall trend analysis of the RDX concentrations. Well R-18 (mean RDX $2 \mu\text{g/L}$), R-63 (mean RDX $1.5 \mu\text{g/L}$), and R-68 (mean RDX $14 \mu\text{g/L}$) show increasing RDX trends. R-25 screen 5 (mean RDX $2 \mu\text{g/L}$) show consistent detections of RDX with no concentration trend. Newly installed well R-69 has only been sampled with the permanent sampling system since January 2019. Based on the first five samples the mean RDX concentration of screen 1 is $14 \mu\text{g/L}$ and screen 2 is $18 \mu\text{g/L}$. Regional wells R-47, R-48, R-58, CdV-R-15-3 screen 4, and CdV-R37-2 screen 2 do not show RDX concentration for the period of record. Table 3.1-5 lists the mean, most recent values, concentration range, and trend of the RDX concentrations.

RDX is present at levels greater than the $9.66 \mu\text{g/L}$ tap-water screening level for drinking water in wells R-68 and R-69 and greater than half the screening level in well R-18. Figures 3.1-4 and 3.1-5 illustrate a cross-sectional view and plan view of the RDX in the regional aquifer, respectively. The RDX contour plots in these plots are based on the current well network, regional groundwater gradients, and process knowledge that the primary source of RDX is the 260 Outfall and downgradient infiltration zones in Cañon de Valle. The extent of RDX in the regional aquifer is well constrained by regional monitoring wells for the south and east parts of the RDX plume depicted in Figures 3.1-4 and 3.1-5. The west and north parts of the plume are largely unconstrained because of a lack of regional monitoring wells in those areas. The occurrence of RDX above standards in both R-68 and R-69 is one of the most significant developments since the 2011 Investigation Report and potential pathways are discussed further in Section 3.2.

The regional groundwater zone contains between 35 and 415 kg of RDX according to inventory performed in 2017 (LANL 2018, 602963). With the installation of wells R-68 and R-69, the RDX inventory in the regional aquifer was updated for this report. The new RDX inventory estimate, which is described in Appendix E, is 18.4 kg within the whole plume area and 15.3 kg within the area defined by the $10\text{-}\mu\text{g/L}$ contour based on a three-dimensional model of the plume based on Figures 3.1-4 and 3.1-5. The three-dimensional model considered concentration contours on the plane of the water table and on a longitudinal cross-section connecting R-25 and R-18. The two planes were used to characterize the plume in three dimensions. The resulting three-dimensional RDX plume concentrations were gridded at a 2 m-wide x 2 m-long x 2 m-deep cell resolution within the $10\text{-}\mu\text{g/L}$ contour, multiplied by pore volume (bulk volume times porosity), and summed to estimate total inventory $>10 \mu\text{g/L}$. The average porosity over the plume was assumed to be 27% based on analysis of Puye Formation data. The bulk volume within the $10\text{-}\mu\text{g/L}$ contour was calculated to be 4.77 billion liters based on the three-dimensional concentration model.

The 2017 inventory estimate assumed RDX concentrations were defined by a large triangle extending eastward of the 260 Outfall, and the inventory estimate was based on a bulk volume of 74 billion liters

and an average porosity between 18% and 33%. In contrast, this report uses updated information, data, and methodologies that result that resulted in a smaller contour-based plume depiction. The decrease in the inventory estimate compared to previous results is primarily due to the smaller plume representation. Appendix E provides a discussion of the methodology used to generate the updated RDX inventory estimate for this report.

3.1.1.3 Radionuclides and Radioactivity

Radionuclide detections in intermediate and regional groundwater are listed in Table 3.1-6. Only radium-226 and radium-228 have NMED screening levels.

Radium-226 was detected in 28% of the unfiltered groundwater samples, with four samples exceeding the screening level of 5 pCi/L (Table 3.1-6). The maximum value (43.8 pCi/L) was from a sample collected at R-19 screen 4 in 2004. R-19 S3 also reported a single result above screening level (10.4 pCi/L) in 2004. No other samples from R-19 have exceeded the standard. The other two exceedances occurred in well R-18 and R-26 screen 1, both in 2005. Radium-226 is not considered a COPC.

Radium-228 was detected in 19% of the unfiltered groundwater samples, with only one sample exceeding the screening level of 5 pCi/L (Table 3.1-6). The sample was collected from well R-25 screen 8 in 2007 and the value was 14.5 pCi/L. No other radium-228 results exceeded the standard since this single event. Radium-228 is not considered a COPC.

Uranium-234 and uranium-238 were detected in 98% of the unfiltered samples. Tritium was detected in 40% of the samples and at 26 of 34 monitoring locations. Tritium was detected in 100% of the samples at 16-26644, CdV-16-1(i), CDV-16-4ip screen 1, CDV-9-1(i) S1, R-25 screen 3, R-25 screen 6 (Table 3.1-6).

Bismuth-214 was detected in 35% of the samples and at 6 of 17 monitoring locations. Bismuth-214 was detected once at the following locations with no repeated detections: R-18, R-19 screen 4, R-25 screen 7, R-25 screen 8, R-26 screen 1, and R-63.

Lead-214 was detected in 18% and at 3 of 17 monitoring locations. Lead-214 was detected once at the following locations with no repeated detections: R-19 screen 4, R-25 screen 7, and R-63.

Strontium-85 was detected in 13% and at 2 of 16 monitoring locations. Strontium-85 was detected once at the following locations with no repeated detections: R-25 screen 1 and R-25 screen 7. Radionuclides are not considered COPCs.

3.1.2 Major-Ion Characteristics of Waters in Different Hydrologic Zones

The major-ion characteristics of waters in the surface system inclusive of springs, baseflow, and alluvial wells, intermediate aquifer, and regional aquifer were analyzed to determine differences and similarities within the respective zones. Trilinear (Piper) plots are commonly used to identify waters with similar chemistries that plot in a distinct position on the Piper plot or that appear to be evolving along similar paths. Relative percentages of major cations and major anions (expressed in milliequivalents (meqs) per liter) are plotted on separate ternary plots. Major cations are calcium (Ca^{+2}), magnesium (Mg^{+2}), and sodium (Na^{+}) + potassium (K^{+}). Major anions are generally chloride (Cl^{-}), sulfate (SO_4^{-2}), and bicarbonate (HCO_3^{-}) + carbonate (CO_3^{-2}). Points plotted on the two ternary plots are then projected upwards where they intersect on the central diamond. Figure 3.1-6 is the trilinear plot for springs, surface water, alluvial groundwater, perched-intermediate groundwater, and regional groundwater. The most recent results for each monitoring location are plotted.

The surface system comprising the Cañon de Valle springs, baseflows, and alluvial wells are similar to each other and plot in separate compositional fields from the perched-intermediate and regional wells (Figure 3.1-6). Differences in water chemistry between the surface waters and perched-intermediate and regional groundwater probably reflect the different rock-water interactions affecting these waters. Water associated with springs, baseflow, and alluvial wells interacts primarily with rhyolitic Bandelier Tuff, whereas flow paths for deeper groundwater include greater interaction with dacitic rocks of the Puye and Tschicoma Formations. Well 16-26644, which taps shallow bedrock groundwater in the Tshirege Member, is chemically similar to the surface system. Fishladder Canyon alluvial well FLC-16-25280 has distinct $\text{HCO}_3^- + \text{CO}_3^{2-}$, and Cl^- signature, and CDV-16-611937 has very high Cl^- and lower $\text{HCO}_3^- + \text{CO}_3^{2-}$ compared to other Cañon de Valle alluvial wells. This indicates there is some spatial heterogeneity in the alluvial system in the study area.

The perched-intermediate wells form two distinct chemical groups in the trilinear diagram (Figure 3.1-6). The water chemistry in one group, including wells CdV-16-2ir, CdV-16-4ip screen 1, CdV-16-4ip screen 2, and R-26 screen 1, R-47i, is the same as that found in the regional aquifer wells. The similarity in water chemistries supports the conceptual model that much of the perched-intermediate groundwater was derived from regional groundwater that was diverted into the vadose zone beneath the mountain block. The second perched-intermediate group, including wells CdV-9-1i, CdV-16-1i, R-25 screen 1, and R-25 screen 4, has water chemistry that is intermediate between surface water and regional groundwater end members. Groundwater in the second perched-intermediate group is probably largely derived from regional groundwater beneath the mountain block, but it may be mixed with a higher proportion of local recharge from Cañon de Valle and TA-16 mesa tops. The water chemistry in well R-25b is anomalous compared other perched-intermediate wells. The anomalous chemistry of R-25b water is probably the residual effect of disulfonate tracer injected in the well during the 2015 tracer study.

The regional wells plot together within a tight compositional range on the trilinear plot with the exception of R-25 screen 5 and R-25 screen 6 (Figure 3.1-6). The close clustering of regional well chemistry supports the conceptual model in that the mountain block is the dominant source of recharge for the regional aquifer and that rock/water reactions are similar along mountain block infiltration pathways. R-25 screen 5 and R-25 screen 6 contain slightly more Ca^{2+} and slightly less $\text{Na}^+ + \text{K}^+$, and $\text{HCO}_3^- + \text{CO}_3^{2-}$ than other regional groundwater.

Stiff diagrams are another method to illustrate the relative concentrations of major cations (Ca^{2+} , Mg^{2+} , and Na^+ , and K^+) to major anions (Cl^- , SO_4^{2-} , HCO_3^- , and CO_3^{2-}) in water samples. Figures 3.1-7, 3.1-8, and 3.1-9 present stiff diagrams for the surface system inclusive of springs baseflow and alluvial wells, intermediate wells, and regional wells respectively. The delineation of separate chemical groups in the stiff diagrams is similar to the groupings described above for the piper diagram. The surface system exhibits the most variability within plots. Some intermediate wells are distinct and others are very similar to regional wells as noted above. The regional wells show remarkably similar cation and anion composition with the exception of R-25 screen 5 and R-25 screen 6 as noted above. The benefit of the stiff diagrams is that individual signatures of the wells can be easily identified.

The following CSM discussion focuses on the fate and transport of RDX because it is the principal contamination affecting perched-intermediate and regional groundwater underlying the TA-16 area. Environmental sampling indicates the most significant source of RDX in the watershed was Consolidated Unit 16-021(c)-99, which included building 16-260. Building 16-260 released thousands of pounds of HE (primarily RDX and HMX) to Cañon de Valle through the 260 Outfall (Figure 1.0-21).

3.2 Updated Conceptual Site Model

This section summarizes the main elements of the physical system CSM that describe the fate and transport of HE in the TA-16 area. The discussion is largely based on the CSM presented in the “Investigation Report for Water Canyon/Cañon de Valle” (LANL 2011, 207069) that is modified to include new and updated information collected since 2011. Figure 3.2-1 is an east-west geologic cross section, and Figure 3.2-2 is a block diagram that illustrates key aspects of the physical system CSM. The conceptual model is described in terms of increasing depth, progressing from the surface to the regional aquifer.

3.2.1 Surface Water Pathways

HE was initially released from mesa-top locations and transported in drainages as solid particulates and/or dissolved in water or adsorbed onto sediment particles and solid organic material. Deposition of a significant inventory of contaminants occurred in mesa-top settling ponds or in sediments in small drainages near outfalls (Figure 3.2-2). Soils and sediments stored in ponds and drainages act as a secondary source of contaminants that are remobilized by snowmelt and storm runoff. Infiltration of surface water at ponds and beneath drainages transports soluble contaminants to shallow bedrock groundwater in the upper Tshirege Member, 100 to 200 ft beneath the mesa. Infiltration is predominately via fast pathways such as fractures and surge beds (high-porosity beds within the Bandelier Tuff). Such transport results in the deposition of RDX within the vadose zone, which represents a secondary source for deeper subsurface perched-intermediate and regional groundwater. The two SWMUs associated with Consolidated Unit 16-021(c)-99 are considered the largest source of subsurface RDX, and its estimated mass of RDX in the vadose zone beneath the former pond, outfall area, drainage channel, and surge bed below the pond is between 545 kg and 940 kg of RDX (LANL 2018, 602963).

Much of the RDX released from the 260 Outfall was transported to Cañon de Valle by surface-water flow and sediment transport (Figure 3.2-2). In Cañon de Valle, RDX occurs as solid particulates or is adsorbed onto sediment and organic particles in the streambed. These contaminants are redistributed by floods that scour the streambed and mobilize the bed sediment. RDX associated with coarse-size fractions (coarse sand and coarser) is generally transported as bed load along the streambed, whereas contaminants associated with fine-size fractions (fine sand and finer) are generally transported in suspension. During floods, sediment from a variety of sources, much of it not contaminated with RDX, is mixed, generally diluting RDX concentrations longitudinally along the channel. The net result is a general downcanyon decrease in RDX concentrations in sediment with distance from a contaminant source area (LANL 2011, 207069). The estimated mass of RDX stored in Cañon de Valle sediments is between 5 and 10 kg (LANL 2011, 207069) (LANL 2018, 602963).

Under base-flow conditions, surface-water transport of RDX is limited to relatively small segments of Cañon de Valle, Fishladder Canyon, and S-Site Canyons. Intermittent or ephemeral flow during snowmelt and storm runoff causes seasonal flow over larger portions of the watershed. In Cañon de Valle, surface water is ephemeral in much of the canyon due to infiltration losses in the mountain block and mountain-front areas of upper Cañon de Valle. Discharges from SWSC and Burning Ground Springs result in perennial surface-water flow in Cañon de Valle from the 260 Outfall to MDA P, but flow rates are low and infiltrate the canyon floor alluvium and underlying bedrock tuffs (Figures 3.2-1 and 3.2-2).

Similarly, Fishladder and S-Site Canyons flow over short distances in response to spring discharge and alluvial groundwater discharge, but flow is ephemeral along most of the length of these canyons and occurs primarily during storm events (Figure 3.2-2). Under current conditions, the perennial surface-water reach in Cañon de Valle is 0.3 mi to 0.6 mi long. The maximum extent of persistent surface water in

Cañon de Valle was probably greater in the 1950s to early 1990s when natural surface flow was augmented by effluent that was routinely discharged into the canyon from the 260 Outfall. Ephemeral or intermittent runoff from storm events and snowmelt occasionally causes Cañon de Valle to flow into Water Canyon and surface water to flow as far east as the eastern Laboratory boundary. During large runoff events, surface water can reach the Rio Grande, but these events are infrequent. From 1999 to 2019 there have been 36 events with potential to reach the Rio Grande, as measured from Gage Station E265 (Water Canyon below New Mexico State Road 4). These events are measured >5 cfs (cubic feet per second) at the gage station. This is the same standard used at the lower Los Alamos and Pueblo Canyon gages to determine potential to reach the Rio Grande. On average, there are about 2 events per year, but there were 10 events in the first year after Cerro Grande fire and 4 events the following year. In the last few dry years, there have been zero events.

3.2.2 Vadose Zone Pathways

The vadose zone at TA-16 is approximately 1280 ft thick beneath mesa tops and 1080 ft thick beneath Cañon de Valle. The following discussion divides the vadose zone into upper and lower parts. The upper vadose zone extends from the surface to a depth of about 600 ft and is made up of thick deposits of variably welded Bandelier Tuff and interbedded Cerro Toledo fluvial deposits. The upper vadose zone includes thin zones of shallow bedrock-perched groundwater within 200 ft of the surface. The lower vadose zone extends from a depth of 600 ft to the top of the regional aquifer (1280 ft) and includes the lowermost deposits of the Bandelier Tuff as well as thick fluvial sediments of the Puye Formation. Significant zones of RDX-containing perched-intermediate groundwater occur in the lower vadose zone.

3.2.2.1 Upper Vadose Zone

Infiltration of surface water and alluvial groundwater into bedrock units results in the vertical transport of RDX into the upper vadose zone. Water percolation into bedrock is greater beneath the canyon floors than mesa tops because surface water flow and alluvial groundwater provide hydrologic drivers for infiltration. The estimated mass of RDX in the vadose zone beneath Cañon de Valle is between 8 kg and 64 kg, but the lack of concentration data in the vadose zone make these estimates uncertain (LANL 2018, 602963).

The shallow bedrock tuffs in this part of Cañon de Valle are strongly welded and relatively impermeable, and percolation of water through these rocks may be largely controlled by fractures and faults (Figures 3.2-2 and 3.2-3). A broad zone of deformation extends approximately 1.25 mi eastwards from the Pajarito fault system to the 260 Outfall area (Gardner et al. 2001, 070106; Figure D-1 in Appendix D; Lewis et al. 2002, 073785). The main structural elements in this zone of deformation include (1) the north-south TA-09 graben that lies between building 16-260 and well R-25; (2) north-northwest-striking fractures and rare faults bounding the zone of deformation that may be the surface expression of deeper faulting; (3) northeast trending open or rubble-filled fissures within the Tshirege Member, some of which are very large; and (4) rare small east-west-trending. (Gardner et al. 2001, 070106) (Lewis et al. 2002, 073785). The largest structure in the 260 Outfall area is the north-trending TA-09 graben (Figures 2.3-1 and 3.2.2) (Lewis et al. 2002, 073785). The graben is about 2000 ft wide at its southern end and about 1000 ft wide at its northern end in Pajarito Canyon. The western bounding fault of the TA-09 graben is a high-angle normal fault with 5 ft of down-to-the-east displacement. The eastern boundary of the graben is defined by three closely spaced high-angle normal faults with a total of 10 ft of down-to-the-west displacement. A shallow north-trending syncline adjacent to the eastern bounding fault accounts for an additional 10 ft of down-to-the-west displacement. The 260 Outfall discharged into the TA-09 graben. Faults and associated fractures on the eastern side of the graben are crossed by perennial surface water

flow in Cañon de Valle downgradient of the 260 Outfall and may be important infiltration pathways through the relatively impermeable tuffs that underlie the canyon floor (Figures 3.2-2 and 3.2-3).

A DC electrical resistivity geophysical survey collected six lines of electrical resistivity within and next to Cañon de Valle in 2014 (LANL 2014, 600004). Three lines were run parallel to the canyon and were over 5000 ft in length. The remaining three lines were placed perpendicular to the canyon to help tie resistivity features together. Two- and three-dimensional processing of the data showed that the vadose zone has a layered electrical structure characterized by a relatively thin conductive surface layer of older alluvial deposits atop the mesas, a thick resistive layer consisting of the Tshirege Member, and a deep layer of conductive rocks made up of the Otowi Member and Puye Formation. The electrical resistivity collected along the axis of Cañon de Valle shows that the tuffs beneath the floor of the canyon, including normally resistive Tshirege tuffs, are relatively conductive west of MDA P (LANL 2014, 600004). These data are consistent with surface water and alluvial well data that indicate the main infiltration pathway for surface water in Cañon de Valle is located downcanyon of the 260 Outfall and extends eastward to the vicinity of MDA P (Reid et al. 2005, 093660; LANL 2011, 207069). Vertical conductivity anomalies are associated with faults bordering the west and east margins of the TA-09 graben. These vertical anomalies penetrate the resistive Tshirege Member layer and may represent local zones of enhanced infiltration of surface water (LANL 2014, 600004).

Local areas of increased infiltration also occur beneath mesas where sufficient hydrologic drivers, such as ponded water, are available (e.g., the 90s Line Pond and 260 Outfall pond) or beneath tributary drainages that receive runoff from snowmelt or storm events. The 2014 DC electrical resistivity survey identified vertical conductivity anomalies associated with mesa top drainages. A strong vertical anomaly is associated with storm drainage for building TA-16-260 and a smaller anomaly occurs at the 260 Outfall. Another deep-penetrating high-conductivity anomaly occurs on the mesa north of Cañon de Valle between wells CdV-9-1(i) and R-68. The source of this electrical anomaly is not known but it may be related to enhanced infiltration near the headwaters of a tributary drainage to Cañon de Valle or it may represent an unmapped fault.

Springs and shallow bedrock groundwater less than 200 ft deep at TA-16 appear to be part of a widespread shallow bedrock perched-groundwater system (Figures 3.2-1 and 3.2-2). SWSC and Burning Ground Springs discharge at elevations from 7422.6 to 7481.9 ft and issue from the same geologic unit (lower Qbt 3t) as springs in upper Pajarito Canyon and upper Twomile Canyon. Additionally, several shallow mesa-top wells encountered perched groundwater at the same stratigraphic level. The shallow bedrock perched-groundwater system is probably largely recharged by infiltration of surface water in the mountain block and mountain-front areas near the Pajarito fault zone (Figures 3.2-1 and 3.2-2). The presence of contaminants, such as RDX and HMX, in shallow bedrock groundwater at widely spaced locations at TA-16 indicates that local infiltration of surface water also recharges the shallow bedrock perched groundwater in the vicinity of outfalls near buildings used for HE processing (such as the 260 Outfall) and beneath mesa-top ponding areas (such as the 90s Line Pond) (Figure 3.2-2). This local recharge comingles with uncontaminated groundwater derived from mountain block and mountain-front recharge. Most shallow boreholes (<200 ft) drilled on TA-16 mesas are dry; however, three wells, 16-260E-02712, MSC-16-02665, and 90LP-SE-16-02669, are intermittently saturated and one well, 16-26644, is perennially saturated (Figure 3.2-2). The spotty distribution of groundwater associated with the springs and shallow boreholes supports the interpretation that the shallow bedrock perched-groundwater occurs as ribbons of saturation that are stratigraphically controlled.

Martin Spring is located near the head of Martin Spring Canyon at an elevation of 7448 ft, similar in elevation to springs in Cañon de Valle and upper Pajarito Canyon and their tributaries. Unlike the springs of Cañon de Valle and Pajarito Canyon, Martin Spring discharges at the Qbt 4/Qbt 3t contact.

Martin Spring has a variable discharge and has been dry in recent drought years. Martin Spring's flow and chemistry are substantially different from those in Cañon de Valle springs, suggesting a different source of recharge (LANL 2003, 077965).

Fishladder Spring is located near the head of Fishladder Canyon at an elevation of 7355 ft; about 100 ft lower than other springs at TA-16. This spring is approximately 2000 ft east of the former outfall discharge area for former building 16-340 and is also downgradient of the discharge area of the former HE wastewater treatment plant at the Burning Grounds. Before releases were discontinued the mid-1990s, millions of gallons of effluent per year were discharged from the building 16-340 outfall, and surface water flowed as far east as the confluence with Cañon de Valle. Water in Fishladder Spring was probably largely recharged by infiltration of discharges from the former outfalls. Today Fishladder Canyon contains flowing water only during snowmelt and storm events and alluvial groundwater occasionally discharges at Fishladder Spring.

Beneath the shallow bedrock perched groundwater, percolation of local infiltration through upper vadose zone rocks is the source of RDX found in perched-intermediate groundwater zones in the lower vadose zone and in the regional aquifer (Figures 3.2-1, 3.2-2, and 3.2-3). Downward flux of moisture is expected to be temporally and spatially variable and impacted by spatial heterogeneity of the flow medium and temporal/spatial distribution of the infiltration recharge of the vadose zone. Moisture flux through the vadose zone is expected to be predominantly vertical and controlled by gravity and hydrogeological properties of the medium and structural features, such as faults and fractures (Figures 3.2-2 and 3.2-3). Significant vertical anisotropy occurs because of the layered nature of the stratigraphic units, with vertical hydraulic conductivities significantly lower than horizontal hydraulic conductivities. Moisture is likely diverted laterally at capillarity barriers associated with bedding contacts (Figures 3.2-3). Direction of groundwater flow is likely controlled in part by the dip of bedding within the major stratigraphic units and hydraulic gradients. Figure 3.2-4 presents structure contour maps that show bedding orientations for the major geologic units in the TA-16 area. Based on bedding attitudes (LANL 2018, 602963), downward moisture flux through the upper vadose zone will have a tendency to stairstep towards the east and southeast (Figures 3.2-2, 3.2-3, and 3.2-4).

Groundwater pathways in the upper part of the upper vadose zone appear to be controlled by bedding features in strongly welded ash-flow tuffs of Tshirege units Qbt 3t, Qbt 3 and Qbt 2. For example, the shallow bedrock perched groundwater zones described above exhibit a strong association with the basal contacts of Tshirege units Qbt 3t and Qbt 4. Groundwater accumulation and flow in these welded tuffs are probably controlled by a combination of horizontal fracture flow along partings and porous flow in sandy pyroclastic surge deposits, with flow generally towards the east-southeast. Some of the perched water daylights as springs (e.g. SWSC, Burning Ground, and Martin Springs) in deeply incised canyons, and the remainder eventually infiltrates to deeper levels of the vadose zone, acting as a local source of recharge to the perched-intermediate groundwater zones in the area (Figures 3.2-2 and 3.2-3). Vertical pathways through the welded tuffs probably occur where horizontal flows intersect fractures and faults (Figures 3.2-2 and 3.2-3).

Rocks in the lower part of the upper vadose zone are much less compacted than the overlying welded tuffs. Tshirege units Qbt 1v and Qbt 1g, Cerro Toledo Formation, and Otowi Member are highly porous and variably stratified tuffaceous deposits. Vertical, gravity-driven moisture flow through these rocks is likely diverted laterally at bedding contacts, particularly in beds that are well stratified (Figures 3.2-2 and 3.2-3). Bedding orientations in these geologic units favor dispersion of moisture flow towards the east and southeast in these units (Figure 3.2-4). Based on observations from outcrops, fractures are much less common in non-welded tuffs and fluvial sediments than in strongly welded tuffs; however, open fractures

are known to occur in the Otowi Member in wells R-25 and CdV-16-1(i) from drill core and borehole videos (LANL 2018, 602963) and they may provide vertical and lateral pathways for groundwater flow.

3.2.2.2 Lower Vadose Zone and Perched-Intermediate Groundwater

Two perched-intermediate groundwater zones occur beneath Cañon de Valle at wells R-26, R-25b, R-25, CdV-16-1(i), CdV-9-1(i), R-68, CdV-16-4ip, R-63, R-63i, CdV-16-2(i)r, and R-47i (Figure 3.2-5). These perched-intermediate zones are lateral and vertical pathways for the transport of groundwater containing RDX, and vertical leakage from these zones is a local source of recharge to the regional aquifer. The upper of the two perched-intermediate zones is more laterally extensive, thicker, and has higher RDX concentrations than the lower zone. The top of the upper perched-intermediate zone decreases in elevation eastward, ranging from about 7034 ft amsl near well R-26 (screen 1) to about 6100 ft amsl near well R-47i. Portions of these perched zones are in direct hydraulic communication locally, especially near wells R-25 and CdV-16-4ip. The geometry of these perched zones is complex because they occur at multiple stratigraphic levels and the aquifer media are extremely heterogeneous. The lower confining beds that underlie these zones appear to include local features (e.g., thin silt beds) that appear to have limited areal extent. In some locations, perched groundwater was identified at only one depth interval (e.g., wells R-26, CdV-16-2(i)r, and R-47i), whereas other locations have groundwater at two depth intervals (e.g., R-25, CdV-9-1(i), and CdV-16-4ip). Figures 3.2-6, 3.2-7, and 3.2-8 are conceptual cross-sections for Cañon de Valle that show the interpreted distribution of perched groundwater zones and their possible interconnections.

Groundwater in the two perched-intermediate zones is a mixture of uncontaminated MBR and RDX-containing mountain-front recharge. Mountain-block recharge occurs in the highlands west of the Pajarito fault zone and consists of diffuse subsurface infiltration of snow melt and surface water that percolates through the rock and recharges the regional aquifer (Figures 3.2-1 and 3.2-2). As regional groundwater flows eastward from the mountain block towards TA-16, some groundwater is diverted laterally into the vadose zone, where steep gradients in the regional water table intersect gently dipping transmissive geologic strata. Lateral diversion of regional groundwater into the vadose zone is believed to be the principal source of recharge for groundwater in both perched-intermediate zones. In the vicinity of the 260 Outfall, mountain-block recharge makes up approximately 66% of perched groundwater (LANL 2018, 602963).

MFR occurs along the Pajarito fault zone and in a zone that extends up to 2 km eastward from the mountain front into the TA-16 area (Figure 3.2-1). MFR is characterized by infiltration of streamflow in major canyons such as Cañon de Valle as well as by infiltration of snowmelt and overland flow on mesa tops. MFR occurs near the 260 Outfall where spring-fed perennial surface water flow occurs in Cañon de Valle. From 1951 to 1996, perennial surface water flow was augmented by effluent releases from the 260 Outfall. Infiltration of RDX-containing surface water in Cañon de Valle during the period of effluent releases is the primary source of RDX found in perched-intermediate and regional groundwater zones at TA-16. Additional local recharge may occur at mesa-top infiltration sites or from shallow bedrock perched groundwater in the upper Bandelier Tuff. Based on hydrogeochemical investigations, approximately 34% of the water in the perched-intermediate zones in the vicinity of the 260 Outfall originated as local mountain-front recharge (LANL 2018, 602963).

In map view, the upper perched-intermediate zone forms a tongue-like body centered on Cañon de Valle that extends approximately 11,000 ft east of the Pajarito fault zone (Figure 3.2-5). The upper perched-intermediate zone is poorly constrained in the west where there are few deep wells, but it is likely that focused recharge of the zone occurs beneath Cañon de Valle both as MBR and MFR. Near the 260 outfall, the perched zone extends approximately 2500 ft in the north-south direction and has a

maximum saturated thickness of 415 ft near well CdV-9-1(i) (Figures 3.2-6 through 3.2-8). Saturation occurs in ash-flow tuffs of the lower Otowi Member, pumice-fall deposits of the Guaje Pumice Bed, and sedimentary deposits of the upper Puye Formation. Water heads measured in wells and piezometers define a potential groundwater mound on top of the perched water table that is characterized by high water levels and elevated RDX concentrations. The mound lies north of Cañon de Valle (Figure 3.1-3), suggesting that rather than percolating vertically beneath the canyon floor, local canyon-floor infiltration near the 260 Outfall follows pathways through the vadose zone that stair-step eastwards at geologic contacts before recharging the upper perched-intermediate zone in the vicinity of well CdV-9-1(i) (Figures 3.2-2 and 3.2-3). Hydraulic gradients in the upper perched zone are largely towards east and southeast, but it is likely that steep gradients occur the north edge of the recharge mound near well R-68 (Figures 3.1-3 and 3.2-3).

Responses in perched-intermediate groundwater to surface runoff events in the TA-16 area are limited to depths of less than about 900 ft and to an area west of the Burning Grounds. Water-level responses to snowmelt runoff occur in shallow bedrock perched groundwater at R-26 PZ-2 and 16-26644 and in the upper perched-intermediate zone at R-25 screens 1 and 2, CdV-16-1(i), R-25b, and CdV-9-1(i). Perched-intermediate wells CdV-16-2(i)r and R-47i east of the Burning Grounds do not exhibit responses to snowmelt runoff, possibly because recharge for these wells takes place along pathways that are less well connected to surface-water infiltration pathways, and their response to snowmelt and other runoff events occurs over longer time periods, perhaps spanning years. In well CdV-9-1(i) screen 1, the water level rose >80 ft during the spring snow melt event of 2017 and >110 ft in 2019. During the same periods, water levels in CdV-9-1(i) PZ2 rose approximately 10 ft and 23 ft, respectively. The water level changes during these recharge events are most likely driven by upgradient infiltration of snowmelt in the mountain block rather than by local recharge in Cañon de Valle. The isotopic similarity of water sampled at CdV-9-1(i) during the 2017 recharge event to other perched-intermediate zone well samples, as well as an increase in temperature during the recharge event, supports the concept that this groundwater is old, well-mixed water derived from the mountain block to the west rather than direct snowmelt recharge through the canyon in the vicinity of the 260 Outfall (LANL 2018, 602963).

Lateral hydraulic connectivity within the upper perched-intermediate groundwater is demonstrated by water level responses during drilling and pumping tests. Penetration of the upper perched-intermediate zone during drilling activities at R-25c caused detectable water level responses at R-25 (screens 1 and 2), located about 100 ft to the east, and at CdV-16-1(i), located about 330 ft to the north (LANL 2011, 207069). Additionally, drilling of well CdV-16-4ip produced a water level response in well R-25 screen 2, located about 430 ft to the east.

Fluctuations in water levels observed in the upper perched-intermediate zone during drilling are likely the result of pressure responses associated with drilling with compressed air and demonstrate lateral hydraulic connectivity within the zone. In 2011, a step-drawdown test and 10-day pump test at well CdV-16-4ip screen 1 produced a muted water level response at well R-25 screen 2 of 0.4 ft, but there was no apparent responses at wells CdV-16-1(i), R-25 screen 1, R-25 regional screens 5-8, R-25b, CdV-16-2(i)r, R-63 (regional), or R-47i (LANL 2011, 203711). The pump test results were interpreted as showing that CDV-16-4ip screen 1 is located in a limited pocket or channel of highly transmissive sediments. The CDV-16-4ip screen 1 pumping test indicates that hydraulic connectivity in the upper perched-intermediate zone is spatially complex, reflecting the highly heterogeneous nature of aquifer media.

The lower perched-intermediate zone is located within sedimentary deposits of the Puye Formation (Figures 3.2-3 and 3.2-6 through 3.2-8). Because it is penetrated by fewer wells than the upper zone, less is known about the overall size and distribution of this zone. Based on available well data, the lower

perched-intermediate zone appears to be a relatively thin groundwater body that extends over a limited area (Figure 3.2-5). It has a saturated thickness of about 30 to 80 ft and is separated from the upper perched-intermediate zone by 80 to 150 ft of dry or variably saturated rock (Figures 3.2-6 through 3.2-8). Hydraulic gradients in the lower perched zone appear to be largely southeast and south based on limited water level data from wells R-25 screen 4 and R-63i and during drilling at wells CdV-9-1(i) and CdV-16-4ip. Lower perched-intermediate groundwater in R-25 screen 4 does not respond to seasonal surface runoff events and may be recharged largely by regional groundwater in the mountain block (Figures 3.2-1 and 3.2-2).

Step-drawdown and pumping test results for CdV-16-4ip screen 2 in the lower perched-intermediate zone suggest that the flow medium has low to moderate permeability and is spatially extensive (LANL 2011, 203711). Pumping in screen 2 did not cause measurable drawdown in screen 1 or at any of the nearby monitoring locations. Based on pumping test results, it appears the upper and lower perched-intermediate zones near Cañon de Valle are not hydraulically connected to each other or to regional groundwater.

The perched-intermediate groundwater systems are characterized by significant downward vertical gradients. Water-level heads in the lower perched-intermediate zone are about 200 to 280 ft lower than in the upper perched-intermediate zone (Figures 3.2-6 through 3.2-8). Water-level data from the multiple screens in well R-25 and CdV-16-4ip indicate the downward vertical gradient is approximately 1, with water levels declining proportionally to decreasing elevation in the vertical profile (LANL 2011, 207069). The water level data suggest a strong, gravity-controlled downward component of flow within and between the perched-intermediate systems, eventually recharging the regional aquifer. The data support a CSM under which both saturated and unsaturated conditions exist between the perched zones and between the lower perched zone and the regional aquifer. A lateral component of the groundwater flow is also expected because of medium anisotropy. The flux of the downward groundwater flow through the vadose zone is expected to be temporally and spatially variable and impacted by spatial heterogeneity of the flow medium and temporal/spatial distribution of the infiltration recharge of the vadose zone.

The geologic media that hosts the two perched-intermediate zones at TA-16 includes rocks of the lower Bandelier Tuff and the Puye Formation. Perched water in the upper perched-intermediate zone occurs partly in the lower Otowi Member and in the Guaje Pumice Bed (Figures 3.2-3 and 3.2-6 through 3.2-8). These tuffs are made up of ash-flow, pumice-fall, and ash-fall deposits. A stratified sequence of highly porous non-welded ash-flow tuffs makes up the bulk of the Otowi Member (40-50%) (Figure 3.2-9).

Despite high porosity, transmissivity through ash-flow tuffs is likely to be low because the tuffs are poorly sorted and their matrix is ash-rich. Transmissivity is likely to be greater within pumice-fall deposits that are interbedded with the ash flows of the Otowi Member and that make up the bulk of the Guaje Pumice Bed. Pumice falls are stratified, highly porous, fines-depleted deposits made up of well-sorted pumices, lithics, and crystals. Thin fine-grain ash beds that are interbedded with the ash-flow and pumice fall deposits may act as confining or semi-confining beds supporting lateral groundwater flow through the ash-flow and pumice-fall tuffs. High-angle fractures occur in the Otowi Member at well R-25 and CdV-16-1(i). These fractures are potential vertical and lateral groundwater pathways (Figure 3.2-9a). Potential clay-silt soil horizons occur at the top of the Puye Formation in several wells and may act as confining beds for perched groundwater in the overlying tuffs.

The Puye Formation is the primary geologic unit in the lower part of the upper perched-intermediate zone and in the lower perched-intermediate zone (Figures 3.2-3 and 3.2-6 through 3.2-8). It was deposited as broad, coalescing alluvial fans shed eastward from the Jemez Mountains volcanic field into the subsiding Española basin (Griggs and Hem 1964, 092516) (Bailey et al. 1969, 021498). The source areas for these alluvial-fan deposits were canyons draining Tschicoma volcanic centers that were active in the eastern Jemez Mountains between about 3 and 5 Ma (Broxton et al. 2007, 106121). The Puye Formation is more

than 1092 ft thick in well R-25, but the base of the unit has not been penetrated by wells in the TA-16 area. Because of their proximity to mountain front, Puye deposits at TA-16 are very coarse-grained, consisting of heterogeneous clast- to matrix-supported conglomerates and associated gravels and lithic sandstones (Figure 3.2-9). The depositional history of the alluvial fan spans 5 Ma, and many features of the deposits were controlled partly by erosional and tectonic changes in the drainage basin located in the mountain block to the west.

Puye conglomeratic deposits tend to be thickly bedded (up to 5 ft) and are commonly separated by thin beds of sandy gravels and silty sands (Figure 3.2-9). Cementation and clay minerals are sparse to absent. Hydraulically, there is considerable vertical anisotropy of the Puye Formation due to the stratification of highly heterogeneous strata with variable hydraulic properties. Lateral anisotropy is expected to be less than vertical anisotropy because the lateral extent of individual strata greatly exceeds their thickness. As a result, horizontal hydraulic conductivities are greater than vertical hydraulic conductivities. Dips of strata in the Puye Formation, determined from borehole Formation Microimager (FMI) logs, are highly variable but are generally eastward, with directions ranging from northeast to southeast. Though relatively uncommon, silt beds 1 to 3 ft thick are believed to be important local confining beds for perched groundwater (Figure 3.2-9). In several wells, water levels in perched zones dropped significantly when these silt beds were penetrated during drilling. The depositional environment for the silt beds is uncertain, and they may form aquicludes over relatively limited areas.

Collectively, silt beds that overlap aerially but occur at different stratigraphic levels may provide leaky confining conditions for perched groundwater. Confining conditions may also develop above conglomerate beds with a silt-rich matrix. The leaky nature of confining beds is supported by thinning and eventual disappearance of perched groundwater to the east and southeast.

A facies model of the Puye Formation is presented in Figure 3.2-10 to provide a stratigraphic framework for understanding the architecture of the highly heterogeneous alluvial fan deposits of the Puye Formation. FMI images of Puye deposits at wells CdV-16-4ip and R-18 were used to constrain the thickness and lithologic character of the depositional units portrayed in the facies model. Alluvial fans facies models were used to visualize the distribution and geometry of the deposits in the areas between the control wells. The facies model augments the site conceptual model by identifying lithologies that likely control groundwater movement and their lateral hydraulic connectivity. For simplicity, most figures in this report portray the perched-intermediate groundwater zones as thick zones of continuous saturation that appear to have extensive hydraulic connectivity (e.g. Figures 3.2-1, 3.2-3 and 3.2-6 through 3.2-8). The facies model presented here, however, provides a more realistic picture of these perched systems in which groundwater flow is limited to certain types of transmissive deposits that have limited vertical and lateral distributions. Networks of flow paths are created where saturated rocks with high conductivity are juxtaposed by erosional and depositional processes.

The Puye deposit at TA-16 is a thick sequence of fluvial sediments dominated by aggrading stream channel deposits in the proximal part of the alluvial fan. Stream channels radiate from the apex of a cone-shaped fan surface, downslope from the point where drainages emerge from the mountain front (Figure 3.2-10). These proximal channels are filled by a combination of debris flow and stream flow deposits. Debris flow deposits include boulders, cobbles, and gravels supported by a silt-rich sandy matrix that generally has poor hydraulic conductivity. Stream flow deposits include both stream flow and flood sediments in which boulders and cobbles are clast supported or occur in a fines-depleted sandy matrix.

Hydraulic conductivity is generally greater in fines-depleted stream flow deposits, and they likely form the primary perched groundwater pathways at TA-16. Sheet flow deposits also formed on the alluvial fan when stream flow overtopped the channels and flooded the fan surface as sheet flow (Figure 3.2-10).

The sheet flow deposits tend to be thin compared to channel deposits and are made up of silts or sands with conglomeratic lenses. These deposits are usually more stratified and better sorted than the channel deposits. Hydraulic conductivity in sheet flow deposits depends on the silt content of individual beds and is likely to be variable. Silt beds that may form local perching horizons for perched-intermediate groundwater were likely deposited by sheet flow on alluvial fan surfaces.

High-runoff flood events in the proximal part of the alluvial fan scour older channel deposits and deposit new sediments. A single flood can result in deposits with large down-slope facies variations, including boulder and cobble channel deposits in proximal areas of the fan, sand and silt channel deposits in more distal parts of the fan, and sheet flow deposits where stream flow overtopped the channels and flood the fan surface. Over time, stream channels migrate back and forth across the fan surface as older channels fill with sediments, causing new channels to form. The scouring of older deposits and aggradation of new sediments buried older, partly eroded channel deposits. As the alluvial fan grows, thick sequences of lobate channel deposits that are elongated in a down-fan direction accumulate in the proximal part of the fan. Consequently, the alluvial fan deposits at TA-16 is largely made up of thick stacks of U-shaped channels filled with coarse-grained sediments that are elongated in a down-fan direction that is generally eastward.

As described above, horizontal hydraulic conductivities are greater than vertical hydraulic conductivities in the deposits. Because the width of channel deposits is less than their length, however, north-south lateral anisotropy (cross-sectional to channels) is expected to be greater than east-west anisotropy (longitudinal to channels). Because of erosion and stream migration, channel deposits are commonly truncated against other channel deposits. Groundwater pathways in this type of environment are likely controlled by the juxtaposition of deposits that have high hydraulic conductivities. Anastomosing networks of interconnected stream channels filled with fines-free stream flow deposits are probably the most favorable groundwater pathways in proximal alluvial fan deposits.

The facies model is consistent with large-scale heterogeneities of aquifer media and high lateral to vertical anisotropy ratios demonstrated by hydrological data collected during source-removal pump tests conducted at CdV-16-4ip screen 1 in 2014 (LANL 2014, 600004) and the extended cross-hole aquifer tests that were conducted at monitoring wells CdV-9-1(i), CdV-16-1(i), and CdV-16-4ip in 2016 (LANL 2017, 602288). A major conclusion of the 2014 CdV-16-4ip pump test is that the well screen is located in a laterally limited pocket or channel of highly transmissive sediments. The 2016 cross-hole aquifer tests showed that the boundary effects observed in the 2014 pump tests at CdV-16-4ip are likely due to contrasts in aquifer properties (i.e. facies changes) and that hydraulic communication in the upper Puye Formation occurs as a laterally interconnected saturated zone that is at least as large as the triangle formed by CdV-9-1(i), CdV-16-4ip, and R-25 screen 2. The preferential lateral communication across the upper Puye Formation is likely driven by a network of permeable interconnected stream channels and water production is largely confined to a few favorable beds intersected by the pumping wells. For example, during the 2014 pump tests at CdV-16-4ip, the drawdown curve showed multiple inflection points caused by hydraulic boundaries near the well. Initially, the pumping caused a rapid, almost linear, water-level decline until the water level reached an elevation of about 6620 ft. Then, the rate of water-level decline slowed until the water-level elevation reached approximately 6615 ft. Below 6615 ft, the water-level decline again accelerated until the water level was about 6603 ft. Below 6603 ft, the water level declined rapidly, suggesting dewatering of the borehole. The recovery curve in CdV-16-4ip after pumping followed a similar pattern with similar inflection points. The water-level data suggest that the groundwater flow to CdV-16-4ip screen 1 occurs primarily between elevations of 6603 and 6620 ft (27% of the well screen interval) and a high-yield zone occurs between elevations of 6615 and 6620 ft (8% of the well screen interval).

Although laterally connected, the 2016 cross-hole aquifer tests also demonstrated the upper perched-intermediate zone does not behave as a single, vertically integrated reservoir. In 30 days of pumping, CdV-9-1(i) screen 1 generated no water-level response in CdV-9-1(i) PZ-2, even though both screens were completed in the upper Puye Formation. The lack of pumping response is consistent with observations that PZ-2 water levels are 300 ft higher than those in CdV-9-1(i) screen 1, even though there is only 75 ft of vertical separation between the two wells. High vertical anisotropy in the upper perched-intermediate zone was also demonstrated by the lack of response in monitored screens within the Otowi Member during pumping from wells within the upper Puye Formation, including monitoring points that are very close to the pumping locations.

Based on the discussion above, the upper perched-intermediate zone is a complex groundwater system that may represent multiple groundwater entities that have a range of hydraulic interconnections with each other. The complexity of the system reflects the extreme heterogeneity of proximal alluvial fan deposits laid down near the apex of the fan where it emerges from the mountain block into the adjacent basin. Although the general nature of the upper perched-intermediate zone is characterized by existing boreholes, prediction of groundwater flux and contaminant migration in this type of hydrologic setting will have significant uncertainties because of difficulties in characterizing the network of hydrologic connections that occur both vertically and laterally in this system.

3.2.3 Regional Groundwater

The shape of the regional water table generally dictates groundwater flow directions and fluxes that control contaminant transport in the aquifer. The general shape of the regional water table beneath the Pajarito Plateau is predominantly controlled by the areas of regional recharge to the west (the mountain block areas of the Sierra de los Valles) and discharge to the east (the Rio Grande and the White Rock Canyon springs) (Figure 2.5-1). The structure of the regional phreatic flow is also expected to be impacted by local infiltration zones beneath wet canyons, heterogeneity and anisotropy in the aquifer properties, and discharge zones (water-supply wells and springs).

The predominant direction of groundwater flow in the regional aquifer is generally from west to east across the Pajarito Plateau (Figure 2.5-1). The lateral regional groundwater flow gradients are relatively high to the west (close to recharge in the Sierra de los Valles) and to the east (close to the Rio Grande), varying between 0.003 and 0.05 m/m (LANL 2011, 207069). Local groundwater recharge potentially affects the shape of regional water table in the area near well R-25, where elevated regional water levels may be the result of vertical canyon-focused recharge. The water-table map suggests northeastward and southeastward components of flow away from the R-25 area (Figures 2.5-1 and 3.2-11).

The regional water table is located approximately 1000 to 1300 ft bgs at TA-16 (Figure 3.2-1 and 3.2-3). The water table is primarily in the Puye Formation in the area of greatest concern for groundwater contamination (Cañon de Valle and potential downgradient areas), but it is within thick Tschicoma dacite lavas in the southern part of TA-16 (Figure 3.2-11). East of well R-27, the upper few hundred feet of regional aquifer is mainly within Cerros del Rio lavas, and it drops into the Puye Formation, Totavi Lentil, and Miocene sediments and Miocene basalt near the Rio Grande.

The regional groundwater system is a complex heterogeneous system that includes shallow, predominantly unconfined and deep, predominantly confined zones (LANL 2011, 207069). There are no clearly defined aquitards or confining layers that provide hydraulic separation between the shallow and deep zones of the regional aquifer; however, the vertical hydraulic stratification of the regional aquifer has been observed at numerous aquifer locations where shallow and deep monitoring-well screens are installed. The vertical hydraulic stratification is indicated by pronounced vertical differences in hydraulic

heads and a lack of vertical propagation of pumping drawdown caused by pumping tests and pumping of municipal water supply. The vertical stratification of the regional aquifer is also demonstrated by the PM-2 spinner test, which demonstrated that discrete units within the 1200-ft screened interval of the production well had a much higher permeability and were responsible for most of the groundwater production (LANL 2009, 106939). The vertical hydraulic separation is likely caused by pronounced vertical aquifer anisotropy, with the lateral permeability substantially higher than the vertical permeability. The anisotropy is likely caused by the depositional layering of the hydrostratigraphic units. Based on the existing observations, the degree of hydraulic communication between these zones is relatively poor and spatially variable depending on local hydrogeologic conditions and hydrostratigraphy. The poor hydraulic communication between the two zones does not preclude the possibility that some contaminant migration may occur between the shallow and deep zones. Between the two zones, the hydraulic gradient has a downward vertical component, creating the possibility that downward contaminant flow may occur along “hydraulic windows,” although these flows have not been directly observed.

Lateral hydraulic connections in the regional aquifer were demonstrated during drilling, well development, and well pump tests associated with installation of wells R-63 and R-69. During drilling and development of well R-63, injection of pressurized air and water produced water-level responses at well R-25 screens 5, 6, and 7. An aquifer test at well R-63 produced water-level responses at well R-25 screens 5, 6, 7, and 8 (LANL 2011, 204541). The greatest drawdown at well R-25 (0.44 ft) occurred in screen 6, which is submerged 92 ft below the regional water table. During drilling of well R-69, injection of pressurized air and water produced water-level responses at wells R-18 and R-47. Unfortunately, R-68 transducer data are not available for these pressure responses because of a dead telemetry battery. The pressure responses at R-18 and R-47 first appeared after R-69 penetrated approximately 33 ft into the regional aquifer, and maximum pressure responses occurred when drilling penetrated 50 ft into the aquifer. After well R-69 was installed, aquifer tests were conducted in both well screens, and water levels were monitored in observation wells R-18, R-47, R-63, and R-68. Pumping of R-69 screen 1 did not produce water level responses in any of the observation wells. Pumping of R-69 screen 2 produced a clear response at R-18, but no responses at the other observation wells.

Analysis of transient water levels observed in regional aquifer monitoring wells near Water Canyon and Cañon de Valle was conducted to determine the magnitude of pumping drawdowns caused by the water-supply wells PM-2, PM-4, and PM-5 (LANL 2011, 207069). The analysis included a hydraulic survey of transients observed at monitoring wells R-26, R-25, R-48, CdV-R-15-3, CdV-R-37-2, DT-5A, R-29, R-30, R-19, R-27, DT-10, DT-9, and R-31. Except for well R-19, there was no apparent impact on water levels at the monitoring wells by water-supply pumping in the (LANL 2011, 207069) study. R-19 screens 4–7 contain water level transients that correspond to pumping at water-supply wells PM-2 and PM-4. Although not included as an observation well in the (LANL 2011, 207069) study, well R-17 responds to pumping at PM-2, PM-4, and PM-5 (Koch and Schmeer 2011, 201566).

In wells with multiple screens, the difference in water levels between two screens divided by the distance separating screen centers is used to estimate the vertical head gradient at those locations. There are several multiscreen wells in the area that can be used to estimate vertical gradients in the regional aquifer. These include R-25, R-69, R-17, and R-19; and CdV-R-15-3 and CdV-R-37-2 prior to redevelopment as single completion wells. Because these wells do not have a single overlapping time period of record, gradients were computed during different time periods. The month of May 2010 was selected for R-17, R-19, R-25, CdV-R-15-3, and CdV-R-37-2, and the month of February 2014, was selected for R-17, R-19, and R-25 for comparison. The month of February 2019 was selected for R-69 as well as R-19 and R-25 for comparison with prior values from 2010 and 2014.

Table 3.2-1 summarizes the vertical gradients between regional aquifer screens at these wells and times. Negative values represent downward vertical gradients. The only upward gradient observed in this analysis is between screens 4 and 5 of CdV-R-15-3, but the overall gradient is downward in this well in these regional aquifer screens. In the central portion of the RDX plume area, vertical gradients are strongly vertically downward at R-25 (ranging from -0.24 ft/ft between screens 5 and 6 to -0.12 ft/ft between screens 7 and 8) and R-69 (-0.18 ft/ft between screens 1 and 2). For the time periods described above, the average downward vertical gradients are smallest at CdV-R-37-2 (-0.004 ft/ft) and also low at the other eastern well locations (CdV-R-15-3, -0.095 ft/ft; R-17, -0.037 ft/ft; R-19, -0.033 ft/ft).

Temporal variability can be significant, with R-17's vertical gradient changing by 60% between May 2010 and February 2014. The likely cause is the onset of consistent pumping at municipal water-supply well PM-2 in early 2012. Figure 3.2-12 shows water levels in R-17 screens 1 and 2 along with pumping at PM-2, PM-4, and PM-5. Pumping at PM-2 appears to have a stronger effect on R-17 screen 2 than screen 1, leading to the change in vertical gradient between the two dates shown in Table 3.2-1. Although R-19 is closer to PM-2 than R-17, a lack of significant change in gradient indicates that all screens possibly are affected similarly.

The existing monitoring well network satisfies the objective to provide for the detection of potential contaminants upgradient of water-supply wells. As discussed in section 3.1, regional groundwater in wells R-18, R-25, R-63, R-68, and R-69 contain RDX and other HE COPCs. RDX in wells R-68 and R-69 is present at levels greater than the 9.66 µg/L tap-water screening level for drinking water and in well R-18 is greater than half the screening level. The downgradient extent of RDX in the regional aquifer is constrained by regional monitoring wells R-14, R-17, R-19, R-27, R-29, R-30, R-46, R-47, R-48, R-51, R-58, R-60, CdV-R-15-3, and CdV-R37-2 that do not contain RDX (Figure 3.2-13). This network of regional groundwater monitoring wells provides early warning of RDX approaching municipal supply wells (primarily PM-2, PM-4, and PM-5), which are located 2.9 to 3.9 mi. east of the RDX plume at TA-16 (Figure 3.2-13). The TA-16 well network analysis (LANL 2007, 100113) (LANL 2008, 101875.5) concluded that the existing network of near- and far-field regional monitoring wells has a greater than 95% chance of detecting TA-16 contaminants before they reach water-supply wells. That finding was supported by the updated TA-16 well network evaluation (LANL 2012, 213573) that found the existing monitoring well network, when supplemented by the addition of regional monitoring wells R-47 and R-58, provides high detection efficiency for all high- and medium-priority contaminant sources at TA-16.

4.0 SUMMARY AND CONCLUSIONS

The purpose of this DGIR is to present a comprehensive description of current conditions of dissolved phase RDX in deep groundwater. This report has met objectives identified in section 1.1 by characterizing the nature and extent of RDX in deep groundwater, updating the conceptual site model, assessing current risk to human health, and recommending next steps.

This report describes the results of the investigations and studies performed pursuant to comments received from NMED in April 2008 on the 2007 CME. Table 1.0-1 lists in chronological order the work plans implemented to address NMED's comments. These investigations, studies, and work plans resulted in a reduction in the uncertainties identified by NMED. As this report documents, the following actions have been completed:

- Installed and reconfigured existing monitoring wells and collected groundwater samples to better characterize the nature and extent of the RDX in the perched-intermediate zone.

- Installed additional monitoring wells and collected groundwater samples to better characterize the nature and extent of RDX in the regional aquifer.
- Collected geologic and hydrogeologic information during the drilling and testing of monitoring wells and performed laboratory studies to better characterize the hydrogeologic properties (e.g., borehole lithology, hydraulic conductivity, partitioning coefficients) in the regional aquifer.
- Collected geologic and hydrogeologic information during the drilling and testing of monitoring wells and performed laboratory studies to better characterize the hydrogeologic and hydrogeochemical properties (e.g., borehole lithology, geochemistry, geophysical properties, hydraulic conductivity, degradation rates, partitioning coefficients) in the perched-intermediate zone.
- Conducted laboratory studies to determine the environmental fate of RDX.
- Performed a monitoring well network evaluation, installed new monitoring wells, and reconfigured a monitoring well to enhance the groundwater monitoring network, resulting in 11 perched-intermediate groundwater monitoring wells and 14 regional aquifer monitoring wells being used to monitor RDX in perched-intermediate and regional groundwater zones.
- Collected data during cross-hole aquifer tests for use in evaluating the feasibility of remedy implementation for remedial alternatives.
- Collected information to update the CSM.

In total, these actions address the uncertainties identified in the NMED's NOD to the 2007 CME (NMED 2008, 101311).

This report presents the physical system CSM for fate and transport of HE in the TA-16 area, with particular emphasis on sources and pathways that affect the distribution of RDX in perched-intermediate and regional groundwater. The discussion builds on the CSM presented in the "Investigation Report for Water Canyon/Cañon de Valle" (LANL 2011, 207069) that was modified to include new and updated information collected since 2011.

The 260 Outfall was the most significant source for HE release at TA-16 based on data collected from previous investigations showing the spatial distribution of these constituents in the Cañon de Valle watershed. The outfalls and surface release sites primarily responsible for RDX in surface water and groundwater are no longer active, and source removal actions have been completed at the key RDX sources.

The pathway for RDX found in perched-intermediate groundwater zones in the lower vadose zone and in the regional aquifer is percolation of local infiltration through the upper vadose zone. Infiltration through the vadose zone is expected to be predominantly vertical and controlled by gravity and the hydrogeological properties of the medium. Stratigraphic and structural features (e.g., silt layers, faults) appear to be locally significant. Significant vertical anisotropy occurs because of the layered nature of the stratigraphic units, and horizontal hydraulic conductivities within stratigraphic units are significantly greater than vertical hydraulic conductivities across bedding within and between units. As a result, downward percolating moisture is likely to be diverted laterally at capillary barriers associated with bedding contacts in the stratigraphic sequence. Downward moisture flux through the upper vadose zone will have a tendency to staircase towards the east and southeast, following the dips of the geologic units.

Two significant zones of perched-intermediate groundwater occur in the lower vadose zone as a result of perching on less permeable strata. These perched-intermediate zones are lateral pathways for the transport of RDX in the vadose zone. Both perched-intermediate zones contain RDX at concentrations

greater than the 9.66 µg/L NMED tap water screening level for drinking. RDX concentrations are higher in the upper perched-intermediate zone relative to the lower perched-intermediate zone. The estimated mass of RDX in both perched-intermediate zones combined is between 263 kg and 1478 kg.

Groundwater in the two perched-intermediate zones is a mixture of clean MBR and MFR containing varying concentrations of RDX. Based on hydrogeochemical investigations, approximately a third of the water in the perched-intermediate zones near the 260 Outfall originated as local MFR. Infiltration of surface water containing RDX in Cañon de Valle during the period of effluent releases (1951–1996) is the primary source of the RDX currently found in perched-intermediate and regional groundwater zones at TA-16.

The upper perched-intermediate zone is located in ash-flow tuffs of the lower Otowi Member, pumice-fall deposits of the Guaje Pumice Bed, and sedimentary deposits of the upper Puye Formation. The lower perched-intermediate zone is located within sedimentary deposits of the Puye Formation. Because of its proximity to the mountain front, the Puye Formation at TA-16 is largely made up of overlapping paleo stream channels filled by boulders, cobbles, and gravels. The particle size of the matrix materials largely controls the hydraulic conductivity of individual beds. The paleo channels of the Puye Formation are elongated in a down-fan direction, which was generally eastward. Thin fine-grained sediments deposited in interchannel areas may provide local aquitards that underlie perched-intermediate groundwater. Groundwater pathways in this type of environment are likely controlled by the juxtaposition of fines-depleted deposits that have high hydraulic conductivities and form networks of favorable pathways for groundwater flow. The facies model is consistent with hydrologic observations during pump tests and cross-hole aquifer tests. The heterogeneity and limited areal extent associated with these paleo channels presents significant challenges to effectively removing quantities of water in volumes required for either water supply or remediation.

The regional groundwater system is a complex heterogeneous system that includes shallow, predominantly unconfined and deep, predominantly confined zones. Vertical hydraulic stratification in the regional aquifer is indicated by pronounced vertical differences in hydraulic heads in multiscreen wells and a lack of vertical propagation of pumping drawdown caused by pumping tests and pumping of municipal water supply wells. There are no clearly defined aquitards or confining layers that provide hydraulic separation between the shallow and deep zones of the regional aquifer. The vertical hydraulic separation is likely caused by pronounced vertical aquifer anisotropy, with the lateral permeability substantially higher than the vertical permeability. The anisotropy is related to the complex depositional layering of the Puye Formation.

This report documents the comparison of groundwater data to applicable NMED water-quality criteria. This screening process compared over 19,100 analytical results collected since 2000 to NMED standards and screening levels. This screening process confirmed that RDX is the only COPC in perched-intermediate and regional groundwater based on concentrations greater than the NMED tap-water screening level, which is consistent with past conclusions. The NMED's Risk Assessment Guidance for Site Investigations and Remediation (Risk Assessment Guidance) states that "NMED tap water screening levels were developed for residential land-use only." Also, "Exposure to contaminants can occur through the ingestion of and dermal contact with domestic/household water..." (NMED 2019, 700550). Additionally, the screening level is based on assumed average chronic (daily) exposure duration of 70 yr.

Based on this application of the tap water screening level to the site conditions, the extent of RDX contamination in the perched-intermediate and regional groundwater beneath the site does not currently pose an unacceptable risk to human health due to the following considerations.

- The extent of perched-intermediate groundwater containing RDX at concentrations above the NMED's tap water screening level is spatially limited to an area beneath the site and above the regional aquifer.
- Regional groundwater containing RDX in concentrations above the tap water screening level is more than 3 mi from the nearest water-supply wells, PM-2, PM-4, and PM-5.
- Land-use restrictions and LANL's project review process inherently prohibit drilling of new wells for water supply within or near portions of the aquifer containing RDX in excess of the tap water screening level.
- The groundwater contained in the perched-intermediate zone occurs in complex and heterogeneous strata that do not make up a continuous water-bearing unit sufficient to extract the volumes needed to support a sustainable water supply.

Currently, RDX concentrations in the perched-intermediate groundwater are stable or decreasing. RDX concentrations in regional aquifer monitoring wells are largely below the tap water screening level. Groundwater samples from well R-18 show increasing RDX over time, but concentrations are currently less than half the screening level. The extent to which the footprint of RDX in the regional aquifer might expand or whether RDX in perched-intermediate groundwater would continue to be a source of RDX to the regional groundwater in a manner that could cause the footprint to expand needs to be assessed. The scientific way to evaluate this potential is through the use of fate and transport modeling. Consent Order Section IX.C states

...the corrective action process employs both screening levels and cleanup levels. Screening levels are contaminant concentrations that indicate the potential for unacceptable risk. If contaminants are present at concentrations above screening levels, it does not necessarily indicate that cleanup is required, but it does indicate that additional risk evaluation is needed to determine the potential need for cleanup. Cleanup levels are the contaminant concentrations that indicate when cleanup objectives are met. The need for cleanup is triggered by potential unacceptable risk and not by exceedance of screening levels."

Further Section IX.F of the Consent Order states "NMED's tap water screening levels shall be used as groundwater screening levels for protection of human health if groundwater is a current or reasonably foreseeable source of drinking water."

5.0 RECOMMENDATIONS

The current conditions pertaining to RDX above the tap water screening level in the perched-intermediate and regional groundwater indicate that there is currently no complete pathway to potential exposure. Because of institutional controls at the Laboratory site, the only feasible exposure scenario for the foreseeable future would be withdrawal of contaminated groundwater at an existing water-supply well that is owned and operated by Los Alamos County. There are, however, uncertainties regarding the potential for RDX presently in a localized portion of the regional aquifer, or that might reach the regional aquifer from the source in the perched-intermediate zone, to expand beyond its current footprint and potentially pose a risk of exposure under the assumptions set forth in NMED Risk Assessment Guidance.

To address the uncertainties and to be consistent with NMED Risk Assessment Guidance, it is recommended that a risk assessment be developed for the RDX contamination in groundwater. The risk assessment would incorporate a fate and transport modeling analysis as input to the evaluation. The model would address the long-term fate of the perched-intermediate and vadose-zone RDX inventory and potential for expansion of the extent of RDX in the regional groundwater. It would also be a necessary component of a subsequent CME.

During this process, monitoring in perched-intermediate and regional groundwater will continue under the IFGMP. Changes to the frequency of monitoring specifically for RDX are proposed for wells within TA-16 Monitoring Group (R-18, R-47, R-48, R-58, R-63, R-68, R-69, CdV-R-15-3, CdV-R-37-2), MDA C Monitoring Group (R-14, R-46, R-60), and General Surveillance Group (R-17 and R-19) to ensure protection of water-supply wells. Figure 3.2-13 shows the location of the monitoring wells. The monitoring well frequency would establish a group of wells, sampled quarterly that would monitor any changes in the current extent of RDX in regional groundwater. Another set of wells further downgradient of the current extent of RDX contamination would be sampled semiannually. The wells in the network and their proposed sampling frequency are shown below. Any changes to the RDX monitoring sampling frequency will be proposed in the 2021 IFGMP.

Well	IFGMP HE Sample Frequency	Recommended Frequency
R-48	Quarterly	Quarterly
R-63	Quarterly	Quarterly
R-68	Quarterly	Quarterly
R-69	Quarterly	Quarterly
R-47	Quarterly	Quarterly
R-18	Quarterly	Quarterly
R-58	Quarterly	Quarterly
CdV-R-37-2	Annual	Quarterly
CdV-R-15-3	Semiannual	Semiannual
R-17	Annual	Semiannual
R-60	1/5 yr	Semiannual
R-19*	N/A	Semiannual
R-14	1/5 yr	Annual
R-46	1/5	Annual

* R-19 is part of the early warning well network but is being reconfigured with a Baski System. After installation of the Baski System, R-19 will be sampled quarterly for the first year. After the first year, the sampling frequency will be revisited.

6.0 REFERENCES AND MAP DATA SOURCES

6.1 References

The following reference list includes documents cited in this report. Parenthetical information following each reference provides the author(s), publication date, and ERID, ESHID, or EMID. This information is also included in text citations. ERIDs were assigned by the Laboratory's Associate Directorate for Environmental Management (IDs through 599999); ESHIDs were assigned by the Laboratory's Associate Directorate for Environment, Safety, and Health (IDs 600000 through 699999); and EMIDs are assigned by Newport News Nuclear BWXT-Los Alamos, LLC (N3B) (IDs 700000 and above). IDs are used to locate documents in N3B's Records Management System and in the Master Reference Set. The NMED Hazardous Waste Bureau and N3B maintain copies of the Master Reference Set. The set ensures that NMED has the references to review documents. The set is updated when new references are cited in documents.

- Bailey, R.A., R.L. Smith, and C.S. Ross, 1969. "Stratigraphic Nomenclature of Volcanic Rocks in the Jemez Mountains, New Mexico," in *Contributions to Stratigraphy*, U.S. Geological Survey Bulletin 1274-P, Washington, D.C. (Bailey et al. 1969, 021498)
- Broxton, D., R. Warren, P. Longmire, R. Gilkeson, S. Johnson, D. Rogers, W. Stone, B. Newman, M. Everett, D. Vaniman, S. McLin, J. Skalski, and D. Larssen, March 2002. "Characterization Well R-25 Completion Report," Los Alamos National Laboratory report LA-13909-MS, Los Alamos, New Mexico. (Broxton et al. 2002, 072640)
- Broxton, D., G. WoldeGabriel, L. Peters, J. Budahn, and G. Luedemann, 2007. "Pliocene Volcanic Rocks of the Tschicoma Formation, East-Central Jemez Volcanic Field: Chemistry, Petrography, and Age Constraints," New Mexico Geological Society Guidebook: 58th Field Conference, Geology of the Jemez Mountains Region II, pp. 284–295. (Broxton et al. 2007, 106121)
- Broxton, D.E., and S.L. Reneau, August 1995. "Stratigraphic Nomenclature of the Bandelier Tuff for the Environmental Restoration Project at Los Alamos National Laboratory," Los Alamos National Laboratory report LA-13010-MS, Los Alamos, New Mexico. (Broxton and Reneau 1995, 049726)
- Caporaso, J.G., C.L. Lauber, W.A. Walters, D. Berg-Lyons, J. Huntley, N. Fierer, S.M. Owens, J. Betley, L. Fraser, M. Bauer, N. Gormley, J.A. Gilbert, G. Smith, and R. Knight, March 8, 2012. "Ultra-High-Throughput Microbial Community Analysis on the Illumina HiSeq and MiSeq Platforms," *The ISME Journal*, Vol. 6, pp. 1621-1624. (Caporaso et al. 2012, 700548)
- Cavazza, W., March 1989. "Sedimentation Pattern of a Rift-Filling Unit, Tesuque Formation (Miocene), Española Basin, Rio Grande Rift, New Mexico," *Journal of Sedimentary Petrology*, Vol. 59, No. 2, pp. 287–296. (Cavazza 1989, 021501)
- Daniel B. Stephens & Associates Inc., January 2018. "Long-Range Water Supply Plan, Los Alamos County," report prepared for Los Alamos County by Daniel B. Stephens & Associates, Inc., Albuquerque, New Mexico. (Daniel B. Stephens & Associates, Inc. 2018, 700540)
- DOE (U.S. Department of Energy), August 3, 1995. "Environmental Assessment for the High Explosives Wastewater Treatment Facility, Los Alamos National Laboratory, Los Alamos, New Mexico," U.S. Department of Energy document DOE/EA-1100, Los Alamos Area Office, Los Alamos, New Mexico. (DOE 1995, 700539)
- EPA (U.S. Environmental Protection Agency), 1990. "NPDES Authorization to Discharge Waters of the United States," Water Management Division, EPA Region 6, Dallas, Texas. (EPA 1990, 012454)

- EPA (U.S. Environmental Protection Agency), June 2003. "Environmental Protection Agency National Primary Drinking Water Standards and Secondary Drinking Water Standards," EPA 816-F03-016, Environmental Protection Agency Office of Water, Washington, D.C. (EPA 2003, 093662)
- EPA (U.S. Environmental Protection Agency), October 2004. "EPA Region 9 Preliminary Remediation Goals Table," San Francisco, California. (EPA 2004, 093663)
- EPA (U.S. Environmental Protection Agency), November 2005. "EPA Region 6 Human Health Medium-Specific Screening Levels," U.S. EPA Region 6, Dallas, Texas. (EPA 2005, 091002)
- Ferguson, J.F., W.S. Baldrige, L.W. Braile, S. Biehler, B. Gilpin, and G.R. Jiracek, 1995. "Structure of the Española Basin, Rio Grande Rift, New Mexico, from Stage Seismic and Gravity Data," New Mexico Geological Society Guidebook: 46th Field Conference, Geology of the Santa Fe Region, pp. 105-110. (Ferguson et al. 1995, 056018)
- Galusha, T., and J.C. Blick, April 1971. "Stratigraphy of the Santa Fe Group, New Mexico," *Bulletin of the American Museum of Natural History*, Vol. 144, No. 1, pp. 1-128. (Galusha and Blick 1971, 021526)
- Gard, M.O., and B.D. Newman, November 2005. "The High Explosives Source Term at TA-16," Los Alamos National Laboratory document LA-UR-05-9433, Los Alamos, New Mexico. (Gard and Newman 2005, 093651)
- Gardner, J.L., S.L. Reneau, C.J. Lewis, A. Lavine, D.J. Krier, G. WoldeGabriel, and G.D. Guthrie, 2001. "Geology of the Pajarito Fault Zone in the Vicinity of S-Site (TA-16), Los Alamos National Laboratory, Rio Grande Rift, New Mexico," Los Alamos National Laboratory report LA-13831-MS, Los Alamos, New Mexico. (Gardner et al. 2001, 070106)
- Gardner, J.N., W.S. Baldrige, R. Gribble, K. Manley, K. Tanaka, J.W. Geissman, M. Gonzales, and G. Baron, December 1990. "Results from Seismic Hazards Trench #1 (SHT-1) Los Alamos Seismic Hazards Investigations," Los Alamos National Laboratory document EES1-SH90-19, Los Alamos, New Mexico. (Gardner et al. 1990, 048813)
- Gardner, J.N., F. Goff, S. Kelley, and E. Jacobs, February 2010. "Rhyolites and Associated Deposits of the Valles-Toledo Caldera Complex," *New Mexico Geology*, Vol. 32, No. 1, pp. 3-18. (Gardner et al. 2010, 204421)
- Gardner, J.N., and F.E. Goff, 1984. "Potassium-Argon Dates from the Jemez Volcanic Field: Implications for Tectonic Activity in the North-Central Rio Grande Rift," New Mexico Geological Society Guidebook: 35th Field Conference, Rio Grande Rift, Northern New Mexico, University of New Mexico, Albuquerque, New Mexico. (Gardner and Goff 1984, 044021)
- Gardner, J.N., F.E. Goff, S.R. Garcia, and R.C. Hagan, February 10, 1986. "Stratigraphic Relations and Lithologic Variations in the Jemez Volcanic Field, New Mexico," *Journal of Geophysical Research*, Vol. 91, No. B2, pp. 1763-1778. (Gardner et al. 1986, 059104)
- Gardner, J.N., and L.S. House, October 1987. "Seismic Hazards Investigations at Los Alamos National Laboratory, 1984 to 1985," Los Alamos National Laboratory report LA-11072-MS, Los Alamos, New Mexico. (Gardner and House 1987, 006682)

- Gardner, J.N., A. Lavine, G. WoldeGabriel, D. Krier, J., D.T. Vaniman, F.A. Caporuscio, C.J. Lewis, M.R. Reneau, E.C. Kluk, and M.J. Snow, March 1999. "Structural Geology of the Northwestern Portion of Los Alamos National Laboratory, Rio Grande Rift, New Mexico: Implications for Seismic Surface Rupture Potential from TA-3 to TA-55," Los Alamos National Laboratory report LA-13589-MS, Los Alamos, New Mexico. (Gardner et al. 1999, 063492)
- Golombek, M.P., February 1983. "Geology, Structure, and Tectonics of the Pajarito Fault Zone in the Española Basin of the Rio Grande Rift, New Mexico," *Geological Society of America Bulletin*, Vol. 94, pp. 192–205. (Golombek 1983, 601748)
- Griggs, R.L., and J.D. Hem, 1964. "Geology and Ground-Water Resources of the Los Alamos Area, New Mexico," U.S. Geological Survey Water Supply Paper 1753, Washington, D.C. (Griggs and Hem 1964, 092516)
- Izett, G.A., and J.D. Obradovich, February 10, 1994. "⁴⁰Ar/³⁹Ar Age Constraints for the Jaramillo Normal Subchron and the Matuyama-Brunhes Geomagnetic Boundary," *Journal of Geophysical Research*, Vol. 99, No. B2, pp. 2925–2934. (Izett and Obradovich 1994, 048817)
- Kelley, V.C., 1978. "Geology of Española Basin, New Mexico," Map 48, ISSN: 0545-2899, New Mexico Bureau of Mines and Mineral Resources, Socorro, New Mexico. (Kelley 1978, 011659)
- Kleinfelder, May 7, 2004. "Final Well CdV-16-1(i) Completion Report," report prepared for Los Alamos National Laboratory, Project No. 37151/9.12, Albuquerque, New Mexico. (Kleinfelder 2004, 087844)
- Koch, R.J., and S. Schmeer, March 2011. "Groundwater Level Status Report for 2010, Los Alamos National Laboratory," Los Alamos National Laboratory report LA-14437-PR, Los Alamos, New Mexico. (Koch and Schmeer 2011, 201566)
- LANL (Los Alamos National Laboratory), November 1990. "Solid Waste Management Units Report," Vol. II of IV (TA-10 through TA-25), Los Alamos National Laboratory document LA-UR-90-3400, Los Alamos, New Mexico. (LANL 1990, 007512)
- LANL (Los Alamos National Laboratory), July 1993. "RFI Work Plan for Operable Unit 1082," Los Alamos National Laboratory document LA-UR-93-1196, Los Alamos, New Mexico. (LANL 1993, 020948)
- LANL (Los Alamos National Laboratory), July 1993. "RFI Work Plan for Operable Unit 1086," Los Alamos National Laboratory document LA-UR-92-3968, Los Alamos, New Mexico. (LANL 1993, 020946)
- LANL (Los Alamos National Laboratory), May 9, 1994. "Process Flow Reductions from Waste Minimization for Value Engineering Study," Los Alamos National Laboratory, Los Alamos, New Mexico. (LANL 1994, 076858)
- LANL (Los Alamos National Laboratory), July 1994. "RFI Work Plan for Operable Unit 1082, Addendum I," Los Alamos National Laboratory document LA-UR-94-1580, Los Alamos, New Mexico. (LANL 1994, 039440)
- LANL (Los Alamos National Laboratory), 1996. "Interim Action Report for Solid Waste Management Unit 16-021(c), Field Unit 3," Los Alamos National Laboratory document LA-UR-96-419, Los Alamos, New Mexico. (LANL 1996, 053838)
- LANL (Los Alamos National Laboratory), September 1996. "RFI Report for Potential Release Sites in TA-16: 16-003(k), 16-021(c)," Los Alamos National Laboratory document LA-UR-96-3191, Los Alamos, New Mexico. (LANL 1996, 055077)

- LANL (Los Alamos National Laboratory), September 1998. "RFI Report for Potential Release Site 16-021(c)," Los Alamos National Laboratory document LA-UR-98-4101, Los Alamos, New Mexico. (LANL 1998, 059891)
- LANL (Los Alamos National Laboratory), September 1998. "CMS Plan for Potential Release Site 16-021(c)," Los Alamos National Laboratory document LA-UR-98-3918, Los Alamos, New Mexico. (LANL 1998, 062413)
- LANL (Los Alamos National Laboratory), September 1999. "Addendum to CMS Plan for Potential Release Site 16-021(c)," Los Alamos National Laboratory document LA-UR-98-3918, Los Alamos, New Mexico. (LANL 1999, 064873)
- LANL (Los Alamos National Laboratory), February 2000. "Interim Measures Plan for Consolidated Potential Release Site 16-021(c)-99," Los Alamos National Laboratory document LA-UR-99-6767, Los Alamos, New Mexico. (LANL 2000, 064355)
- LANL (Los Alamos National Laboratory), January 2001. "Project Completion Report for the Accelerated Action at TA-16, MDA R," Los Alamos National Laboratory document LA-UR-01-522, Los Alamos, New Mexico. (LANL 2001, 069971)
- LANL (Los Alamos National Laboratory), July 2002. "Interim Measure Report for Potential Release Site 16-021(c)-99," Los Alamos National Laboratory document LA-UR-02-4229, Los Alamos, New Mexico. (LANL 2002, 073706)
- LANL (Los Alamos National Laboratory), March 2003. "Addendum to the CMS Plan for PRS 16-021(c), Revision 1," Los Alamos National Laboratory document LA-UR-02-7366, Los Alamos, New Mexico. (LANL 2003, 075986)
- LANL (Los Alamos National Laboratory), September 2003. "Phase III RFI Report for Solid Waste Management Unit 16-021(c)-99," Los Alamos National Laboratory document LA-UR-03-5248, Los Alamos, New Mexico. (LANL 2003, 077965)
- LANL (Los Alamos National Laboratory), November 2003. "Corrective Measures Study Report for Solid Waste Management Unit 16-021(c)-99," Los Alamos National Laboratory document LA-UR-03-7627, Los Alamos, New Mexico. (LANL 2003, 085531)
- LANL (Los Alamos National Laboratory), August 2005. "Material Disposal Area P Site Closure Certification Report, Revision 1," Los Alamos National Laboratory document LA-UR-05-6536, Los Alamos, New Mexico. (LANL 2005, 092251)
- LANL (Los Alamos National Laboratory), August 2006. "Investigation Report for Intermediate and Regional Groundwater, Consolidated Unit 16-021(c)-99," Los Alamos National Laboratory document LA-UR-06-5510, Los Alamos, New Mexico. (LANL 2006, 093798)
- LANL (Los Alamos National Laboratory), August 6, 2006. "Request for 'Contained In' Determination for the Purged Alluvial Groundwater Collected during the Quarterly Sampling of Monitoring Wells Associated with Consolidated Unit 16-021(c)-99 Investigation within Technical Area 16," Los Alamos National Laboratory letter (EP2006-0700) to J. Bearzi (NMED-HWB) from A. Phelps (LANL) and D. Gregory (DOE-LASO). (LANL 2006, 092717)

- LANL (Los Alamos National Laboratory), April 2007. "Evaluation of the Suitability of Wells Near Technical Area 16 for Monitoring Contaminant Releases from Consolidated Unit 16-021(c)-99," Los Alamos National Laboratory document LA-UR-07-2370, Los Alamos, New Mexico. (LANL 2007, 095787)
- LANL (Los Alamos National Laboratory), May 2007. "Corrective Measures Implementation Plan for Consolidated Unit 16-021(c)-99," Los Alamos National Laboratory document LA-UR-07-2019, Los Alamos, New Mexico. (LANL 2007, 096003)
- LANL (Los Alamos National Laboratory), June 2007. "Drilling Work Plan for Intermediate Aquifer Well R-25b," Los Alamos National Laboratory document LA-UR-07-3952, Los Alamos, New Mexico. (LANL 2007, 098121)
- LANL (Los Alamos National Laboratory), July 2007. "Corrective Measures Implementation Plan for Consolidated Unit 16-021(c)-99, Revision 1," Los Alamos National Laboratory document LA-UR-07-4715, Los Alamos, New Mexico. (LANL 2007, 098192)
- LANL (Los Alamos National Laboratory), August 2007. "Corrective Measures Evaluation Report, Intermediate and Regional Groundwater, Consolidated Unit 16-021(c)-99," Los Alamos National Laboratory document LA-UR-07-5426, Los Alamos, New Mexico. (LANL 2007, 098734)
- LANL (Los Alamos National Laboratory), September 2007. "Evaluation of the Suitability of Wells Near Technical Area 16 for Monitoring Contaminant Releases from Consolidated Unit 16-021(c)-99, Revision 1," Los Alamos National Laboratory document LA-UR-07-6433, Los Alamos, New Mexico. (LANL 2007, 100113)
- LANL (Los Alamos National Laboratory), February 2008. "Drilling Work Plan for Well R-25c," Los Alamos National Laboratory document LA-UR-08-0337, Los Alamos, New Mexico. (LANL 2008, 100696)
- LANL (Los Alamos National Laboratory), March 2008. "Drilling Work Plan for Well CdV-16-3(i)," Los Alamos National Laboratory document LA-UR-08-1534, Los Alamos, New Mexico. (LANL 2008, 101875.11)
- LANL (Los Alamos National Laboratory), March 2008. "Addendum to the 'Evaluation of the Suitability of Wells Near Technical Area 16 for Monitoring Contaminant Releases from Consolidated Unit 16-021(c)-99, Revision 1'," Los Alamos National Laboratory document LA-UR-08-1536, Los Alamos, New Mexico. (LANL 2008, 101875.5)
- LANL (Los Alamos National Laboratory), June 2008. "Supplemental Investigation Work Plan for Intermediate and Regional Groundwater at Consolidated Unit 16-021(c)-99," Los Alamos National Laboratory document LA-UR-08-3991, Los Alamos, New Mexico. (LANL 2008, 103165)
- LANL (Los Alamos National Laboratory), September 2008. "Completion Report for Well R-25c," Los Alamos National Laboratory document LA-UR-08-5878, Los Alamos, New Mexico. (LANL 2008, 103408)
- LANL (Los Alamos National Laboratory), December 2008. "Completion Report for Well R-25b, Revision 1," Los Alamos National Laboratory document LA-UR-08-7831, Los Alamos, New Mexico. (LANL 2008, 105018)
- LANL (Los Alamos National Laboratory), January 2009. "Phase II Investigation Report for the TA-16-340 Complex [Consolidated Units 13-003(a)-99 and 16-003(n)-99 and Solid Waste Management Units 16-003(o), 16-026(j2), and 16-029(f)], Revision 1," Los Alamos National Laboratory document LA-UR-09-0309, Los Alamos, New Mexico. (LANL 2009, 105061.17)

- LANL (Los Alamos National Laboratory), August 2009. "Pajarito Canyon Investigation Report, Revision 1," Los Alamos National Laboratory document LA-UR-09-4670, Los Alamos, New Mexico. (LANL 2009, 106939)
- LANL (Los Alamos National Laboratory), November 2009. "Work Plan for Redrilling Well R-47," Los Alamos National Laboratory document LA-UR-09-7269, Los Alamos, New Mexico. (LANL 2009, 107505)
- LANL (Los Alamos National Laboratory), January 2010. "Supplemental Investigation Report for Consolidated Units 16-007(a)-99 and 16-008(a)-99 at Technical Area 16," Los Alamos National Laboratory document LA-UR-09-8193, Los Alamos, New Mexico. (LANL 2010, 108279)
- LANL (Los Alamos National Laboratory), February 2010. "Completion Report for Regional Aquifer Well R-48," Los Alamos National Laboratory document LA-UR-10-0864, Los Alamos, New Mexico. (LANL 2010, 108778)
- LANL (Los Alamos National Laboratory), February 2010. "Hydrologic Testing Work Plan for Consolidated Unit 16-021(c)-99," Los Alamos National Laboratory document LA-UR-10-0404, Los Alamos, New Mexico. (LANL 2010, 108534)
- LANL (Los Alamos National Laboratory), March 2010. "Summary Report for the Corrective Measures Implementation at Consolidated Unit 16-021(c)-99," Los Alamos National Laboratory document LA-UR-10-0947, Los Alamos, New Mexico. (LANL 2010, 108868)
- LANL (Los Alamos National Laboratory), April 2010. "Completion Report for Intermediate Aquifer Well R-47i," Los Alamos National Laboratory document LA-UR-10-2207, Los Alamos, New Mexico. (LANL 2010, 109188)
- LANL (Los Alamos National Laboratory), April 2010. "Drilling Work Plan for Perched-Intermediate Pumping Well CdV-16-4ip," Los Alamos National Laboratory document LA-UR-10-2147, Los Alamos, New Mexico. (LANL 2010, 109268)
- LANL (Los Alamos National Laboratory), June 2011. "Hydrologic Testing Report for Consolidated Unit 16-021(c)-99," Los Alamos National Laboratory document LA-UR-11-3072, Los Alamos, New Mexico. (LANL 2011, 203711)
- LANL (Los Alamos National Laboratory), July 2011. "Completion Report for Regional Well R-63," Los Alamos National Laboratory document LA-UR-11-3673, Los Alamos, New Mexico. (LANL 2011, 204541)
- LANL (Los Alamos National Laboratory), September 2011. "2010/2011 Monitoring Summary Report for the Technical Area 16 Permeable Reactive Barrier and Associated Corrective Measures Implementation Projects," Los Alamos National Laboratory document LA-UR-11-4911, Los Alamos, New Mexico. (LANL 2011, 206408)
- LANL (Los Alamos National Laboratory), September 2011. "Investigation Report for Water Canyon/ Cañon de Valle," Los Alamos National Laboratory document LA-UR-11-5478, Los Alamos, New Mexico. (LANL 2011, 207069)
- LANL (Los Alamos National Laboratory), January 2012. "Work Plan for a Tracer Test at Consolidated Unit 16-021(c)-99, Technical Area 16," Los Alamos National Laboratory document LA-UR-12-0440, Los Alamos, New Mexico. (LANL 2012, 210352)

- LANL (Los Alamos National Laboratory), March 2012. "Technical Area 16 Well Network Evaluation and Recommendations," Los Alamos National Laboratory document LA-UR-12-1082, Los Alamos, New Mexico. (LANL 2012, 213573)
- LANL (Los Alamos National Laboratory), April 2012. "Work Plan for Direct Current Resistivity Profiling in Cañon de Valle," Los Alamos National Laboratory document LA-UR-12-20546, Los Alamos, New Mexico. (LANL 2012, 215111)
- LANL (Los Alamos National Laboratory), July 12, 2012. "Twenty-Five Year Site Plan, FY2013 - FY2037," Los Alamos National Laboratory document LA-UR-12-22913, Los Alamos, New Mexico. (LANL 2012, 601095)
- LANL (Los Alamos National Laboratory), November 2012. "Work Plan to Reconfigure Well CdV-16-4ip," Los Alamos National Laboratory document LA-UR-12-26150, Los Alamos, New Mexico. (LANL 2012, 232222)
- LANL (Los Alamos National Laboratory), December 2012. "Drilling Work Plan for Regional Aquifer Well R-58," Los Alamos National Laboratory document LA-UR-12-26784, Los Alamos, New Mexico. (LANL 2012, 212117)
- LANL (Los Alamos National Laboratory), February 2013. "Drilling Work Plan for Well R-63i," Los Alamos National Laboratory document LA-UR-13-20150, Los Alamos, New Mexico. (LANL 2013, 235924)
- LANL (Los Alamos National Laboratory), March 2013. "Interim Measures Work Plan for Source Removal Testing at Well CdV-16-4ip," Los Alamos National Laboratory document LA-UR-13-21795, Los Alamos, New Mexico. (LANL 2013, 239235)
- LANL (Los Alamos National Laboratory), April 2013. "Drilling Work Plan for Well CdV-9-1(i)," Los Alamos National Laboratory document LA-UR-13-20779, Los Alamos, New Mexico. (LANL 2013, 239226)
- LANL (Los Alamos National Laboratory), September 2013. "Well Reconfiguration of CdV-16-4ip Field Summary Report," Los Alamos National Laboratory document LA-UR-13-26926, Los Alamos, New Mexico. (LANL 2013, 249519)
- LANL (Los Alamos National Laboratory), July 2014. "Geophysical Investigation of Cañon de Valle," Los Alamos National Laboratory document LA-UR-14-25096, Los Alamos, New Mexico. (LANL 2014, 259157)
- LANL (Los Alamos National Laboratory), October 2014. "Interim Measures Report for Source-Removal Testing at Well CdV-16-4ip," Los Alamos National Laboratory document LA-UR-14-27065, Los Alamos, New Mexico. (LANL 2014, 600004)
- LANL (Los Alamos National Laboratory), June 2015. "Completion Report for Intermediate Aquifer Well CdV-9-1(i)," Los Alamos National Laboratory document LA-UR-15-23954, Los Alamos, New Mexico. (LANL 2015, 600503)
- LANL (Los Alamos National Laboratory), July 2015. "Work Plan for a Tracer Test at Consolidated Unit 16-021(c)-99, Technical Area 16, Revision 1," Los Alamos National Laboratory document LA-UR-15-24089, Los Alamos, New Mexico. (LANL 2015, 600535)
- LANL (Los Alamos National Laboratory), August 2015. "Work Plan for Intermediate Groundwater System Characterization at Consolidated Unit 16-021(c)-99," Los Alamos National Laboratory document LA-UR-15-24545, Los Alamos, New Mexico. (LANL 2015, 600686)

- LANL (Los Alamos National Laboratory), September 2015. "Completion Report for Intermediate Aquifer Well R-63i," Los Alamos National Laboratory document LA-UR-15-26729, Los Alamos, New Mexico. (LANL 2015, 600934)
- LANL (Los Alamos National Laboratory), April 2016. "Completion Report for Regional Aquifer Well R-58," Los Alamos National Laboratory document LA-UR-16-21912, Los Alamos, New Mexico. (LANL 2016, 601364)
- LANL (Los Alamos National Laboratory), September 2016. "Evaluation Report for Surface Corrective Measures Implementation Closure, Consolidated Unit 16-02I(c)-99," Los Alamos National Laboratory document LA-UR-16-27153, Los Alamos, New Mexico. (LANL 2016, 601837)
- LANL (Los Alamos National Laboratory), September 2016. "Groundwater Investigation Work Plan for Consolidated Unit 16-021(c)-99, Including Drilling Work Plans for Wells R-68 and R-69," Los Alamos National Laboratory document LA-UR-16-26493, Los Alamos, New Mexico. (LANL 2016, 601779)
- LANL (Los Alamos National Laboratory), February 2017. "Status Report for the Tracer Tests at Consolidated Unit 16-021(c)-99, Technical Area 16," Los Alamos National Laboratory document LA-UR-17-20782, Los Alamos, New Mexico. (LANL 2017, 602161)
- LANL (Los Alamos National Laboratory), April 2017. "Summary Report for Intermediate Groundwater System Characterization Activities at Consolidated Unit 16-02I(c)-99," Los Alamos National Laboratory document LA-UR-17-22550, Los Alamos, New Mexico. (LANL 2017, 602288)
- LANL (Los Alamos National Laboratory), July 27, 2017. "Completion Report for Regional Aquifer Well R-68," Los Alamos National Laboratory document LA-UR-17-26063, Los Alamos, New Mexico. (LANL 2017, 602539)
- LANL (Los Alamos National Laboratory), September 2017. "Remedy Completion Report for Corrective Measures Implementation at Consolidated Unit 16-021(c)-99," Los Alamos National Laboratory document LA-UR-17-27678, Los Alamos, New Mexico. (LANL 2017, 602597)
- LANL (Los Alamos National Laboratory), March 2018. "Compendium of Technical Reports Related to the Deep Groundwater Investigation for the RDX Project at Los Alamos National Laboratory," Los Alamos National Laboratory document LA-UR-18-21326, Los Alamos, New Mexico. (LANL 2018, 602963)
- Lewis, C.J., A. Lavine, S.L. Reneau, J.N. Gardner, R. Channell, and C.W. Criswell, December 2002. "Geology of the Western Part of Los Alamos National Laboratory (TA-3 to TA-16), Rio Grande Rift, New Mexico," Los Alamos National Laboratory report LA-13960-MS, Los Alamos, New Mexico. (Lewis et al. 2002, 073785)
- Lewis, C.L., J.N. Gardner, E.S. Schultz-Fellenz, A. Lavine, and S.L. Reneau, June 2009. "Fault Interaction and Along-Strike Variation in Throw in the Pajarito Fault System, Rio Grande Rift, New Mexico," *Geosphere*, Vol. 5, No. 3, pp. 252–269. (Lewis et al. 2009, 111708)
- McGehee, E.D., S. McCarthy, K. Towery, J. Ronquillo, K.L.M. Garcia, and J. Isaacson, March 28, 2003. "Sentinels of the Atomic Dawn: A Multiple-Property Evaluation of the Remaining Manhattan Project Properties at Los Alamos (1942-1946)," Historic Building Survey Report No. 215, Los Alamos National Laboratory document LA-UR-03-0726, Los Alamos, New Mexico. (McGehee et al. 2003, 700541)

- N3B (Newport News Nuclear BWXT-Los Alamos, LLC), May 2018. "Interim Facility-Wide Groundwater Monitoring Plan for the 2019 Monitoring Year, October 2018–September 2019," Newport News Nuclear BWXT-Los Alamos, LLC, document EM2018-0004, Los Alamos, New Mexico. (N3B 2018, 700000)
- N3B (Newport News Nuclear BWXT-Los Alamos, LLC), September 2018. "First Annual Long-Term Monitoring and Maintenance Report for the Corrective Measures Implementation at Consolidated Unit 16-021(c)-99," Newport News Nuclear BWXT-Los Alamos, LLC, document EM2018-0033, Los Alamos, New Mexico. (N3B 2018, 700089)
- N3B (Newport News Nuclear BWXT-Los Alamos, LLC), November 2018. "Annual Progress Report for the Corrective Measures Evaluation for the Deep Groundwater Investigation for Consolidated Unit 16-021(c)-99," Newport News Nuclear BWXT-Los Alamos, LLC, document EM2018-0095, Los Alamos, New Mexico. (N3B 2018, 700127)
- N3B (Newport News Nuclear BWXT-Los Alamos, LLC), March 2019. "Completion Report for Regional Aquifer Well R-69," Newport News Nuclear BWXT-Los Alamos, LLC, document EM2019-0053, Los Alamos, New Mexico. (N3B 2019, 700346)
- NMED (New Mexico Environment Department), January 20, 1998. "Approval Upon Modification, 16-003(k) and 16-021(c), RCRA Facility Investigation Report (EM/ER:96-502) and Response to Supplemental Information (EM/ER:97-476)," New Mexico Environment Department letter to T. Taylor (DOE-LAAO) and J. Browne (LANL Director) from B. Garcia (NMED-HRMB), Santa Fe, New Mexico. (NMED 1998, 093664)
- NMED (New Mexico Environment Department), September 8, 1999. "Approval, 16-021(c) RFI Report and CMS Plan," New Mexico Environment Department letter to T. Taylor (DOE-LAAO) and J. Browne (LANL Director) from J.E. Kieling (NMED-HRMB), Santa Fe, New Mexico. (NMED 1999, 093666)
- NMED (New Mexico Environment Department), January 7, 2000. "Contained-in Determination," New Mexico Environment Department letter to J. Browne (LANL), and T. Taylor (DOE ER), Santa Fe, New Mexico. (NMED 2000, 064730)
- NMED (New Mexico Environment Department), April 4, 2000. "Area of Contamination Approval 16-021(c)-99 Interim Measures Activities," New Mexico Environment Department letter to J. Browne (LANL Director) and T. Taylor (DOE-LAAO) from J.E. Kieling (Acting Manager/RCRA Permits Management Program), Santa Fe, New Mexico. (NMED 2000, 070649)
- NMED (New Mexico Environment Department), June 5, 2000. "In Situ Blending Authorization during 16-021(c)-99 Interim Measures Activities," New Mexico Environment Department letter HRMB-LANL-00-006 to J. Browne (LANL), and T. Taylor (DOE ER), Santa Fe, New Mexico. (NMED 2000, 067094)
- NMED (New Mexico Environment Department), June 21, 2004. "Approval as Modified, Phase III RFI Report for Solid Waste Management Unit (SWMU) 16-021(c)-99," New Mexico Environment Department letter to D. Gregory (DOE-LASO) and G.P. Nanos (LANL Director) from J.P. Bearzi (NMED-HWB), Santa Fe, New Mexico. (NMED 2004, 093248)
- NMED (New Mexico Environment Department), November 10, 2005. "Approval of the Material Disposal Area P Site Closure Certification Report, Revision 1," New Mexico Environment Department letter to G. Turner (DOE LASO) and R.W. Kuckuck (LANL Director) from J.P. Bearzi (NMED-HWB), Santa Fe, New Mexico. (NMED 2005, 093247)

- NMED (New Mexico Environment Department), October 13, 2006. "Final Decision, Remedy Selection for Solid Waste Management Unit 16-021(c)," New Mexico Environment Department letter to D. Gregory (DOE LASO) and D. McInroy (LANL) from R. Curry (NMED), Santa Fe, New Mexico. (NMED 2006, 095631)
- NMED (New Mexico Environment Department), August 15, 2007. "Notice of Disapproval of the Evaluation of the Suitability of Wells Near Technical Area 16 for Monitoring Contaminant Releases from Consolidated Unit 16-021(c)-99," New Mexico Environment Department letter to D. Gregory (DOE LASO) and D. McInroy (LANL) from J.P. Bearzi (NMED HWB), Santa Fe, New Mexico. (NMED 2007, 097874)
- NMED (New Mexico Environment Department), August 17, 2007. "Notice of Approval, Corrective Measures Implementation Plan for Consolidated Unit 16-021(c)-99, Revision 1," New Mexico Environment Department letter to D. Gregory (DOE-LASO) and D. McInroy (LANL) from J.P. Bearzi (NMED-HWB), Santa Fe, New Mexico. (NMED 2007, 098449)
- NMED (New Mexico Environment Department), November 2, 2007. "Approval of the Drilling Work Plan for Regional Aquifer Well R-25b," New Mexico Environment Department letter to D. Gregory (DOE-LASO) and D. McInroy (LANL) from J.P. Bearzi (NMED-HWB), Santa Fe, New Mexico. (NMED 2007, 098996)
- NMED (New Mexico Environment Department), March 11, 2008. "Notice of Approval, Drilling Work Plan for Well R-25c," New Mexico Environment Department letter to D. Gregory (DOE-LASO) and D. McInroy (LANL) from J.P. Bearzi (NMED-HWB), Santa Fe, New Mexico. (NMED 2008, 100575)
- NMED (New Mexico Environment Department), March 28, 2008. "Approval with Direction, Drilling Work Plans for Well CdV-16-3(i) and CdV-R-15-1," New Mexico Environment Department letter to D. Gregory (DOE-LASO) and D. McInroy (LANL) from J.P. Bearzi (NMED-HWB), Santa Fe, New Mexico. (NMED 2008, 101114)
- NMED (New Mexico Environment Department), April 22, 2008. "Notice of Disapproval Corrective Measures Evaluation Report, Intermediate and Regional Groundwater Consolidated Unit 16-021(c)-99," New Mexico Environment Department letter to D. Gregory (DOE-LASO) and D. McInroy (LANL) from J.P. Bearzi (NMED-HWB), Santa Fe, New Mexico. (NMED 2008, 101311)
- NMED (New Mexico Environment Department), January 26, 2009. "Approval with Modifications, Supplemental Investigation Work Plan for Intermediate and Regional Groundwater at TA-16 (Consolidated Unit 16-021(c)-99)," New Mexico Environment Department letter to D. Gregory (DOE-LASO) and D. McInroy (LANL) from J.P. Bearzi (NMED-HWB), Santa Fe, New Mexico. (NMED 2009, 104973)
- NMED (New Mexico Environment Department), June 20, 2012. "Approval with Modifications, Technical Area 16 Well Network Evaluation and Recommendations," New Mexico Environment Department letter to P. Maggiore (DOE-LASO) and M.J. Graham (LANL) from J.E. Kielling (NMED-HWB), Santa Fe, New Mexico. (NMED 2012, 520747)
- NMED (New Mexico Environment Department), December 21, 2012. "Approval with Modifications, Work Plan to Reconfigure Well CdV-16-4ip," New Mexico Environment Department letter to P. Maggiore (DOE-LASO) and J.D. Mousseau (LANL) from J.E. Kielling (NMED-HWB), Santa Fe, New Mexico. (NMED 2012, 521747)

- NMED (New Mexico Environment Department), December 31, 2012. "Approval with Modifications, Drilling Work Plan for Regional Aquifer Well R-58," New Mexico Environment Department letter to P. Maggiore (DOE-LASO) and J.D. Mousseau (LANL) from J.E. Kieling (NMED-HWB), Santa Fe, New Mexico. (NMED 2012, 521741)
- NMED (New Mexico Environment Department), March 8, 2013. "Approval with Modification, Drilling Work Plan for Well R-63i," New Mexico Environment Department letter to P. Maggiore (DOE-LASO) and J.D. Mousseau (LANL) from J.E. Kieling (NMED-HWB), Santa Fe, New Mexico. (NMED 2013, 522166)
- NMED (New Mexico Environment Department), May 31, 2013. "Approval with Modification, Drilling Work Plan for Well CdV-9-1(i)," New Mexico Environment Department letter to P. Maggiore (DOE-LASO) and J.D. Mousseau (LANL) from J.E. Kieling (NMED-HWB), Santa Fe, New Mexico. (NMED 2013, 522693)
- NMED (New Mexico Environment Department), October 21, 2016. "Approval, Evaluation Report for Surface Corrective Measures Implementation Closure, Consolidated Unit 16-021(c)-99," New Mexico Environment Department letter to D. Hintze (DOE-EM-LA) and M. Brandt (LANL) from J.E. Kieling (NMED-HWB), Santa Fe, New Mexico. (NMED 2016, 601914)
- NMED (New Mexico Environment Department), November 27, 2017. "Approval with Modifications, Remedy Completion Report for Corrective Measures Implementation at Consolidated Unit 16-021(c)-99," New Mexico Environment Department letter to D. Hintze (DOE-NA-LA) and B. Robinson (LANL) from J.E. Kieling (NMED-HWB), Santa Fe, New Mexico. (NMED 2017, 602758)
- NMED (New Mexico Environment Department), June 19, 2019. "Risk Assessment Guidance for Site Investigations and Remediation, Volume 1, Soil Screening Guidance for Human Health Risk Assessments," February 2019 (Revision 2, 6/19/19), Hazardous Waste Bureau and Ground Water Quality Bureau, Santa Fe, New Mexico. (NMED 2019, 700550)
- Reid, K.D., S.L. Reneau, B.D. Newman, and D.D. Hickmott, August 2005. "Barium and High Explosives in a Semiarid Alluvial System, Cañon de Valle, New Mexico," *Vadose Zone Journal*, Vol. 4, pp. 744–759. (Reid et al. 2005, 093660)
- Reneau, S.L., and E.V. McDonald, September 12–15, 1996. "Landscape History and Processes on the Pajarito Plateau, Northern New Mexico," in *Rocky Mountain Cell, Friends of the Pleistocene Field Trip Guidebook*, Los Alamos National Laboratory document LA-UR-96-3035, Los Alamos, New Mexico. (Reneau and McDonald 1996, 055538)
- Reneau, S.L., E.V. McDonald, J.N. Gardner, T.R. Kolbe, J.S. Carney, P.M. Watt, and P.A. Longmire, 1996. "Erosion and Deposition on the Pajarito Plateau, New Mexico, and Implications for Geomorphic Responses to Late Quaternary Climatic Changes," New Mexico Geological Society Guidebook: 47th Field Conference, Jemez Mountains Region, New Mexico, pp. 391-398. (Reneau et al. 1996, 055539)
- Samuels, K.E., D.E. Broxton, D.T. Vaniman, G. WoldeGabriel, J.A. Wolff, D.D. Hickmott, E.C. Kluk, and M.M. Fittipaldo, 2007. "Distribution of Dacite Lavas beneath the Pajarito Plateau, Jemez Mountains, New Mexico," New Mexico Geological Society Guidebook: 58th Field Conference, Geology of the Jemez Mountains Region II, pp. 296–308. (Samuels et al. 2007, 204422)
- Smith, R.L., and R.A. Bailey, 1966. "The Bandelier Tuff: A Study of Ash-Flow Eruption Cycles from Zoned Magma Chambers," *Bulletin Volcanologique*, Vol. 29, pp. 83-103. (Smith and Bailey 1966, 021584)

- Smith, R.L., R.A. Bailey, and C.S. Ross, 1970. "Geologic Map of the Jemez Mountains, New Mexico," U.S. Geological Survey Miscellaneous Investigations Series, Map I-571, Washington, D.C. (Smith et al. 1970, 009752)
- Spell, T.L., I. McDougall, and A.P. Dougeris, December 1996. "Cerro Toledo Rhyolite, Jemez Volcanic Field, New Mexico: $^{40}\text{Ar}/^{39}\text{Ar}$ Geochronology of Eruptions between Two Caldera-Forming Events," *Geological Society of America Bulletin*, Vol. 108, No. 12, pp. 1549-1566. (Spell et al. 1996, 055542)
- Turbeville, B.N., D.B. Waresback, and S. Self, February 1989. "Lava-Dome Growth and Explosive Volcanism in the Jemez Mountains, New Mexico: Evidence from the Pilo-Pliestocene Puye Alluvial Fan," *Journal of Volcanology and Geothermal Research*, Vol. 36, pp. 267-291. (Turbeville et al. 1989, 021587)
- WoldeGabriel, G., D.J. Koning, D. Broxton, and R.G. Warren, 2013. "Chronology of Volcanism, Tectonics, and Sedimentation Near the Western Boundary Fault of the Española Basin, Rio Grande Rif, New Mexico," *Geological Society of America Special Papers*, Vol. 494, pp. 221-238. (WoldeGabriel et al. 2013, 601750)

6.2 Map Data Sources

Monitoring well and spring point features; Former LANL ER-DB Database pull; 02 February 2004; As published 02 February 2004.

Infiltration area outline; Los Alamos National Laboratory, ER-ES, As published, project folder 11-0015; \\172.30.0.10\n3b-shares\GIS Data and Projects\11-Projects\11-0057\gdb\gdb_11-057.mdb\infiltration_lines_buffer; 2012.

SWMU or AOC; Los Alamos National Laboratory, Site Planning & Project Initiation Group, Infrastructure Planning Office; September 2007; As published 13 August 2010.

Structures; Los Alamos National Laboratory, KSL Site Support Services, Planning, Locating and Mapping Section; 06 January 2004; As published 29 November 2010.

Contours, 100, 20-ft interval; Los Alamos National Laboratory, Site Planning & Project Initiation Group, Infrastructure Planning Office; September 2007; As published 13 August 2010.

Paved Road; Los Alamos National Laboratory, FWO Site Support Services, Planning, Locating and Mapping Section; 06 January 2004; As published 29 November 2010.

Unpaved Road; Los Alamos National Laboratory, ER-ES, As published, GIS projects folder; \\slip\GIS\Projects\14-Projects\14-0062\project_data.gdb; digitized_site_features; digitized_road; 2017.

Drainage Channel; Los Alamos National Laboratory, ER-ES, As published, GIS projects folder; \\slip\GIS\Projects\11-Projects\11-0108\gdb\gdb_11-0108_generic.mdb; drainage; 2017.

Watersheds; Los Alamos National Laboratory, ENV Environmental Remediation and Surveillance Program; EP2006-0942; 1:2,500 Scale Data; 27 October 2006

TA-16 260 Outfall, As Published, GIS project folder: Q:\14-Projects\14-0080\project_data.gdb\
polygon\outfall_260

Technical Area Boundaries; Los Alamos National Laboratory, Database
Connections\GIS.PUB.PRD1.sde\PUB.Boundaries\PUB.tecareas_line

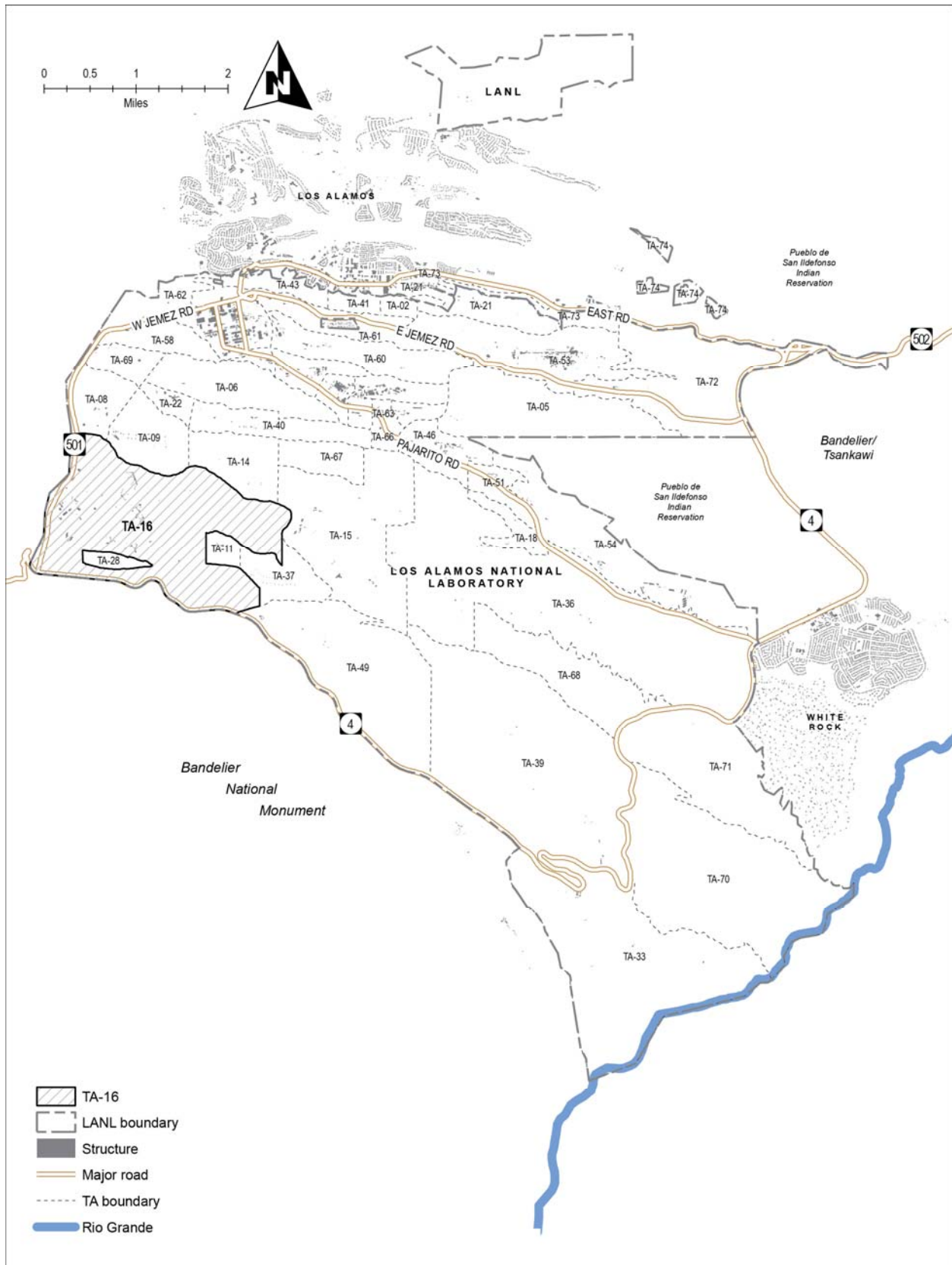


Figure 1.0-1 Location TA-16 within LANL

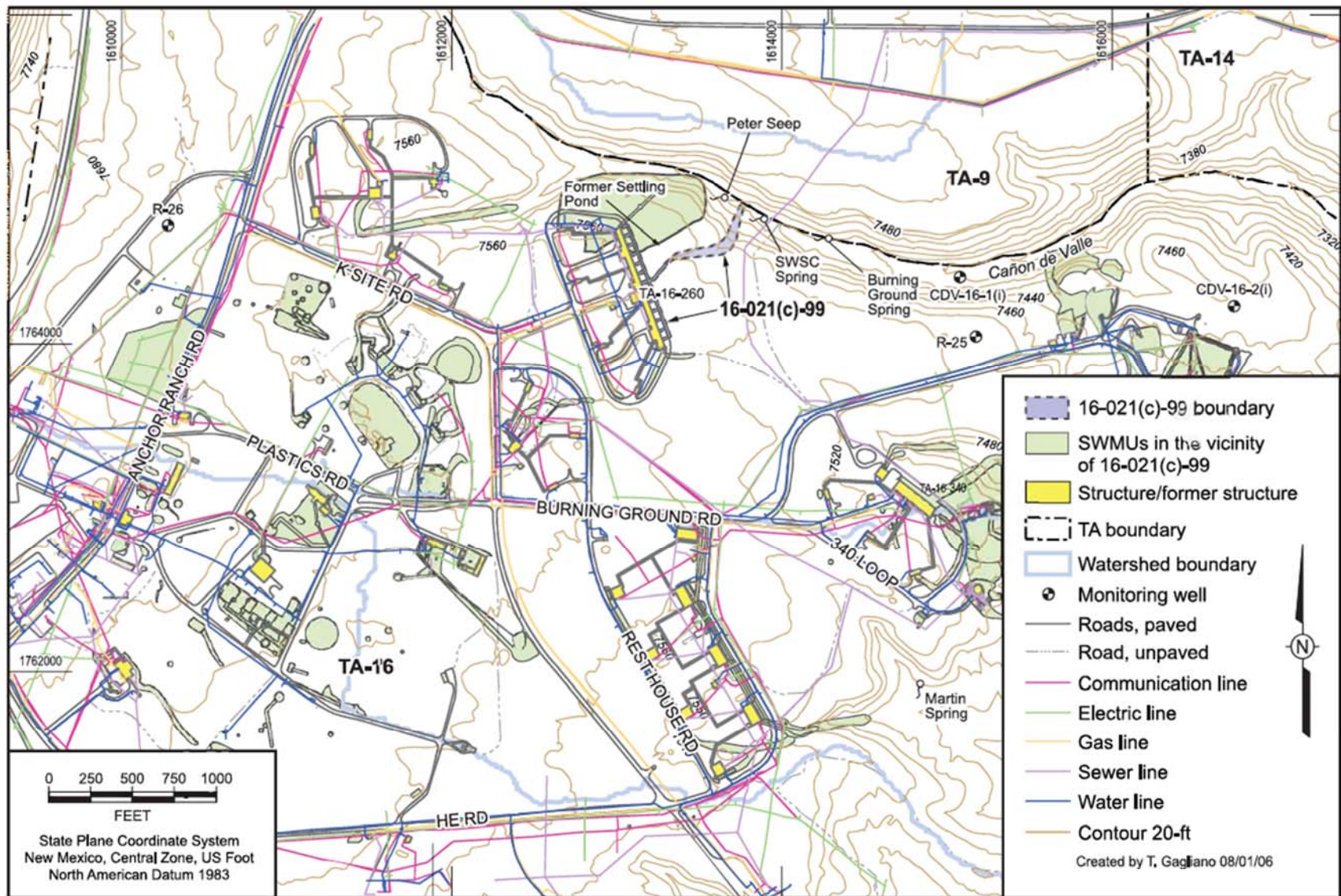


Figure 1.0-2 TA-16 boundary

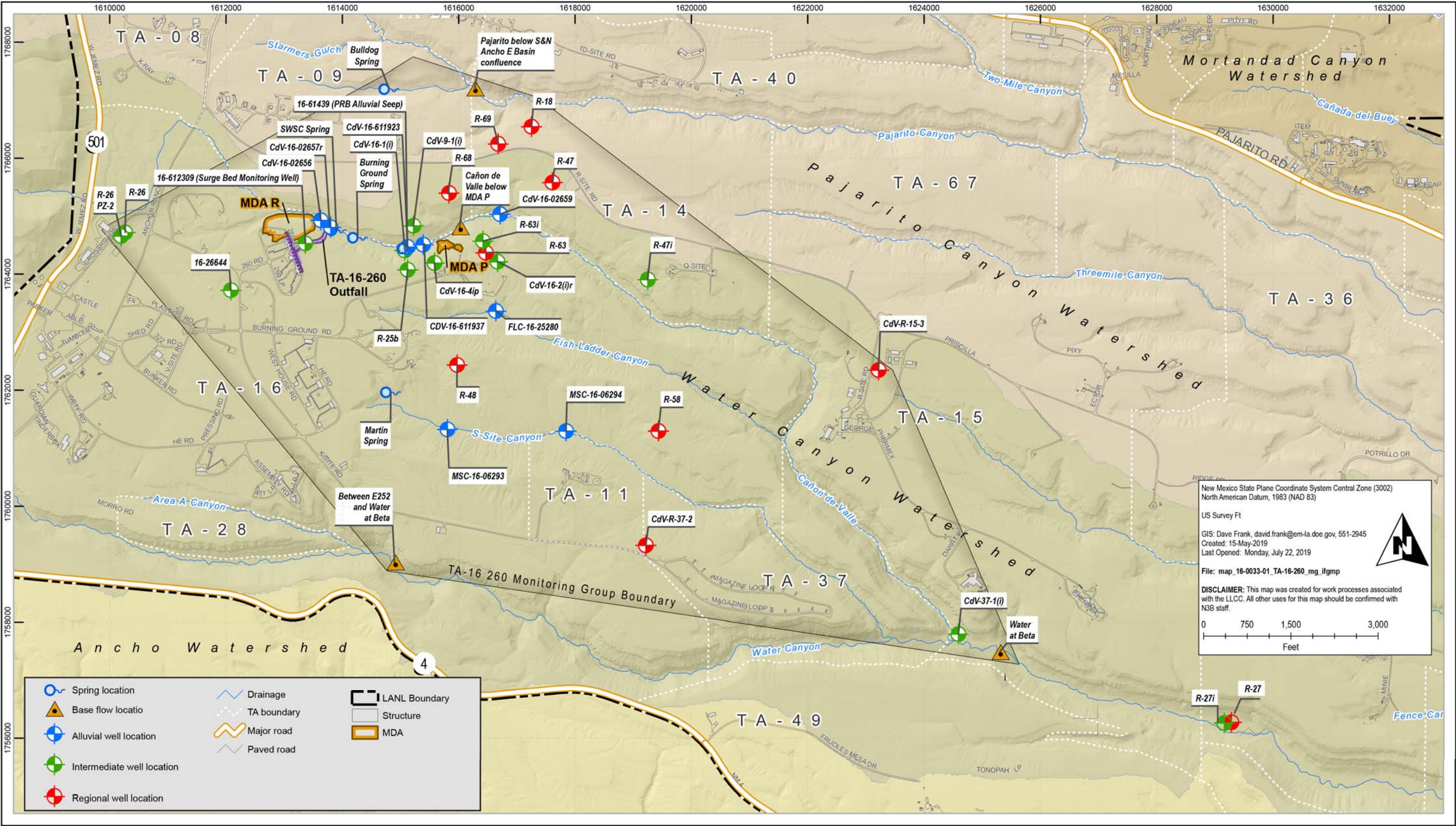


Figure 1.0-3 TA-16 Monitoring Group

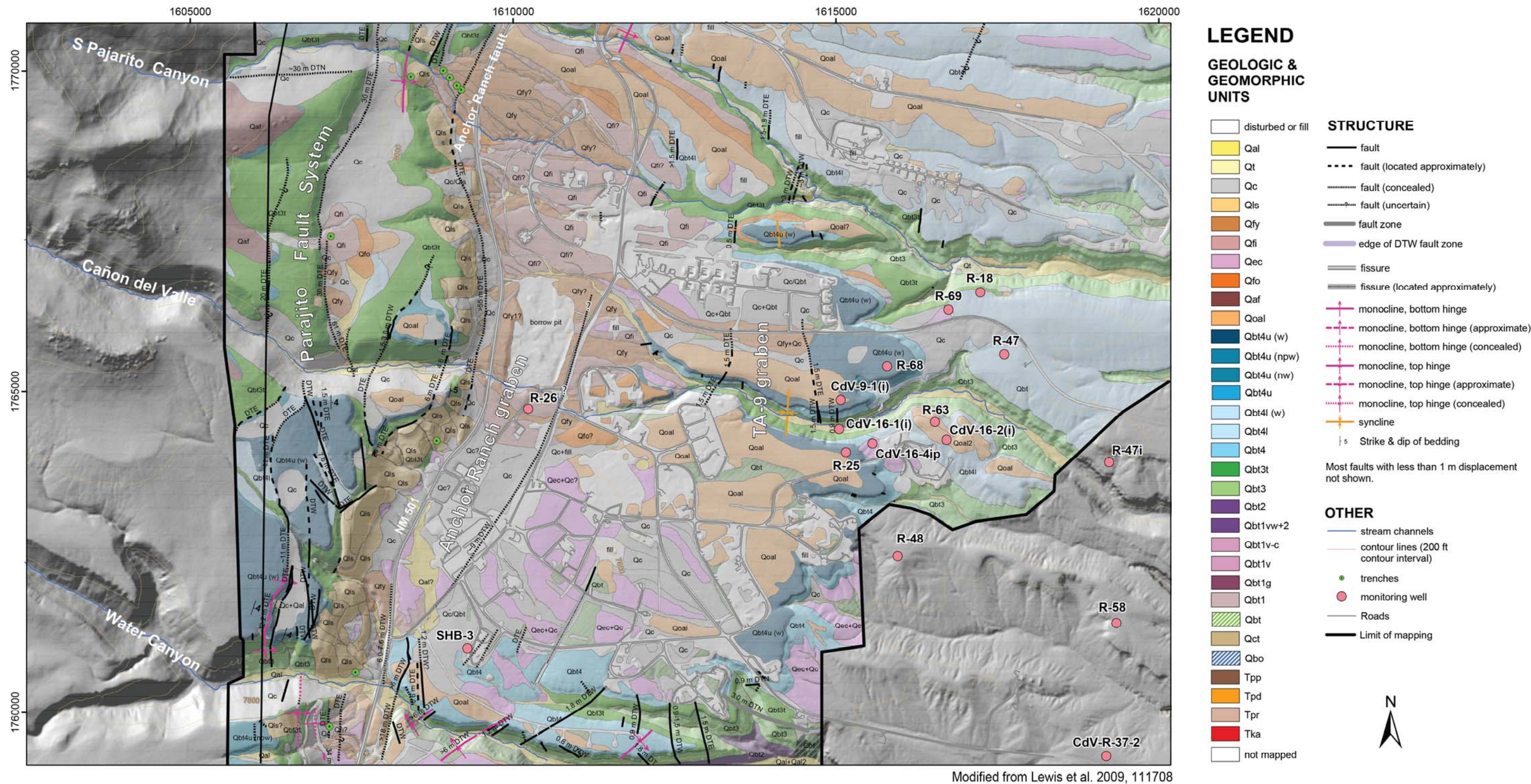


Figure 2.3-1 Geologic map of TA-16 and surrounding areas

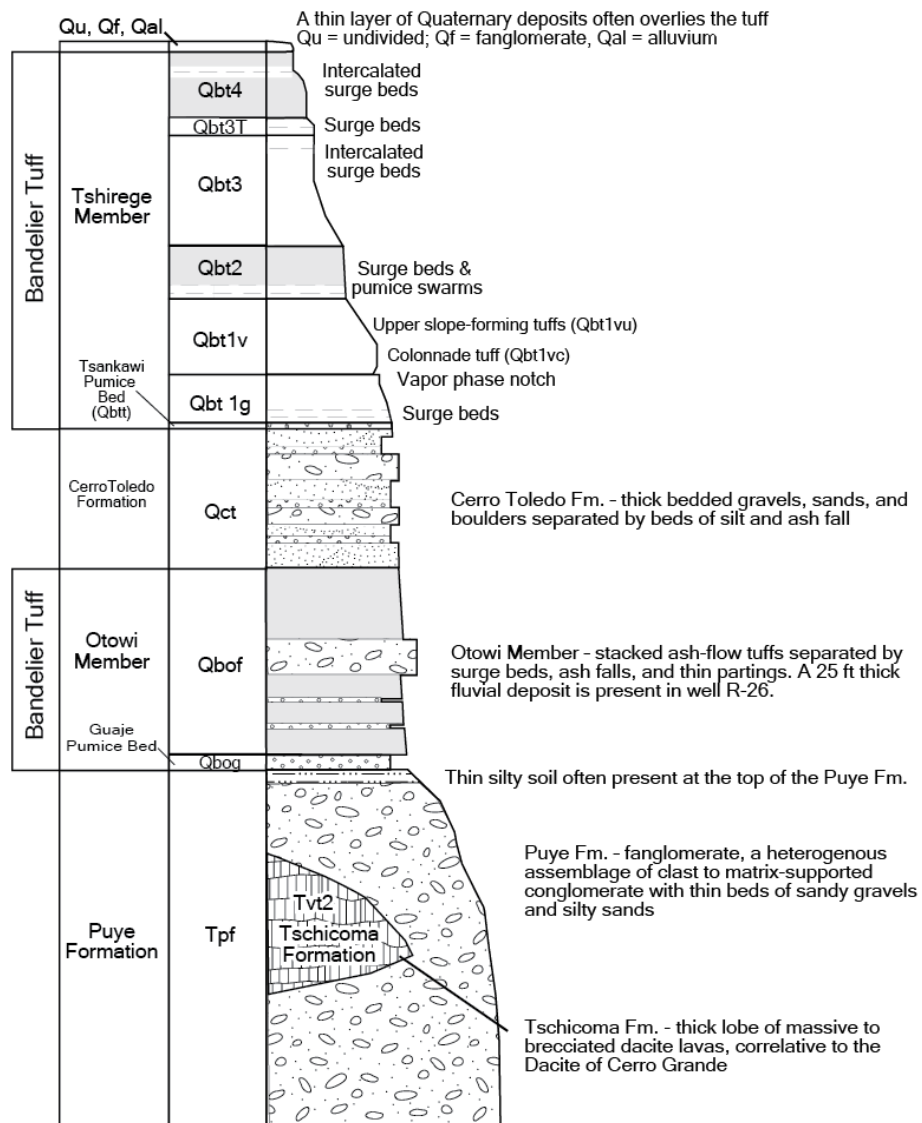


Figure 2.4-1 Stratigraphy of the geologic units at TA-16

Note: Section is schematic with thickness of units taken from well CdV-9-1(i). Descriptions of units compiled from lithologic descriptions of wells and outcrops

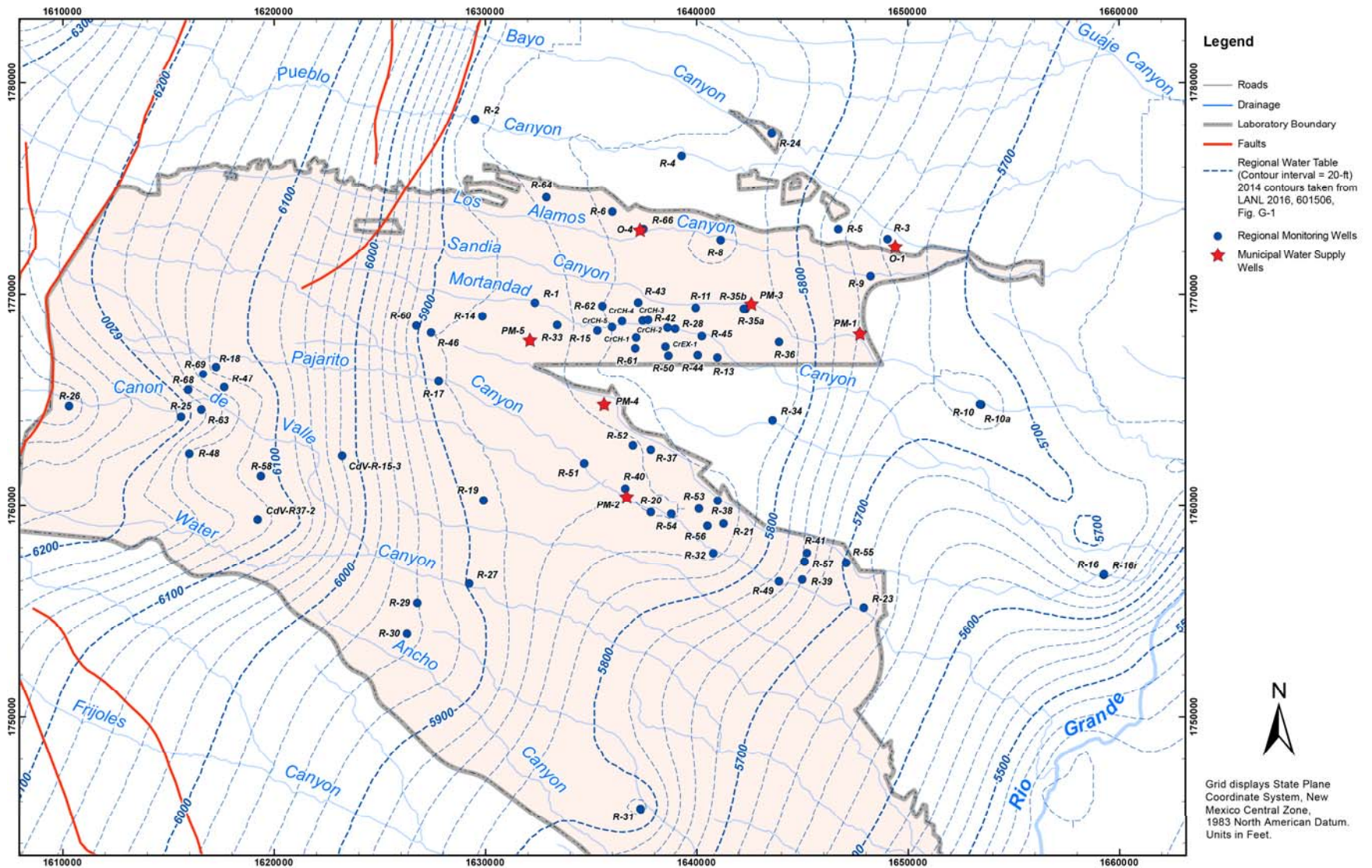


Figure 2.5-1 Map of regional water table at Los Alamos National Laboratory

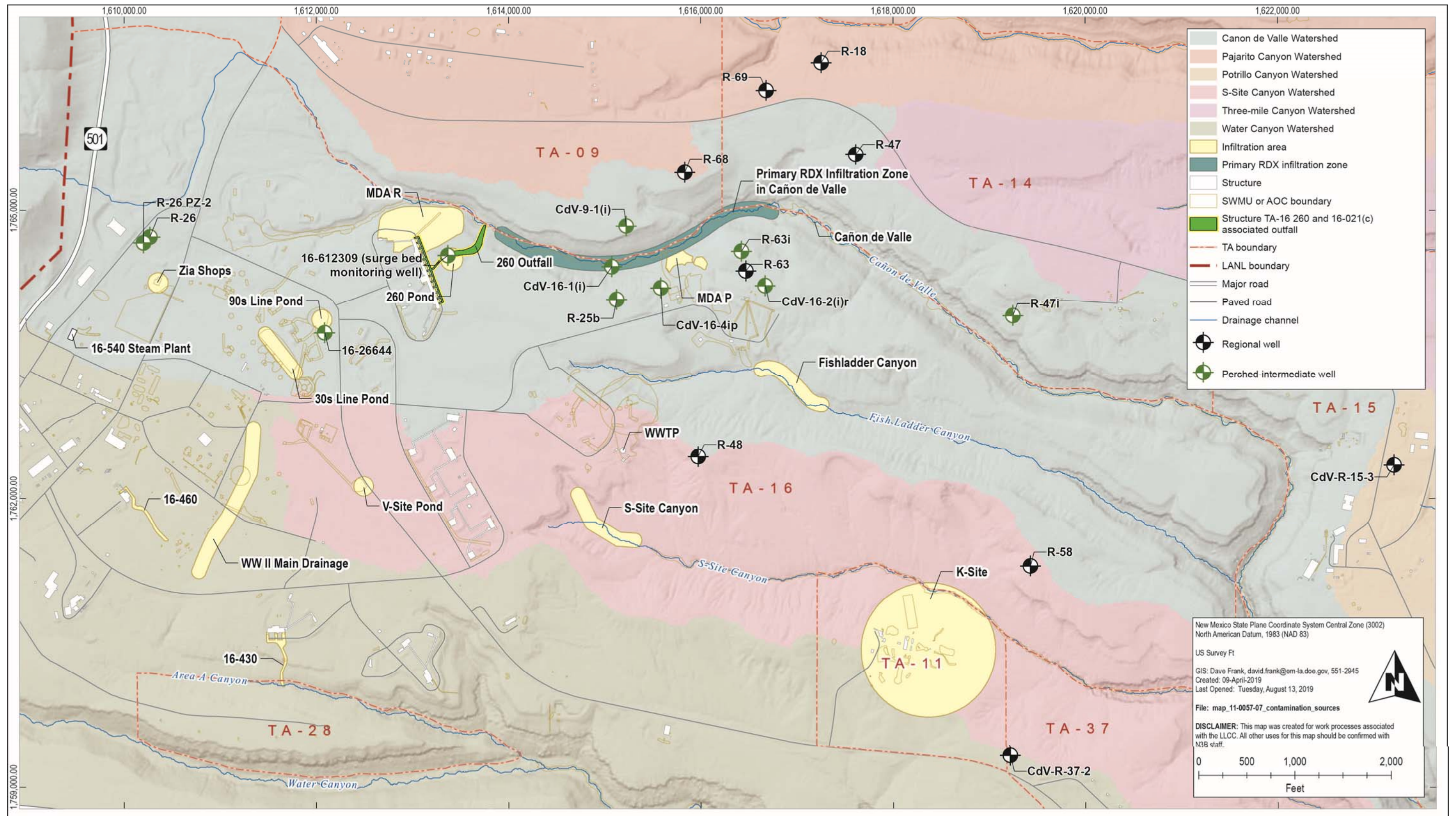


Figure 2.6-1 TA-16 source locations



Figure 3.1-1 Time series trend plots for alluvial wells (circle), springs (square), and baseflow (triangle) monitoring locations

Note: Sites with significant trends include the linear trend line. Non-detected results have open fill.

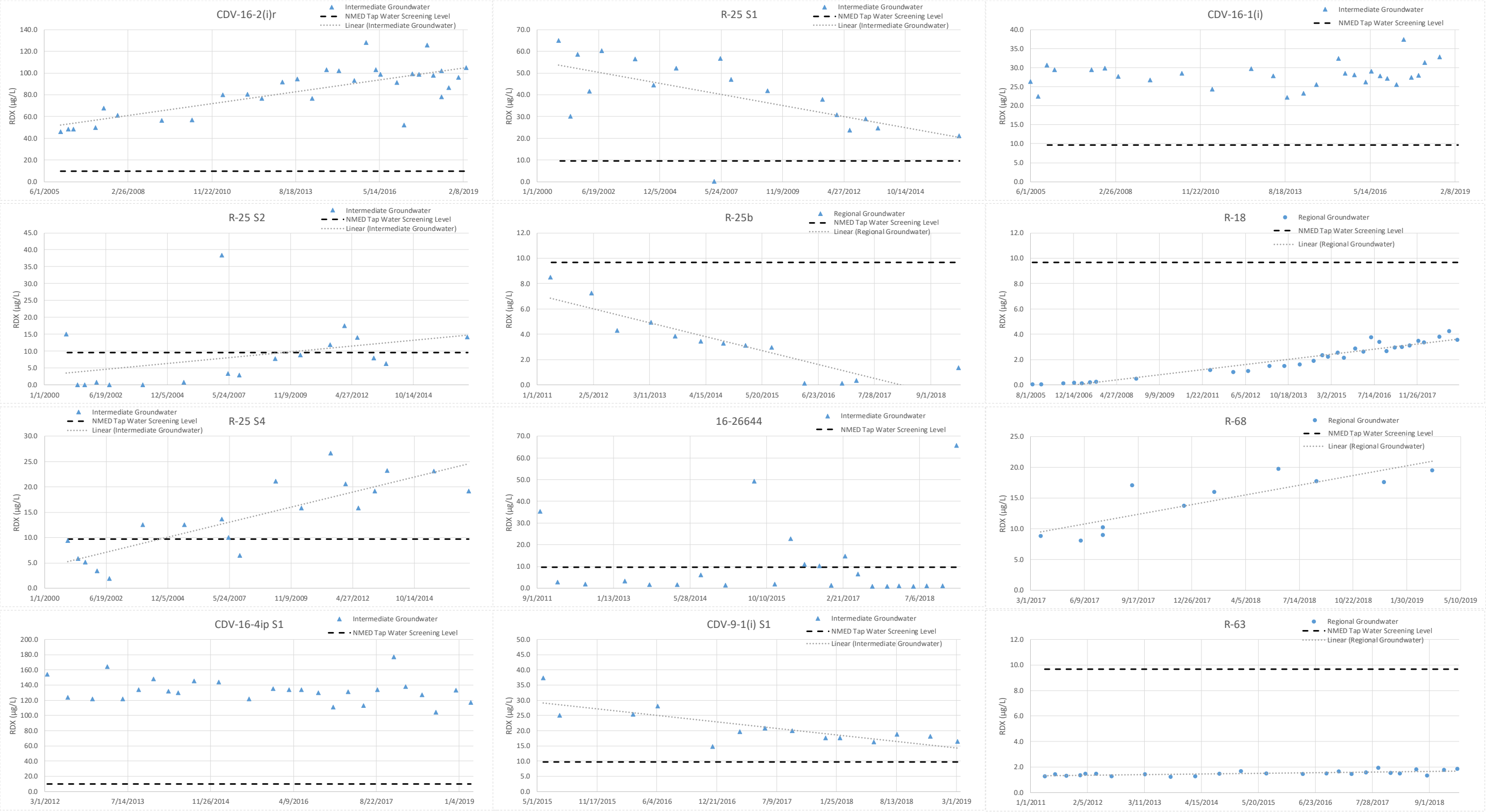


Figure 3.1-2 Time series trend plots for intermediate (triangle) and regional (square) monitoring wells

Note: Sites with significant trends include the linear trend line. Time series for R-68 and CdV-9-1i range from May 2014 to May 2019, all other time series range from January 2000 to June 2019. Non-detected results have open fill.

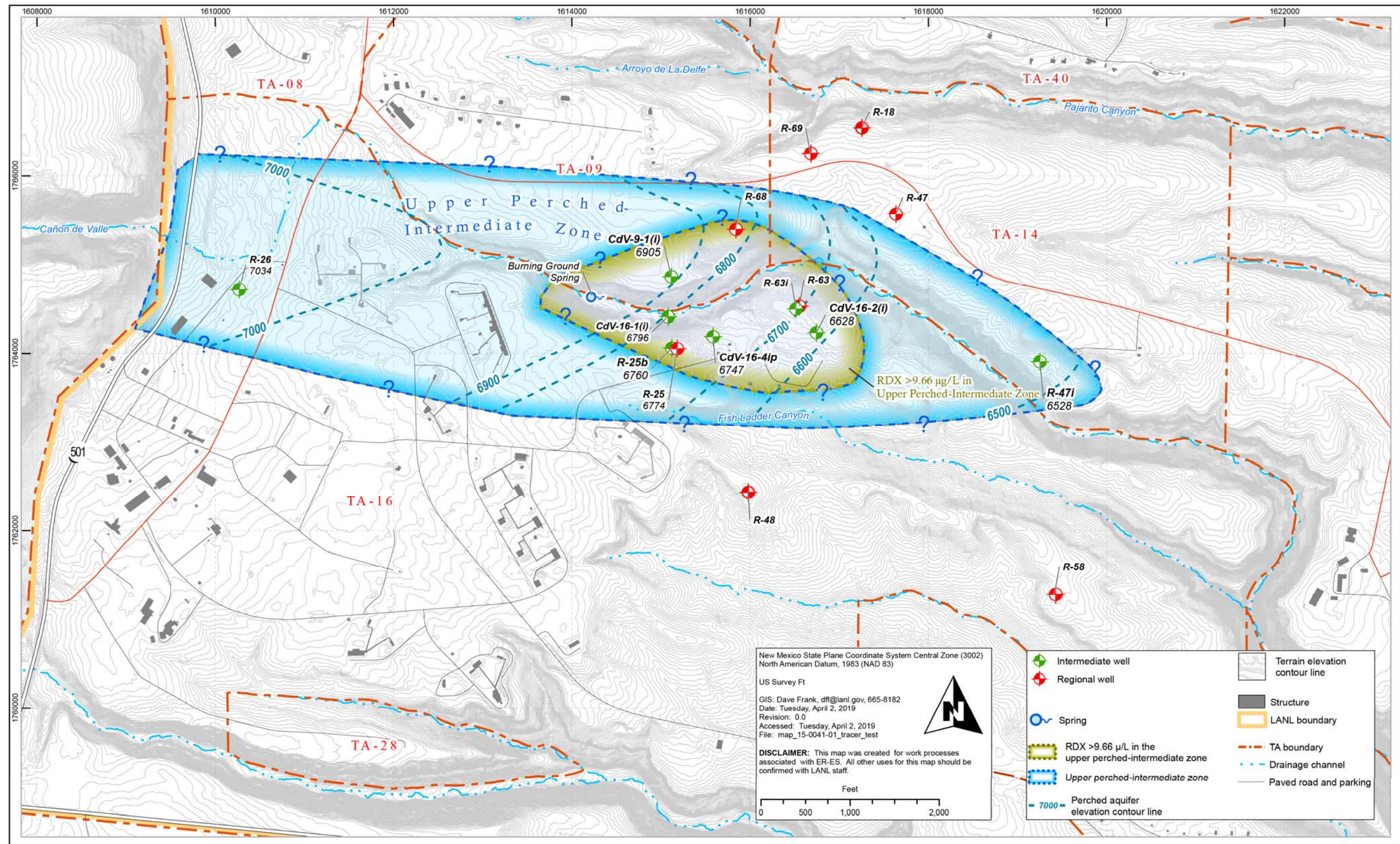


Figure 3.1-3 Map showing RDX extent and water table contours for the upper perched-intermediate groundwater zone at TA-16

Note: Green inner zone is extent of RDX contamination >9.66 µg/L in the upper perched-intermediate groundwater (LANL 2015, 600535).

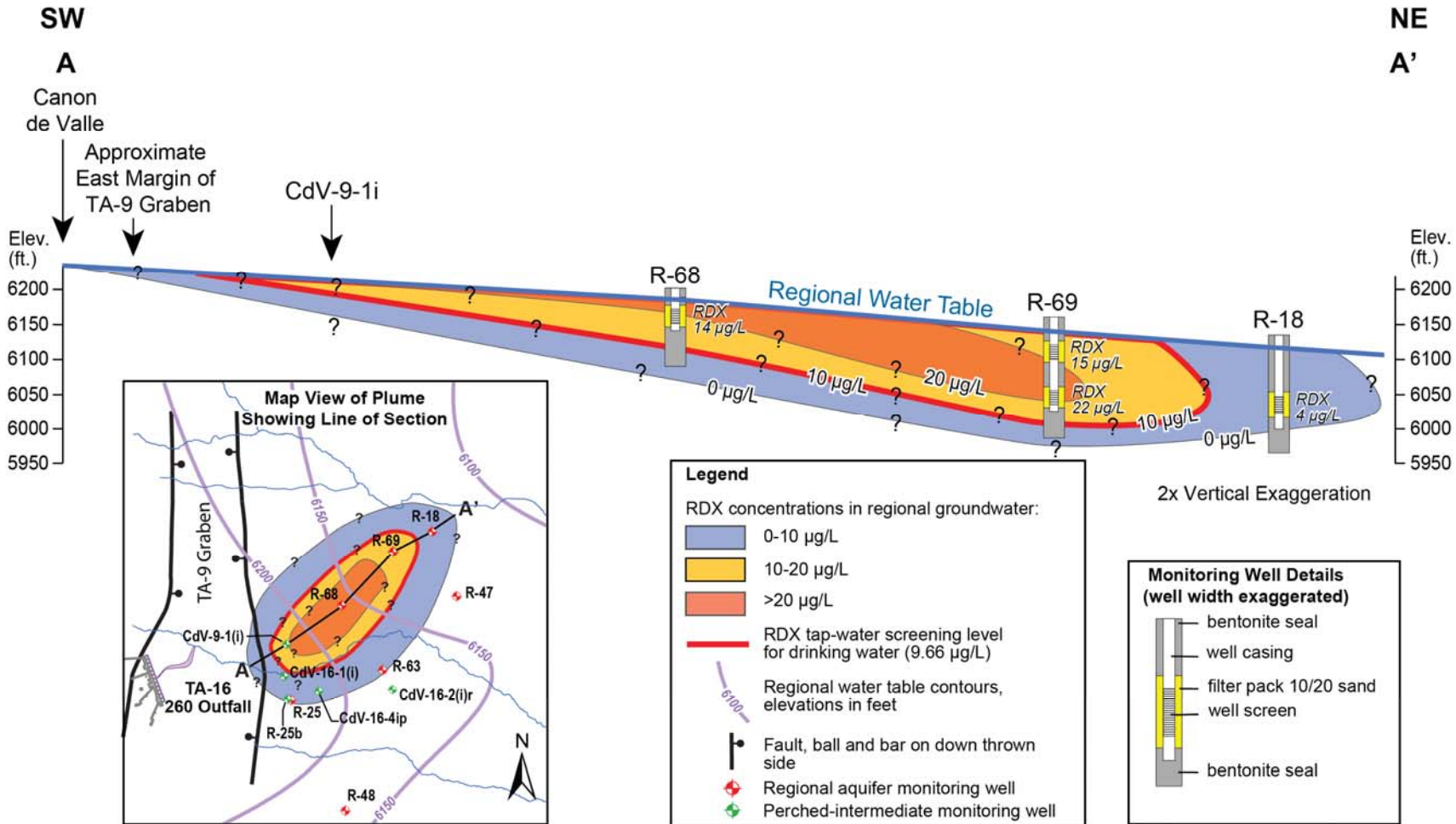


Figure 3.1-4 Southwest to northeast cross section of RDX concentrations in the regional aquifer at TA-16

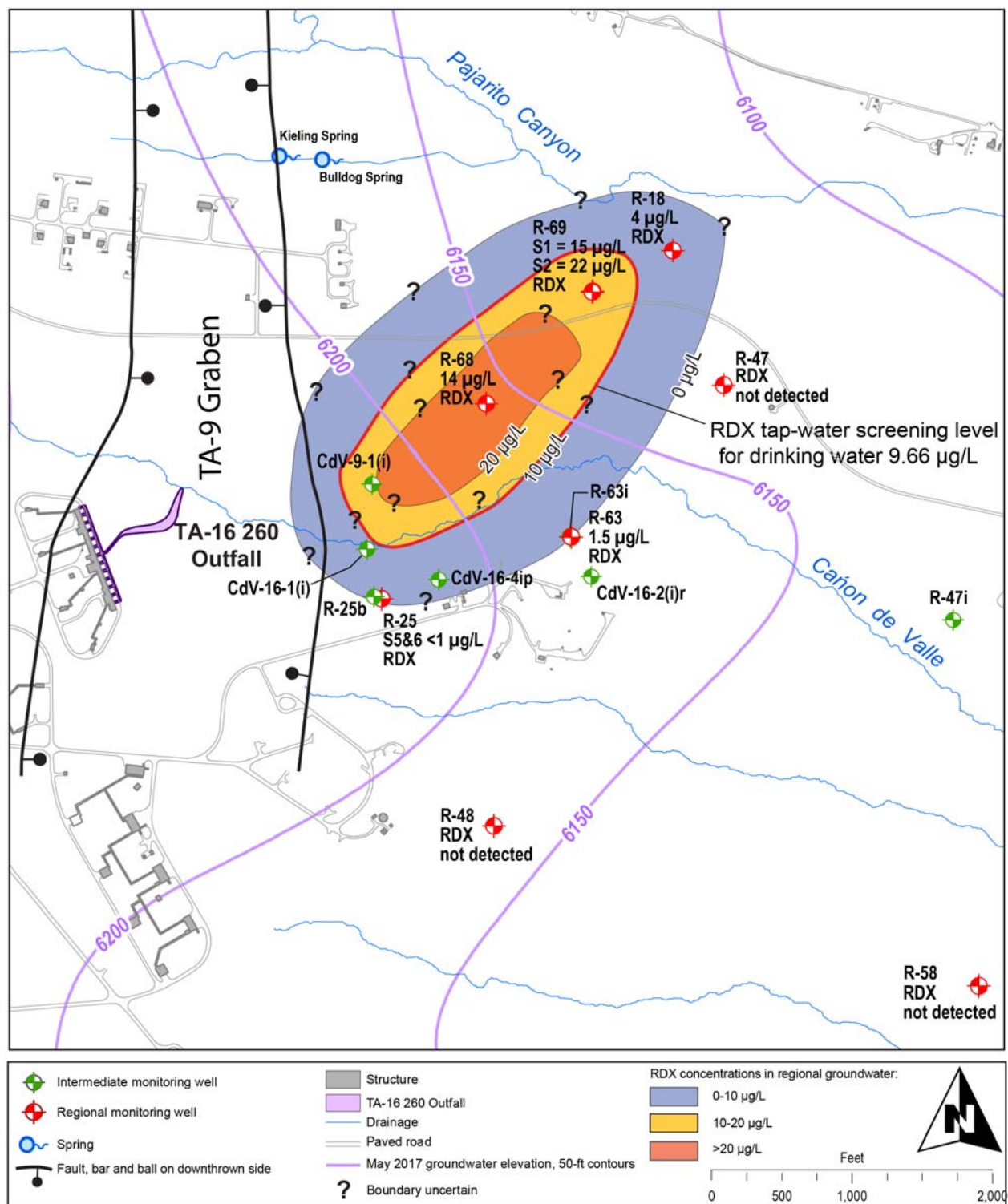


Figure 3.1-5 Map view of RDX concentrations in the regional aquifer at TA-16

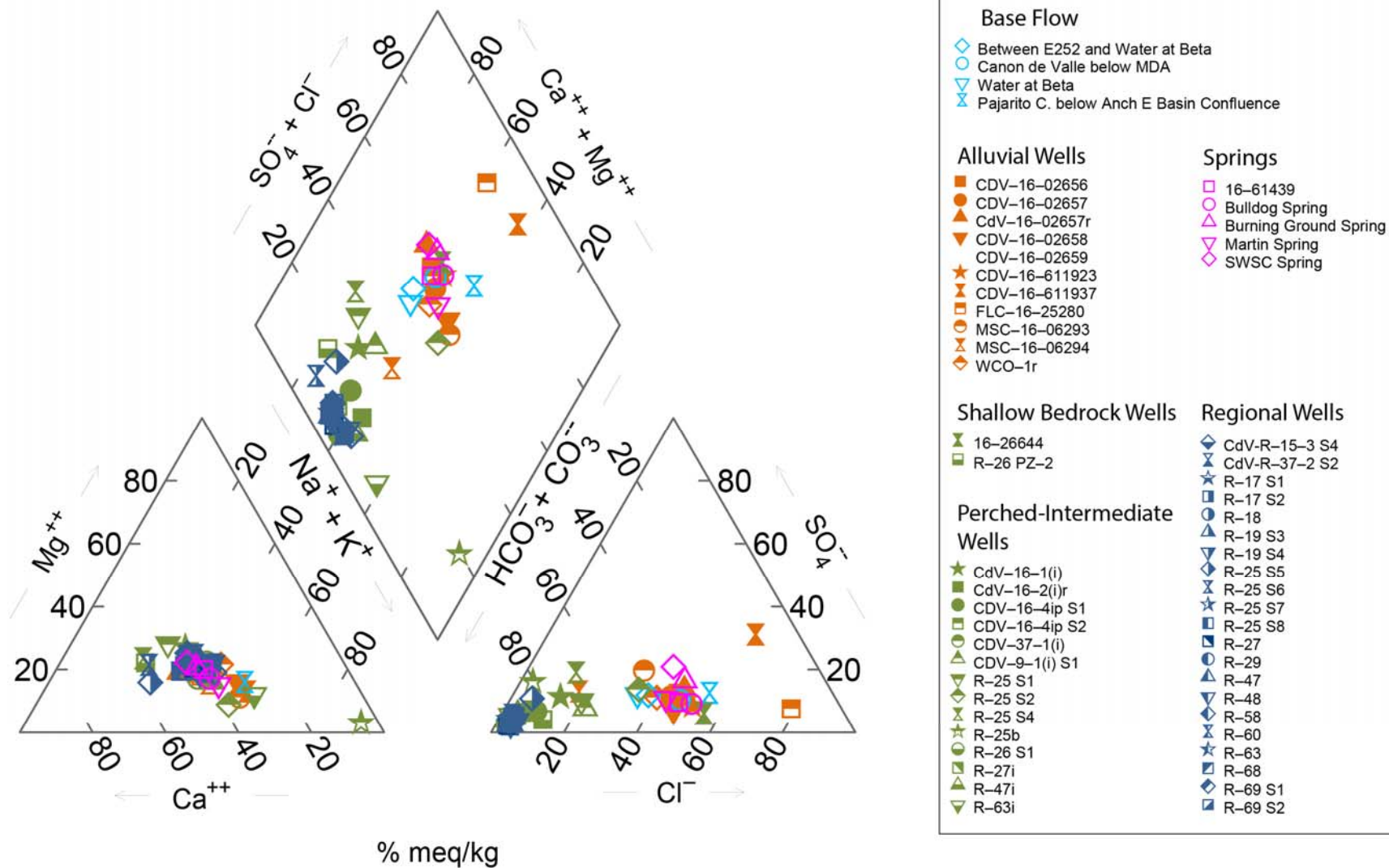


Figure 3.1-6 Trilinear (Piper) plots for springs, surface water, alluvial groundwater, perched-intermediate groundwater, and regional groundwater

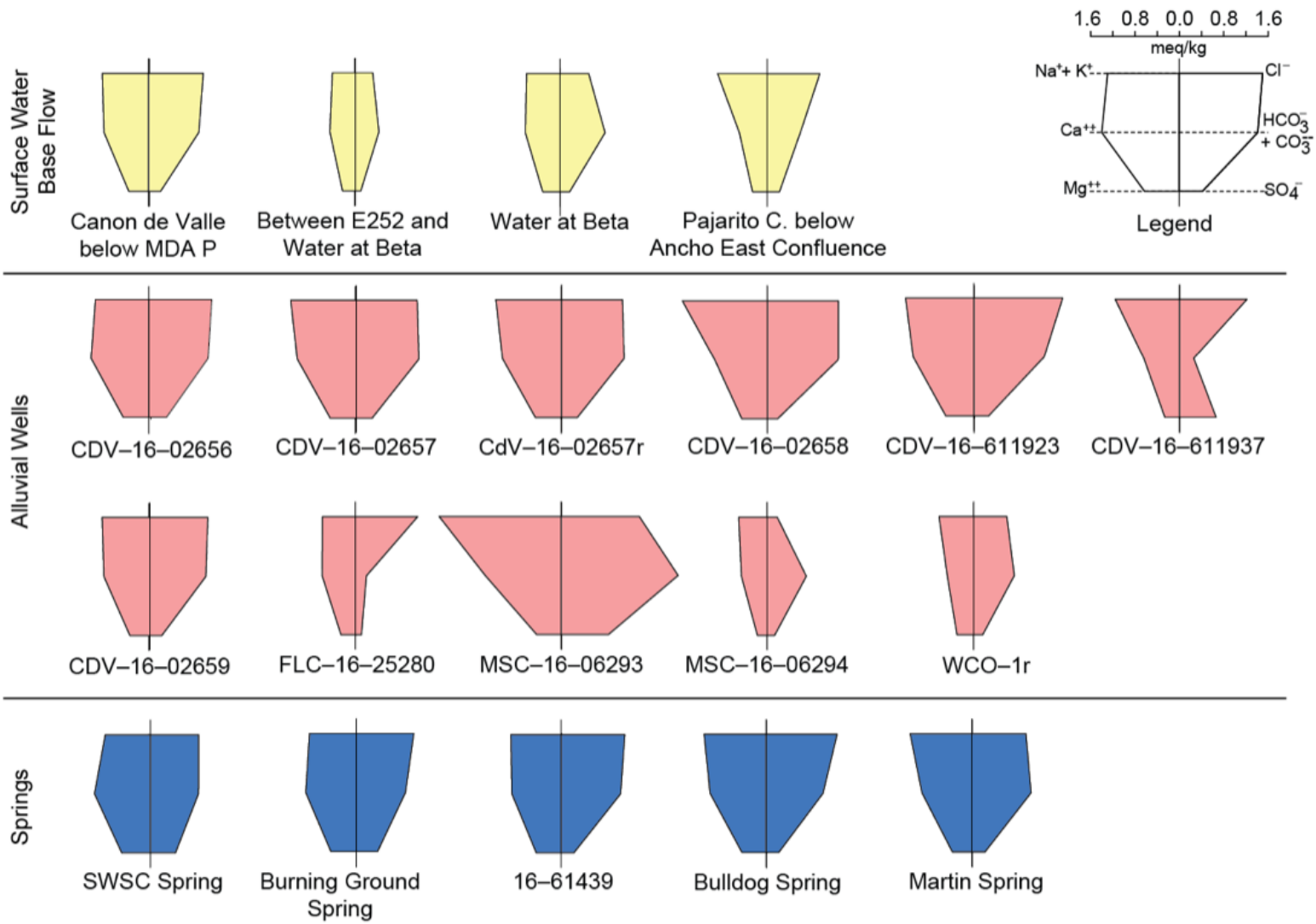


Figure 3.1-7 Stiff diagrams for surface and near-surface water systems

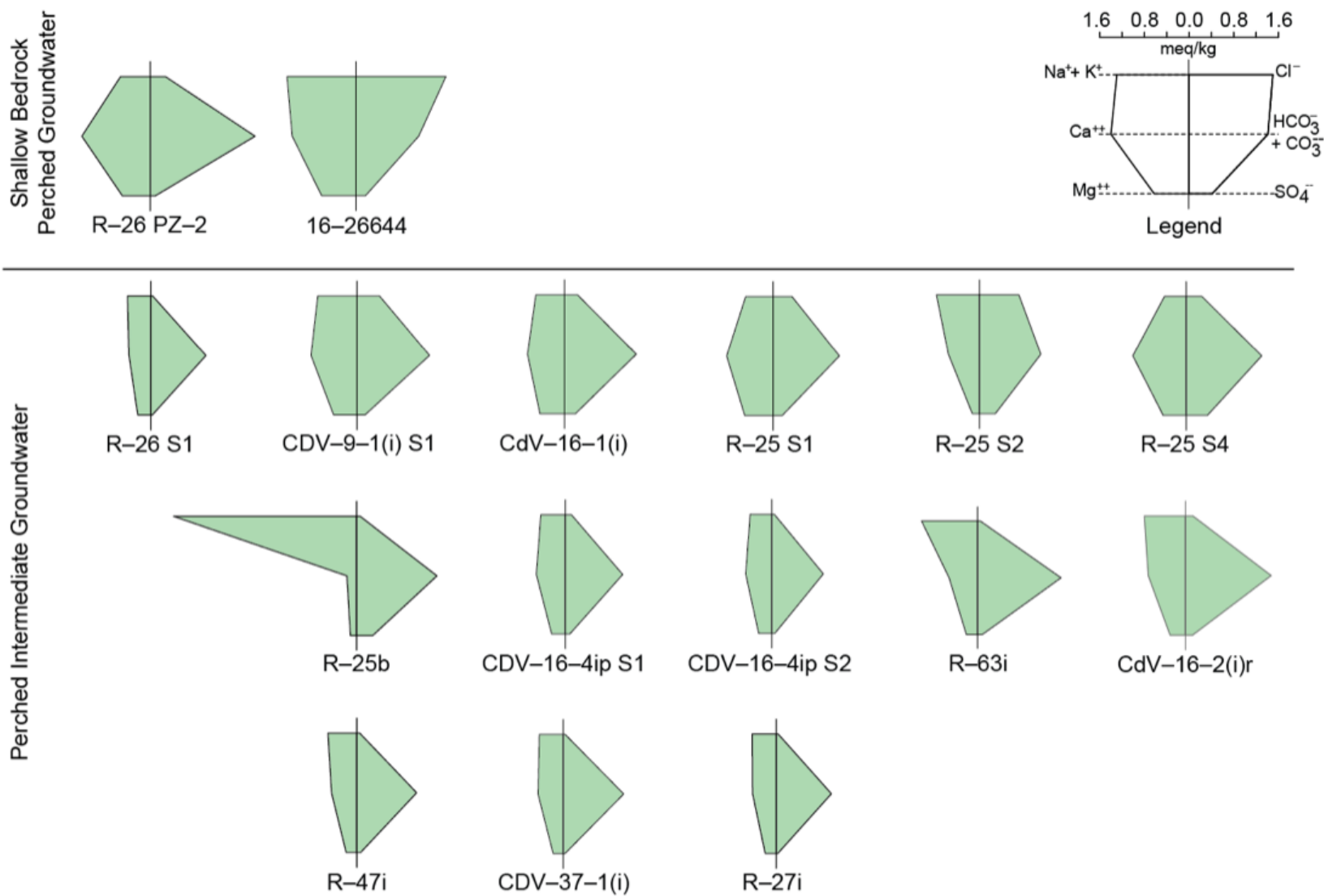


Figure 3.1-8 Stiff diagrams for perched-intermediate groundwater

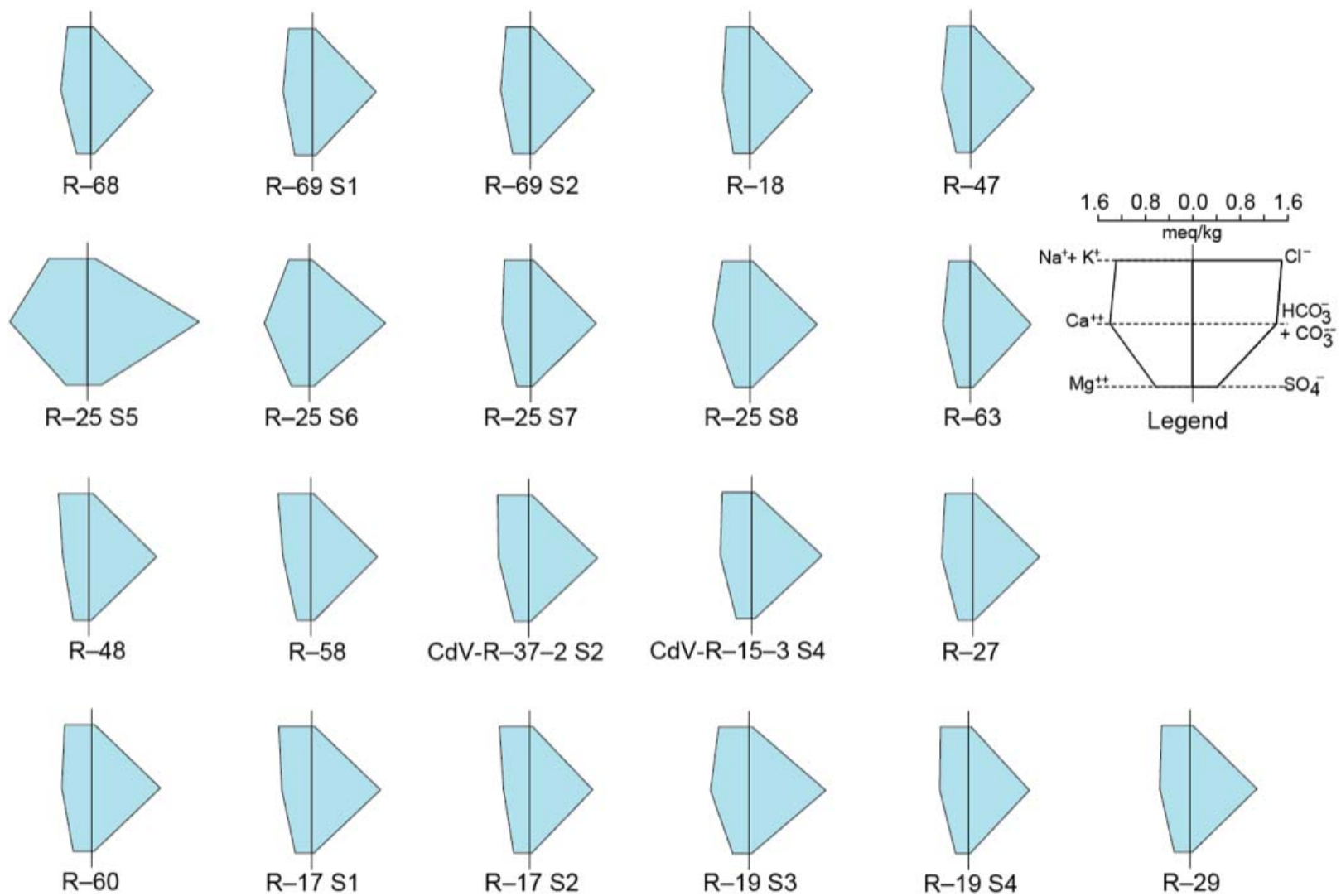


Figure 3.1-9 Stiff diagrams for regional groundwater

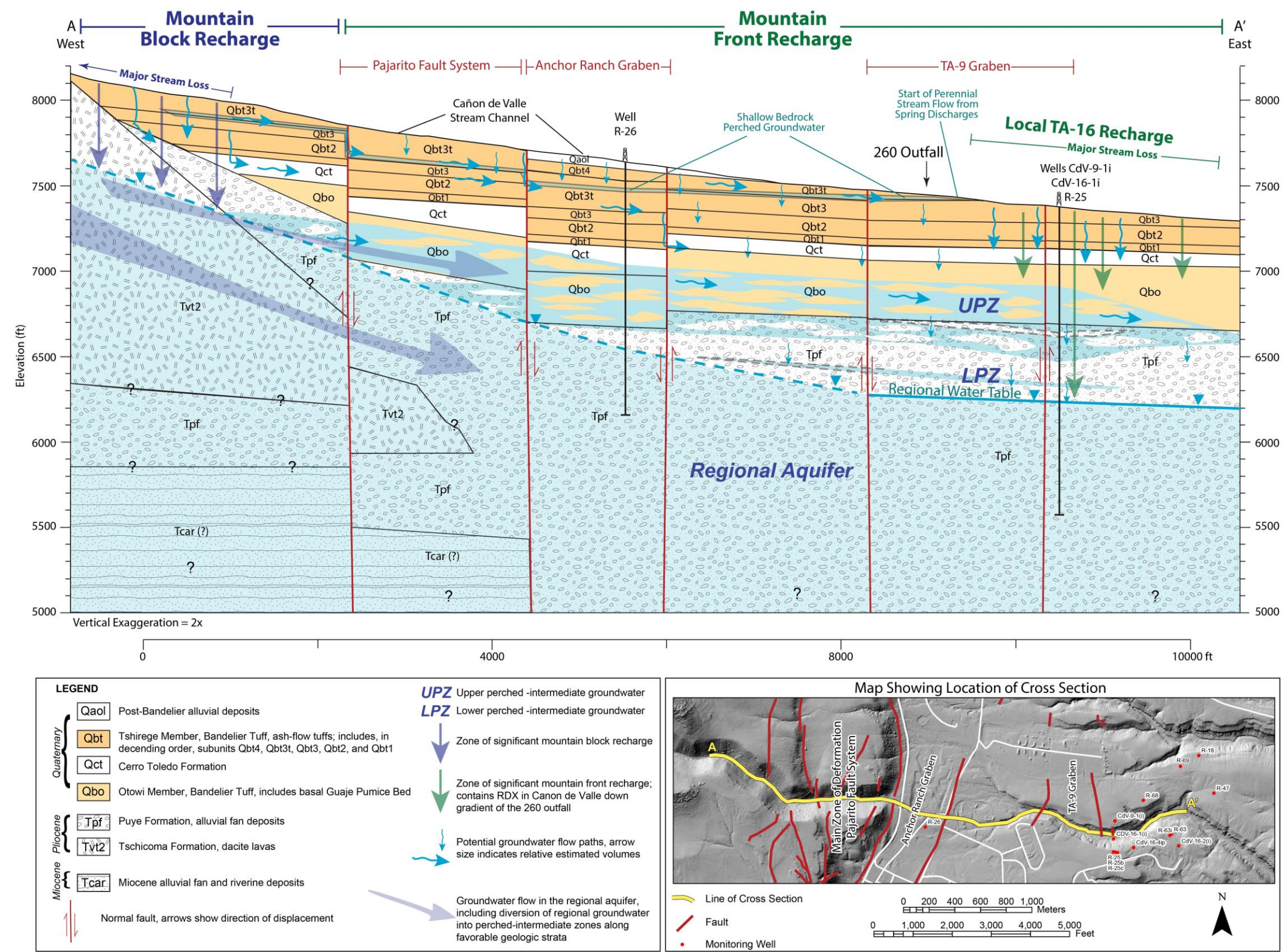


Figure 3.2-1 Conceptual E-W cross section showing of groundwater in the vicinity of TA-16

Note: Top of cross section is the floor of Cañon de Valle.

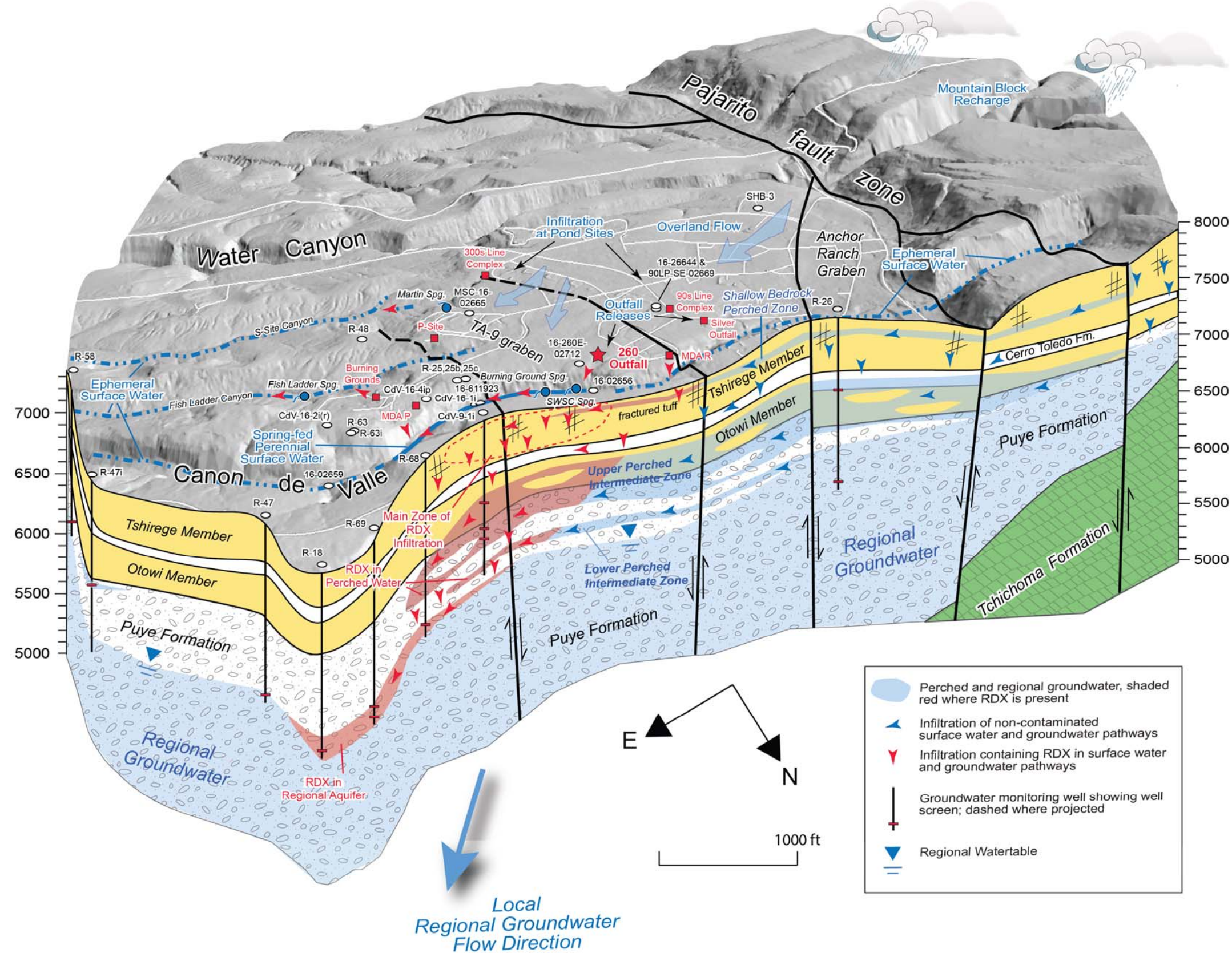


Figure 3.2-2 Conceptual block diagram showing RDX release sites and monitoring wells in the vicinity of TA-16

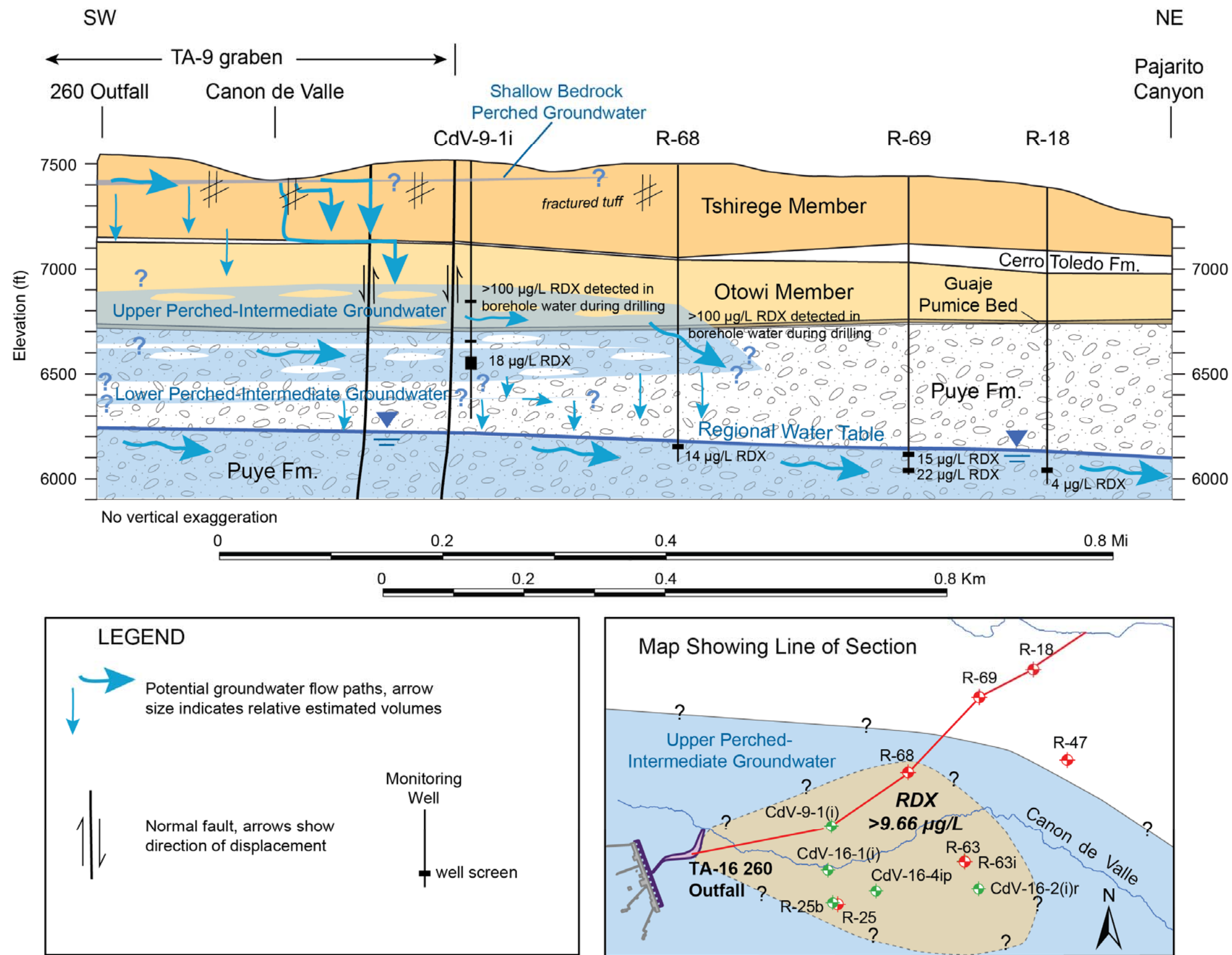


Figure 3.2-3 Southwest-northeast geologic cross section showing groundwater pathways from the 260 Outfall to well R-18

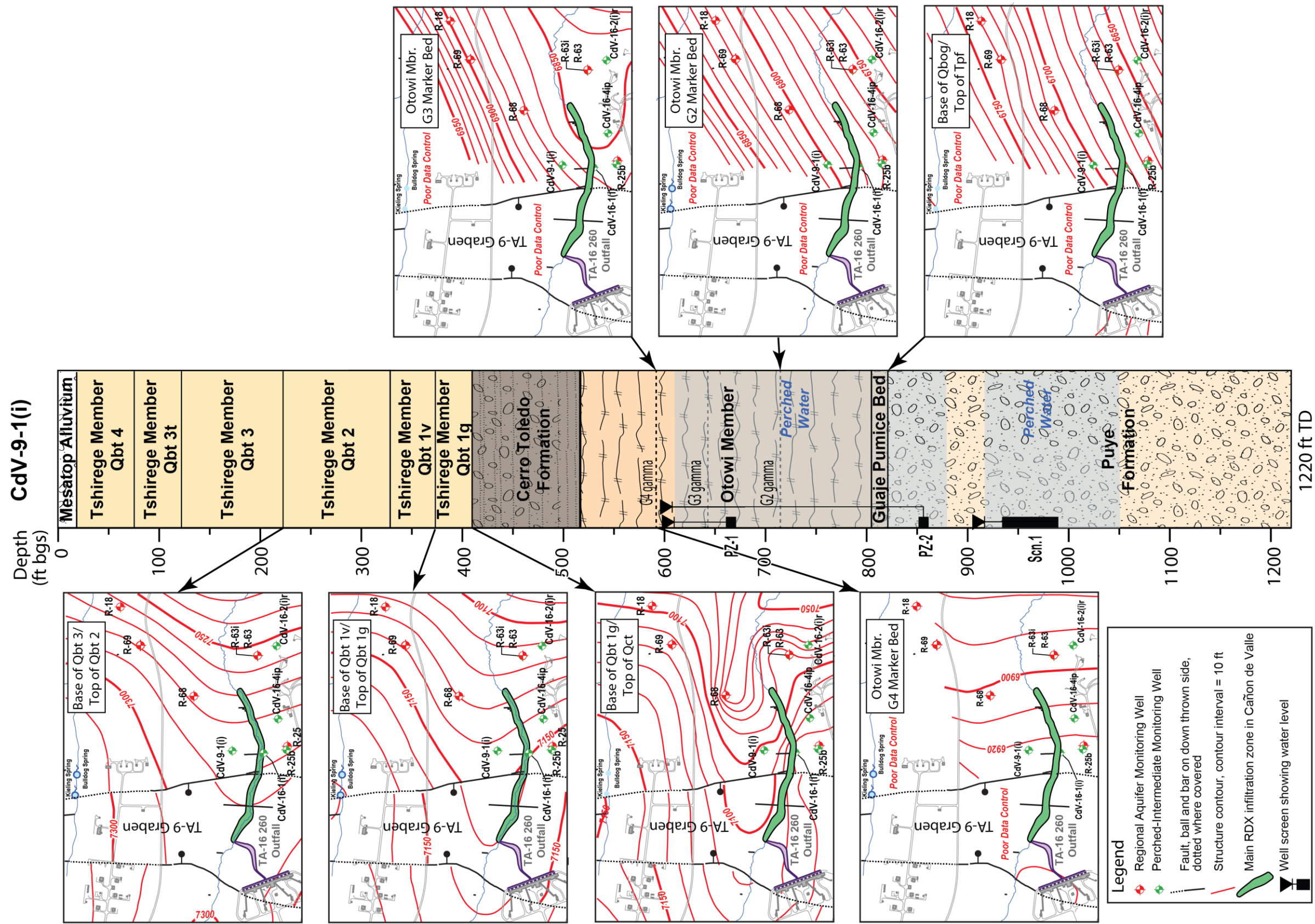


Figure 3.2-4 Structure contour maps for geologic contacts in the TA-16 area

Note: Geologic contacts and internal bedding are likely to divert vertical percolation pathways towards down-dip directions.

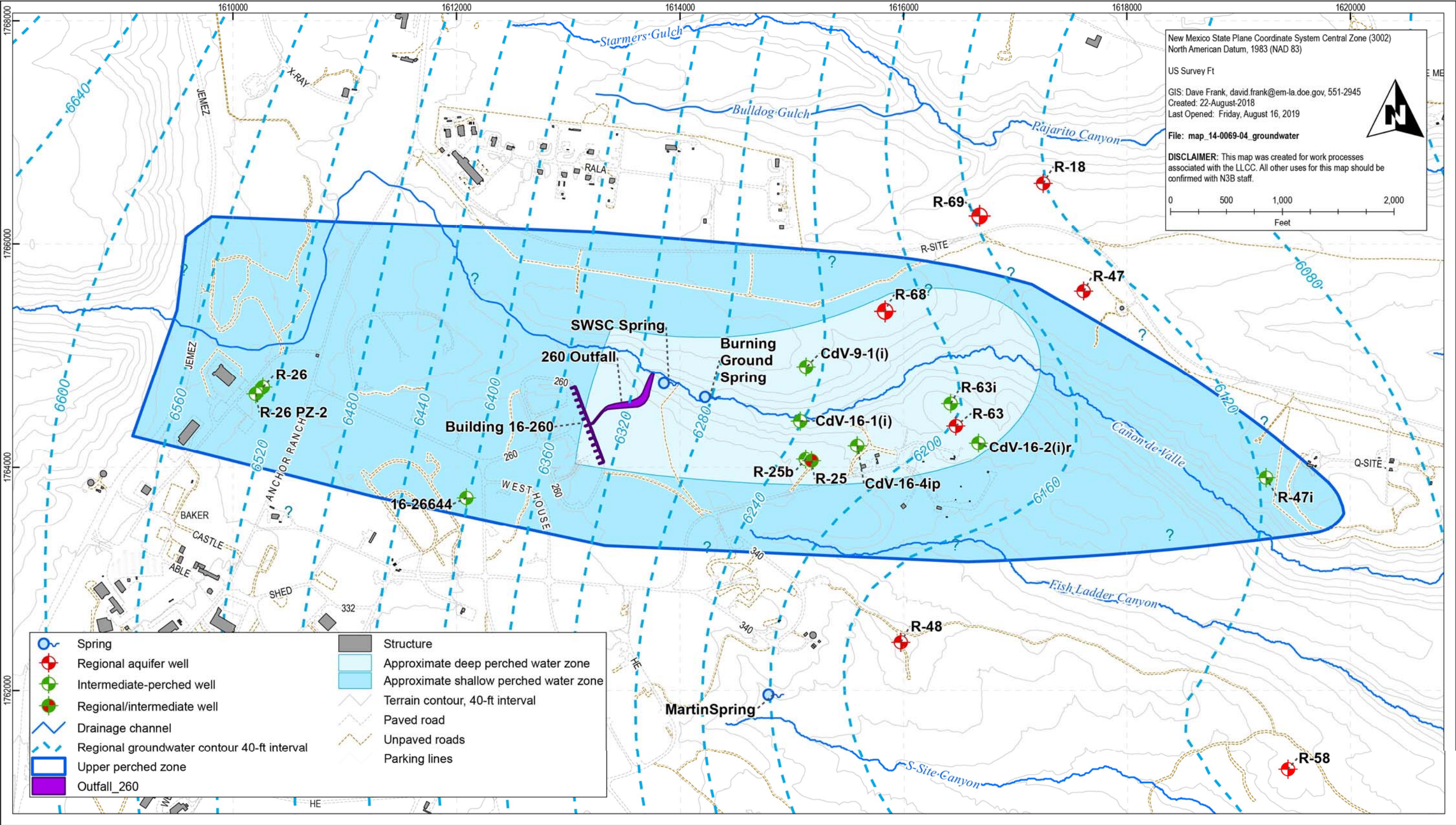


Figure 3.2-5 Map showing approximate extent of perched-intermediate groundwater zones at TA-16

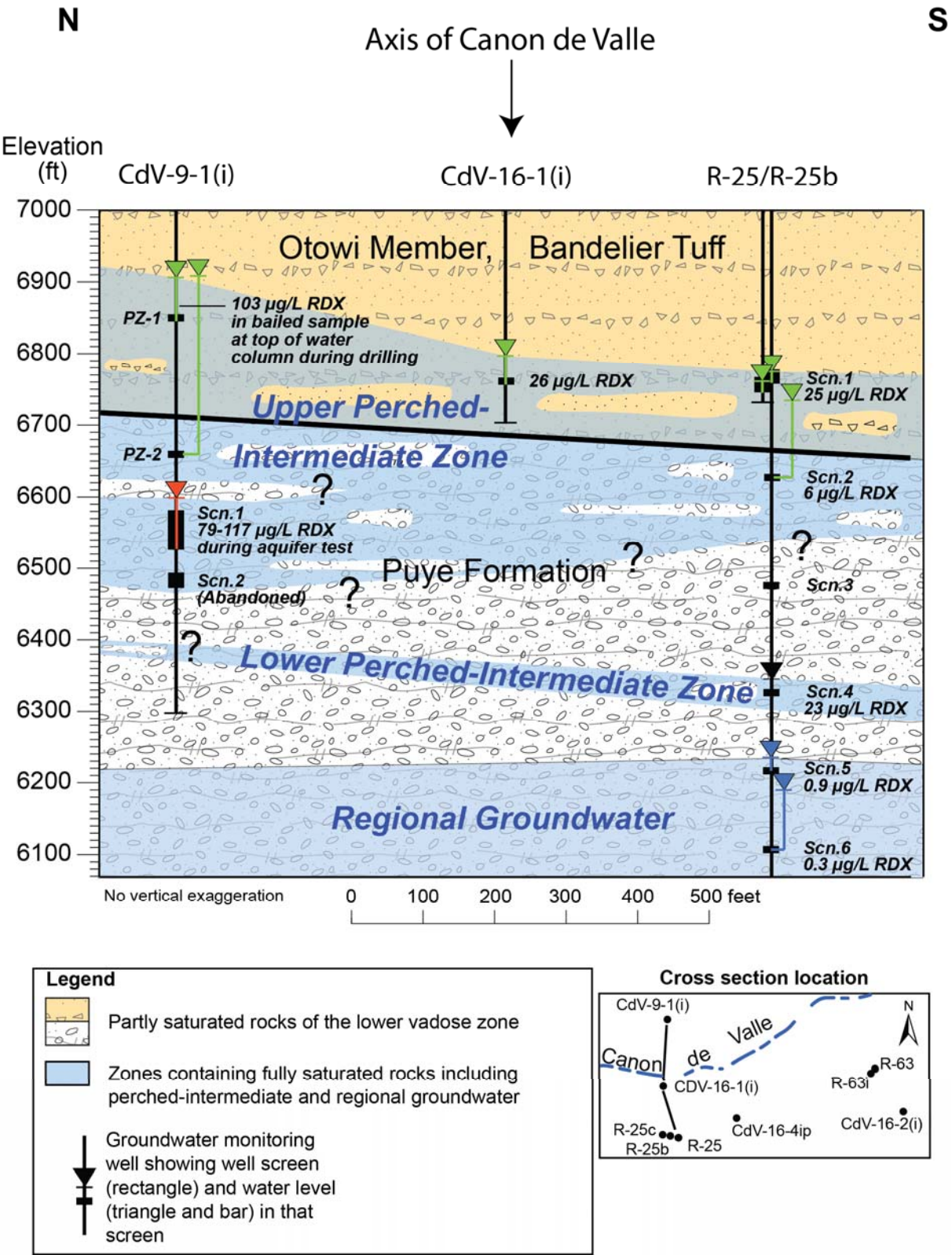


Figure 3.2-6 North-south geologic cross-section for the lower part of the vadose zone showing geologic contacts and groundwater occurrences in wells CdV-9-1(i), CdV-16-1(i), R-25b, and R-25

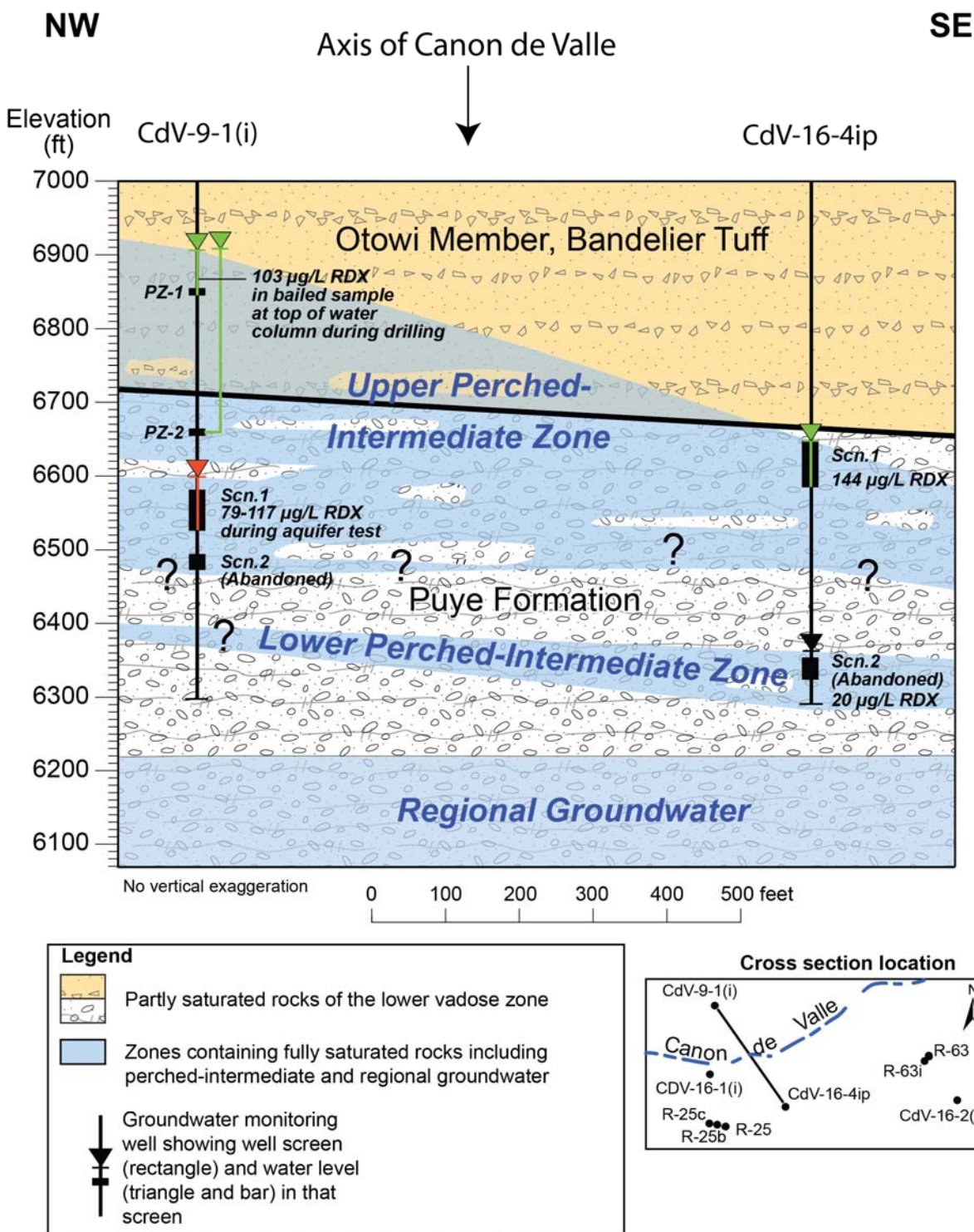


Figure 3.2-7 Northwest-southeast geologic cross-section for the lower part of the vadose zone showing geologic contacts and groundwater occurrences in wells CdV-9-1(i) and CdV-16-4ip

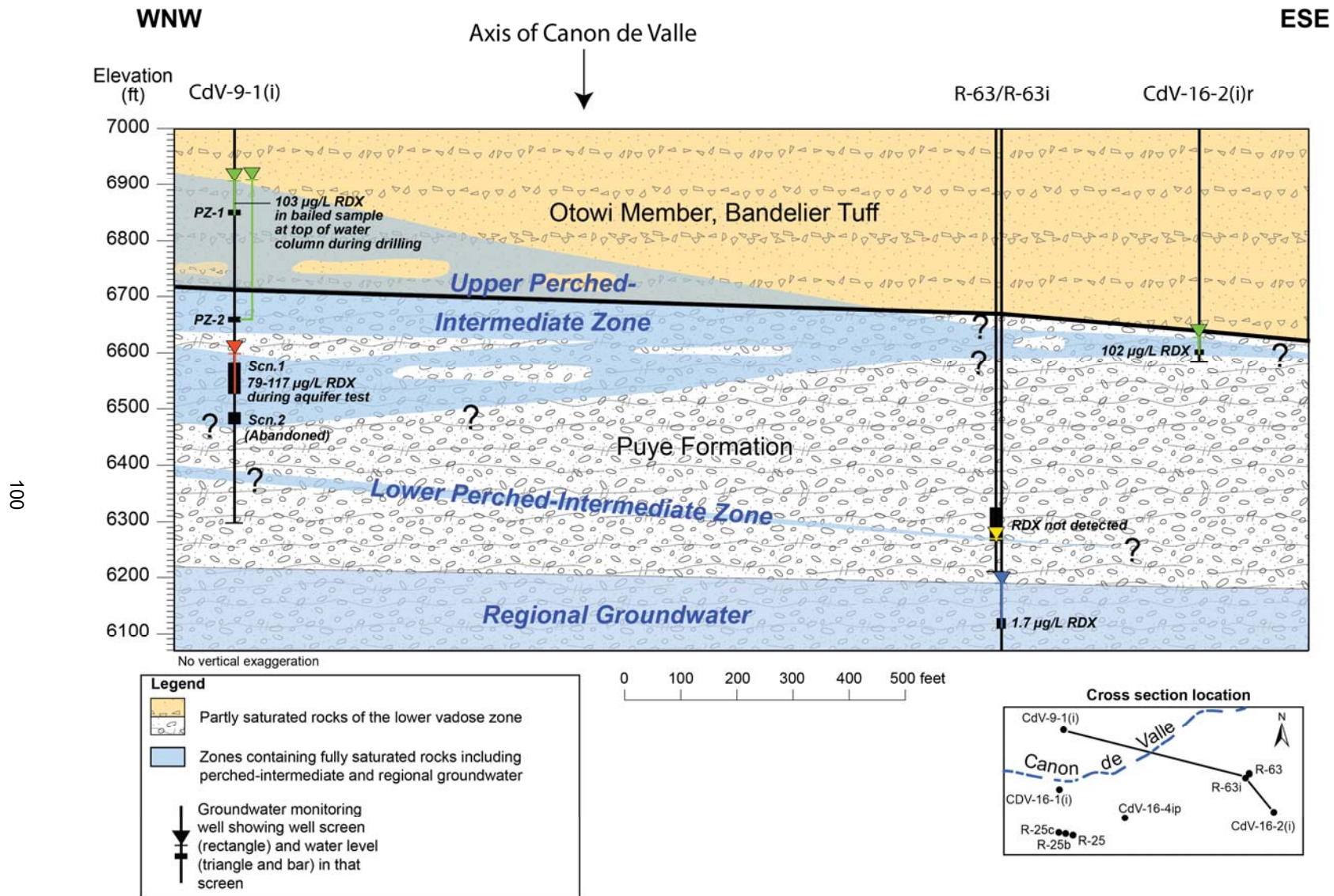


Figure 3.2-8 West-northwest to east-southeast geologic cross-section for the lower part of the vadose zone showing contacts and groundwater occurrences in wells CdV-9-1(i), R-63i, R-63, and CdV-16-2(i)r

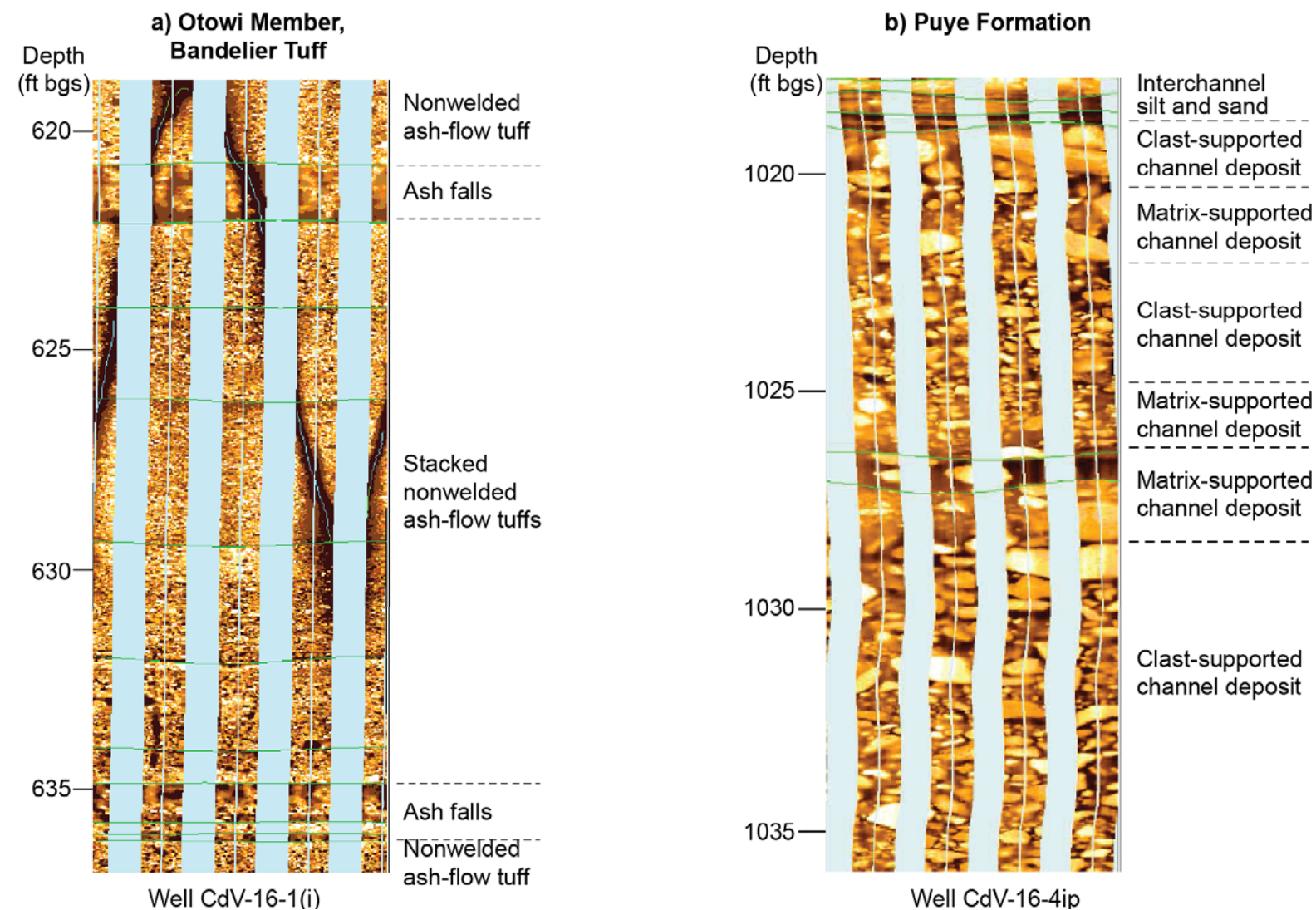


Figure 3.2-9 Geologic media hosting perched-intermediate groundwater at TA-16

Note: a) Well CdV-16-1(i) FMI log showing stratified ash-flow tuffs that make up the bulk of the of the Otowi Member of the Bandelier Tuff. Thin fall deposits are intercalated between some of the ash flows. A high-angle fracture lies within the well screen at CdV-16-1(i) and may be a vertical and lateral pathway for groundwater. b) Well CdV-16-4ip FMI log showing proximal alluvial fan deposits of the Puye Formation made up of a sequence of thick-bedded, poorly sorted, coarse-grained strata. In some beds, the cobbles and boulders are supported in a fine-grained matrix of silt and sand, indicating they were probably deposited as debris flows in stream channels. Other beds lack a significant matrix, and the cobbles and boulders are clast supported. These fines-depleted strata were deposited in channels by stream flow processes.

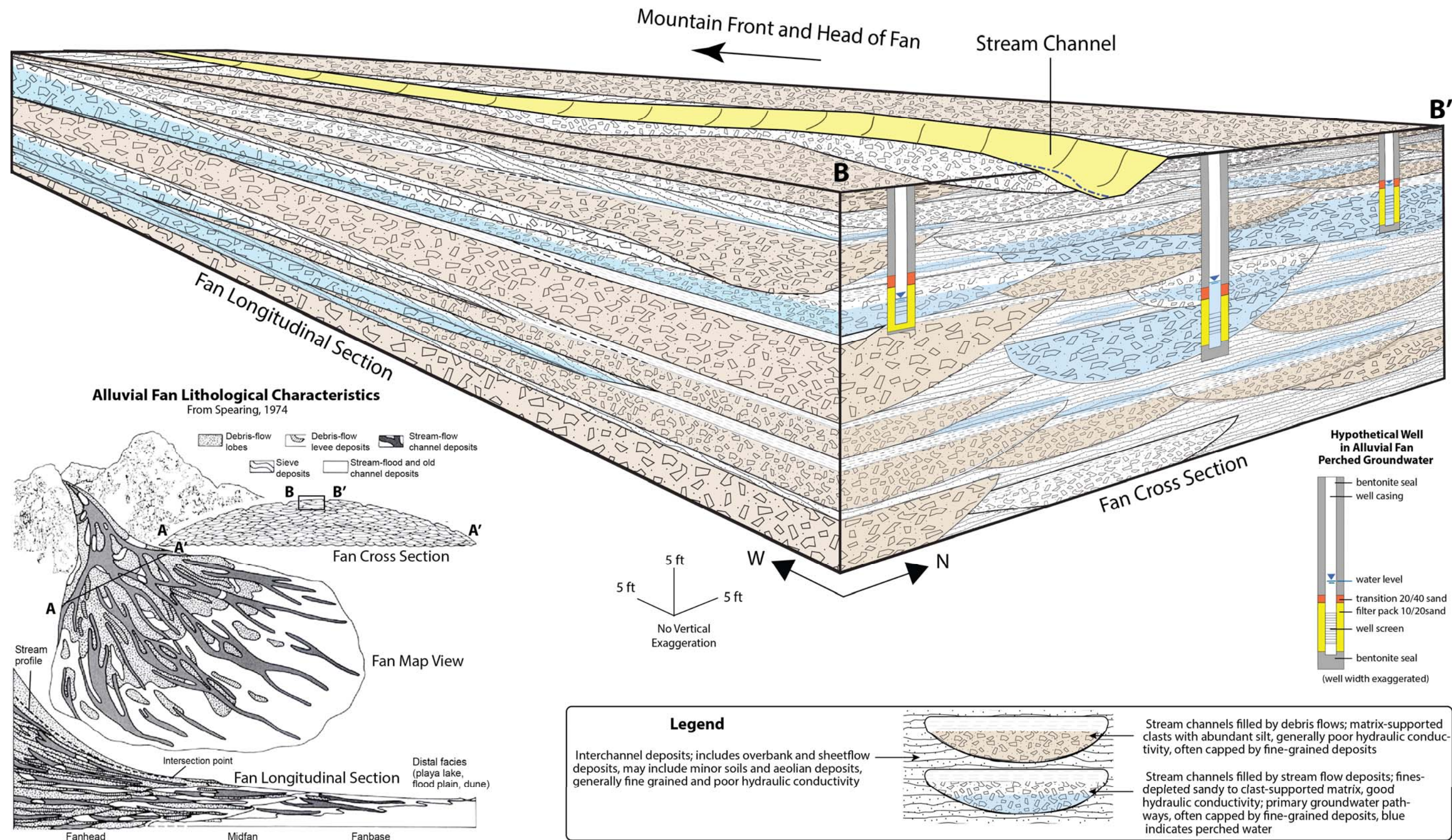


Figure 3.2-10 Block diagram showing conceptual facies model of Puye Formation proximal alluvial fan deposits at TA-16

Note: The figure in the lower left corner shows alluvial fan lithological characteristics in map, cross section, and longitudinal views (from Spearing, 1974). The main figure (top) is a conceptual block diagram showing a more detailed view of rock facies making up the alluvial fan at TA-16.

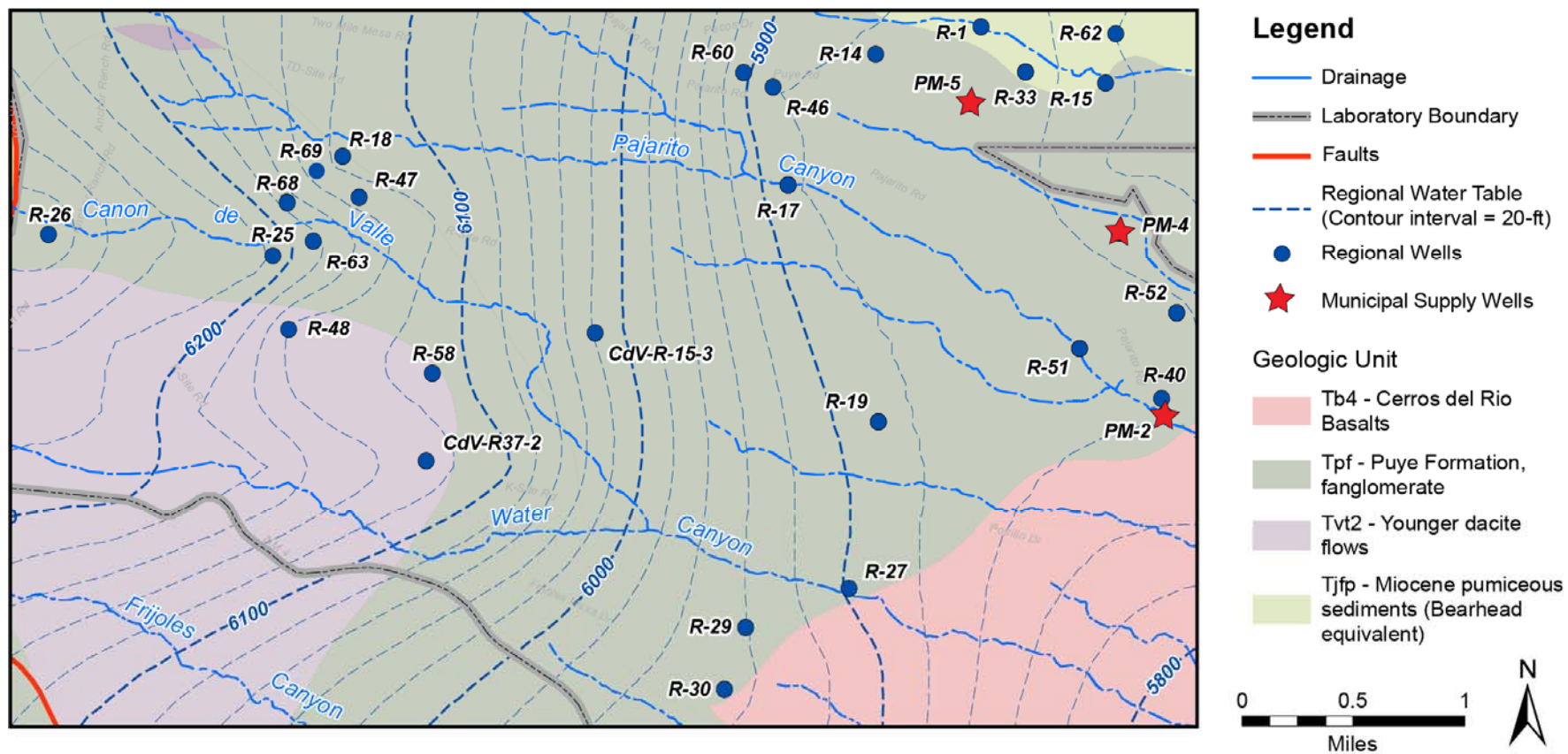


Figure 3.2-11 Regional water table map for the Pajarito Plateau and geologic units intersected by the water table

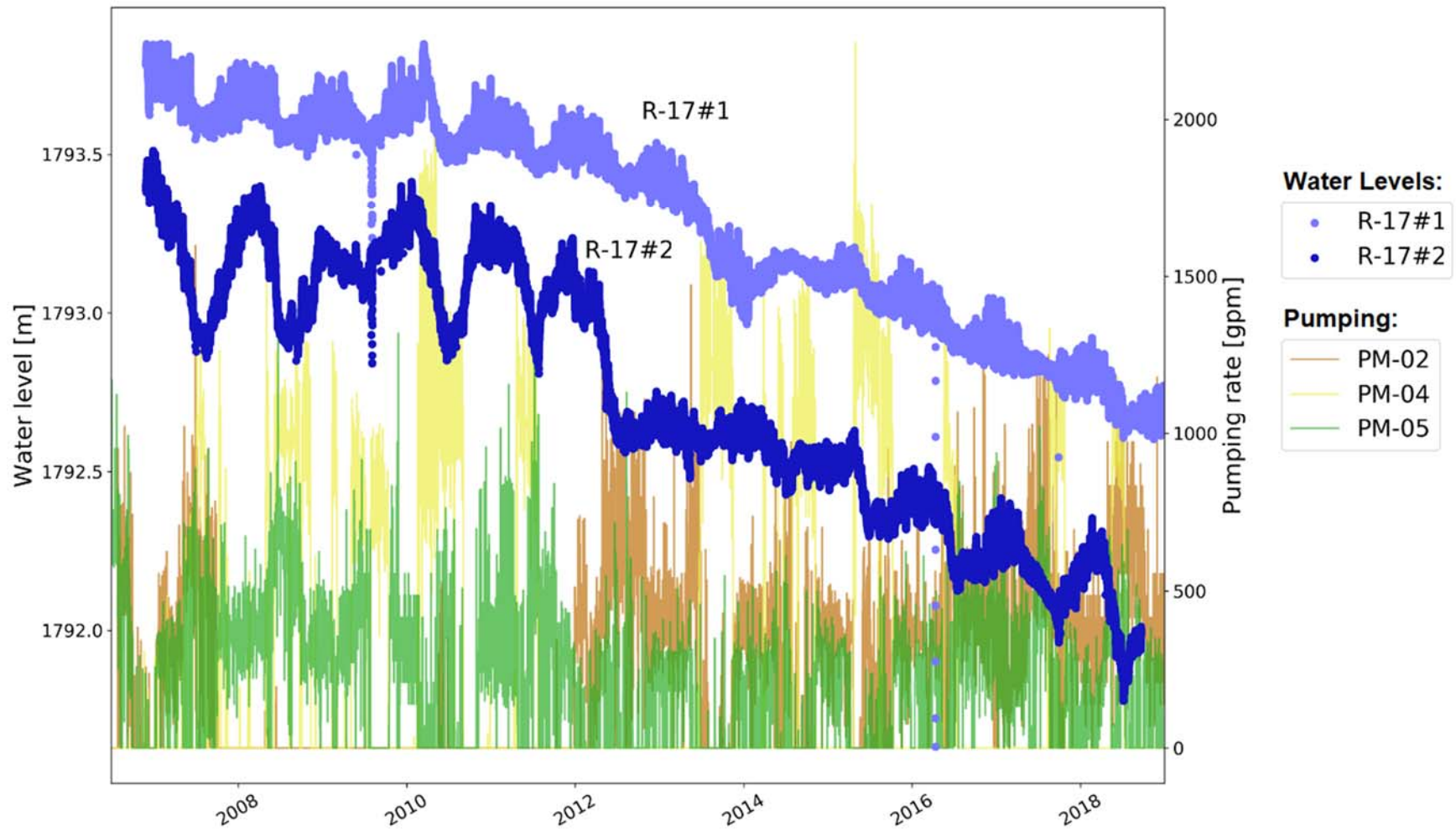


Figure 3.2-12 R-17 screen 1 and screen 2 water levels along with pumping rates at municipal water-supply wells PM-2, PM-4, and PM-5

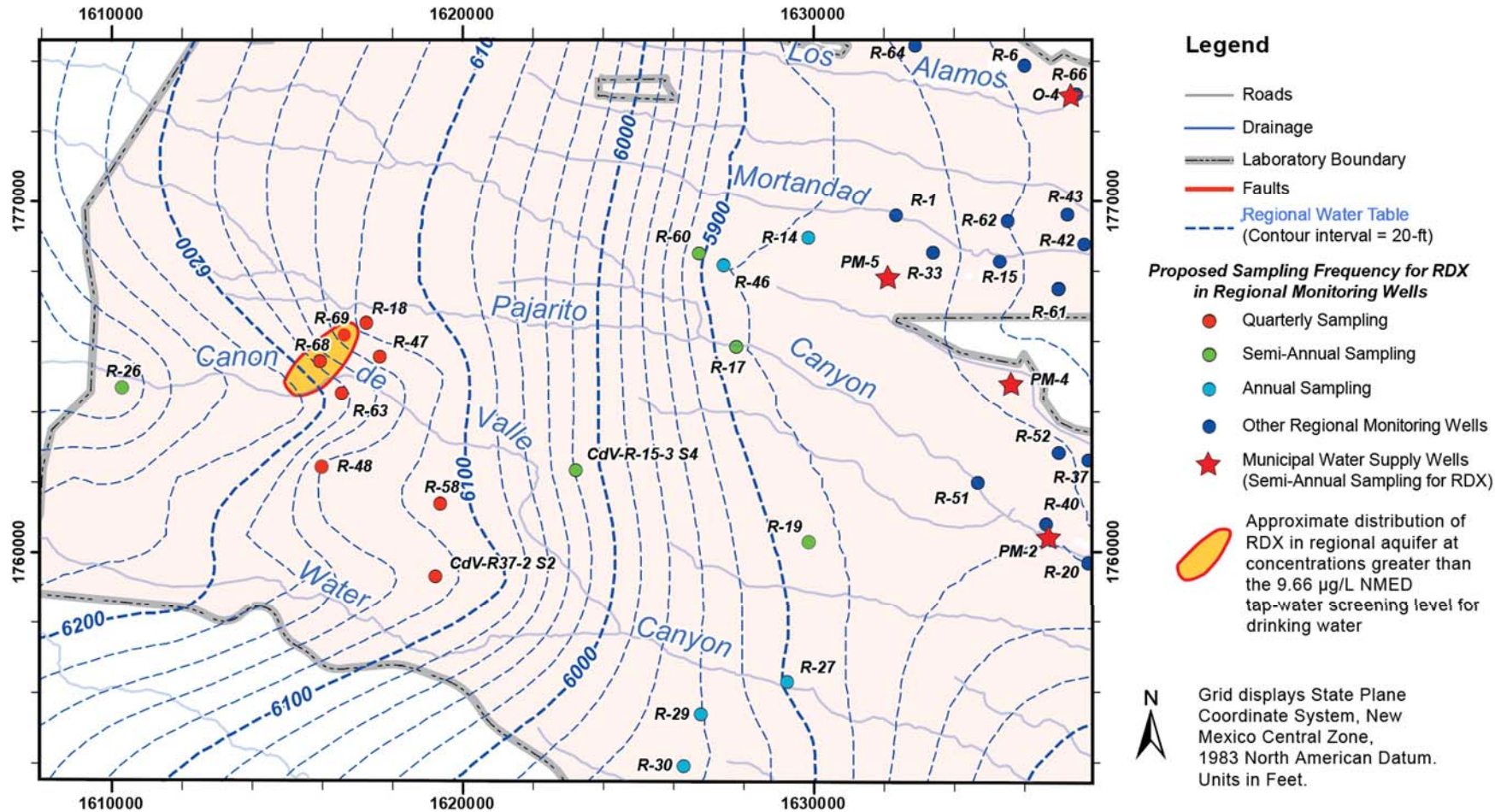


Figure 3.2-13 Map showing the location of RDX concentrations >9.66 µg/L in regional groundwater relative to the existing groundwater monitoring wells and downgradient water supply wells

Table 1.0-1
TA-16 Activities Summary

Date	Activity (Reference)	Synopsis of Activity
1990	RCRA facility assessment (RFA) (LANL 1990, 007512)	RFA initial site assessment is completed. The RFA summarizes previous studies and documents extensive contamination in TA-16-260 sump water.
July 1993	Phase I RFI work plan—site characterization plan (LANL 1993, 020948)	“RFI Work Plan for Operable Unit 1082” is issued. Plan addresses Phase I sampling at SWMU 16-021(c).
July 1994	First addendum to Phase I RFI work plan (LANL 1994, 039440)	“RFI Work Plan for Operable Unit 1082, Addendum 1” is issued. Plan is approved by NMED in January 1995.
April 1995–November 1995	Phase I RFI site characterization	Phase I RFI is implemented, including Phase I investigation of SWMU 16-021(c)-99.
1995–1996	Interim action—best management practices (LANL 1996, 053838)	Sandbag dam and diversion pipe are installed upgradient from the former HE pond; sandbag dam is located east of the parking lot behind TA-16-260; geotextile fabric matting is placed in former HE pond area; eight hay bale check dams are placed within the SWMU drainage between the rock dam and the 15-ft-high cliff. These controls were subsequently removed in 2000 during the 260 Outfall interim measure (IM).
September 1996	Phase I RFI report (LANL 1996, 055077)	Phase I RFI report is issued. Data show widespread HE contamination at SWMU 16-021(c)-99, extending from the 260 Outfall discharge point down to the sediment and waters of Cañon de Valle. Report is approved by NMED in March 1998.
September 1996	Phase II RFI work plan (included in LANL 1996, 055077)	Phase II RFI work plan is included in Phase I RFI report. Report is approved by NMED in March 1998.
November 1, 1996–December 23, 1996; May 1997–November 9, 1997	Phase II RFI site characterization	Phase II RFI is implemented at SWMU 16-021(c)-99.
September 1998	Phase II RFI report (LANL 1998, 059891)	Phase II RFI report is issued. Data confirm widespread HE contamination extending from the 260 Outfall discharge point down to the sediment and waters of Cañon de Valle and show deeper subsurface contamination. Up to 1% total HE is detected in surge bed at a depth of 17 ft. Report documents risk to human health and the environment. Report is approved by NMED in September 1999.
September 30, 1998	CMS plan (LANL 1998, 062413)	CMS plan is issued. Alternatives are evaluated. Report includes Phase III RFI sampling plan and describes ongoing hydrogeologic investigations for the site. Report is approved by NMED in September 1999.
October 1998–2003	Phase III RFI site characterization	Continued monitoring and sampling are used to characterize the temporal and spatial variability of site contamination; components of the site hydrogeologic system are undergoing continued evaluation.

Table 1.0-1 (continued)

Date	Activity (Reference)	Synopsis of Activity
October 1998–2006	CMS—ongoing evaluation of alternatives	CMS is initiated. A series of soil and water corrective measures technologies is evaluated. Investigation of components of the site hydrogeologic system continues.
September 30, 1999	Addendum to CMS plan (LANL 1999, 064873)	Addendum to CMS plan is issued. Addendum expands investigations to include deeper perched and regional groundwater potentially impacted by releases from SWMU 16-021(c)-99.
November 1999	IM plan—abatement of potential risks at the source area (LANL 2000, 064355)	IM plan is issued. Plan specifies removal of the highly contaminated soil and tuff identified in the 260 Outfall drainage channel. Plan is approved by NMED in April 2002.
November 12, 1999–November 18, 2000	Abatement of ongoing risks is initiated	TA-16-260 IM begins. Activities are interrupted by Cerro Grande fire. Initial stage of project is completed in November 2000.
January 7, 2000	Contained-in determination (NMED 2000, 064730)	NMED memo of contained-in determination is sent to the Laboratory (J. Brown) and DOE Environmental Remediation (T. Taylor).
April 4, 2000	Designation of area of contamination (NMED 2000, 070649)	NMED designates SWMU 16-021(c)-99 an area of contamination. Purpose of designation is to allow material from entire drainage area to be excavated, processed, and segregated without invoking RCRA land disposal restrictions. Excavated material considered potentially hazardous waste is staged in covered piles within area-of-contamination boundary.
June 5, 2000	In situ blending authorization (NMED 2000, 067094)	NMED authorizes in situ blending in memo sent to the Laboratory and DOE. To ensure worker health and safety during the IM and after, settling pond soil is robotically blended in situ with clean or low HE concentration material to reduce maximum concentration of settling pond sediment to below-reactive limit.
August 4, 2001–October 13, 2001	Abatement of ongoing risks is completed	Remobilization and removal of isolated areas containing more than 100 mg/kg of RDX is completed. Waste disposal stage of project is completed.
July 2002	260 Outfall IM report (LANL 2002, 073706)	IM results are presented in IM report. Report is approved by NMED in January 2003 (NMED 2003, 076174).
March 2003	Revision 1 to CMS plan addendum—evaluation of alternatives (LANL 2003, 075986)	Addendum to CMS plan is updated. Investigation into deeper perched and regional groundwater and deeper vadose zone potentially impacted by releases from SWMU 16-021(c)-99 is expanded further. Plan is approved by NMED in March 2003.

Table 1.0-1 (continued)

Date	Activity (Reference)	Synopsis of Activity
September 2003	"Phase III RFI Report for Solid Waste Management Unit 16-021(c)-99" (LANL 2003, 077965)	Report focuses on investigations into the surface water, alluvial groundwater, canyon sediment, and springs in Cañon de Valle and Martin Spring Canyon. Report includes analysis of data generated since Phase II RFI report (post-1998) and baseline risk assessments using a comprehensive database of both pre- and post-1998 data and emphasizes greater understanding of site hydrogeology and contaminant behavior. Report presents human health baseline risk assessments—one for source area, one for a selected reach of Cañon de Valle. In addition, a baseline ecological risk assessment is performed for that reach of Cañon de Valle.
November 2003	"Corrective Measures Study Report for Solid Waste Management Unit 16-021(c)-99" (LANL 2003, 085531)	CMS report for SWMU 16-021(c)-99 alluvial system. Report is a companion document to Phase III RFI report and relies heavily on the understanding of site hydrogeology and contaminant behavior outlined in that document. Report evaluates potential remedial technologies for each media and proposes appropriate technologies.
August 2006	Investigation report for intermediate and regional groundwater (LANL 2006, 093798)	Investigation report for the nature and extent of 16-021(c)-99 impacts to intermediate and regional groundwater.
October 2006	NMED approval of CMS (NMED 2006, 095631)	Final remedy approval for Cañon de Valle and Martin Spring Canyon alluvial groundwater and spring water and for 260 Outfall soils.
April 2007	"Evaluation of the Suitability of Wells Near TA-16 for Monitoring Contaminant Releases from Consolidated Unit 16-021(c)-99" (LANL 2007, 095787)	Documents conditions of wells and well screens and evaluates locations of wells for monitoring releases and migration to groundwater for 16-021(c)-99. NOD received August 15, 2007 (NMED 2007, 097874).
May 2007	Corrective Measures Implementation (CMI) Plan for Consolidated Unit 16-021(c)-99 (LANL 2007, 096003)	Presents engineering designs and specifications for CMI remedy for near-surface system associated with Consolidated Unit 16-021(c)-99; NMED approves document August 2007 (NMED 2007, 098449).
August 2007	"Corrective Measures Evaluation Report, Intermediate and Regional Groundwater, Consolidated Unit 16-021(c)-99" (LANL 2007, 098734)	The CME recommended a remediation strategy for monitored natural attenuation in the intermediate and regional groundwater, with possible pump and treat actions to reduce HE contaminant concentrations in groundwater.
April 2008	"Notice of Disapproval Corrective Measures Evaluation Report, Intermediate and Regional Groundwater Consolidated Unit 16-021(c)-99" (NMED 2008, 101311)	NMED required the Laboratory to (1) conduct additional characterization to assess the extent of contamination in perched-intermediate groundwater and in the regional aquifer and (2) further evaluate the feasibility of the remedial alternatives proposed in the CME based on their assessment that insufficient information was available to determine whether the Laboratory's proposed actions were appropriate and protective.

Table 1.0-1 (continued)

Date	Activity (Reference)	Synopsis of Activity
June 2008	"Supplemental Investigation Work Plan for Intermediate and Regional Groundwater at Consolidated Unit 16-021(c)-99" (LANL 2008, 103165)	In response to the CME NOD, the Laboratory proposed additional characterization activities to address uncertainties in the hydrogeologic conceptual model at TA-16. These activities included installing additional perched intermediate and regional groundwater monitoring wells, performing additional groundwater monitoring, and conducting single-well aquifer tests to further characterize hydraulics of the perched-intermediate and the regional aquifer.
March 2010	"Summary Report for the Corrective Measures Implementation at Consolidated Unit 16-021(c)-99" (LANL 2010, 108868)	Presents the results from the 2009–2010 CMI characterization and remediation activities. Details soil removals from the 260 Outfall. Confirmation samples are used to update the mass of RDX in the near-surface soils and sediments around the 260 Outfall and Cañon de Valle.
January 2012	"Work Plan for a Tracer Test at Consolidated Unit 16-021(c)-99, Technical Area 16" (LANL 2012, 210352)	To address hydrogeologic uncertainties, identified in the CME NOD, the Laboratory proposed aquifer tests and cross-hole tracer tests.
March 2012	"Technical Area 16 Well Network Evaluation and Recommendations" (LANL 2012, 213573)	The network evaluation resulted in recommendations to (1) convert several multiscreen wells to improve their reliability, (2) install a monitoring well in the perched-intermediate zone north of Cañon de Valle, and (3) install two additional monitoring wells in the regional aquifer to characterize contaminant flow paths and to monitor for contaminants. NMED approved the TA-16 well network evaluation with modifications in June 2012 (NMED 2012, 520747).
July 2014	"Geophysical Investigation of Cañon de Valle" (LANL 2014, 259157)	To address hydrogeologic uncertainties in the intermediate zone identified in the CME NOD, the Laboratory conducted an electrical resistivity geophysical survey to map the electrical structure of the vadose zone in the vicinity of Cañon de Valle.
July 2015	"Work Plan for a Tracer Test at Consolidated Unit 16-021(c)-99, Technical Area 16, Revision 1" (LANL 2015, 600535)	To address hydrogeologic uncertainties, identified in the CME NOD, the Laboratory proposed aquifer tests and cross-hole tracer tests.
August 2015	"Work Plan for Intermediate Groundwater System Characterization at Consolidated Unit 16-021(c)-99" (LANL 2015, 600686)	Conducted extended-duration (30-day) cross-hole aquifer tests using CdV-9-1(i), CdV-16-4ip, and CdV-16-1(i) as pumping locations and monitoring the effects in surrounding wells in 2016,
September 2016	"Evaluation Report for Surface Corrective Measures Implementation Closure, Consolidated Unit 16-021(c)-99" (LANL 2016, 601837)	Summarized the CMI work completed to date. Recommended removal of PRB; plugging and abandonment of PRB alluvial monitoring wells; removal of spring treatment units at SWSC, Burning Ground, and Martin springs; and replacement of alluvial well CdV-16-02657.

Table 1.0-1 (continued)

Date	Activity (Reference)	Synopsis of Activity
September 2016	"Groundwater Investigation Work Plan for Consolidated Unit 16-021(c)-99, Including Drilling Work Plans for Wells R-68 and R-69" (LANL 2016, 601779)	To address uncertainties related to increasing concentrations of RDX observed in monitoring well R-18, the groundwater investigation work plan recommended installing up to two monitoring wells completed in the regional aquifer. The first well, R-68, was completed in early 2017. R-69 was completed in early 2019.
February 2017	"Status Report for the Tracer Tests at Consolidated Unit 16-021(c)-99, Technical Area 16" (LANL 2017, 602161)	The Laboratory deployed groundwater tracers in perched-intermediate well CdV-9-1(i) with two piezometers, and in monitoring wells R-25b and CdV-16-1(i), and is performing ongoing sampling for tracers in monitoring wells near tracer-injection points.
March 2018	"Compendium of Technical Reports Related to the Deep Groundwater Investigation for the RDX Project at Los Alamos National Laboratory" (LANL 2018, 602963)	This document presents a compendium of technical reports summarizing the results of recent studies on the hydrology, geology, and geochemistry of TA-16, conducted in the period from 2015 to 2018 to support the deep groundwater investigation of RDX contamination at the site. A summary of the groundwater models developed for the deep groundwater investigation is also included, along with some of the preliminary modeling results.
August 2019	"Deep Groundwater Investigation Report for RDX" (<i>This document</i>)	Summarizes the hydrogeologic conceptual model and addresses the remaining data gaps related to the deep groundwater CME identified by NMED in the NOD (NMED 2008, 101311). The DGIR will include the results of a groundwater risk assessment that will evaluate the potential impacts of transport of the RDX inventory in the vadose zone to the regional aquifer. [<i>Note: this summary will be updated as the document develops.</i>]

Table 2.6-1
TA-16 Contaminant Sources and Ranking Based on their Potential to Impact Groundwater

Potential Source	COPCs (Large Inventory and/or Mobile)	Ranking	Rationale for Ranking
Cañon de Valle (alluvial system)	RDX, other HE, barium, solvents	High	Highest water volumes at TA-16, elevated RDX and other HE, evidence of vadose-zone infiltration
TA-16-260 pond	RDX, other HE, barium, solvents	High	Very large (thousands of kilograms) historical HE source. Historical water ponding zone. Known vadose zone migration
S-Site Canyon (alluvial system)/300s Line drainage/Martin Spring	RDX, other HE, boron, solvents	Medium	High water volumes, elevated RDX and other HE
30s Line/90s Line ponds	RDX, other HE, solvents	Medium	Intermittent water ponding. Historical water ponding. Moderate/large historical HE source. Known vadose zone migration
Fishladder Canyon (alluvial system)	Solvents (perchloroethylene), RDX, other HE	Medium	Moderate (intermittently saturated) current water volume. Historically higher water volumes. Moderate solvent/HE source
TA-16-460 drainage	RDX, other HE, solvents	Low	Historically high-water volumes. Low HE/solvent source
TA-16-430 drainage	RDX, other HE	Low	Historically moderate water volumes. Low HE
World War II Area Main Drainage (also known as Mother Ditch)	RDX, other HE	Low	Historically moderate/high water volumes. Unknown historical HE concentrations
Water Canyon (alluvial system)	RDX, other HE (?)	Low	Historically high water volumes. Minimal sediment contamination
MDA P/Burning Ground	RDX, other HE, barium, solvents	Low	Historically large HE, barium source. Intermittent/low water ponding (precipitation only)
MDA R	RDX, other HE, barium	Low	Historically moderate HE, barium source. Intermittent/low water ponding (precipitation only)
K-Site	RDX, other HE, barium	Low	Historically moderate HE source. Intermittent/low water ponding (precipitation only)
V-Site pond	RDX, other HE, boron	Low	Historically low/moderate HE source. Historical ponding area
Zia shops drum storage	Solvents	Low	Historical solvent source. Intermittent/low water ponding (precipitation only). Possible migration in vadose zone
Other HE-processing building outfalls (TA-16-220, 280, 400, 410, 360, 370, 380, etc.) and historic process building outfalls	RDX, other HE, barium, solvents, other COPCs	Low	Historically low HE, other COPC sources. Intermittent/low water ponding (low-flow outfalls and precipitation)

Table 3.1-1a
Analytes, Field Preparation, and Analytical Methods Used by
Accredited Contract Laboratories for Samples Collected under the IFGMP

Analytical Suite	Field Preparation	Analytical Method	Analytes
Metals ^a	Unfiltered	SW-846:6010	Aluminum
		EPA:245.2	Mercury
		SW-846:6020	Selenium
	Filtered	SW-846:6010	Aluminum, barium, beryllium, boron, calcium, cobalt, copper, iron, magnesium, manganese, potassium, silicon dioxide, sodium, strontium, tin, vanadium, zinc
		SW-846:6020	Antimony, arsenic, cadmium, chromium, lead, molybdenum, nickel, selenium, silver, thallium, uranium
VOCs	Unfiltered	SW-846:8260	See Table 3.1-2b
SVOCs ^b	Unfiltered	SW-846:8270	See Table 3.1-2b
PCBs	Unfiltered	SW-846:8082	See Table 3.1-2b
HEXP ^c	Unfiltered	SW-846:8330B	See Table 3.1-2b
HEXMOD ^d	Unfiltered	SW-846:8330B	See Table 3.1-2b
Dioxins/furans	Unfiltered	SW-846:8290	See Table 3.1-2b
Radionuclides	Unfiltered	EPA:900	Gross alpha, gross beta
	Unfiltered	EPA:901.1	Cesium-137, cobalt-60, neptunium-237, potassium-40, sodium-22
		EPA:905.0	Strontium-90
		HASL-300:AM-241	Americium-241
		HASL-300:ISOPU	Plutonium-238, plutonium-239/240
		HASL-300:ISOU	Uranium-234, uranium-235/236, uranium-238
Tritium	Unfiltered	EPA:906.0	Tritium
Low-level tritium	Unfiltered	Generic:Low_Level_Tritium	Tritium
General inorganics	Filtered	EPA:300.0	Bromide, chloride, fluoride, sulfate
		EPA:310.1	Alkalinity-CO ₃ , alkalinity-CO ₃ +HCO ₃
		SW-846:6010	Silicon dioxide
		SW-846:6850	Perchlorate
	Filtered	EPA:353.2	Nitrate-nitrite as nitrogen
		EPA:365.4	Total phosphate as phosphorus
	Unfiltered	EPA:335.4	Cyanide (total)

^a The following metals suite analytical groups and field preparations apply to groundwater samples: WSP-All metals (filtered) and MSGP-Hg (unfiltered).

^b SVOCs = Semivolatile organic compounds.

^c HEXP (analytical suite) = Analysis of samples for HE by SW-846:8330B.

^d HEXMOD (analytical suite) = Analysis of samples for HE and RDX-degradation products by SW-846:8330B.

Table 3.1-1b
Analytical Methods Used by
Contract Laboratories for Samples Collected under the IFGMP

Symbol or CAS ^a No.	Analyte
Analytical Suite: VOCs Analytical Group: WSP-8260B-VOA Analytical Method: SW-846:8260	
67-64-1	Acetone
75-05-8	Acetonitrile
107-02-8	Acrolein
107-13-1	Acrylonitrile
71-43-2	Benzene
108-86-1	Bromobenzene
74-97-5	Bromochloromethane
75-27-4	Bromodichloromethane
75-25-2	Bromoform
74-83-9	Bromomethane
71-36-3	Butanol[1-]
78-93-3	Butanone[2-]
104-51-8	Butylbenzene[n-]
135-98-8	Butylbenzene[sec-]
98-06-6	Butylbenzene[tert-]
75-15-0	Carbon disulfide
56-23-5	Carbon tetrachloride
126-99-8	Chloro-1,3-butadiene[2-]
107-05-1	Chloro-1-propene[3-]
108-90-7	Chlorobenzene
124-48-1	Chlorodibromomethane
75-00-3	Chloroethane
67-66-3	Chloroform
74-87-3	Chloromethane
95-49-8	Chlorotoluene[2-]
106-43-4	Chlorotoluene[4-]
96-12-8	Dibromo-3-chloropropane[1,2-]
106-93-4	Dibromoethane[1,2-]
74-95-3	Dibromomethane
95-50-1	Dichlorobenzene[1,2-]
541-73-1	Dichlorobenzene[1,3-]
106-46-7	Dichlorobenzene[1,4-]
75-71-8	Dichlorodifluoromethane
75-34-3	Dichloroethane[1,1-]

Table 3.1-1b (continued)

Symbol or CAS No.	Analyte
107-06-2	Dichloroethane[1,2-]
75-35-4	Dichloroethene[1,1-]
540-59-0	Dichloroethene[cis/trans-1,2-]
156-59-2	Dichloroethene[cis-1,2-]
156-60-5	Dichloroethene[trans-1,2-]
78-87-5	Dichloropropane[1,2-]
142-28-9	Dichloropropane[1,3-]
594-20-7	Dichloropropane[2,2-]
563-58-6	Dichloropropene[1,1-]
10061-01-5	Dichloropropene[cis-1,3-]
10061-02-6	Dichloropropene[trans-1,3-]
60-29-7	Diethyl ether
123-91-1	Dioxane[1,4-]
97-63-2	Ethyl methacrylate
100-41-4	Ethylbenzene
87-68-3	Hexachlorobutadiene
591-78-6	Hexanone[2-]
74-88-4	Iodomethane
78-83-1	Isobutyl alcohol
98-82-8	Isopropylbenzene
99-87-6	Isopropyltoluene[4-]
126-98-7	Methacrylonitrile
80-62-6	Methyl methacrylate
1634-04-4	Methyl tert-butyl ether
108-10-1	Methyl-2-pentanone[4-]
75-09-2	Methylene chloride
91-20-3	Naphthalene
107-12-0	Propionitrile
103-65-1	Propylbenzene[1-]
100-42-5	Styrene
630-20-6	Tetrachloroethane[1,1,1,2-]
79-34-5	Tetrachloroethane[1,1,2,2-]
127-18-4	Tetrachloroethene
108-88-3	Toluene
76-13-1	Trichloro-1,2,2-trifluoroethane[1,1,2-]
87-61-6	Trichlorobenzene[1,2,3-]
120-82-1	Trichlorobenzene[1,2,4-]
71-55-6	Trichloroethane[1,1,1-]
79-00-5	Trichloroethane[1,1,2-]

Table 3.1-1b (continued)

Symbol or CAS No.	Analyte
79-01-6	Trichloroethene
75-69-4	Trichlorofluoromethane
96-18-4	Trichloropropane[1,2,3-]
95-63-6	Trimethylbenzene[1,2,4-]
108-67-8	Trimethylbenzene[1,3,5-]
108-05-4	Vinyl acetate
75-01-4	Vinyl chloride
95-47-6	Xylene[1,2-]
Xylene[m+p]	Xylene[1,3-]+xylene[1,4-]
Analytical Suite: SVOCs Analytical Group: WSP-8270C-SVOA Analytical Method: SW-846:8270	
83-32-9	Acenaphthene
208-96-8	Acenaphthylene
62-53-3	Aniline
120-12-7	Anthracene
1912-24-9	Atrazine
103-33-3	Azobenzene
92-87-5	Benzidine
56-55-3	Benzo(a)anthracene
50-32-8	Benzo(a)pyrene
205-99-2	Benzo(b)fluoranthene
191-24-2	Benzo(g,h,i)perylene
207-08-9	Benzo(k)fluoranthene
65-85-0	Benzoic acid
100-51-6	Benzyl alcohol
111-91-1	Bis(2-chloroethoxy)methane
111-44-4	Bis(2-chloroethyl)ether
117-81-7	Bis(2-ethylhexyl)phthalate
101-55-3	Bromophenyl-phenylether[4-]
85-68-7	Butylbenzylphthalate
59-50-7	Chloro-3-methylphenol[4-]
106-47-8	Chloroaniline[4-]
91-58-7	Chloronaphthalene[2-]
95-57-8	Chlorophenol[2-]
7005-72-3	Chlorophenyl-phenyl[4-] Ether
218-01-9	Chrysene
53-70-3	Dibenz(a,h)anthracene
132-64-9	Dibenzofuran

Table 3.1-1b (continued)

Symbol or CAS No.	Analyte
95-50-1	Dichlorobenzene[1,2-]
541-73-1	Dichlorobenzene[1,3-]
106-46-7	Dichlorobenzene[1,4-]
91-94-1	Dichlorobenzidine[3,3'-]
120-83-2	Dichlorophenol[2,4-]
84-66-2	Diethylphthalate
131-11-3	Dimethyl phthalate
105-67-9	Dimethylphenol[2,4-]
84-74-2	Di-n-butylphthalate
534-52-1	Dinitro-2-methylphenol[4,6-]
51-28-5	Dinitrophenol[2,4-]
121-14-2	Dinitrotoluene[2,4-]
606-20-2	Dinitrotoluene[2,6-]
117-84-0	Di-n-octylphthalate
88-85-7	Dinoseb
123-91-1	Dioxane[1,4-]
122-39-4	Diphenylamine
206-44-0	Fluoranthene
86-73-7	Fluorene
118-74-1	Hexachlorobenzene
87-68-3	Hexachlorobutadiene
77-47-4	Hexachlorocyclopentadiene
67-72-1	Hexachloroethane
193-39-5	Indeno(1,2,3-cd)pyrene
78-59-1	Isophorone
90-12-0	Methylnaphthalene[1-]
91-57-6	Methylnaphthalene[2-]
95-48-7	Methylphenol[2-]
106-44-5	Methylphenol[4-]
91-20-3	Naphthalene
88-74-4	Nitroaniline[2-]
99-09-2	Nitroaniline[3-]
100-01-6	Nitroaniline[4-]
98-95-3	Nitrobenzene
88-75-5	Nitrophenol[2-]
100-02-7	Nitrophenol[4-]
55-18-5	Nitrosodiethylamine[N-]
62-75-9	Nitrosodimethylamine[N-]
924-16-3	Nitroso-di-n-butylamine[N-]

Table 3.1-1b (continued)

Symbol or CAS No.	Analyte
621-64-7	Nitroso-di-n-propylamine[N-]
86-30-6	Nitrosodiphenylamine[N-]
930-55-2	Nitrosopyrrolidine[N-]
108-60-1	Oxybis(1-chloropropane)[2,2'-]
608-93-5	Pentachlorobenzene
87-86-5	Pentachlorophenol
85-01-8	Phenanthrene
108-95-2	Phenol
129-00-0	Pyrene
110-86-1	Pyridine
95-94-3	Tetrachlorobenzene[1,2,4,5]
58-90-2	Tetrachlorophenol[2,3,4,6-]
120-82-1	Trichlorobenzene[1,2,4-]
95-95-4	Trichlorophenol[2,4,5-]
88-06-2	Trichlorophenol[2,4,6-]
Analytical Suite: Polychlorinated Biphenyls (PCBs)	
Analytical Group: WSP-8082-PCB	
Analytical Method: SW-846:8082	
12674-11-2	Aroclor-1016
11104-28-2	Aroclor-1221
11141-16-5	Aroclor-1232
53469-21-9	Aroclor-1242
12672-29-6	Aroclor-1248
11097-69-1	Aroclor-1254
11096-82-5	Aroclor-1260
37324-23-5	Aroclor-1262
Analytical Suite: HEXP (High Explosives)	
Analytical Group: WSP-8330B-NMED HEXP	
Analytical Method: SW-846:8330B	
6629-29-4	2,4-diamino-6-nitrotoluene
59229-75-3	2,6-diamino-4-nitrotoluene
618-87-1	3,5-dinitroaniline
19406-51-0	Amino-2,6-dinitrotoluene[4-]
35572-78-2	Amino-4,6-dinitrotoluene[2-]
99-65-0	Dinitrobenzene[1,3-]
121-14-2	Dinitrotoluene[2,4-]
606-20-2	Dinitrotoluene[2,6-]
2691-41-0	HMX
98-95-3	Nitrobenzene
88-72-2	Nitrotoluene[2-]

Table 3.1-1b (continued)

Symbol or CAS No.	Analyte
99-08-1	Nitrotoluene[3-]
99-99-0	Nitrotoluene[4-]
78-11-5	PETN ^b
121-82-4	RDX
3058-38-6	TATB
479-45-8	Tetryl
99-35-4	Trinitrobenzene[1,3,5-]
118-96-7	Trinitrotoluene[2,4,6-]
78-30-8	Tris (o-cresyl) phosphate
Analytical Suite: HEXMOD (High Explosives and RDX [Hexahydro-1,3,5, trinitro-1,3,5-triazine] Degradation Products) Analytical Group: WSP-8330B-NMED HEXMOD Analytical Method: SW-846:8330B	
6629-29-4	2,4-diamino-6-nitrotoluene
59229-75-3	2,6-diamino-4-nitrotoluene
618-87-1	3,5-dinitroaniline
19406-51-0	Amino-2,6-dinitrotoluene[4-]
35572-78-2	Amino-4,6-dinitrotoluene[2-]
99-65-0	Dinitrobenzene[1,3-]
121-14-2	Dinitrotoluene[2,4-]
606-20-2	Dinitrotoluene[2,6-]
2691-41-0	HMX
98-95-3	Nitrobenzene
88-72-2	Nitrotoluene[2-]
99-08-1	Nitrotoluene[3-]
99-99-0	Nitrotoluene[4-]
78-11-5	PETN
121-82-4	RDX
3058-38-6	TATB
479-45-8	Tetryl
99-35-4	Trinitrobenzene[1,3,5-]
118-96-7	Trinitrotoluene[2,4,6-]
78-30-8	Tris (o-cresyl) phosphate
80251-29-2	DNX ^c
5755-27-1	MNX ^c
13980-04-6	TNX ^c

Table 3.1-1b (continued)

Symbol or CAS No.	Analyte
Analytical Suite: Dioxins/Furans (D/F)	
Analytical Group: WSP-8290-D/F	
Analytical Method SW-846:8290	
35822-46-9	Heptachlorodibenzodioxin[1,2,3,4,6,7,8-]
37871-00-4	Heptachlorodibenzodioxins (total)
67562-39-4	Heptachlorodibenzofuran[1,2,3,4,6,7,8-]
55673-89-7	Heptachlorodibenzofuran[1,2,3,4,7,8,9-]
38998-75-3	Heptachlorodibenzofurans (total)
39227-28-6	Hexachlorodibenzodioxin[1,2,3,4,7,8-]
57653-85-7	Hexachlorodibenzodioxin[1,2,3,6,7,8-]
19408-74-3	Hexachlorodibenzodioxin[1,2,3,7,8,9-]
34465-46-8	Hexachlorodibenzodioxins (total)
70648-26-9	Hexachlorodibenzofuran[1,2,3,4,7,8-]
57117-44-9	Hexachlorodibenzofuran[1,2,3,6,7,8-]
72918-21-9	Hexachlorodibenzofuran[1,2,3,7,8,9-]
60851-34-5	Hexachlorodibenzofuran[2,3,4,6,7,8-]
55684-94-1	Hexachlorodibenzofurans (total)
3268-87-9	Octachlorodibenzodioxin[1,2,3,4,6,7,8,9-]
39001-02-0	Octachlorodibenzofuran[1,2,3,4,6,7,8,9-]
40321-76-4	Pentachlorodibenzodioxin[1,2,3,7,8-]
36088-22-9	Pentachlorodibenzodioxins (total)
57117-41-6	Pentachlorodibenzofuran[1,2,3,7,8-]
57117-31-4	Pentachlorodibenzofuran[2,3,4,7,8-]
30402-15-4	Pentachlorodibenzofurans (total)
1746-01-6	Tetrachlorodibenzodioxin[2,3,7,8-]
41903-57-5	Tetrachlorodibenzodioxins (total)
51207-31-9	Tetrachlorodibenzofuran[2,3,7,8-]
55722-27-5	Tetrachlorodibenzofurans (total)

Note: Table 3.1-2b is referenced in Table 3.1-2a and serves to complete the analyte lists in Table 3.1-2a.

^a CAS = Chemical Abstracts Service.

^b PETN = Pentaerythritol tetranitrate.

^c DNX, MNX, and TNX are RDX degradation products.

Table 3.1-2
Sample Location Descriptions for Water Samples Collected in
Alluvial Wells, Base Flow, Intermediate Wells, and Regional Wells

Location ID	Type	Top Screen Interval (bgs)	Bottom Screen Interval (bgs)	Geologic Unit
CDV-16-02656	Alluvial	3	8	Quaternary alluvium
CDV-16-02657	Alluvial	0.4	5.4	Quaternary alluvium
CDV-16-02657r	Alluvial	1.35	3.7	Quaternary alluvium
CDV-16-02658	Alluvial	1.9	6.9	Quaternary alluvium
CDV-16-02659	Alluvial	1.7	6.7	Quaternary alluvium
CDV-16-611923	Alluvial	3.2	8.2	Quaternary alluvium
CDV-16-611937	Alluvial	3	8	Quaternary alluvium
FLC-16-25280	Alluvial	2.6	4.2	Quaternary alluvium
MSC-16-06293	Alluvial	2	7	Quaternary alluvium
MSC-16-06294	Alluvial	2.5	7.3	Quaternary alluvium
WCO-1r	Alluvial	6	16	Quaternary alluvium
Between E252 and Water at Beta	Base flow	NA*	NA	Quaternary alluvium
Cañon de Valle below MDA P	Base flow	NA	NA	Quaternary alluvium
Water at Beta	Base flow	NA	NA	Quaternary alluvium
Pajarito below S&N Ancho E Basin Confluence	Base flow	NA	NA	Quaternary alluvium
16-26644	Intermediate	129	144	Tshirege Member – top of Qbt 3, tuff
CdV-16-1(i)	Intermediate	624	634	Otowi Member, tuff
CdV-16-2(i)r	Intermediate	850	859.7	Puye Formation, fanglomerates
CDV-16-4ip S1	Intermediate	815.6	879.2	Puye Formation, fanglomerates
CDV-16-4ip S2	Intermediate	1110	1141.1	Puye Formation, fanglomerates
CDV-37-1(i)	Intermediate	632	652.5	Puye Formation, fanglomerates
CDV-9-1(i) S1	Intermediate	937.4	992.4	Puye Formation, fanglomerates
R-25 S1	Intermediate	737.6	758.4	Otowi Member, tuff
R-25 S2	Intermediate	882.6	893.4	Puye Formation, fanglomerates
R-25 S3	Intermediate	1054.6	1064.6	Puye Formation, fanglomerates
R-25 S4	Intermediate	1184.6	1194.6	Puye Formation, fanglomerates
R-25b	Intermediate	750	770.8	Otowi Member, tuff
R-26 PZ-2	Intermediate	150	180	Tshirege Member - Qbt 3t, tuff
R-26 S1	Intermediate	654.8	669.9	Cerro Toledo Formation
R-27i	Intermediate	619	629	Puye Formation, fanglomerates
R-47i	Intermediate	840	860.6	Puye Formation, fanglomerates
R-63i	Intermediate	1122.5	1189	Puye Formation, fanglomerates
CdV-R-15-3 S4	Regional	1235.1	1278.9	Puye Formation, fanglomerates
CdV-R-37-2 S2	Regional	1188.7	1213.8	Tschicoma Formation dacite lava

Table 3.1-2 (continued)

Location ID	Type	Top Screen Interval (bgs)	Bottom Screen Interval (bgs)	Geologic Unit
R-17 S1	Regional	1057	1080	Puye Formation, fanglomerates
R-17 S2	Regional	1124	1134	Puye Formation, fanglomerates
R-18	Regional	1358	1381	Puye Formation, fanglomerates
R-19 S3	Regional	1171.4	1215.4	Puye Formation, fanglomerates
R-19 S4	Regional	1410.2	1417.4	Puye Formation, fanglomerates
R-19 S5	Regional	1582.6	1589.8	Puye Formation, fanglomerates
R-25 S5	Regional	1294.7	1304.7	Puye Formation, fanglomerates
R-25 S6	Regional	1404.7	1414.7	Puye Formation, fanglomerates
R-25 S7	Regional	1604.7	1614.7	Puye Formation, fanglomerates
R-25 S8	Regional	1794.7	1804.7	Puye Formation, fanglomerates
R-27	Regional	852	875	Puye Formation, fanglomerates
R-29	Regional	1170	1180	Puye Formation, fanglomerates
R-47	Regional	1322	1343.3	Puye Formation, fanglomerates
R-48	Regional	1500	1520.63	Tschicoma Formation, dacite lava
R-58	Regional	1257	1277.3	Tschicoma Formation, dacite lava
R-60	Regional	1330	1350.9	Puye Formation, fanglomerates
R-63	Regional	1325	1345.3	Puye Formation, fanglomerates
R-68	Regional	1340	1360.4	uye Formation
R-69 S1	Regional	1310	1330.2	Puye Formation, fanglomerates
R-69 S2	Regional	1375.5	1395.8	Puye Formation, fanglomerates
16-61439 (PRB Alluvial Seep)	Spring	NA	NA	Quaternary alluvium
Bulldog Spring	Spring	NA	NA	Tshirege Member base of Qbt 3t, tuff
Burning Ground Spring	Spring	NA	NA	Tshirege Member base of Qbt 3t, tuff
Martin Spring	Spring	NA	NA	Tshirege Member base of Qbt 3t, tuff
SWSC Spring	Spring	NA	NA	Tshirege Member base of Qbt 3t, tuff

* NA = Not analyzed.

Table 3.1-3
Frequency of Detections for Inorganic Constituents in Water Samples Collected in Intermediate and Regional Wells

Field Preparation Code	Analyte	Unit	Number of Analyses	Number of Detects	Detection (%)	Min	Avg	Max	Screening Value (Reference ^a)	Number Greater than Screening Value
F ^b	Alkalinity-CO ₃ +HCO ₃	mg/L	645	644	99.8	15.9	59.9	286	— ^c	—
F	Aluminum	µg/L	675	70	10.4	15.3	295	2140	5000 (4)	0
F	Antimony	µg/L	705	39	5.5	0.08	0.96	5.67	6 (4)	0
F	Arsenic	µg/L	675	128	19	1.5	2.61	8.8	10 (2)	0
F	Barium	µg/L	675	666	98.7	1.89	25.5	260	2000 (4)	0
F	Beryllium	µg/L	705	23	3.3	0	0.55	10.1	4 (4)	1
F	Boron	µg/L	661	280	42.4	8.4	49.2	640	750 (4)	0
F	Bromide	mg/L	656	106	16.2	0.06	0.14	2.44	—	—
F	Cadmium	µg/L	701	10	1.4	0.07	0.27	1.28	5 (2)	0
F	Calcium	mg/L	676	676	100	3.45	12.8	140	—	—
F	Chloride	mg/L	658	655	99.5	1.06	3.75	66.5	250 (4)	0
F	Chromium	µg/L	675	253	37.5	0.24	15.3	3080	50 (4)	1
F	Cobalt	µg/L	675	91	13.5	0.31	6.87	95	50 (4)	4
F	Copper	µg/L	675	63	9.3	0.43	9.71	116	1000 (4)	0
F	Cyanide (Total)	mg/L	30	3	10	0	0.01	0.03	0.2 (4)	0
UF ^d	Cyanide (Total)	mg/L	412	17	4.1	0	0.01	0.01	0.2 (4)	0
F	Fluoride	mg/L	658	625	95	0.04	0.15	0.53	1.6 (4)	0
F	Iron	µg/L	675	192	28.4	14.1	2060	29,300	1000 (4)	32
F	Lead	µg/L	702	29	4.1	0.03	0.97	3.31	15 (4)	0
F	Magnesium	mg/L	676	675	99.9	1.2	3.48	15.1	—	—
F	Manganese	µg/L	675	305	45.2	0.54	205	3720	200 (4)	39
UF	Mercury	µg/L	502	5	1	0.06	0.17	0.52	2 (4)	0
F	Molybdenum	µg/L	658	505	76.7	0.29	2.25	40.3	1000 (4)	0
F	Nickel	µg/L	675	454	67.3	0.51	58.6	7520	200 (4)	13

Table 3.1-3 (continued)

Field Preparation Code	Analyte	Unit	Number of Analyses	Number of Detects	Detection (%)	Min	Avg	Max	Screening Value (Reference ^a)	Number Greater than Screening Value
F	Nitrate-Nitrite as Nitrogen	mg/L	648	598	92.3	0.01	1.8	793	10 (2)	1
F	Perchlorate	µg/L	622	538	86.5	0.05	0.3	2.05	13.8 (3)	0
F	Potassium	mg/L	676	669	99	0.2	1.5	10.3	—	—
F	Selenium	µg/L	670	8	1.2	1	2.56	3.8	50 (4)	0
F	Silicon Dioxide	mg/L	597	589	98.7	12.5	149	28,700	—	—
F	Silver	µg/L	675	5	0.7	0.22	0.51	0.87	50 (4)	0
F	Sodium	mg/L	675	675	100	3.96	15.6	1910	—	—
F	Strontium	µg/L	657	657	100	23	71.3	750	11800 (3)	0—
F	Sulfate	mg/L	657	634	96.5	0.36	5.47	280	600 (4)	0
F	Thallium	µg/L	704	53	7.5	0.01	0.72	5.2	2 (4)	4
F	Tin	µg/L	601	26	4.3	2.51	4.96	10.4	1200 (1)	0
F	Titanium	µg/L	1	0	0	—	—	—	—	—
F	Uranium	µg/L	660	617	93.5	0.03	0.54	14.5	30 (2)	0
F	Vanadium	µg/L	675	553	81.9	0.46	4.42	12.9	63.1 (1)	0
F	Zinc	µg/L	675	346	51.3	1.4	17.1	1420	10000 (4)	0

^a Screening value reference:

(1) = EPA Regional Screening Levels for Tap Water

(2) = EPA Maximum Contaminant Levels

(3) = NMED Tap Water Screening Levels specified in the June 2019 Table A-1 of "Risk Assessment Guidance for Site Investigations and Remediation"

(4) = New Mexico Water Quality Control Commission (NMWQCC) Groundwater Standards

^b F = Filtered.^c — = Not applicable.^d UF = Unfiltered.

Table 3.1-4
Frequency of Detections for Organic Constituents in Water Samples Collected in Intermediate and Regional Wells

Field Preparation Code	Analyte	Unit	Number of Analyses	Number of Detects	Detection (%)	Min	Avg	Max	Screening Value (Reference ^a)	Number Greater than Screening Value
UF ^b	2,4-Diamino-6-nitrotoluene	µg/L	527	7	1.3	0.28	0.5	0.92	— ^c	—
UF	2,6-Diamino-4-nitrotoluene	µg/L	527	1	0.2	0.25	0.25	0.25	—	—
UF	3,5-Dinitroaniline	µg/L	527	4	0.8	0.35	0.48	0.85	—	—
UF	Acenaphthene	µg/L	327	0	0	—	—	—	535 (3)	—
UF	Acenaphthylene	µg/L	327	1	0.3	0.2	0.2	0.2	—	—
UF	Acetone	µg/L	568	45	7.9	1.29	8.87	68.7	14100 (3)	0
UF	Acetonitrile	µg/L	486	0	0	—	—	—	130 (1)	—
UF	Acrolein	µg/L	546	0	0	—	—	—	0.0415 (3)	—
UF	Acrylonitrile	µg/L	546	0	0	—	—	—	0.523 (3)	—
UF	Aldrin	µg/L	72	0	0	—	—	—	0.00198 (3)	—
UF	Amino-2,6-dinitrotoluene[4-]	µg/L	623	160	25.7	0.1	0.9	4.5	39 (1)	0
UF	Amino-4,6-dinitrotoluene[2-]	µg/L	623	90	14.4	0.08	0.83	8	39 (1)	0
UF	Aniline	µg/L	301	0	0	—	—	—	130 (1)	—
UF	Anthracene	µg/L	327	1	0.3	0.25	0.25	0.25	1720 (3)	0
UF	Aroclor-1016	µg/L	107	0	0	—	—	—	0.5 (2)	—
UF	Aroclor-1221	µg/L	107	0	0	—	—	—	0.5 (2)	—
UF	Aroclor-1232	µg/L	107	0	0	—	—	—	0.5 (2)	—
UF	Aroclor-1242	µg/L	107	1	0.9	0.17	0.17	0.17	0.5 (2)	0
UF	Aroclor-1248	µg/L	107	0	0	—	—	—	0.5 (2)	—
UF	Aroclor-1254	µg/L	107	0	0	—	—	—	0.5 (2)	—
UF	Aroclor-1260	µg/L	107	0	0	—	—	—	0.5 (2)	—
UF	Aroclor-1262	µg/L	89	0	0	—	—	—	0.5 (2)	—
UF	Atrazine	µg/L	284	0	0	—	—	—	3 (4)	—

Table 3.1-4 (continued)

Field Preparation Code	Analyte	Unit	Number of Analyses	Number of Detects	Detection (%)	Min	Avg	Max	Screening Value (Reference ^a)	Number Greater than Screening Value
UF	Azobenzene	µg/L	321	0	0	—	—	—	1.2 (1)	—
UF	Benzene	µg/L	568	3	0.5	0.22	0.32	0.4	5 (4)	0
UF	Benzidine	µg/L	334	0	0	—	—	—	0.00109 (3)	—
UF	Benzo(a)anthracene	µg/L	327	0	0	—	—	—	0.12 (3)	—
UF	Benzo(a)pyrene	µg/L	327	0	0	—	—	—	0.2 (4)	—
UF	Benzo(b)fluoranthene	µg/L	327	1	0.3	0.17	0.17	0.17	0.343 (3)	0
UF	Benzo(g,h,i)perylene	µg/L	327	0	0	—	—	—	—	—
UF	Benzo(k)fluoranthene	µg/L	327	0	0	—	—	—	3.43 (3)	—
UF	Benzoic Acid	µg/L	301	3	1	14.6	48.6	98.6	75,000 (1)	0
UF	Benzyl Alcohol	µg/L	301	0	0	—	—	—	2000 (1)	—
UF	BHC[alpha-]	µg/L	72	0	0	—	—	—	0.0693 (3)	—
UF	BHC[beta-]	µg/L	72	0	0	—	—	—	0.243 (3)	—
UF	BHC[delta-]	µg/L	72	0	0	—	—	—	—	—
UF	BHC[gamma-]	µg/L	72	0	0	—	—	—	—	—
UF	Bis(2-chloroethoxy)methane	µg/L	301	0	0	—	—	—	59 (1)	—
UF	Bis(2-chloroethyl)ether	µg/L	353	0	0	—	—	—	0.137 (3)	—
UF	Bis(2-ethylhexyl)phthalate	µg/L	301	13	4.3	0.25	2.98	5.48	6 (2)	0
UF	Bromobenzene	µg/L	568	0	0	—	—	—	62 (1)	—
UF	Bromochloromethane	µg/L	568	0	0	—	—	—	83 (1)	—
UF	Bromodichloromethane	µg/L	568	6	1.1	0.35	3.47	16.2	1.34 (3)	2
UF	Bromoform	µg/L	568	5	0.9	0.72	2.05	4.91	80 (2)	0
UF	Bromomethane	µg/L	568	0	0	—	—	—	7.54 (3)	—
UF	Bromophenyl-phenylether[4-]	µg/L	301	0	0	—	—	—	—	—
UF	Butanol[1-]	µg/L	448	0	0	—	—	—	2000 (1)	—
UF	Butanone[2-]	µg/L	568	5	0.9	4.35	8.89	11.7	5560 (3)	0

Table 3.1-4 (continued)

Field Preparation Code	Analyte	Unit	Number of Analyses	Number of Detects	Detection (%)	Min	Avg	Max	Screening Value (Reference ^a)	Number Greater than Screening Value
UF	Butylbenzene[n-]	µg/L	568	0	0	—	—	—	1000 (1)	—
UF	Butylbenzene[sec-]	µg/L	568	0	0	—	—	—	2000 (1)	—
UF	Butylbenzene[tert-]	µg/L	568	0	0	—	—	—	690 (1)	—
UF	Butylbenzylphthalate	µg/L	301	0	0	—	—	—	160 (1)	—
UF	Carbazole	µg/L	8	0	0	—	—	—	1800 (1)	—
UF	Carbon Disulfide	µg/L	568	6	1.1	1.36	2.23	4.9	810 (3)	—
UF	Carbon Tetrachloride	µg/L	568	0	0	—	—	—	5 (4)	—
UF	Chlordane[alpha-]	µg/L	72	0	0	—	—	—	0.448 (3)	—
UF	Chlordane[gamma-]	µg/L	72	0	0	—	—	—	0.448 (3)	—
UF	Chloro-1-propene[3-]	µg/L	486	0	0	—	—	—	7.3 (1)	—
UF	Chloro-1,3-butadiene[2-]	µg/L	525	0	0	—	—	—	0.187 (3)	—
UF	Chloro-3-methylphenol[4-]	µg/L	301	0	0	—	—	—	1400 (1)	—
UF	Chloroaniline[4-]	µg/L	301	0	0	—	—	—	3.7 (1)	—
UF	Chlorobenzene	µg/L	568	3	0.5	0.73	1.31	2.3	100 (2)	0
UF	Chlorodibromomethane	µg/L	568	6	1.1	0.76	1.94	4.15	1.68 (3)	2
UF	Chloroethane	µg/L	568	1	0.2	0.42	0.42	0.42	20,900 (3)	0
UF	Chloroethyl vinyl ether[2-]	µg/L	43	0	0	—	—	—	—	—
UF	Chloroform	µg/L	568	6	1.1	0.3	16.3	90.9	80 (2)	0
UF	Chloromethane	µg/L	568	4	0.7	0.33	0.94	2.7	20.3 (3)	0
UF	Chloronaphthalene[2-]	µg/L	322	0	0	—	—	—	733 (3)	—
UF	Chlorophenol[2-]	µg/L	301	0	0	—	—	—	91 (3)	—
UF	Chlorophenyl-phenyl[4-] Ether	µg/L	301	0	0	—	—	—	—	—
UF	Chlorotoluene[2-]	µg/L	568	0	0	—	—	—	233 (3)	—
UF	Chlorotoluene[4-]	µg/L	567	0	0	—	—	—	250 (1)	—
UF	Chrysene	µg/L	327	0	0	—	—	—	34.3 (3)	—

Table 3.1-4 (continued)

Field Preparation Code	Analyte	Unit	Number of Analyses	Number of Detects	Detection (%)	Min	Avg	Max	Screening Value (Reference ^a)	Number Greater than Screening Value
UF	D[2,4-] ^d	µg/L	30	0	0	—	—	—	70 (2)	—
UF	Dalapon	µg/L	30	0	0	—	—	—	200 (2)	—
UF	DB[2,4-] ^e	µg/L	30	0	0	—	—	—	450 (1)	—
UF	DDD[4,4'-] ^f	µg/L	72	0	0	—	—	—	0.317 (3)	—
UF	DDE[4,4'-] ^g	µg/L	72	0	0	—	—	—	0.462 (3)	—
UF	DDT[4,4'-] ^h	µg/L	72	1	1.4	0.02	0.02	0.02	2.29 (3)	0
UF	Di-n-butylphthalate	µg/L	301	0	0	—	—	—	885 (3)	—
UF	Di-n-octylphthalate	µg/L	301	0	0	—	—	—	200 (1)	—
UF	Dibenz(a,h)anthracene	µg/L	327	0	0	—	—	—	0.0343 (3)	—
UF	Dibenzofuran	µg/L	301	0	0	—	—	—	7.9 (1)	—
UF	Dibromo-3-Chloropropane[1,2-]	µg/L	565	0	0	—	—	—	0.2 (2)	—
UF	Dibromoethane[1,2-]	µg/L	565	0	0	—	—	—	0.05 (4)	—
UF	Dibromomethane	µg/L	568	0	0	—	—	—	0.0747 (3)	—
UF	Dicamba	µg/L	30	0	0	—	—	—	570 (1)	—
UF	Dichlorobenzene[1,2-]	µg/L	869	0	0	—	—	—	600 (4)	—
UF	Dichlorobenzene[1,3-]	µg/L	869	1	0.1	0.79	0.79	0.79	—	—
UF	Dichlorobenzene[1,4-]	µg/L	869	1	0.1	0.21	0.21	0.21	75 (4)	0
UF	Dichlorobenzidine[3,3'-]	µg/L	353	0	0	—	—	—	1.25 (3)	—
UF	Dichlorodifluoromethane	µg/L	568	0	0	—	—	—	197 (3)	—
UF	Dichloroethane[1,1-]	µg/L	568	0	0	—	—	—	25 (4)	—
UF	Dichloroethane[1,2-]	µg/L	568	1	0.2	0.49	0.49	0.49	5 (4)	0
UF	Dichloroethene[1,1-]	µg/L	568	0	0	—	—	—	5 (4)	—
UF	Dichloroethene[cis-1,2-]	µg/L	547	0	0	—	—	—	70 (4)	—
UF	Dichloroethene[cis/trans-1,2-]	µg/L	1	0	0	—	—	—	70 (4)	—
UF	Dichloroethene[trans-1,2-]	µg/L	568	0	0	—	—	—	100 (4)	—

Table 3.1-4 (continued)

Field Preparation Code	Analyte	Unit	Number of Analyses	Number of Detects	Detection (%)	Min	Avg	Max	Screening Value (Reference ^a)	Number Greater than Screening Value
UF	Dichlorophenol[2,4-]	µg/L	301	0	0	—	—	—	45.3 (3)	—
UF	Dichloropropane[1,2-]	µg/L	568	0	0	—	—	—	5 (4)	—
UF	Dichloropropane[1,3-]	µg/L	568	0	0	—	—	—	370 (1)	—
UF	Dichloropropane[2,2-]	µg/L	568	0	0	—	—	—	—	—
UF	Dichloropropene[1,1-]	µg/L	568	0	0	—	—	—	—	—
UF	Dichloropropene[cis-1,3-]	µg/L	568	0	0	—	—	—	4.71 (3)	—
UF	Dichloropropene[cis/trans-1,3-]	µg/L	4	0	0	—	—	—	4.71 (3)	—
UF	Dichloropropene[trans-1,3-]	µg/L	568	0	0	—	—	—	4.71 (3)	—
UF	Dichloroprop	µg/L	30	0	0	—	—	—	—	—
UF	Dieldrin	µg/L	72	0	0	—	—	—	0.0175 (3)	—
UF	Diethyl Ether	µg/L	448	2	0.4	0.32	0.35	0.39	3930 (3)	0
UF	Diethylphthalate	µg/L	301	2	0.7	2.35	16.8	31.2	14800 (3)	0
UF	Dimethyl Phthalate	µg/L	301	0	0	—	—	—	612 (3)	—
UF	Dimethylphenol[2,4-]	µg/L	301	0	0	—	—	—	354 (3)	—
UF	Dinitro-2-methylphenol[4,6-]	µg/L	332	0	0	—	—	—	1.52 (3)	—
UF	Dinitrobenzene[1,3-]	µg/L	623	1	0.2	0.22	0.22	0.22	2 (1)	0
UF	Dinitrophenol[2,4-]	µg/L	301	0	0	—	—	—	38.7 (3)	—
UF	Dinitrotoluene[2,4-]	µg/L	924	21	2.3	0.07	0.46	1.15	2.37 (3)	0
UF	Dinitrotoluene[2,6-]	µg/L	924	1	0.1	0.39	0.39	0.39	0.485 (3)	0
UF	Dinoseb	µg/L	281	0	0	—	—	—	7 (2)	—
UF	Dioxane[1,4-]	µg/L	312	1	0.3	1.94	1.94	1.94	4.59 (3)	0
UF	Diphenylamine	µg/L	291	0	0	—	—	—	1300 (1)	—
UF	Diphenylhydrazine[1,2-]	µg/L	10	0	0	—	—	—	0.78 (3)	—
UF	DNX	µg/L	448	80	17.9	0.08	0.26	3.48	—	—
UF	Endosulfan I	µg/L	72	0	0	—	—	—	—	—

Table 3.1-4 (continued)

Field Preparation Code	Analyte	Unit	Number of Analyses	Number of Detects	Detection (%)	Min	Avg	Max	Screening Value (Reference ^a)	Number Greater than Screening Value
UF	Endosulfan II	µg/L	72	0	0	—	—	—	—	—
UF	Endosulfan Sulfate	µg/L	72	0	0	—	—	—	—	—
UF	Endrin Aldehyde	µg/L	72	0	0	—	—	—	—	—
UF	Endrin Ketone	µg/L	72	0	0	—	—	—	—	—
UF	Endrin	µg/L	72	0	0	—	—	—	2 (2)	—
UF	Ethyl Methacrylate	µg/L	486	0	0	—	—	—	455 (3)	—
UF	Ethylbenzene	µg/L	568	1	0.2	0.28	0.28	0.28	700 (4)	0
UF	Fluoranthene	µg/L	327	1	0.3	0.22	0.22	0.22	802 (3)	0
UF	Fluorene	µg/L	327	0	0	—	—	—	288 (3)	—
UF	Heptachlor	µg/L	72	1	1.4	0.02	0.02	0.02	0.4 (2)	0
UF	Heptachlorodibenzodioxin[1,2,3,4,6,7,8-]	µg/L	28	0	0	—	—	—	—	—
UF	Heptachlorodibenzodioxins (Total)	µg/L	28	0	0	—	—	—	—	—
UF	Heptachlorodibenzofuran[1,2,3,4,6,7,8-]	µg/L	28	0	0	—	—	—	—	—
UF	Heptachlorodibenzofuran[1,2,3,4,7,8,9-]	µg/L	28	0	0	—	—	—	—	—
UF	Heptachlorodibenzofurans (Total)	µg/L	28	0	0	—	—	—	—	—
UF	Hexachlorobenzene	µg/L	351	0	0	—	—	—	1 (2)	—
UF	Hexachlorobutadiene	µg/L	837	0	0	—	—	—	1.39 (3)	—
UF	Hexachlorocyclopentadiene	µg/L	301	0	0	—	—	—	50 (2)	—
UF	Hexachlorodibenzodioxin[1,2,3,4,7,8-]	µg/L	28	0	0	—	—	—	—	—
UF	Hexachlorodibenzodioxin[1,2,3,6,7,8-]	µg/L	28	0	0	—	—	—	—	—
UF	Hexachlorodibenzodioxin[1,2,3,7,8,9-]	µg/L	28	0	0	—	—	—	—	—
UF	Hexachlorodibenzodioxins (Total)	µg/L	28	0	0	—	—	—	—	—
UF	Hexachlorodibenzofuran[1,2,3,4,7,8-]	µg/L	28	0	0	—	—	—	—	—
UF	Hexachlorodibenzofuran[1,2,3,6,7,8-]	µg/L	28	0	0	—	—	—	—	—
UF	Hexachlorodibenzofuran[1,2,3,7,8,9-]	µg/L	28	0	0	—	—	—	—	—

Table 3.1-4 (continued)

Field Preparation Code	Analyte	Unit	Number of Analyses	Number of Detects	Detection (%)	Min	Avg	Max	Screening Value (Reference ^a)	Number Greater than Screening Value
UF	Hexachlorodibenzofuran[2,3,4,6,7,8-]	µg/L	28	0	0	—	—	—	—	—
UF	Hexachlorodibenzofurans (Total)	µg/L	28	0	0	—	—	—	—	—
UF	Hexachloroethane	µg/L	301	0	0	—	—	—	3.28 (3)	—
UF	Hexanone[2-]	µg/L	568	0	0	—	—	—	38 (1)	—
UF	HMX	µg/L	644	207	32.1	0.04	2.62	11.9	1000 (3)	0
UF	Indeno(1,2,3-cd)pyrene	µg/L	327	0	0	—	—	—	0.343 (3)	—
UF	Iodomethane	µg/L	568	0	0	—	—	—	—	—
UF	Isobutyl alcohol	µg/L	486	0	0	—	—	—	5910 (3)	—
UF	Isophorone	µg/L	301	0	0	—	—	—	781 (3)	—
UF	Isopropylbenzene	µg/L	568	8	1.4	0.32	0.5	0.69	447 (3)	0
UF	Isopropyltoluene[4-]	µg/L	568	1	0.2	0.35	0.35	0.35	—	—
UF	MCPA ⁱ	µg/L	30	0	0	—	—	—	7.5 (1)	—
UF	MCPPI ^j	µg/L	30	0	0	—	—	—	16 (1)	—
UF	Methacrylonitrile	µg/L	506	0	0	—	—	—	1.91 (3)	—
UF	Methoxychlor[4,4'-]	µg/L	72	0	0	—	—	—	40 (2)	—
UF	Methyl-2-pentanone[4-]	µg/L	568	2	0.4	1.4	3.38	5.35	1240 (3)	0
UF	Methyl Methacrylate	µg/L	486	0	0	—	—	—	1390 (3)	—
UF	Methyl tert-Butyl Ether	µg/L	448	82	18.3	0.3	0.75	1.48	100 (3)	0
UF	Methylene Chloride	µg/L	568	7	1.2	0.53	1.57	3.2	5 (4)	0
UF	Methylnaphthalene[1-]	µg/L	279	0	0	—	—	—	11.4 (3)	—
UF	Methylnaphthalene[2-]	µg/L	327	0	0	—	—	—	35.1 (3)	—
UF	Methylphenol[2-]	µg/L	301	0	0	—	—	—	930 (1)	—
UF	Methylphenol[3-,4-]	µg/L	118	0	0	—	—	—	930 (1)	—
UF	Methylphenol[4-]	µg/L	183	0	0	—	—	—	1900 (1)	—
UF	Methylpyridine[2-]	µg/L	21	0	0	—	—	—	—	—

Table 3.1-4 (continued)

Field Preparation Code	Analyte	Unit	Number of Analyses	Number of Detects	Detection (%)	Min	Avg	Max	Screening Value (Reference ^a)	Number Greater than Screening Value
UF	MNX	µg/L	448	101	22.5	0.09	0.39	2.53	—	—
UF	Naphthalene	µg/L	863	2	0.2	0.26	0.33	0.41	1.65 (3)	0
UF	Nitroaniline[2-]	µg/L	301	0	0	—	—	—	190(1)	—
UF	Nitroaniline[3-]	µg/L	301	0	0	—	—	—	—	—
UF	Nitroaniline[4-]	µg/L	301	0	0	—	—	—	38 (1)	—
UF	Nitrobenzene	µg/L	924	1	0.1	0.02	0.02	0.02	1.4 (3)	0
UF	Nitroglycerin	µg/L	11	0	0	—	—	—	1.96 (3)	—
UF	Nitrophenol[2-]	µg/L	301	0	0	—	—	—	—	—
UF	Nitrophenol[4-]	µg/L	301	0	0	—	—	—	—	—
UF	Nitroso-di-n-butylamine[N-]	µg/L	303	0	0	—	—	—	0.0273 (3)	—
UF	Nitroso-di-n-propylamine[N-]	µg/L	353	0	0	—	—	—	0.11 (1)	—
UF	Nitrosodiethylamine[N-]	µg/L	303	0	0	—	—	—	0.00167 (3)	—
UF	Nitrosodimethylamine[N-]	µg/L	353	1	0.3	1.57	1.57	1.57	0.00491 (3)	1
UF	Nitrosodiphenylamine[N-]	µg/L	10	0	0	—	—	—	122 (3)	—
UF	Nitrosopyrrolidine[N-]	µg/L	305	0	0	—	—	—	0.37 (3)	—
UF	Nitrotoluene[2-]	µg/L	623	11	1.8	0.09	0.47	1.6	3.14 (3)	0
UF	Nitrotoluene[3-]	µg/L	623	3	0.5	0.12	0.29	0.56	1.74 (3)	0
UF	Nitrotoluene[4-]	µg/L	623	0	0	—	—	—	42.7 (3)	—
UF	Octachlorodibenzodioxin[1,2,3,4,6,7,8,9-]	µg/L	28	0	0	—	—	—	—	—
UF	Octachlorodibenzofuran[1,2,3,4,6,7,8,9-]	µg/L	28	0	0	—	—	—	—	—
UF	Oxybis(1-chloropropane)[2,2'-]	µg/L	332	0	0	—	—	—	710 (1)	—
UF	Pentachlorobenzene	µg/L	251	0	0	—	—	—	3.07 (3)	—
UF	Pentachlorodibenzodioxin[1,2,3,7,8-]	µg/L	28	0	0	—	—	—	—	—
UF	Pentachlorodibenzodioxins (Total)	µg/L	28	0	0	—	—	—	—	—
UF	Pentachlorodibenzofuran[1,2,3,7,8-]	µg/L	28	0	0	—	—	—	—	—

Table 3.1-4 (continued)

Field Preparation Code	Analyte	Unit	Number of Analyses	Number of Detects	Detection (%)	Min	Avg	Max	Screening Value (Reference ^a)	Number Greater than Screening Value
UF	Pentachlorodibenzofuran[2,3,4,7,8-]	µg/L	28	0	0	—	—	—	—	—
UF	Pentachlorodibenzofurans (Totals)	µg/L	28	0	0	—	—	—	—	—
UF	Pentachlorophenol	µg/L	326	0	0	—	—	—	1 (4)	—
UF	PETN ^k	µg/L	538	1	0.2	0.19	0.19	0.19	190 (1)	0
UF	Phenanthrene	µg/L	327	1	0.3	0.28	0.28	0.28	170 (3)	0
UF	Phenol	µg/L	301	2	0.7	3.62	9.71	15.8	5 (4)	1
UF	Propionitrile	µg/L	486	0	0	—	—	—	—	—
UF	Propylbenzene[1-]	µg/L	568	0	0	—	—	—	660 (1)	—
UF	Pyrene	µg/L	327	1	0.3	0.23	0.23	0.23	117 (3)	0
UF	Pyridine	µg/L	245	1	0.4	2.34	2.34	2.34	20 (1)	0
UF	RDX	µg/L	621	306	49.3	0.03	29.6	177	9.66 (3)	164
UF	Styrene	µg/L	568	6	1.1	0.26	0.65	1	100 (4)	0
UF	T[2,4,5-] ^l	µg/L	30	0	0	—	—	—	160 (1)	—
UF	TATB	µg/L	527	0	0	—	—	—	—	—
UF	Tetrachlorobenzene[1,2,4,5]	µg/L	253	0	0	—	—	—	1.66 (3)	—
UF	Tetrachlorodibenzodioxin[2,3,7,8-]	µg/L	28	0	0	—	—	—	0.00003 (2)	—
UF	Tetrachlorodibenzodioxins (Total)	µg/L	28	0	0	—	—	—	—	—
UF	Tetrachlorodibenzofuran[2,3,7,8-]	µg/L	28	0	0	—	—	—	0.00000184 (3)	—
UF	Tetrachlorodibenzofurans (Totals)	µg/L	28	0	0	—	—	—	—	—
UF	Tetrachloroethane[1,1,1,2-]	µg/L	568	0	0	—	—	—	5.74 (3)	—
UF	Tetrachloroethane[1,1,2,2-]	µg/L	568	0	0	—	—	—	10 (4)	—
UF	Tetrachloroethene	µg/L	568	157	27.6	0.29	1.02	5.03	5 (4)	1
UF	Tetrachlorophenol[2,3,4,6-]	µg/L	253	0	0	—	—	—	240 (1)	—
UF	Tetryl	µg/L	623	0	0	—	—	—	39.4 (3)	—
UF	TNX	µg/L	448	87	19.4	0.09	0.31	2.53	—	—

Table 3.1-4 (continued)

Field Preparation Code	Analyte	Unit	Number of Analyses	Number of Detects	Detection (%)	Min	Avg	Max	Screening Value (Reference ^a)	Number Greater than Screening Value
UF	Toluene	µg/L	568	68	12	0.18	5.72	119	1000 (4)	0
UF	Total Petroleum Hydrocarbons Diesel Range Organics	µg/L	11	0	0	—	—	—	—	—
UF	Toxaphene (Technical Grade)	µg/L	72	0	0	—	—	—	3 (2)	—
UF	TP[2,4,5-] ^m	µg/L	30	0	0	—	—	—	50 (2)	—
UF	Trichloro-1,2,2-trifluoroethane[1,1,2-]	µg/L	568	0	0	—	—	—	55,000 (3)	—
UF	Trichlorobenzene[1,2,3-]	µg/L	515	1	0.2	0.9	0.9	0.9	7 (1)	0
UF	Trichlorobenzene[1,2,4-]	µg/L	816	0	0	—	—	—	70 (4)	—
UF	Trichloroethane[1,1,1-]	µg/L	568	0	0	—	—	—	200 (4)	—
UF	Trichloroethane[1,1,2-]	µg/L	568	0	0	—	—	—	5 (4)	—
UF	Trichloroethene	µg/L	568	98	17.3	0.29	0.88	4.14	5 (4)	0
UF	Trichlorofluoromethane	µg/L	568	0	0	—	—	—	1140 (3)	—
UF	Trichlorophenol[2,4,5-]	µg/L	301	0	0	—	—	—	1170 (3)	—
UF	Trichlorophenol[2,4,6-]	µg/L	301	0	0	—	—	—	11.9 (3)	—
UF	Trichloropropane[1,2,3-]	µg/L	608	0	0	—	—	—	0.00835 (3)	—
UF	Trichlorotrifluoroethane	µg/L	1	0	0	—	—	—	55,000 (3)	—
UF	Trimethylbenzene[1,2,4-]	µg/L	568	0	0	—	—	—	56 (1)	—
UF	Trimethylbenzene[1,3,5-]	µg/L	568	0	0	—	—	—	60 (1)	—
UF	Trinitrobenzene[1,3,5-]	µg/L	623	61	9.8	0.03	1.01	12.4	590 (1)	0
UF	Trinitrotoluene[2,4,6-]	µg/L	644	47	7.3	0.09	2.32	9.36	9.8 (3)	0
UF	Tris (o-cresyl) phosphate	µg/L	527	0	0	—	—	—	—	—
UF	Vinyl acetate	µg/L	486	0	0	—	—	—	409 (3)	—
UF	Vinyl Chloride	µg/L	568	0	0	—	—	—	2 (4)	—
UF	Xylene (Total)	µg/L	68	0	0	—	—	—	620 (4)	—
UF	Xylene[1,2-]	µg/L	553	0	0	—	—	—	193 (3)	—

Table 3.1-4 (continued)

Field Preparation Code	Analyte	Unit	Number of Analyses	Number of Detects	Detection (%)	Min	Avg	Max	Screening Value (Reference ^a)	Number Greater than Screening Value
UF	Xylene[1,3-]+Xylene[1,4-]	µg/L	523	2	0.4	0.26	0.35	0.45	193 (3)	0

^a Screening value reference:

(1) = EPA Regional Screening Levels for Tap Water

(2) = EPA Maximum Contaminant Levels

(3) = NMED Tap Water Screening Levels specified in the June 2019 Table A-1 of "Risk Assessment Guidance for Site Investigations and Remediation"

(4) = New Mexico Water Quality Control Commission (NMWQCC) Groundwater Standards

^b UF = Unfiltered.

^c — = Not applicable.

^d D[2,4] = 2,4-dichlorophenoxyacetic acid.

^e DB[2,4-] = 4-(2,4-dichlorophenoxy)butanoic acid.

^f DDD[4,4'-] = 4,4'-dichlorodiphenyldichloroethane.

^g DDE[4,4'-] = 4,4'-dichlorodiphenyldichloroethylene.

^h DDT[4,4'-] = 4,4'-dichlorodiphenyltrichloroethane.

ⁱ MCPA = Methyl-4-chlorophenoxyacetic(2-) acid.

^j MCPP = Methyl-4-chlorophenoxypropionic(2-) acid.

^k PETN = Pentaerythritol tetranitrate.

^l T[2,4,5-] = 2,4,5-trichlorophenoxyacetic acid.

^m TP[2,4,5] = 2(2,4,5-trichlorophenoxy) propionic acid.

Table 3.1-5
Mean, Most Recent Values, and Mann-Kendall Trend Analysis of the RDX Concentrations in Water Samples

Media	Location Name	Most Recent RDX Value (µg/L)	Mean RDX (µg/L)	Concentration Range	Number of Samples	Mann-Kendall Trend Test: p<0.05	Notes
Base Flow	CdV below MDA P (E256)	20.6	11	<1–55	46	No trend	
	Between E252 and Water at Beta	<1, U ^a	<1, U	<1	23	No trend	
	Paj bl S-N Anch E Basin Conf	<1	1	<1–5	17	No trend	
	Water at Beta	<1, U	<1, U	<1	20	No trend	
Springs	Burning Ground Spring	45.4	20	2–100	74	Decreasing	
	Martin Spring	26	98	<1–230	70	Decreasing	
	SWSC Spring	296	51	1–296	36	Decreasing	
	Bulldog Spring	1.84	4	1–8	32	No trend	
	PRB Alluvial Seep (16-61439)	12.8	11	7–13	7	Not enough data for test	Limited data
Alluvial Groundwater	CDV-16-02656	3.9	1	<1–9	51	Decreasing	
	CDV-16-02659	4.5	20	<1–112	52	Decreasing	
	CDV-16-02657	148	68	0–759	22	No trend	Well damaged in 2011 floods; replaced by CDV-16-02657r.
	CDV-16-02658	0.7	5	<1–27	33	No trend	Well damaged in 2011 floods; replaced by CDV-16-611923.
	CDV-16-611923	5.1	3	<1–15	22	No trend	
	MSC-16-06293	0.1	<1	<1–5	9	No trend	
	MSC-16-06294	<1, U	<1	<1	26	No trend	
	CdV-16-611937	1.6	<1	<1–2	13	No trend	
	FLC-16-25280	3.9	4	2-7	5	Not enough data for test	Limited data

Table 3.1-5 (continued)

Media	Location Name	Most Recent RDX Value (µg/L)	Mean RDX (µg/L)	Concentration Range	Number of Samples	Mann-Kendall Trend Test: p<0.05	Notes
Intermediate Groundwater	16-26644	65.7	11	<1–66	23	Decreasing	Shallow bedrock perched zone
	CdV-9-1(i) S ^b 1	16.4	21	15–37	14	Decreasing	Upper perched-intermediate zone
	CdV-16-4ip S1	117	133	104–177	26	Decreasing	Upper perched-intermediate zone
	R-25 S1	21.2	40	<1–65	18	Decreasing	Upper perched-intermediate zone
	R-25b	1.3	3	<1–8	13	Decreasing	Upper perched-Intermediate zone; data affected by tracer injection 2016.
	CdV-16-2(i)r	105	84	46–128	31	Increasing	Upper perched-intermediate zone
	R-25 S2	14.1	8	<1–38	18	Increasing	Upper perched-intermediate zone
	R-25 S4	19.2	14	2–27	19	Increasing	Lower perched-intermediate zone
	CdV-16-1(i)	32.9	28	22–37	26	No trend	Upper perched-intermediate zone
	CdV-37-1(i)	<1, U	<1	<1, U	10	No trend	Upper perched-intermediate zone
	R-26 PZ-2	<1, U	<1	<1, U	13	No trend	Lower perched-intermediate zone
	R-26 S1	<1, U	<1, U	<1, U	25	No trend	Upper perched-intermediate zone
	R-47i	<1, U	<1	<1, U	15	No trend	Upper perched-intermediate zone
	R-63i	<1	<1	<1, U	1	Not enough data for test	Lower perched-intermediate zone; limited data.
Regional Groundwater	R-63	1.8	1	1–2	25	Increasing	
	R-68	19.5	14	8–20	11	Increasing	
	R-18	3.5	2	0–4	32	Increasing	
	R-47	<1, U	<1	<1, U	19	No trend	
	CdV-R-15-3 S4	<1, U	<1	<1	47	No trend	
	CdV-R-37-2 S2	<1, U	<1	<1, U	38	No trend	
	R-25 S5	<1	2	<1–22	20	No trend	
	R-25 S6	<1	3	<1–17	16	Decreasing	Early data affected by crossflow
	R-48	<1, U	<1	<1, U	15	No trend	
	R-58	<1, U	<1	<1 U	12	No trend	
	R-69 S1	15.0	14	13–15	5	Not enough data for test	Limited data
	R-69 S2	22.1	18	15–22	5	Not enough data for test	Limited data

^a U = Not detected.^b S = Screen.

Table 3.1-6
Frequency of Detections for Radionuclide Constituents in Water Samples Collected in Intermediate and Regional Wells

Field Preparation Code	Analyte	Unit	Number of Analyses	Number of Detects	Detection (%)	Min	Avg	Max	Screening Value (Reference ^a)	Number Greater than Screening Value
F ^b	Actinium-228	pCi/L	12	1	8	17.7	17.7	17.7	— ^c	—
UF ^d	Actinium-228	pCi/L	9	0	0	—	—	—	—	—
F	Americium-241	pCi/L	106	1	1	71	71	71	—	—
UF	Americium-241	pCi/L	199	0	0	—	—	—	—	—
F	Annihilation Radiation	pCi/L	12	0	0	—	—	—	—	—
UF	Annihilation Radiation	pCi/L	6	0	0	—	—	—	—	—
UF	Antimony-124	pCi/L	2	0	0	—	—	—	—	—
F	Antimony-125	pCi/L	4	0	0	—	—	—	—	—
UF	Antimony-125	pCi/L	2	0	0	—	—	—	—	—
UF	Barium-133	pCi/L	2	0	0	—	—	—	—	—
F	Barium-140	pCi/L	12	0	0	—	—	—	—	—
UF	Barium-140	pCi/L	6	0	0	—	—	—	—	—
UF	Beryllium-7	pCi/L	2	0	0	—	—	—	—	—
F	Bismuth-211	pCi/L	4	0	0	—	—	—	—	—
UF	Bismuth-211	pCi/L	10	0	0	—	—	—	—	—
F	Bismuth-212	pCi/L	12	1	8	54	54	54	—	—
UF	Bismuth-212	pCi/L	9	0	0	—	—	—	—	—
F	Bismuth-214	pCi/L	16	1	6	32	32	32	—	—
UF	Bismuth-214	pCi/L	17	6	35	10.9	27.8	43.8	—	—
F	Cadmium-109	pCi/L	12	0	0	—	—	—	—	—
UF	Cadmium-109	pCi/L	16	0	0	—	—	—	—	—
F	Cerium-139	pCi/L	12	0	0	—	—	—	—	—
UF	Cerium-139	pCi/L	16	0	0	—	—	—	—	—
UF	Cerium-141	pCi/L	2	0	0	—	—	—	—	—
F	Cerium-144	pCi/L	12	0	0	—	—	—	—	—

Table 3.1-6 (continued)

Field Preparation Code	Analyte	Unit	Number of Analyses	Number of Detects	Detection (%)	Min	Avg	Max	Screening Value (Reference ^a)	Number Greater than Screening Value
UF	Cerium-144	pCi/L	8	0	0	—	—	—	—	—
F	Cesium-134	pCi/L	17	0	0	—	—	—	—	—
UF	Cesium-134	pCi/L	17	0	0	—	—	—	—	—
F	Cesium-137	pCi/L	89	0	0	—	—	—	—	—
UF	Cesium-137	pCi/L	187	0	0	—	—	—	—	—
UF	Chromium-51	pCi/L	2	0	0	—	—	—	—	—
F	Cobalt-57	pCi/L	12	0	0	—	—	—	—	—
UF	Cobalt-57	pCi/L	8	0	0	—	—	—	—	—
F	Cobalt-60	pCi/L	89	0	0	—	—	—	—	—
UF	Cobalt-60	pCi/L	187	1	1	6.5	6.5	6.5	—	—
F	Europium-152	pCi/L	17	0	0	—	—	—	—	—
UF	Europium-152	pCi/L	16	0	0	—	—	—	—	—
F	Europium-154	pCi/L	4	0	0	—	—	—	—	—
UF	Europium-154	pCi/L	2	0	0	—	—	—	—	—
F	Europium-155	pCi/L	4	0	0	—	—	—	—	—
F	Gross alpha	pCi/L	48	4	8	1.53	2.99	3.92	—	—
UF	Gross alpha	pCi/L	198	19	10	1.02	7.57	62.8	—	—
UF	Gross alpha/beta	pCi/L	8	2	25	1.31	3.78	6.24	—	—
F	Gross beta	pCi/L	48	11	23	1.85	3.23	4.79	—	—
UF	Gross beta	pCi/L	207	72	35	1.15	27.5	1530	—	—
F	Gross gamma	pCi/L	73	0	0	—	—	—	—	—
UF	Gross gamma	pCi/L	83	16	19	58	150	190	—	—
F	Iodine-129	pCi/L	2	0	0	—	—	—	—	—
UF	Iodine-129	pCi/L	9	0	0	—	—	—	—	—
UF	Iodine-133	pCi/L	2	0	0	—	—	—	—	—
UF	Iron-59	pCi/L	2	0	0	—	—	—	—	—
F	Lanthanum-140	pCi/L	12	0	0	—	—	—	—	—

Table 3.1-6 (continued)

Field Preparation Code	Analyte	Unit	Number of Analyses	Number of Detects	Detection (%)	Min	Avg	Max	Screening Value (Reference ^a)	Number Greater than Screening Value
UF	Lanthanum-140	pCi/L	6	0	0	—	—	—	—	—
F	Lead-211	pCi/L	12	0	0	—	—	—	—	—
UF	Lead-211	pCi/L	8	0	0	—	—	—	—	—
F	Lead-212	pCi/L	16	0	0	—	—	—	—	—
UF	Lead-212	pCi/L	17	0	0	—	—	—	—	—
F	Lead-214	pCi/L	16	0	0	—	—	—	—	—
UF	Lead-214	pCi/L	17	3	18	11.7	27.8	46.4	—	—
F	Manganese-54	pCi/L	12	0	0	—	—	—	—	—
UF	Manganese-54	pCi/L	8	0	0	—	—	—	—	—
F	Mercury-203	pCi/L	12	0	0	—	—	—	—	—
UF	Mercury-203	pCi/L	16	0	0	—	—	—	—	—
F	Neptunium-237	pCi/L	84	1	1	20	20	20	—	—
UF	Neptunium-237	pCi/L	178	0	0	—	—	—	—	—
UF	Neptunium-239	pCi/L	2	0	0	—	—	—	—	—
UF	Niobium-95	pCi/L	2	0	0	—	—	—	—	—
F	Plutonium-238	pCi/L	90	0	0	—	—	—	—	—
UF	Plutonium-238	pCi/L	185	0	0	—	—	—	—	—
F	Plutonium-239/240	pCi/L	90	1	1	0.16	0.16	0.16	—	—
UF	Plutonium-239/240	pCi/L	185	1	1	0.06	0.06	0.06	—	—
F	Potassium-40	pCi/L	88	0	0	—	—	—	—	—
UF	Potassium-40	pCi/L	187	0	0	—	—	—	—	—
F	Protactinium-231	pCi/L	12	0	0	—	—	—	—	—
UF	Protactinium-231	pCi/L	8	0	0	—	—	—	—	—
F	Protactinium-233	pCi/L	16	0	0	—	—	—	—	—
UF	Protactinium-233	pCi/L	8	0	0	—	—	—	—	—
F	Protactinium-234m	pCi/L	12	1	8	860	860	860	—	—
UF	Protactinium-234m	pCi/L	9	0	0	—	—	—	—	—

Table 3.1-6 (continued)

Field Preparation Code	Analyte	Unit	Number of Analyses	Number of Detects	Detection (%)	Min	Avg	Max	Screening Value (Reference ^a)	Number Greater than Screening Value
F	Radium-223	pCi/L	12	0	0	—	—	—	—	—
UF	Radium-223	pCi/L	16	0	0	—	—	—	—	—
UF	Radium-224	pCi/L	5	0	0	—	—	—	—	—
F	Radium-226	pCi/L	16	2	13	0.3	0.79	1.28	5 (1)	0
UF	Radium-226	pCi/L	46	13	28	0.37	6.99	43.8	5 (1)	4
F	Radium-228	pCi/L	4	2	50	0.66	0.72	0.78	5 (1)	0
UF	Radium-228	pCi/L	31	6	19	0.57	3.44	14.5	5 (1)	1
F	Radon-219	pCi/L	12	0	0	—	—	—	—	—
UF	Radon-219	pCi/L	8	0	0	—	—	—	—	—
UF	Rhodium-106	pCi/L	2	0	0	—	—	—	—	—
UF	Ruthenium-103	pCi/L	2	0	0	—	—	—	—	—
F	Ruthenium-106	pCi/L	17	0	0	—	—	—	—	—
UF	Ruthenium-106	pCi/L	16	0	0	—	—	—	—	—
F	Selenium-75	pCi/L	12	0	0	—	—	—	—	—
UF	Selenium-75	pCi/L	8	0	0	—	—	—	—	—
F	Sodium-22	pCi/L	85	0	0	—	—	—	—	—
UF	Sodium-22	pCi/L	187	0	0	—	—	—	—	—
F	Strontium-85	pCi/L	12	1	8	3.6	3.6	3.6	—	—
UF	Strontium-85	pCi/L	16	2	13	3.4	4.6	5.8	—	—
F	Strontium-90	pCi/L	90	1	1	0.38	0.38	0.38	—	—
UF	Strontium-90	pCi/L	185	0	0	—	—	—	—	—
F	Technetium-99	pCi/L	2	0	0	—	—	—	—	—
UF	Technetium-99	pCi/L	10	0	0	—	—	—	—	—
F	Thallium-208	pCi/L	16	0	0	—	—	—	—	—
UF	Thallium-208	pCi/L	17	0	0	—	—	—	—	—
F	Thorium-227	pCi/L	16	0	0	—	—	—	—	—
UF	Thorium-227	pCi/L	16	0	0	—	—	—	—	—

Table 3.1-6 (continued)

Field Preparation Code	Analyte	Unit	Number of Analyses	Number of Detects	Detection (%)	Min	Avg	Max	Screening Value (Reference ^a)	Number Greater than Screening Value
UF	Thorium-228	pCi/L	4	0	0	—	—	—	—	—
UF	Thorium-230	pCi/L	4	0	0	—	—	—	—	—
UF	Thorium-231	pCi/L	4	0	0	—	—	—	—	—
UF	Thorium-232	pCi/L	4	0	0	—	—	—	—	—
F	Thorium-234	pCi/L	16	1	6	310	310	310	—	—
UF	Thorium-234	pCi/L	17	1	6	169	169	169	—	—
F	Tin-113	pCi/L	12	0	0	—	—	—	—	—
UF	Tin-113	pCi/L	16	0	0	—	—	—	—	—
UF	Tritium	pCi/L	328	130	40	-0.13	19.8	140	—	—
F	Uranium-234	pCi/L	109	103	95	0.02	0.38	2.13	—	—
UF	Uranium-234	pCi/L	203	198	98	0.13	0.37	2.47	—	—
F	Uranium-235	pCi/L	16	1	6	58	58	58	—	—
UF	Uranium-235	pCi/L	17	0	0	—	—	—	—	—
F	Uranium-235/236	pCi/L	109	8	7	0.02	0.06	0.16	—	—
UF	Uranium-235/236	pCi/L	203	9	4	0.03	0.07	0.15	—	—
F	Uranium-238	pCi/L	109	100	92	0.07	0.21	1.43	—	—
UF	Uranium-238	pCi/L	205	200	98	0.03	0.21	1.51	—	—
F	Yttrium-88	pCi/L	12	0	0	—	—	—	—	—
UF	Yttrium-88	pCi/L	16	1	6	6.4	6.4	6.4	—	—
F	Zinc-65	pCi/L	12	0	0	—	—	—	—	—
UF	Zinc-65	pCi/L	8	0	0	—	—	—	—	—
UF	Zirconium-95	pCi/L	2	0	0	—	—	—	—	—

^a Screening value reference:

(1) = EPA Maximum Concentration Limit

^b F = Filtered.^c — = Not applicable.^d UF = Unfiltered.

**Table 3.2-1
Vertical Head Gradients in Multiscreen Wells**

Well Location	Screens	Screen Center Separation (ft)	May 2010 Gradient (ft/ft)	February 2014 Gradient (ft/ft)	February 2019 Gradient (ft/ft)	Average Gradient (ft/ft)	Overall Gradient in Well (ft/ft)
CdV-R-15-3	4 to 5	95	0.003	not measured	not measured	0.003	-0.095
CdV-R-15-3	5 to 6	290	-0.127	not measured	not measured	-0.13	
CdV-R-37-2	2 to 3	164	-0.005	not measured	not measured	-0.005	-0.004
CdV-R-37-2	3 to 4	187	-0.004	not measured	not measured	-0.004	
R-17	1 to 2	60	-0.026	-0.048	not measured	-0.037	-0.037
R-19	3 to 4	220	-0.034	-0.036	-0.035	-0.035	-0.033
R-19	4 to 5	172	-0.018	-0.016	-0.015	-0.016	
R-19	5 to 6	144	-0.055	-0.046	-0.047	-0.049	
R-19	6 to 7	106	-0.030	-0.031	-0.034	-0.032	
R-25	5 to 6	110	-0.24	-0.25	-0.24	-0.24	-0.18
R-25	6 to 7	200	-0.21	-0.21	-0.21	-0.21	
R-25	7 to 8	190	-0.11	-0.12	-0.12	-0.12	
R-69	1 to 2	66	not measured	not measured	-0.18	-0.18	-0.18

Appendix A

*Acronyms and Abbreviations,
Metric Conversion Table, and Data Qualifier Definitions*

A-1.0 ACRONYMS AND ABBREVIATIONS

3-D	three-dimensional
amsl	above mean sea level
AOC	area of concern
bgs	below ground surface
BHC	benzene hexachloride
BSS	blind source separation
CAS	Chemical Abstracts Service
cfs	cubic feet per second
CFU	colony-forming units
CME	corrective measures evaluation
CMI	corrective measures implementation
CMS	corrective measures study
COPC	chemical of potential concern
CSM	conceptual site model
D[2,4]	2,4-dichlorophenoxyacetic acid
DB[2,4-]	4-(2,4-dichlorophenoxy)butanoic acid
DC	direct current
DDD[4,4'-]	4,4'-dichlorodiphenyldichloroethane
DDE[4,4'-]	4,4'-dichlorodiphenyldichloroethylene
DDT[4,4']	4,4'-dichlorodiphenyltrichloroethane
DGIR	deep groundwater investigation report
DOE	Department of Energy (U.S.)
DNX	hexahydro-1,3-dinitro-5-nitro-1,3,5-triazine
EPA	Environmental Protection Agency (U.S.)
F	filtered
FMI	Formation Microimager
GGRL	Geochemistry and Geomaterials Research Laboratory
gpd	gallons per day
gpm	gallons per minute
HE	high explosives
HGI	HydroGeophysics, Inc.
HMX	Her Majesty's Explosive
IFGMP	Interim Facility-Wide Groundwater Monitoring Plan
IM	interim measure
IP	induced polarization
K _d	partition distribution
LANL	Los Alamos National Laboratory

LPZ	lower perched-intermediate zone
Ma	million years ago
MCPA	methyl-4-chlorophenoxyacetic(2-) acid
MCP	methyl-4-chlorophenoxypropionic(2-) acid
MBR	mountain-block recharge
MCS	media cleanup standard
MDA	material disposal area
meq	milliequivalent
MFR	mountain-front recharge
MTBE	methyl tert butyl ether
N3B	Newport News Nuclear BWXT-Los Alamos, LLC
NDS	disulfonate
NMAC	New Mexico Administrative Code
NMED	New Mexico Environment Department
NMWQCC	New Mexico Water Quality Control Commission
NTS	trisulfonate
MNX	hexahydro 1 nitroso-3,5-dinitro-1,3,5-triazine
NOD	notice of disapproval (NMED)
NPDES	National Pollutant Discharge Elimination System (CWA)
OUT	operational taxonomic unit
PAH	polycyclic aromatic hydrocarbon
PETN	pentaerythritol tetranitrate
PRB	permeable reactive barrier
PZ	piezometer
QIIME	Quantitative Insights Into Microbial Ecology
RCRA	Resource Conservation and Recovery Act
RDX	Royal Demolition Explosive
RFA	RCRA facility assessment
RFI	RCRA facility investigation
RME	reasonable maximum exposure
rRNA	ribosomal ribonucleic acid
S	screen
SVOC	semivolatile organic compound
SWA	Solid Waste Act (New Mexico)

SWMU	solid waste management unit
SWSC	Sanitation Wastewater Systems Consolidation (Spring)
TA	technical area
TATB	triaminotrinitrobenzene
TNT	trinitrotoluene(2,4,6-) (dynamite)
TNX	2,4,6-trinitroxylyene
TP[2,4,5]	2(2,4,5-trichlorophenoxy) propionic acid
UF	unfiltered
UPZ	upper perched-intermediate zone
VCA	voluntary corrective action
VOC	volatile organic compound
wt%	weight percent

A-2.0 METRIC CONVERSION TABLE

Multiply SI (Metric) Unit	by	To Obtain U.S. Customary Unit
kilometers (km)	0.622	miles (mi)
kilometers (km)	3281	feet (ft)
meters (m)	3.281	feet (ft)
meters (m)	39.37	inches (in.)
centimeters (cm)	0.03281	feet (ft)
centimeters (cm)	0.394	inches (in.)
millimeters (mm)	0.0394	inches (in.)
micrometers or microns (μm)	0.0000394	inches (in.)
square kilometers (km^2)	0.3861	square miles (mi^2)
hectares (ha)	2.5	acres
square meters (m^2)	10.764	square feet (ft^2)
cubic meters (m^3)	35.31	cubic feet (ft^3)
kilograms (kg)	2.2046	pounds (lb)
grams (g)	0.0353	ounces (oz)
grams per cubic centimeter (g/cm^3)	62.422	pounds per cubic foot (lb/ft^3)
milligrams per kilogram (mg/kg)	1	parts per million (ppm)
micrograms per gram ($\mu\text{g/g}$)	1	parts per million (ppm)
liters (L)	0.26	gallons (gal.)
milligrams per liter (mg/L)	1	parts per million (ppm)
degrees Celsius ($^{\circ}\text{C}$)	$9/5 + 32$	degrees Fahrenheit ($^{\circ}\text{F}$)

A-3.0 DATA QUALIFIER DEFINITIONS

Data Qualifier	Definition
U	The analyte was analyzed for but not detected.
J	The analyte was positively identified, and the associated numerical value is estimated to be more uncertain than would normally be expected for that analysis.
J+	The analyte was positively identified, and the result is likely to be biased high.
J-	The analyte was positively identified, and the result is likely to be biased low.
UJ	The analyte was not positively identified in the sample, and the associated value is an estimate of the sample-specific detection or quantitation limit.
R	The data are rejected as a result of major problems with quality assurance/quality control parameters.

Appendix B

Well Completion Diagrams

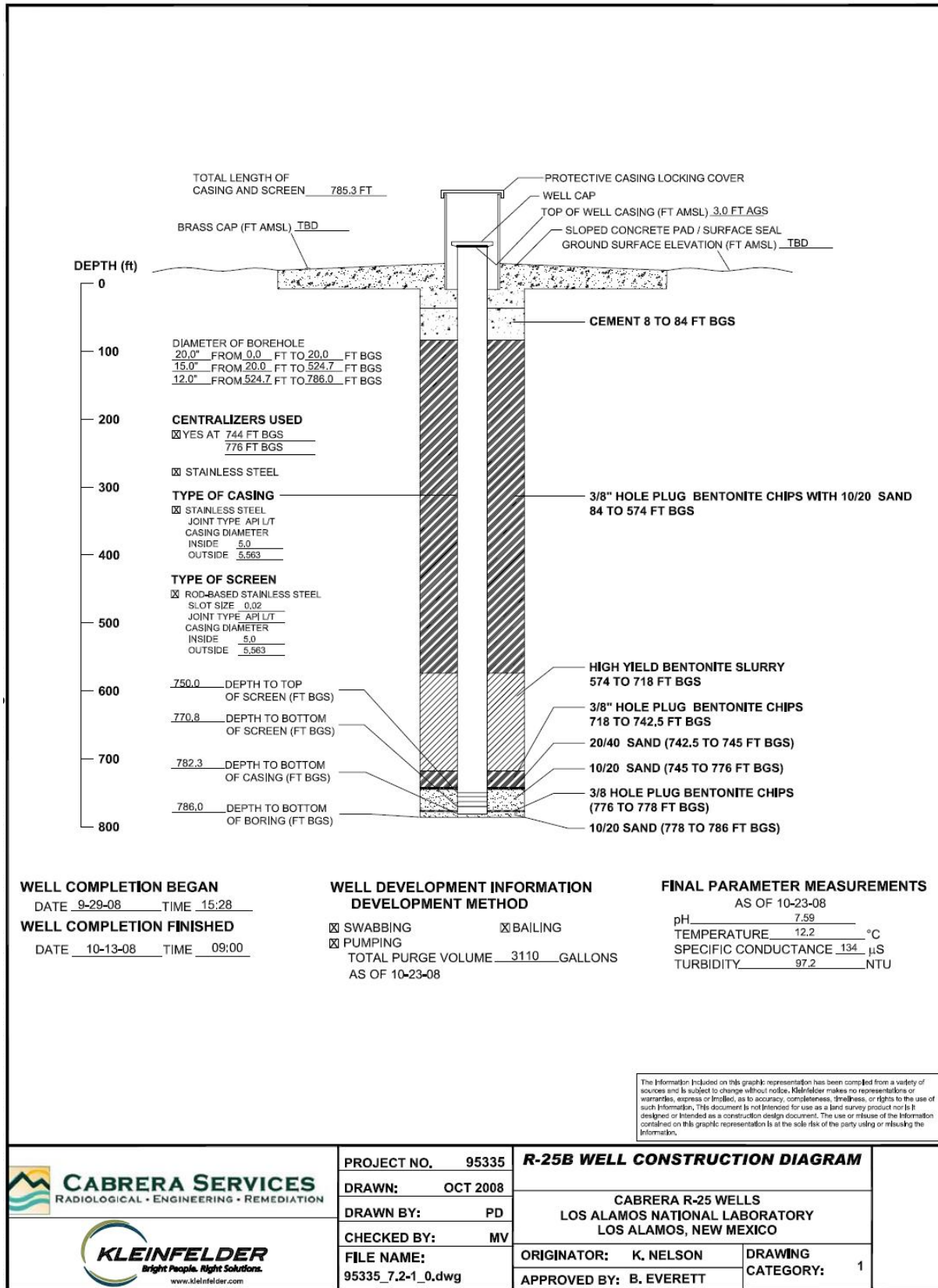


Figure B-1 R-25b well construction diagram

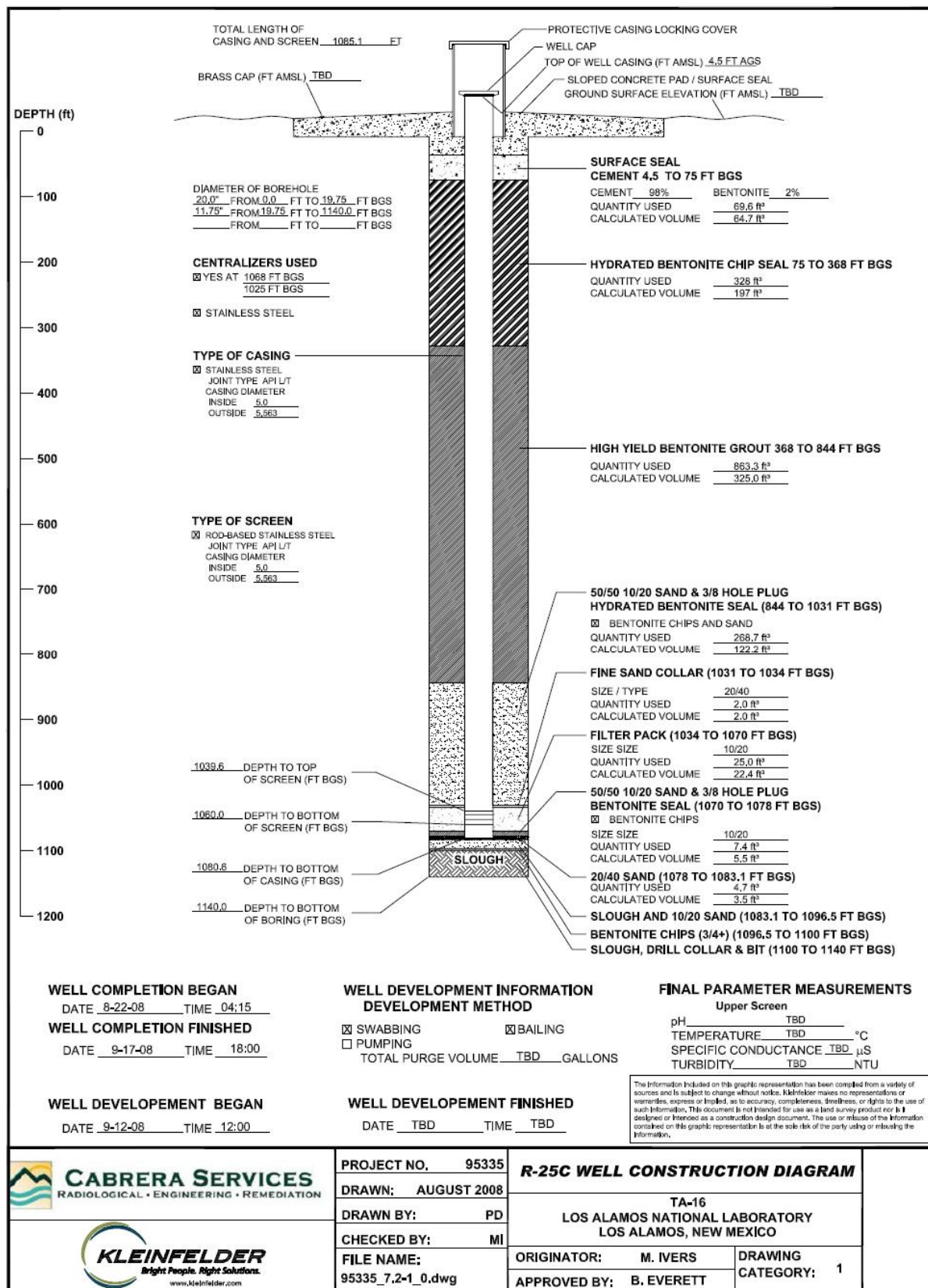


Figure B-2 R-25c well construction diagram

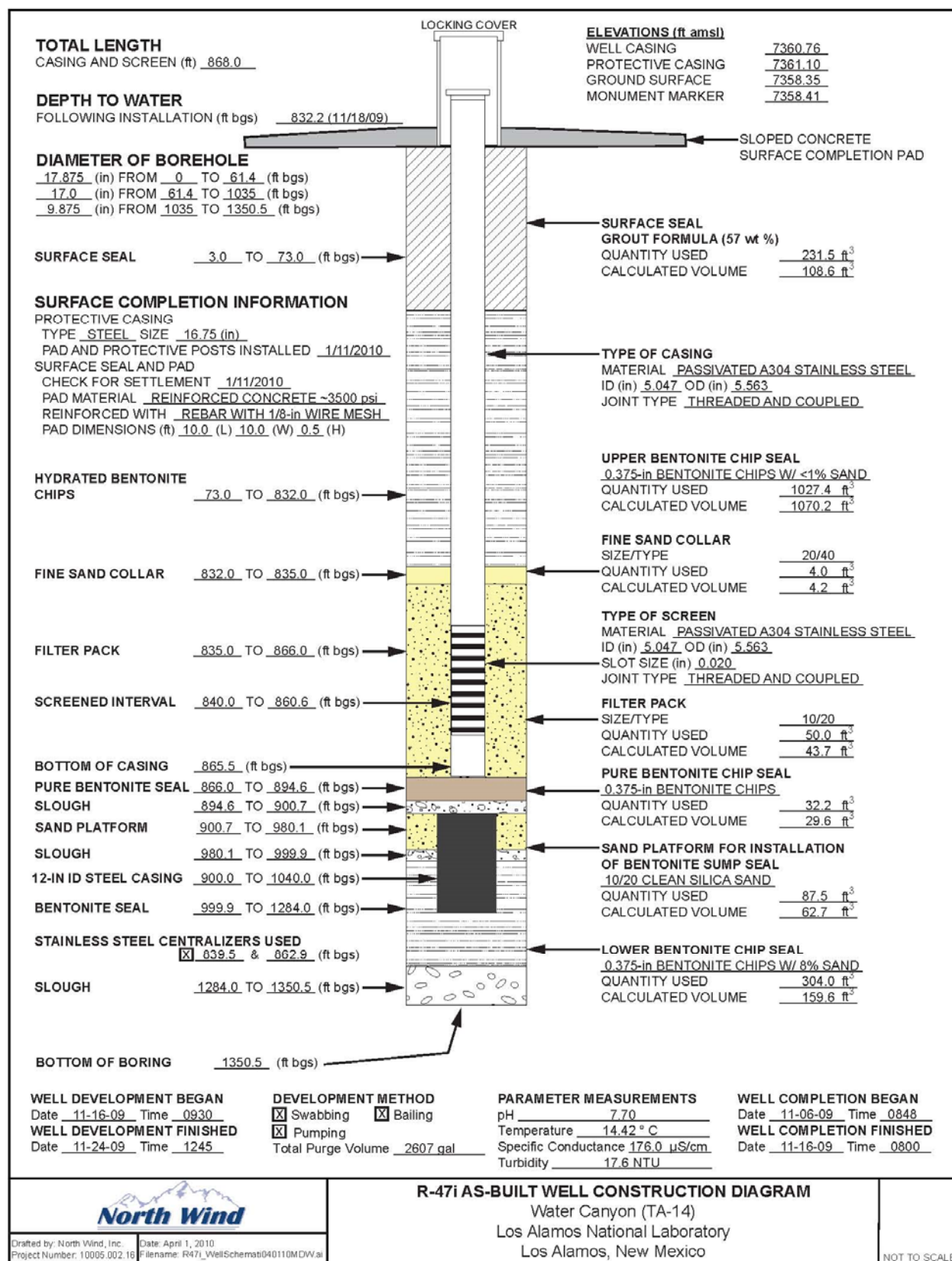


Figure B-3 R-47i as-built well construction diagram

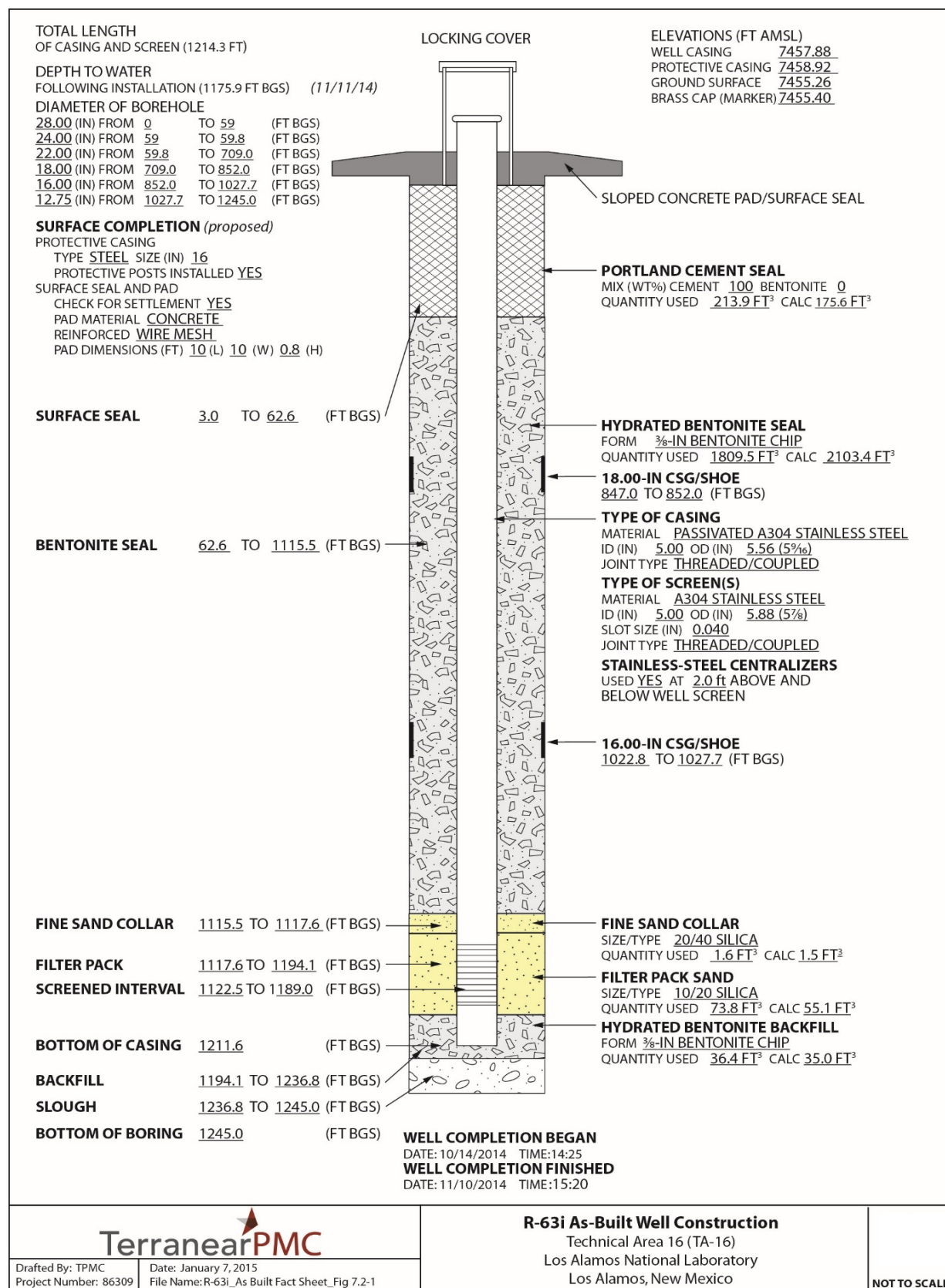


Figure B-4 R-63i as-built well construction diagram



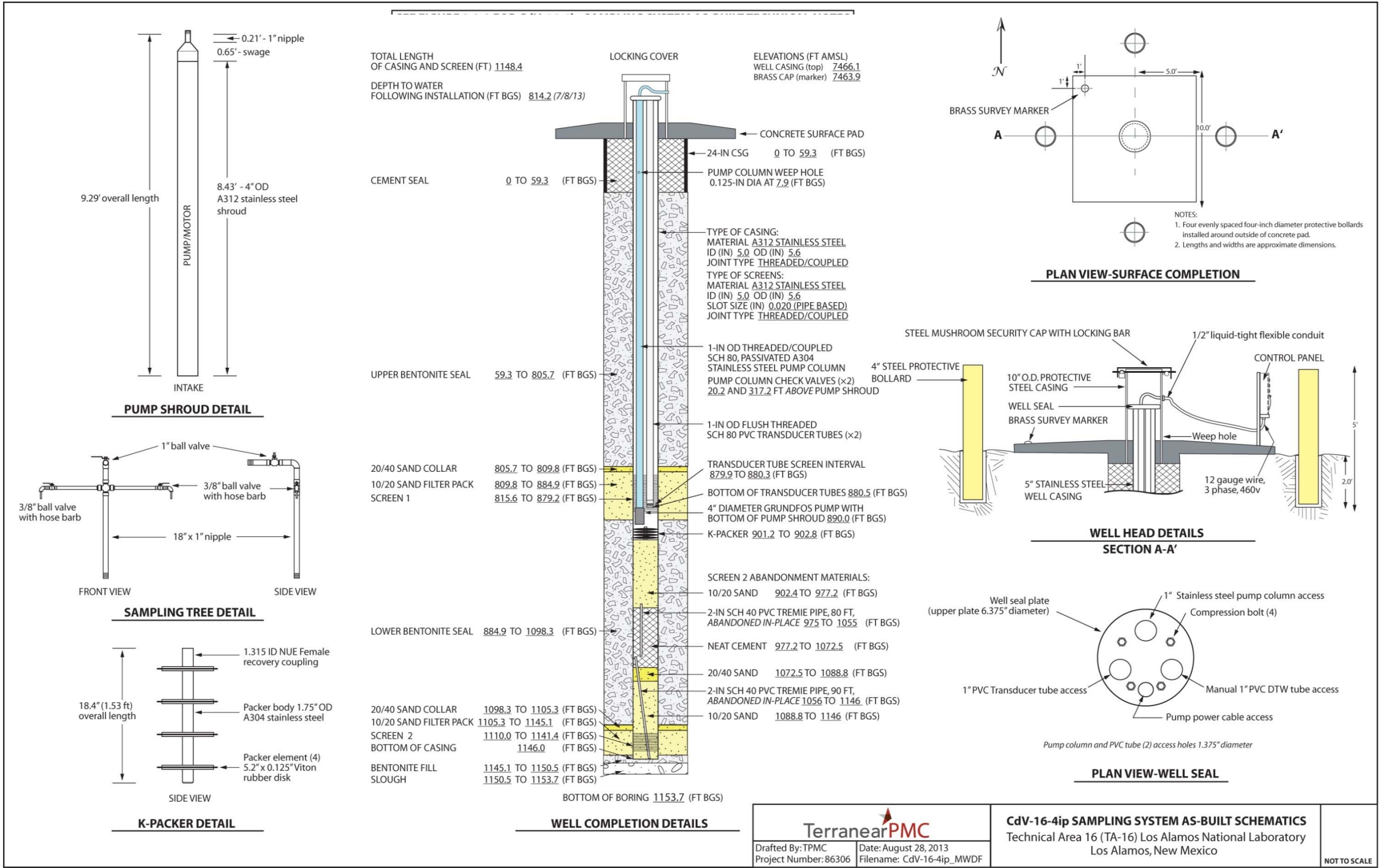


Figure B-6 CdV-16-4ip as-built well construction diagram

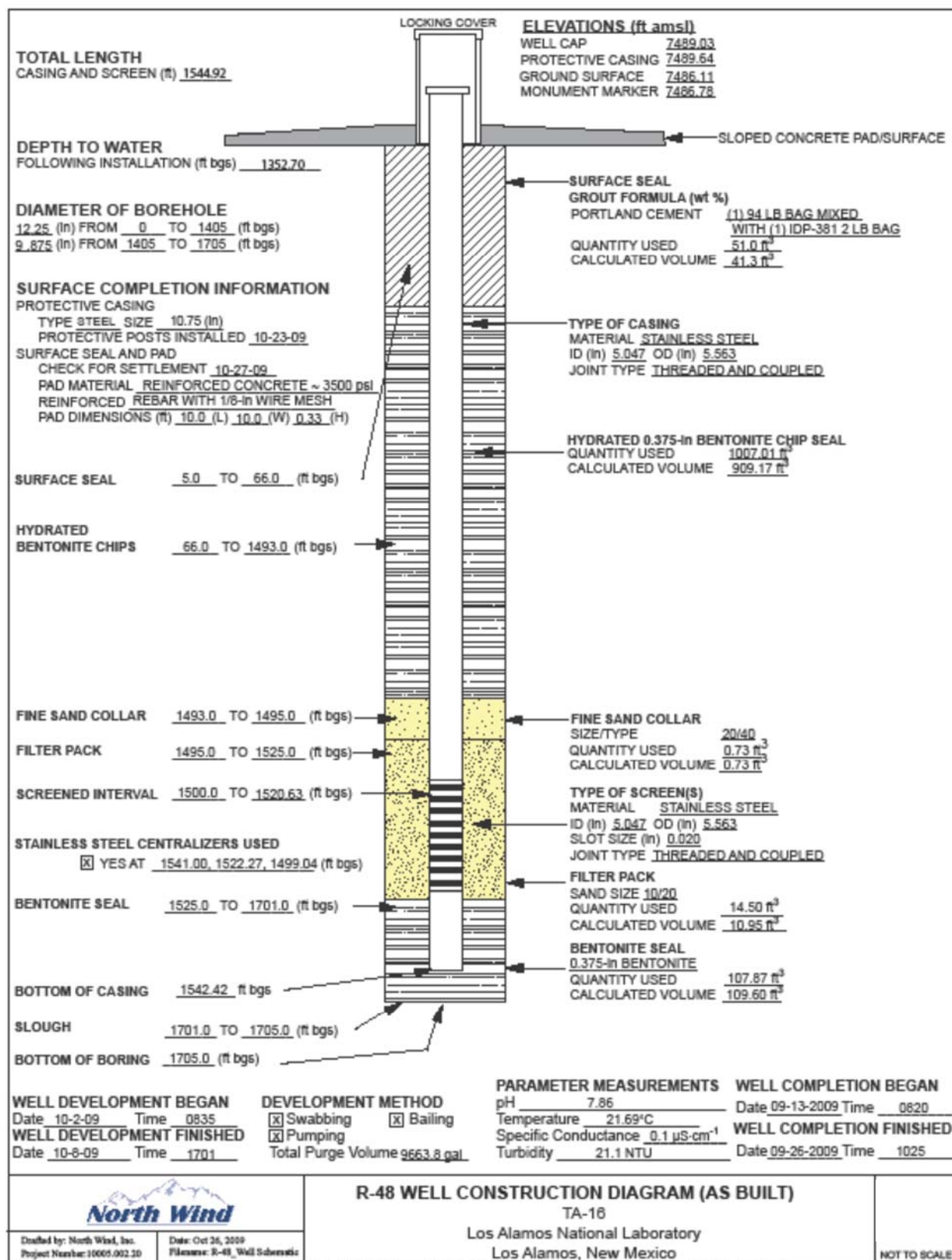


Figure B-7 R-48 as-built well construction diagram

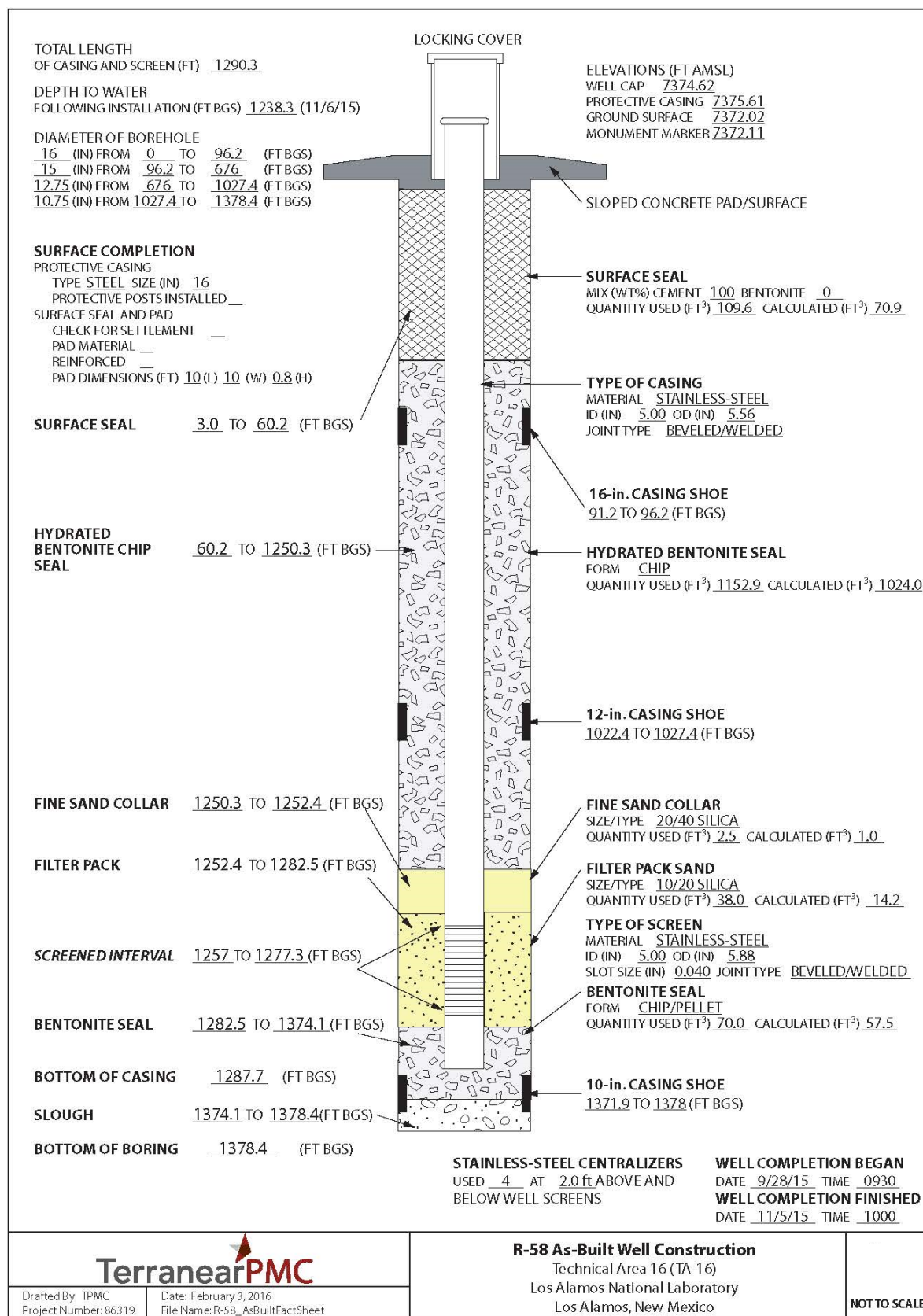


Figure B-8 R-58 as-built well construction diagram

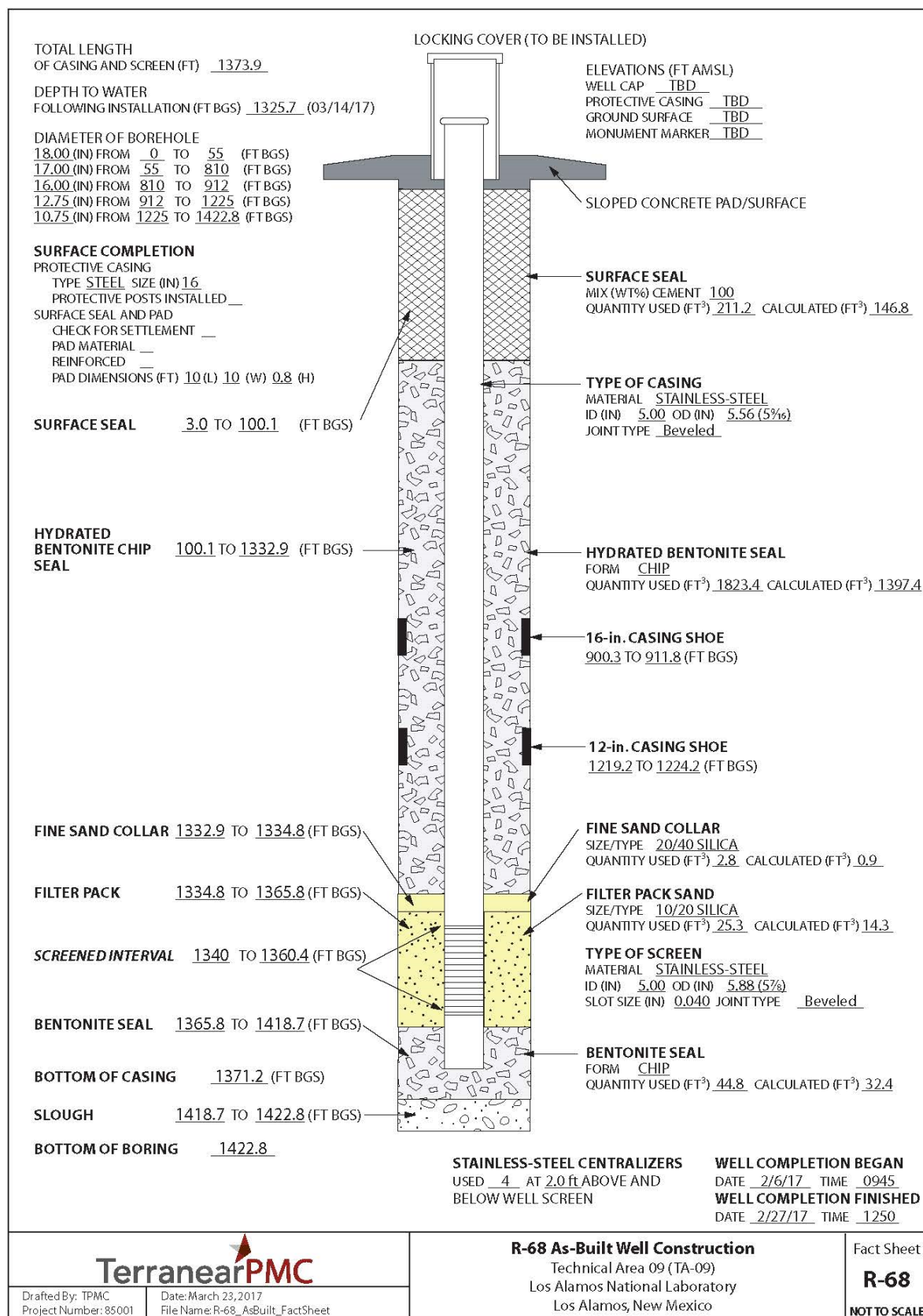


Figure B-9 R-68 as-built well construction diagram

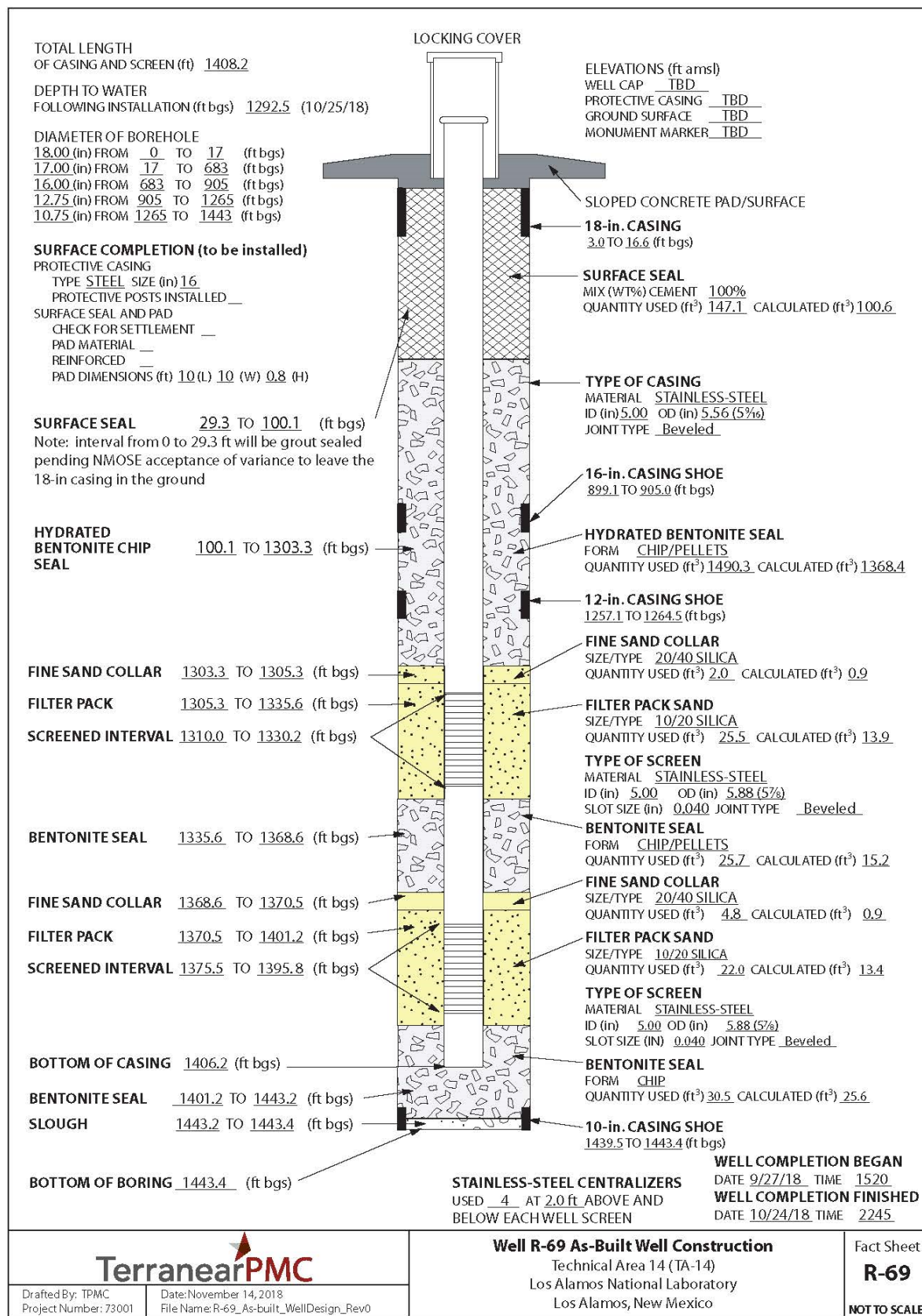


Figure B-10 R-69 as-built well construction diagram

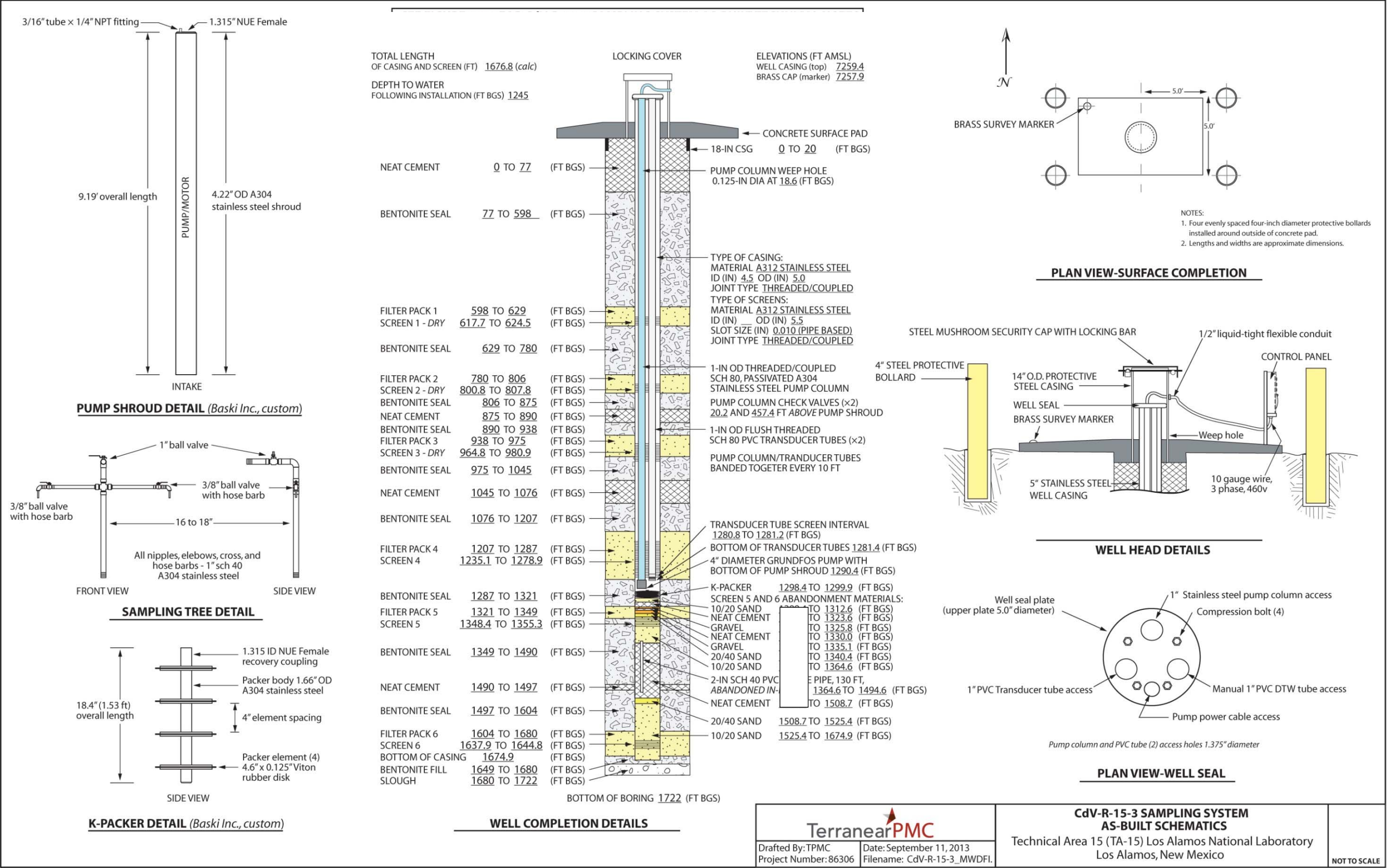


Figure B-11 As-built schematics of monitoring well CdV-R--3 sampling system

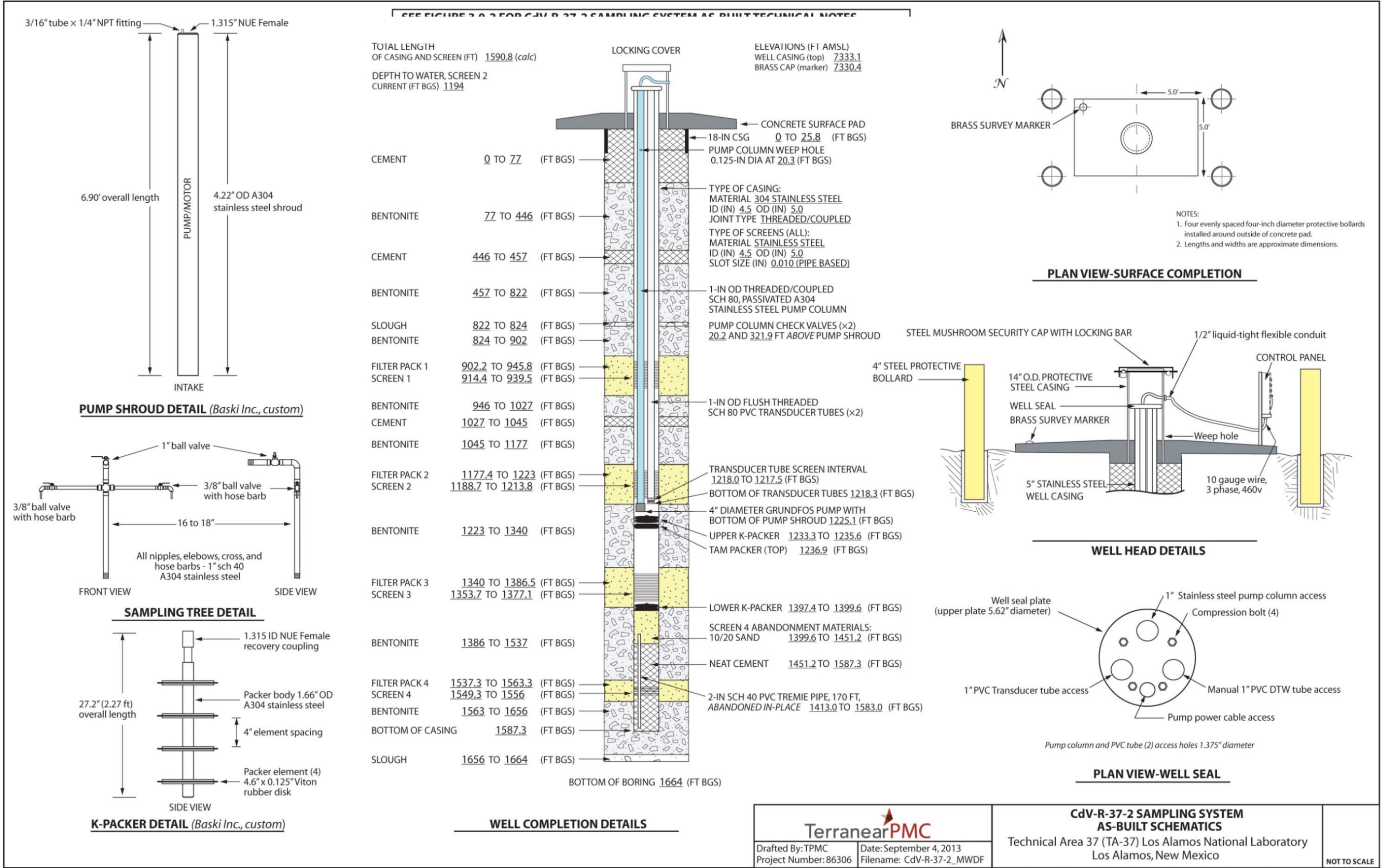


Figure B-12 As-built schematics of monitoring well CdV-R-37-2 sampling system

Appendix C

Tracer Data
(on CD included with this document)

Appendix D

*Groundwater Analytical Results from 2000 to 2019
(on CD included with this document)*


Appendix E

2019 Update of RDX Inventory in the Regional Aquifer



2019 Update of RDX Inventory in the Regional Aquifer

July 23, 2019



Prepared by
NEPTUNE AND COMPANY, INC.
1505 15th St, Suite B, Los Alamos, NM 87544

TABLE OF CONTENTS

1.0	Introduction	1
2.0	Methods	1
2.1	3D Contour Development.....	1
2.2	Porosity Distribution Development	2
2.3	Mathematical Model	2
3.0	Results and Discussion.....	3
3.1	Comparison with Previous Results.....	3
3.2	Uncertainty Analysis.....	4
4.0	References	4

FIGURES

Figure 1.	Contours interpreted based on RDX data available through May 2019.	5
Figure 2.	3D contours extruded from the 2D plan view and cross-sectional hand-drawn contours shown in Figure 1. Vertical exaggeration is 2x.....	6
Figure 3.	A histogram of RDX inventory results from an MC simulation incorporating uncertainty in porosity. The red line is the normal probability distribution fit to the MC results using maximum likelihood methods.	7

TABLES

Table 1.	Plume volume and inventory estimates compared to 2017 results.....	7
----------	--	---

1.0 Introduction

The purpose of this appendix is to describe the estimation of RDX mass within the regional aquifer at Los Alamos National Laboratory (LANL) at the present time (2019).

The following updated inventory analysis uses the latest RDX monitoring well data, subject matter expert (SME)-derived contours of RDX mass at the regional aquifer water table that conform to the current site conceptual model, and a distribution for porosity developed for the Puye Formation. Inventory is calculated using a three-dimensional (3D) model of the plume. The average porosity over the plume is assumed to be 27% based on analysis of Puye data. The bulk volume within the 10-ppb contour is calculated to be 4.77 billion liters based on the 3D plume model. The 2019 RDX inventory estimate within the 10-ppb contour is 15.3 kg, and the total estimate is 18.4 kg.

Prior estimates of RDX mass in the different zones of the hydrogeologic system were completed in previous years. The differences among all methods are summarized in Section 3.1. Uncertainty is discussed in Section 3.2.

2.0 Methods

SMEs used monitoring well data analyzed for RDX (as of May 2019) in conjunction with the conceptual site model to produce contours in both a two-dimensional (2D) plan view and a 2D cross section. The provided contours are shown in Figure 1. The mass of RDX greater than 10 ppb, based on the New Mexico tap water drinking standard of 9.66 ppb (NMED 2019), is estimated from a 3D volume extrusion of the 2D SME contours depicted in Figure 1, as described in the following sections.

2.1 3D Contour Development

The plan view and cross sectional 2D contours were digitized with a projected coordinate system of NAD83 New Mexico Central (EPSG 2826). The transect shown on the 2D contour image ("Transect A") was also digitized, using points labeled along the transect as coordinate locations (A, CdV-9-1(i), R-68, R-69, R-18, and A'). Each contour was saved as a separate set of coordinate points.

Based on these provided contours, the extrusion from 2D to the 3D model is performed as follows. The 2D digitized contours are converted from points to polygons. Based on the SME contours in Figure 1, a minimum and a maximum elevation is set to 1815 m (5950 ft) and 1905 m (6250 ft), respectively. The resolution of the 3D plume is set to 5 m in the northing and easting directions, and a resolution of 5 m with depth, generating a 5 × 5 × 5-m grid cell.

A set of elevation values is generated between the minimum and maximum elevations, at 5 m increments, and a 2D slice of the plume is developed on the northing and easting plane at each elevation in the set. At each elevation, the start and end points of each concentration contour along Transect A are recorded based upon the depth contours in Figure 1. The start and end points of each contour are then converted to EPSG 2826 northing and easting coordinates located on Transect A. Each concentration contour line is defined by lines drawn perpendicular to Transect A in the northing-easting plane at those two points. The result is a 2D depiction of the plume on the northing and easting plane at each elevation. This method assumes that the

depth contours along Transect A apply uniformly to all other longitudinal cross-sections parallel to Transect A within the plume domain.

The resulting collection of contour lines defined at each elevation is then rasterized to define the plume in 3D. Figure 2 shows the 3D plume model developed using this method.

2.2 Porosity Distribution Development

Total porosity, ϕ , defines the volume fraction of a cell that is not occupied by rock material. It is used to calculate total RDX mass if concentrations in the fluid are measured. Porosity is spatially variable and can be highly uncertain in deep aquifer materials.

The porosity distribution utilized in this inventory analysis characterizes the mean porosity over the spatial and temporal domain of the RDX plume. A single value is drawn from the distribution and applied to all grid cells within the plume. Under simplifying assumptions of linearity, additivity, and stationarity, the application of a mean porosity over the plume domain yields the same inventory estimate as would result if a heterogeneous porosity model is applied to explicitly capture small scale differences in porosity from one grid cell to the next.

Data from borehole logs obtained during the drilling of wells in the LANL area are filtered and analyzed to develop a probability distribution for mean porosity of the Puye Formation. The process takes into account the quality and information content of each porosity estimate and relies on sampling theory to quantify uncertainty in the mean value. The distribution of porosity carried forward to this inventory analysis is a normal distribution with a mean of 0.27 and a standard deviation 0.06. The 5th and 95th percentiles of this distribution are 0.17 and 0.37, respectively, providing a range for comparison to porosity values used in prior estimates. As more porosity data and information are collected over time, the distribution could be updated in the future. Results shown here represent a snapshot of the porosity distribution at the present time and are subject to change. Preliminary probabilistic results incorporating uncertainty in porosity are presented in Section 3.2. The mean of the porosity distribution, 0.27, is used to calculate the deterministic 2019 inventory estimate.

2.3 Mathematical Model

A raster math approach is used to calculate inventory based on the 3D plume model developed in Section 2.1. Concentrations are estimated at each grid cell on a $5 \times 5 \times 5$ -m regular grid. For each cell, concentrations are multiplied by porosity and total cell volume. The resulting masses within each cell are summed to estimate total inventory in kilograms:

$$M_{RDX} = \phi \sum_{i=1}^n C_i V_i \quad (1)$$

where

- C_i is the RDX concentration [kg L^{-1}] of cell i ,
- V_i is the total volume [L] of cell i ,
- n is the total number of $5 \times 5 \times 5$ -m grid cells within the plume (643,093), and
- ϕ is the mean porosity [-].

One porosity value is applied at all grid cells within the plume domain, relying on spatial scaling theory (Black et al. 2019) to simplify calculations yet provide an accurate inventory estimate (Section 2.2).

3.0 Results and Discussion

The 2019 RDX inventory estimate calculated using this raster math approach on the 3D plume model is 15.3 kg within the 10-ppb contour and 18.4 kg for the whole plume. The bulk volume within the 10-ppb contour is calculated to be 4.77 billion liters based on the 3D plume model.

3.1 Comparison with Previous Results

Prior estimates of RDX mass in the different zones of the hydrogeologic system were completed in 2005 and 2017, as well as a “geostatistically based” approach in 2016. These studies are summarized in Tables 3.0-1 and 5.0-1 of Attachment 1 of LANL (2018). For the regional aquifer, the 2005 estimate was 135 to 6053 kg and the 2017 estimate was 35 to 415 kg. Updated methodology and a smaller contour-based plume depiction primarily explain the decrease in the 2019 inventory estimate compared to 2005 and 2017 results. The plume volume within the 10-ppb contour, 4.77 billion liters, is substantially less than the 74.1 billion liters considered in 2017. The 2017 volume was based on a triangle extending outward from the TA-260 building, as shown in Figure 3.6-5 of Attachment 1 of LANL (2018), which encompassed a much larger area to the south and east compared to the current depiction (Figure 1).

In 2017, the minimum regional zone inventory estimate (35 kg) was calculated based on the median concentration of all detected samples (2.58 ppb) and a minimum pore volume of 13.7 billion liters (B. Newman, personal communication, 2019). The maximum inventory estimate (415 kg) was based on the assumption that the highest detected concentration from regional groundwater sampling (17.1 ppb) applied to the entire plume, with a maximum pore volume of 24.3 billion liters. The porosity of the Puye Formation was assumed to range from 18 to 33% (Table 1), with a bulk volume of 74.1 billion L.

In 2005, “a large, somewhat arbitrary contaminated volume was assumed below the regional water table” (LANL 2018). The depth assumed in the 2005 calculations was based on the early data at R-25, which suggested a deeper plume with high RDX concentrations. The R-25 concentrations have since been adjusted downward based on long-term trends at that location. The 2017 estimate was thus lower than that of 2005 due to lower RDX concentrations from groundwater sampling at R-25, a “far shallower” depth of contamination within the regional aquifer, and incorporation of other more recent monitoring well data.

The 2016 “geostatistically based” estimate uses a similar SME contour-based method as described here, but two contour scenarios were explored and a sensitivity analysis was performed consisting of 48 iterations with differing interpolation parameters, grid resolution, vertical distribution, and boundary conditions (LANL 2018). The range of RDX in the regional aquifer estimated with this approach was 1.8 to 8.5 kg. The primary limitation of this study was that at the time it was originally published (2016), R-68 and R-69 data were not yet available, so concentrations in the plume were assumed to be smaller and the resulting inventory results for the regional aquifer are smaller than presently estimated.

Current estimates of the plume area at the water table, total volume, porosity, and inventory are compared to the 2017 estimates in Table 1.

3.2 Uncertainty Analysis

Concentration gradients (i.e., the SME contour placement and plume shape) and porosity are primary sources of uncertainty in RDX inventory under the current model. The 2019 inventory estimate is provided as a single estimate without uncertainty because uncertainty in plume shape and contour placements have yet to be quantified. RDX inventory is expected to be most sensitive to contour placement, as illustrated by the larger volumes and inventories from 2017 and 2005. Uncertainty will not be presented until this source of uncertainty is quantified, but preliminary results are provided in this section to quantify uncertainty as it relates solely to porosity.

The impact of porosity uncertainty on RDX inventory is analyzed using a Monte Carlo (MC) simulation based on the porosity distribution. A normal distribution with a mean of 0.27 and a standard deviation of 0.06 is used to characterize uncertainty in mean porosity over the plume area (Section 2.2). The inventory calculations are performed with 1,000 random draws from the porosity distribution, and inventory varies from 5.04 to 24.9 kg within the 10-ppb contour. A probability distribution is fit to the results using maximum likelihood methods, and the MC results are displayed alongside the fitted probability distribution (Figure 3).

4.0 References

- Black, P., et al., 2019. Scaling Input Distributions for Probabilistic Models - 19472, proceedings of the *Waste Management Symposia 2019, March 3-7*, Phoenix AZ, 2019
- LANL, 2018. *Compendium of Technical Reports Related to the Deep Groundwater Investigation for the RDX Project at Los Alamos National Laboratory*, LA-UR-18-21326, EP2018-0006, Los Alamos National Laboratory, Los Alamos NM, March 2018
- NMED, 2019. *Risk Assessment Guidance for Site Investigations and Remediation, Volume I, Soil Screening Guidance for Human Health Risk Assessments, Revision 2*, New Mexico Environment Department, Santa Fe NM, June 2019

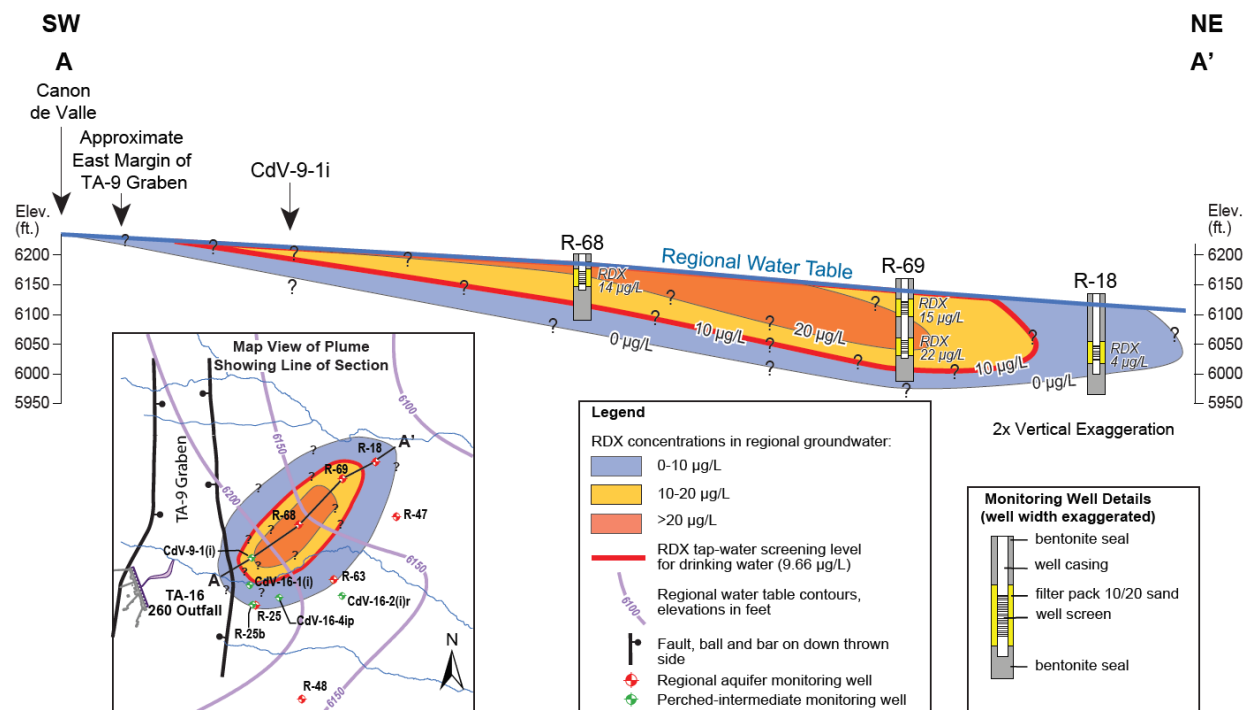


Figure 1. Contours interpreted based on RDX data available through May 2019.

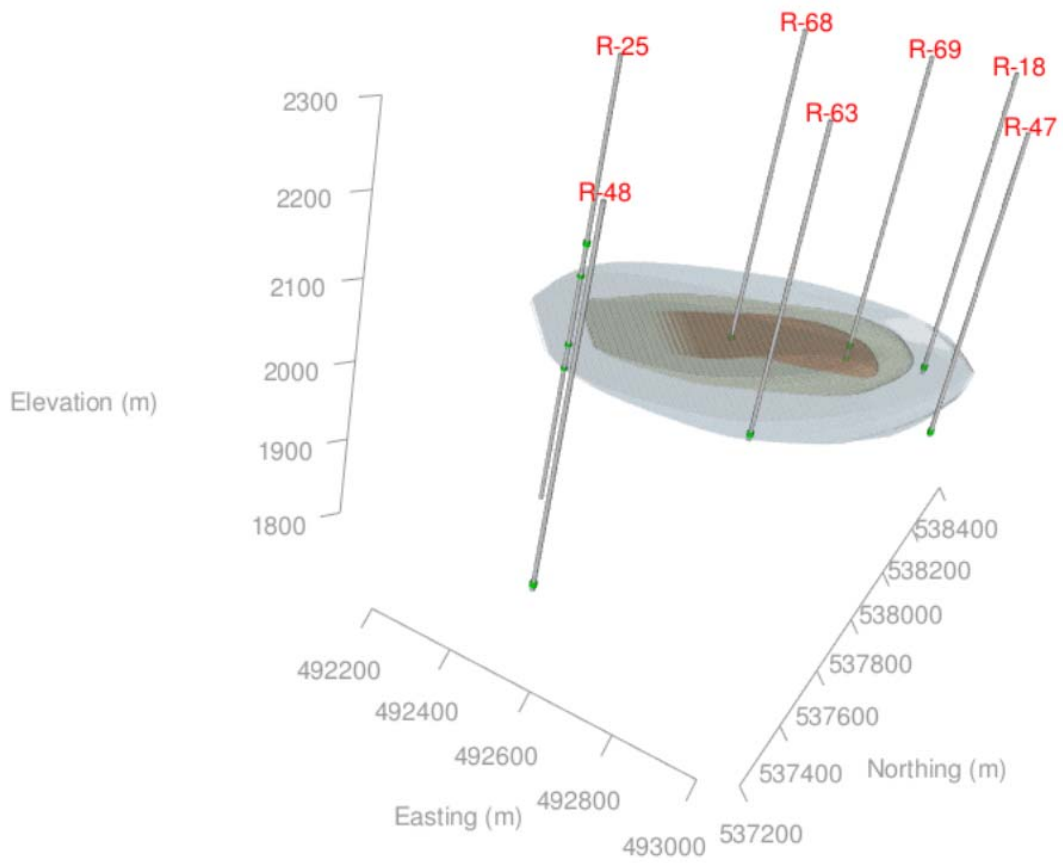


Figure 2. 3D contours extruded from the 2D plan view and cross-sectional hand-drawn contours shown in Figure 1. Vertical exaggeration is 2x.

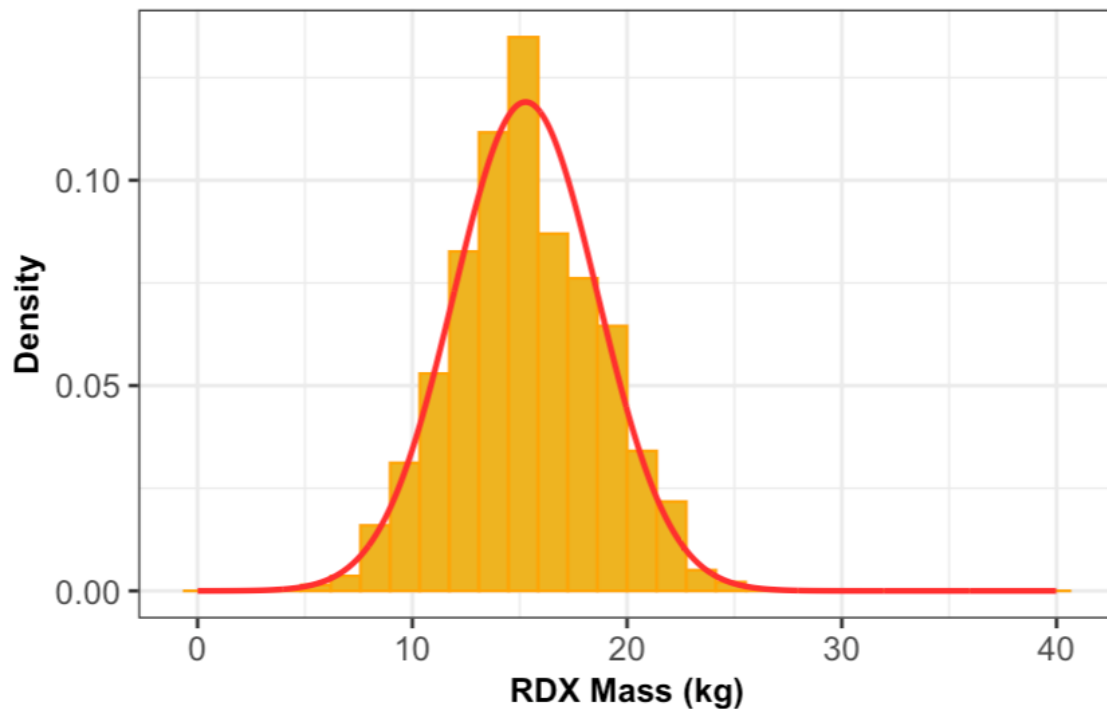


Figure 3. A histogram of RDX inventory results from an MC simulation incorporating uncertainty in porosity. The red line is the normal probability distribution fit to the MC results using maximum likelihood methods.

Table 1. Plume volume and inventory estimates compared to 2017 results.

	2017	2019, >10 ppb	2019, whole plume
Volume (L)	7.41×10^{10}	4.77×10^9	1.61×10^{10}
Porosity	0.18–0.33	0.27	0.27
Inventory (kg)	35–415	15.3	18.4